

Final Report

Groundwater Availability Model for the West Texas Bolsons (Red Light Draw, Green River Valley, and Eagle Flat) Aquifer in Texas

Prepared by:

James A. Beach, P.G.

Leigh Symank

Yun Huang

John B. Ashworth, P.G.

Tyler Davidson, P.E.

Eddie W. Collins, P.G.

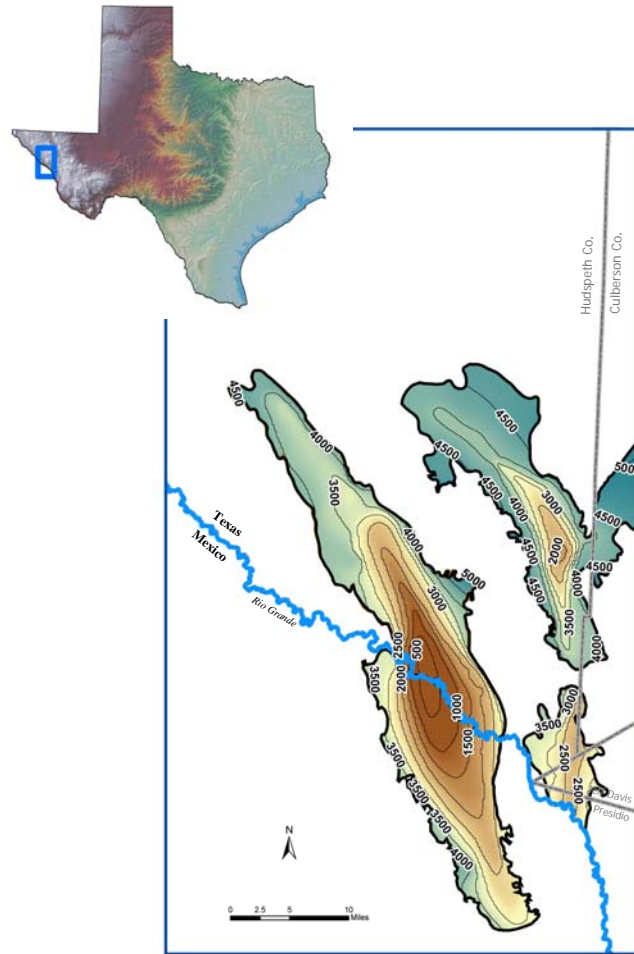
Barry J. Hibbs, Ph.D.

Bruce K. Darling, Ph.D., P.G.

Kevin Urbancyk, Ph.D., P.G.

Kenny Calhoun

Steve Finch, P.G.



Prepared for the

Texas Water Development Board

P.O. Box 1321, Capitol Station
Austin, Texas 78711-3231



November 2008



Texas Water Development Board

Final Report

Groundwater Availability Model For the West Texas Bolsons (Red Light Draw, Green River Valley and Eagle Flat) Aquifer in Texas

Prepared by:

James A. Beach, P.G.

Leigh Symank

Yun Huang

John B. Ashworth, P.G.

Tyler Davidson, P.E.

LBG-Guyton Associates

Eddie W. Collins, P.G.

Bureau of Economic Geology

Barry J. Hibbs, Ph.D.

University of California

Bruce K. Darling, Ph.D., P.G.

Southwest Groundwater Consulting, LLC

Kevin Urbancyk, Ph.D, P.G.

Sul Ross State University

Kenny Calhoun

Daniel B. Stephens and Associates, Inc.

Steve Finch

John Shomaker and Associates, Inc.

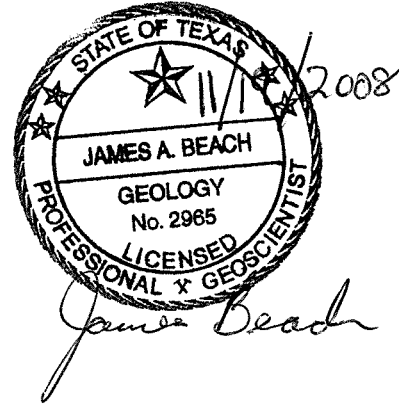
November 2008

GEOSCIENTIST AND ENGINEERING SEAL

This report documents the work of the following Licensed Texas Geoscientists or Licensed Texas Professional Engineers:

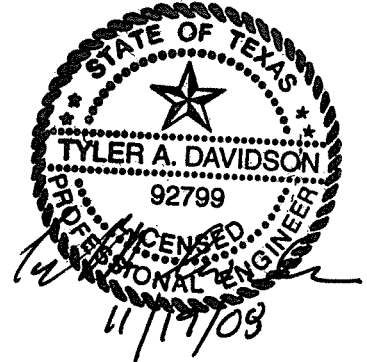
James A. Beach, P.G.

Mr. Beach was the Project Manager and was responsible for overseeing the development of the conceptual model, and for development and calibration of the numerical model.



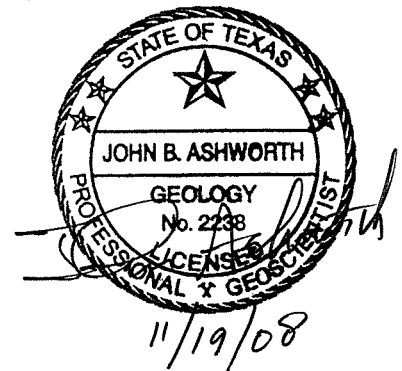
Tyler Davidson, P.E.

Mr. Davidson was responsible for the evaluation of hydraulic properties and water quality in the conceptual model.



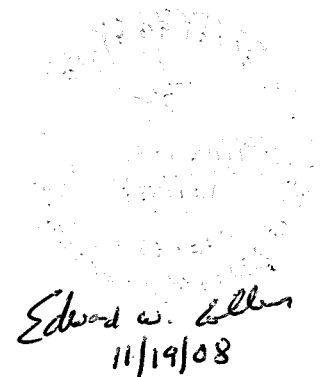
John Ashworth, P.G.

Mr. Ashworth was responsible for helping integrate the geologic structure into the numerical model.



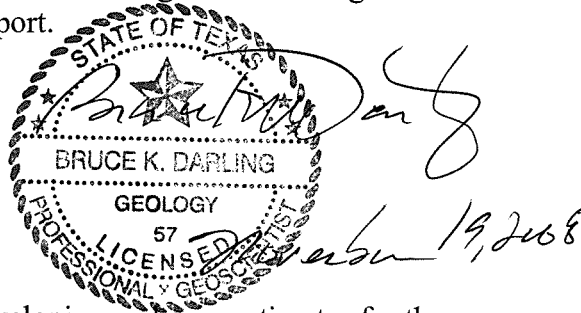
Eddie W. Collins, P.G.

Mr. Collins was responsible for development of the conceptual geologic structure in the model area.



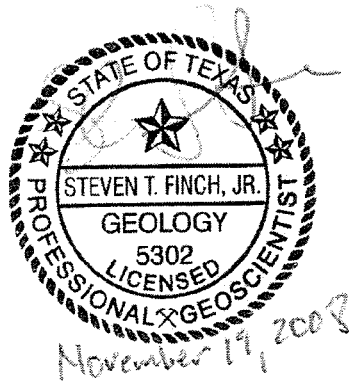
Bruce K. Darling, Ph.D., P.G.

Dr. Darling was responsible for writing and reviewing the geology sections in the report.



Steven Finch, P.G.

Mr. Finch was responsible for developing recharge estimates for the model.



Groundwater Availability Model for the West Texas Bolsons (Red Light Draw, Green River Valley, and Eagle Flat) Aquifer in Texas

TABLE OF CONTENTS

1.0	INTRODUCTION	1-1
2.0	STUDY AREA	2-1
2.1	Location	2-1
2.2	Physiography	2-9
2.3	Climate	2-15
2.4	Vegetation and Land Use	2-23
2.5	Geology	2-26
3.0	PREVIOUS WORK	3-1
3.1	Hydrogeologic Framework	3-1
3.2	Groundwater Models	3-2
4.0	HYDROLOGIC SETTING	4-1
4.1	Hydrostratigraphy	4-1
4.1.1	Red Light Draw	4-2
4.1.2	Northwest Eagle Flat	4-3
4.1.3	Southeast Eagle Flat	4-4
4.1.4	Green River Valley	4-4
4.2	Structure	4-5
4.2.1	Data Sources	4-5
4.2.2	Construction of the Structural Surfaces	4-6
4.2.3	Discussion of Structure	4-6
4.3	Water Levels and Regional Groundwater Flow	4-12
4.3.1	Hydrographs	4-13
4.3.2	Groundwater Flow	4-13
4.3.3	Potentiometric Map	4-17
4.3.4	Flow Systems	4-20
4.3.5	Vertical Flow	4-23
4.4	Recharge	4-25
4.4.1	Recharge Areas	4-25
4.4.2	Recharge Estimates from Previous Work	4-26
4.4.3	Summary of Recharge Method	4-28
4.4.4	Recharge Estimates	4-30
4.5	Rivers, Streams, Springs and Lakes	4-35
4.6	Hydraulic Properties	4-38
4.6.1	Hydraulic Conductivity	4-38
4.6.2	Storage Properties	4-39
4.7	Discharge	4-42
4.8	Water Quality	4-50

5.0	CONCEPTUAL MODEL OF FLOW IN WEST TEXAS BOLSON AQUIFERS.....	5-1
5.1	Conceptual model.....	5-1
6.0	MODEL DESIGN.....	6-1
6.1	Code and Processor.....	6-1
6.2	Model Layers and Grid.....	6-2
6.3	Model Parameters.....	6-11
6.3.1	Hydraulic Conductivity.....	6-11
6.3.2	Storage Coefficients.....	6-12
6.4	Model Boundaries.....	6-13
6.4.1	Lateral Boundaries.....	6-13
6.4.2	Vertical Boundaries.....	6-18
6.4.3	Streams and Springs.....	6-18
6.4.4	Recharge and Evapotranspiration.....	6-18
6.4.5	Pumping Discharge.....	6-19
7.0	MODELING APPROACH.....	7-1
7.1	Calibration.....	7-1
7.1.1	Approach.....	7-1
7.1.2	Calibration Targets and Measures.....	7-2
7.1.3	Calibration Target Uncertainty.....	7-4
7.2	Sensitivity Analyses.....	7-5
8.0	STEADY-STATE MODEL.....	8-1
8.1	Calibration.....	8-1
8.1.1	Calibration Targets.....	8-1
8.1.2	Horizontal and Vertical Hydraulic Conductivities.....	8-1
8.1.3	Recharge.....	8-8
8.1.4	Groundwater Evapotranspiration.....	8-8
8.1.5	General Head Boundaries.....	8-8
8.1.6	Calibration Results and Statistics.....	8-11
8.1.7	Hydraulic Heads.....	8-12
8.1.8	Water Budget.....	8-20
8.2	Sensitivity Analysis.....	8-23
9.0	TRANSIENT MODEL.....	9-1
9.1	Transient Simulation.....	9-1
9.2	Sensitivity Analysis.....	9-1
10.0	LIMITATIONS OF THE MODEL.....	10-2
10.1	Limitations of Supporting Data.....	10-2
10.2	Limiting Assumptions.....	10-2
10.3	Limits for Model Applicability.....	10-3
11.0	FUTURE IMPROVEMENTS.....	11-1
11.1	Supporting Data.....	11-1
11.2	Model Improvements.....	11-1
12.0	CONCLUSIONS.....	12-1
13.0	ACKNOWLEDGEMENTS.....	13-1
14.0	REFERENCES.....	14-1

LIST OF FIGURES

Figure 2.1.1	Location of the Study Area.....	2-4
Figure 2.1.2	Location of the West Texas Bolsons Aquifer.....	2-5
Figure 2.1.3	Regional Water Planning Groups.....	2-6
Figure 2.1.4	Groundwater Conservation Districts	2-7
Figure 2.1.5	Groundwater Management Areas.....	2-8
Figure 2.2.1	Sections Within the Basin and Range Physiographic Province	2-12
Figure 2.2.2	Topography.....	2-13
Figure 2.2.3	Major River Basins and Surface Water Features	2-14
Figure 2.3.1	Texas Climate Classification (from Larkin and Bomar, 1983)	2-16
Figure 2.3.2	Mean Annual Precipitation and Weather Stations.....	2-17
Figure 2.3.3	Selected weather stations with historic precipitation data.....	2-20
Figure 2.3.4	Average annual lake evaporation	2-21
Figure 2.3.5	Average Annual Temperature	2-22
Figure 2.4.1	Distribution of Vegetation.....	2-24
Figure 2.4.2	Land Use.....	2-25
Figure 2.5.1	Surface Geology	2-27
Figure 2.5.2	Location of Geologic Cross Sections	2-36
Figure 2.5.3	Geohydrologic Cross Section A-A'	2-37
Figure 2.5.4	Geohydrologic Cross Section B-B'.....	2-38
Figure 2.5.5	Geohydrologic Cross Section C-C'.....	2-39
Figure 2.5.6	Geohydrologic Cross Section D-D'	2-40
Figure 2.5.7	Geohydrologic Cross Section E-E'	2-41
Figure 2.5.8	Geohydrologic Cross Section F- F'	2-42
Figure 2.5.9	Structural Faulting.....	2-43
Figure 3.2.1	Location of previous modeling studies.....	3-4
Figure 4.2.1	Thickness of West Texas Bolson Aquifer	4-8
Figure 4.2.2	Elevation of the base of the West Texas Bolsons Aquifer	4-9
Figure 4.2.3	Thickness of the underlying units.....	4-10
Figure 4.2.4	Elevation of the base of underlying units.....	4-11
Figure 4.3.1	Histogram showing the number of water level measurements in each year.....	4-12

Figure 4.3.2	Hydrographs for Wells in Eagle Flat, Red Light Draw, Green River Valley and Rio Grande Alluvium.....	4-14
Figure 4.3.3	Water level elevation versus land surface elevation.....	4-15
Figure 4.3.4	Depth to Water	4-18
Figure 4.3.5	Steady-state potentiometric surface based on all available measurements	4-19
Figure 4.3.6	Regional groundwater flow patterns	4-22
Figure 4.4.1	Distribution of potential recharge.....	4-31
Figure 4.4.2	Average annual recharge estimates in five watersheds	4-32
Figure 4.5.1	Monthly Mean Streamflow at Candelaria and Fort Quitman.....	4-36
Figure 4.5.2	Location of Springs	4-37
Figure 4.6.1	Hydraulic conductivity data in the model area.....	4-40
Figure 4.6.2	Histograms of hydraulic conductivity in the West Texas Bolsons Aquifer	4-41
Figure 4.7.1	Total pumping in the study area	4-45
Figure 4.7.2	Total pumping by aquifer	4-45
Figure 4.7.3	Total pumping for portion of the county in the study area by county and type	4-46
Figure 4.7.4	Population density in 1990 and 2000	4-48
Figure 4.7.5	Irrigated land in 1989 and 1994.....	4-49
Figure 4.8.1	Groundwater quality.....	4-53
Figure 5.1.1	Schematic of conceptual model for the WTBGAM.....	5-2
Figure 6.2.1	Model schematic and Layer representation.....	6-4
Figure 6.2.2	Thickness of Layer 2	6-5
Figure 6.2.3	Elevation of the base of Layer 2.....	6-6
Figure 6.2.4	Thickness of Layer 3	6-7
Figure 6.2.5	Model grid	6-10
Figure 6.4.1	Active cells and boundary conditions in Layer 1	6-15
Figure 6.4.2	Active cells and boundary conditions in Layer 2	6-16
Figure 6.4.3	Active cells and boundary conditions in Layer 3	6-17
Figure 8.1.1	Location of Wells Used for Steady-State Calibration Targets (Including Layer Designation)	8-2
Figure 8.1.2	Final distribution of hydraulic conductivity in Layer 1.....	8-5
Figure 8.1.3	Final distribution of hydraulic conductivity in Layer 2	8-6
Figure 8.1.4	Final distribution of hydraulic conductivity in Layer 3	8-7
Figure 8.1.5	Final distribution of recharge rate in the steady-state model	8-9

Figure 8.1.6 Simulated evapotranspiration rates in the steady-state model	8-10
Figure 8.1.7 Crossplot of simulated versus observed heads in the steady-state model	8-14
Figure 8.1.8 Plot of residuals versus observed heads in the steady-state model	8-15
Figure 8.1.9 Simulated steady-state hydraulic heads and residuals in Layer 1	8-16
Figure 8.1.10 Residuals in the steady-state model (all Layers)	8-17
Figure 8.1.11 Simulated steady-state hydraulic heads and residuals in Layer 2	8-18
Figure 8.1.12 Simulated steady-state hydraulic heads and residuals in Layer 3	8-19
Figure 8.1.13 Water budget components in the steady-state model	8-21
Figure 8.2.1 Steady-state sensitivity results for the Bolsons (Layer 1)	8-24
Figure 8.2.2 Steady-state sensitivity results for Layer 2	8-24
Figure 8.2.3 Steady-state sensitivity results for Layer 3	8-25
Figure 8.2.4 Steady-state sensitivity results for all Layers	8-25
Figure 9.1.1 Well locations and water levels after 30 years with production of 9700 af/yr	9-3
Figure 9.1.2 Water level decline after 30 years with production of 9700 af/yr	9-4
Figure 9.1.3 Water level decline during 30-year period with production of 9700 af/yr	9-5
Figure 9.2.1 Transient sensitivity of the model to storage properties and pumping	9-1

LIST OF TABLES

Table 2.1 Generalized stratigraphic units	2-35
Table 4.1 Comparison of Recharge Estimated for West Texas Bolsons by Other Researchers	4-27
Table 4.2 Summary of coefficients used to estimate potential recharge, and corresponding elevation, average annual precipitation, and potential recharge	4-29
Table 4.3 Summary of Recharge Estimates for Red Light Draw-Green River Valley Groundwater Availability Model Study Area	4-30
Table 4.4 Comparison of Recharge Methods for Red Light Draw-Green River Valley Groundwater Availability Model Study Area	4-33
Table 4.5 Hydraulic property data from pumping tests	4-41
Table 4.6 Historical pumping by user group and county	4-47
Table 4.7 Water quality constituents and MCLs	4-52
Table 4.8 Groundwater facies (after Darling, 1997)	4-54

Table 6.1	Generalized stratigraphic units	6-8
Table 7.1	Summary of the steady-state calibration targets	7-2
Table 8.1	Summary of hydraulic properties used in model	8-3
Table 8.2	Summary of steady-state head calibration statistics	8-12
Table 8.3	Summary of steady-state water budget components.....	8-20

LIST OF APPENDICES

Appendix	Description
A	Detailed geologic maps and definitions
B	Recharge estimation methodology
C	Texas and Mexico pumping data
D	Countywide water budgets
E	Response to TWDB comments

EXECUTIVE SUMMARY

The West Texas Bolsons aquifer system of the Trans-Pecos region of West Texas represents the primary source of water supply within their extent. The flow systems of the Red Light Draw, Green River Valley, and Eagle Flat Bolsons are interconnected and complex. Because this aquifer system represents an important resource for West Texas, it is important to understand them and to develop quantitative tools to support all stakeholders in planning the future of these resources.

The model is regional in scale, and was developed with the MODFLOW-2000 groundwater flow code. The conceptual model divides the aquifer system into three Layers. The top Layer represents the bolsons and the two underlying aquifer Layers represent the Cretaceous, Paleozoic, and other water-bearing zones that exist in the basement rocks. The conceptual model was based on data compiled from many sources and included a detailed analysis of recharge for the model area. Estimates of hydraulic conductivity and aquifer storage properties were limited due to the limited historical use of the West Texas Bolsons aquifer. Water level measurements were assimilated for use in developing a calibrated model under steady-state conditions.

The mean absolute error (MAE) of the steady-state calibration targets for the bolsons is 56 feet over a range of 800 feet, resulting in a MAE/range ratio of 7.0%. For Layer 2, MAE was 99 feet over a range of 2,638 feet resulting in a ratio of 3.8% and Layer 3 has a MAE of 119 feet over a range of 1,106 feet for a ratio of 10.8%. Over the entire model, MAE was 93 feet over a range of 2,641 feet, resulting in a 3.5% ratio. These statistics indicate that the model provides a reasonable tool to assess regional groundwater issues.

Due to the lack of water level data that indicate any significant transient responses in the aquifer system and the relatively small amount of pumping in the model, a transient model was not calibrated. Therefore, storage properties from the calibrated Igneous and Bolson GAM (located just to the east of this model) were used in this model and a test production scenario was completed to ensure that the model results were reasonable. If a significant production project is undertaken in the West Texas Bolsons, the model should be refined to incorporate local hydraulic conductivity and storage properties.

1.0 INTRODUCTION

The West Texas Bolsons aquifer system of the Trans-Pecos region of West Texas is classified as a minor aquifer by the Texas Water Development Board (Ashworth and Hopkins, 1995) and generally represents the sole source of water supply within its extent. This report describes the hydrologic flow characteristics of the Red Light Draw, Green River Valley, and Eagle Flat Bolson aquifers and the hydrologically connected Cretaceous, Permian, Paleozoic and Igneous water-bearing rocks that underlie and flank the three western bolson aquifers of the West Texas Bolsons aquifer system. Hydrologic data from these aquifers, as well as adjacent water-bearing formations, were evaluated to establish a conceptual model of the groundwater flow system that is the basis for a groundwater availability model (GAM).

The goal of the Texas Water Development Board (TWDB) GAM program is to provide reliable information on groundwater availability to the citizens of Texas to ensure adequate supplies or recognize inadequate supplies over a 50-year planning period. The West Texas Bolsons Groundwater Availability Model (WTBGAM) conceptual model was developed by assimilating available scientific information about the aquifers in the study area. Existing data was assimilated in the model area to define:

- Physiography, climate, vegetation, and land use
- Geology, hydrostratigraphy and structure of the aquifers
- Groundwater quality
- Hydraulic properties of the aquifers
- Surface water and groundwater interaction
- Recharge rates for the aquifers
- Water levels
- Pumping rates

The WTBGAM numerical computer model (created using the USGS finite difference groundwater modeling code, MODFLOW-2000) of the aquifers provides a scientific, quantitative tool to evaluate aquifer responses to current and projected pumping and to assist in regional water planning efforts and aquifer management decisions. The TWDB GAM program allowed stakeholders the opportunity to provide input and comments during the conceptual model development. The result is a

standardized, documented, and publicly available numerical groundwater flow model and support information.

The WTBGAM can be used as a basis for performing predictive simulations and sensitivity evaluations of regional water management strategies and groundwater availability. The WTBGAM can also be used as a water management tool for the local groundwater conservation districts. If a significant production project is undertaken in the West Texas Bolsons, the model should be refined to incorporate local hydraulic conductivity and storage properties.

2.0 STUDY AREA

2.1 Location

The study area is approximately 100 miles southeast of El Paso, Texas (Figure 2.1.1), and is part of the southernmost extension of the North American Basin-and-Range physiographic province. The area encompassed by the study lies in southern Hudspeth County and includes a small segment of bolson extending across the international border into northern Chihuahua, Mexico (Figure 2.1.1).

The “West Texas Bolsons” include several deep basins filled with erosional sediments of Quaternary and Tertiary age that contain variable quantities of groundwater. These bolsons include Red Light Draw, Eagle Flat, Green River Valley, Presidio-Redford, and Salt Basin (Ashworth and Hopkins, 1995) (Figure 2.1.2). The westernmost system of bolsons includes three basin-fill aquifers targeted in this study. These include the Eagle Flat, Green River Valley, and Red Light Draw aquifers (Figure 2.1.2). Some researchers further divide Eagle Flat into Northwest Eagle Flat and Southeast Eagle Flat (Darling and others, 1994). Previous hydrogeologic studies of the Red Light Draw aquifer terminated at the US/Mexico border (Hibbs and Darling, 2005). The smaller section of this aquifer extending into Mexico is included in the phrase “Red Light Draw aquifer” in this study because of historical precedence and convenience, despite the fact that the aquifer is not named the Red Light Draw in Mexico.

The West Texas Bolsons GAM (WTBGAM) study area includes the full contiguous extent of these three basin-fill aquifers, as well as the basin-bordering mountain areas, as these areas serve as potential areas of recharge to the bolson aquifers. Where depth to groundwater exceeds basin-fill thickness, such as in parts of the Northwest Eagle Flat and Red Light Draw, the Cretaceous and Tertiary bedrock units serve as the main aquifers.

The WTBGAM model area covers the full surface extent of the three bolson aquifers, contained within the following approximate geographic/geologic boundaries (Figure 2.1.2):

- North - groundwater divide that roughly mimics the topographic divide north of I-10
- East - along a line running through the valley that separates the Van Horn Mountains on the south and the Carrizo Mountains to the north, roughly parallel to the Hudspeth/Culberson County Line
- West - west of the westernmost extent of Red Light Draw along the northwestern extent of the Quitman Mountains and running south into Mexico
- South - along the southern extent of the Sierra El Trozado Mountains in Mexico, which is the southern extent of the alluvium that is contiguous with the Red Light Draw

The study area is located within the Far West Texas Water Planning Region (also known as Region E) as shown in Figure 2.1.3. Region F lies just east of the study area boundary. There are four groundwater conservation districts in the study area, as shown in Figure 2.1.4. However, a groundwater conservation district does not regulate the bolson aquifers in southern Hudspeth County at this time. The parts of the bolson aquifers (e.g., Green River Valley) covered by a district are subject to regulation. The study area is also completely contained within TWDB Groundwater Management Area 4, as shown in Figure 2.1.5.

The study area is sparsely populated, with only a few small towns and hamlets and mostly large ranches. The largest settlement, Sierra Blanca, lies in the northwestern part of the study area, approximately 90 miles (144 km) southeast of El Paso, and 33 miles (53 km) west of the City of Van Horn, along Interstate 10 (Figure 2.1.1). Sierra Blanca has most of its municipal drinking water piped in from Van Horn. A small number of wells satisfy the needs of the local population and livestock. A few springs issue from bedrock formations in the mountains and from basin-fill and augment livestock water supplies.

Low-lying areas of Northwest Eagle Flat were disposal areas for interstate municipal sludge in the 1990s and had been identified and studied as possible repositories for disposal of low-level radioactive waste. However, the proposed radioactive waste site located in Northwest Eagle Flat was never licensed. Some of the geologic and

hydrogeologic data that have been collected to support proposed radioactive waste disposal by Darling and others (1994) are integrated in the WTBGAM.

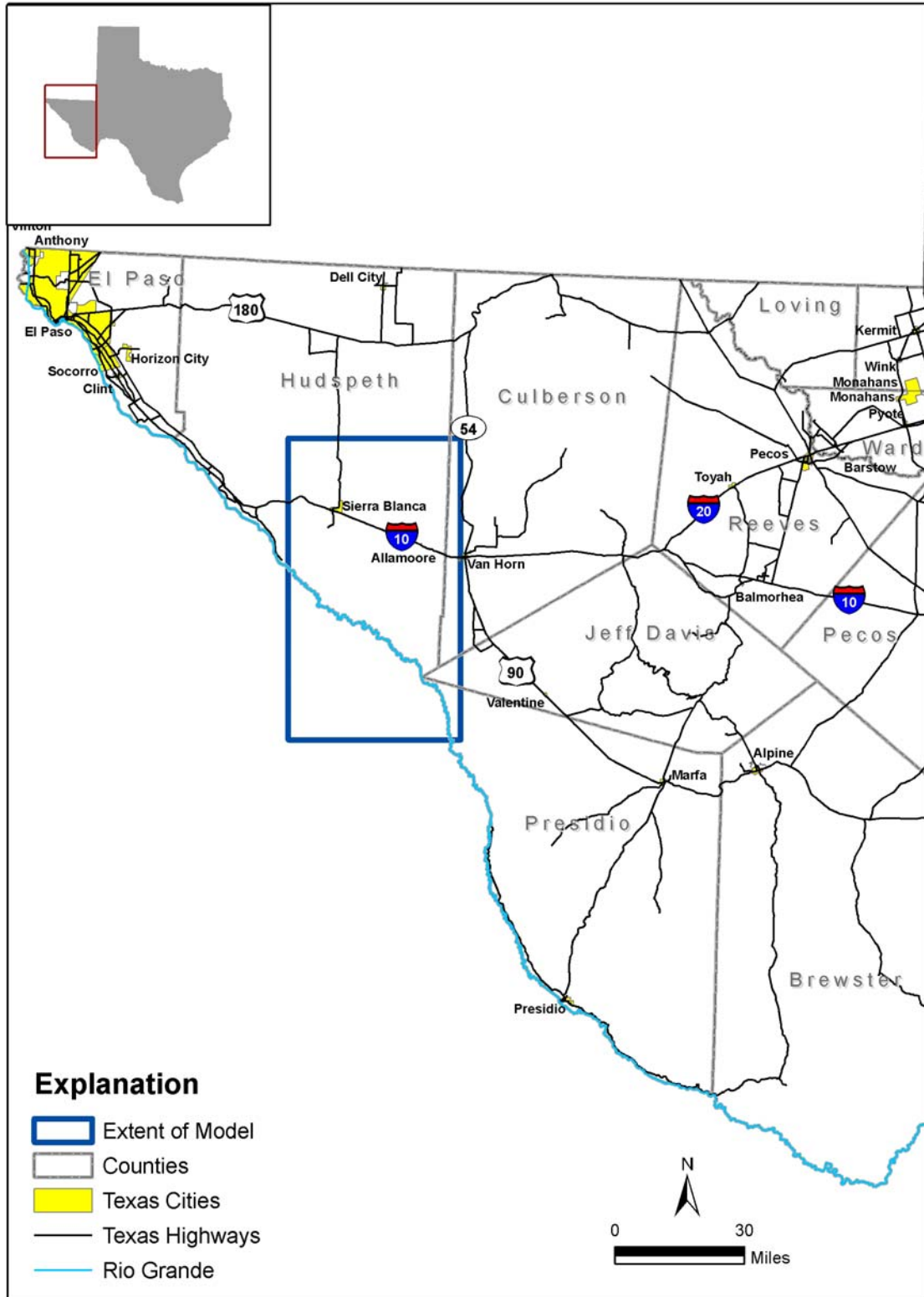


Figure 2.1.1 Location of the Study Area

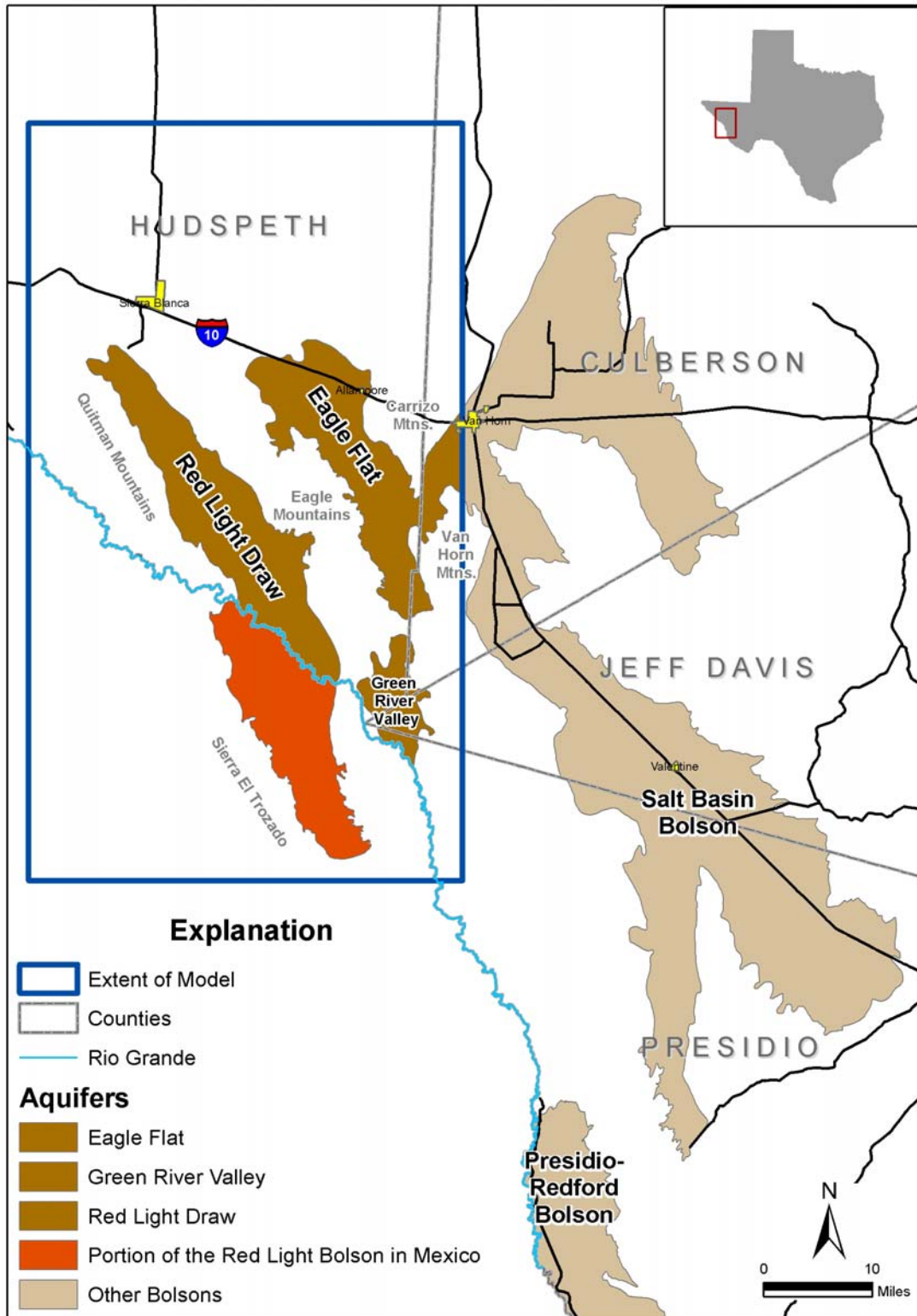


Figure 2.1.2 Location of the West Texas Bolsons Aquifer

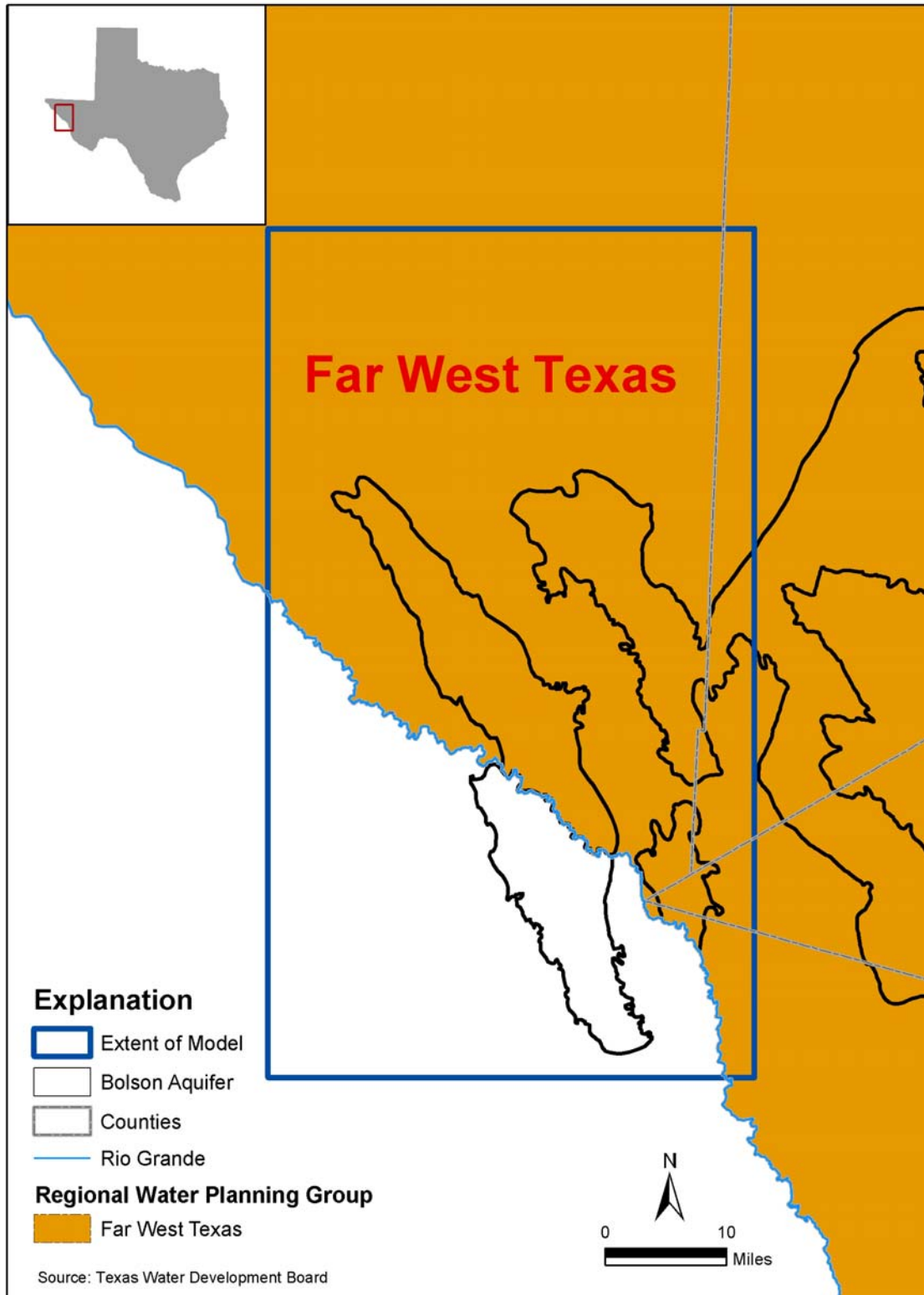


Figure 2.1.3 Regional Water Planning Groups

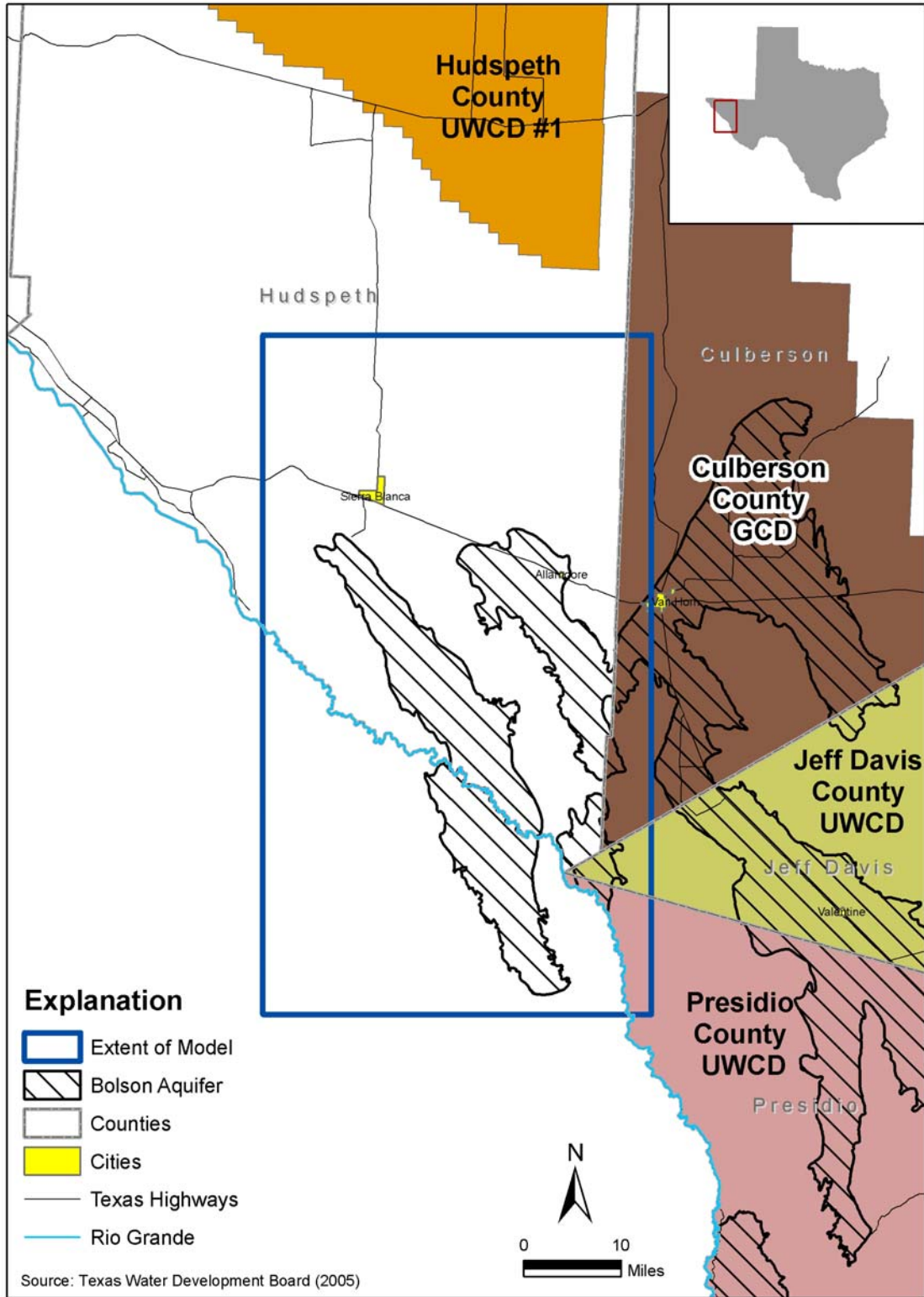


Figure 2.1.4 Groundwater Conservation Districts

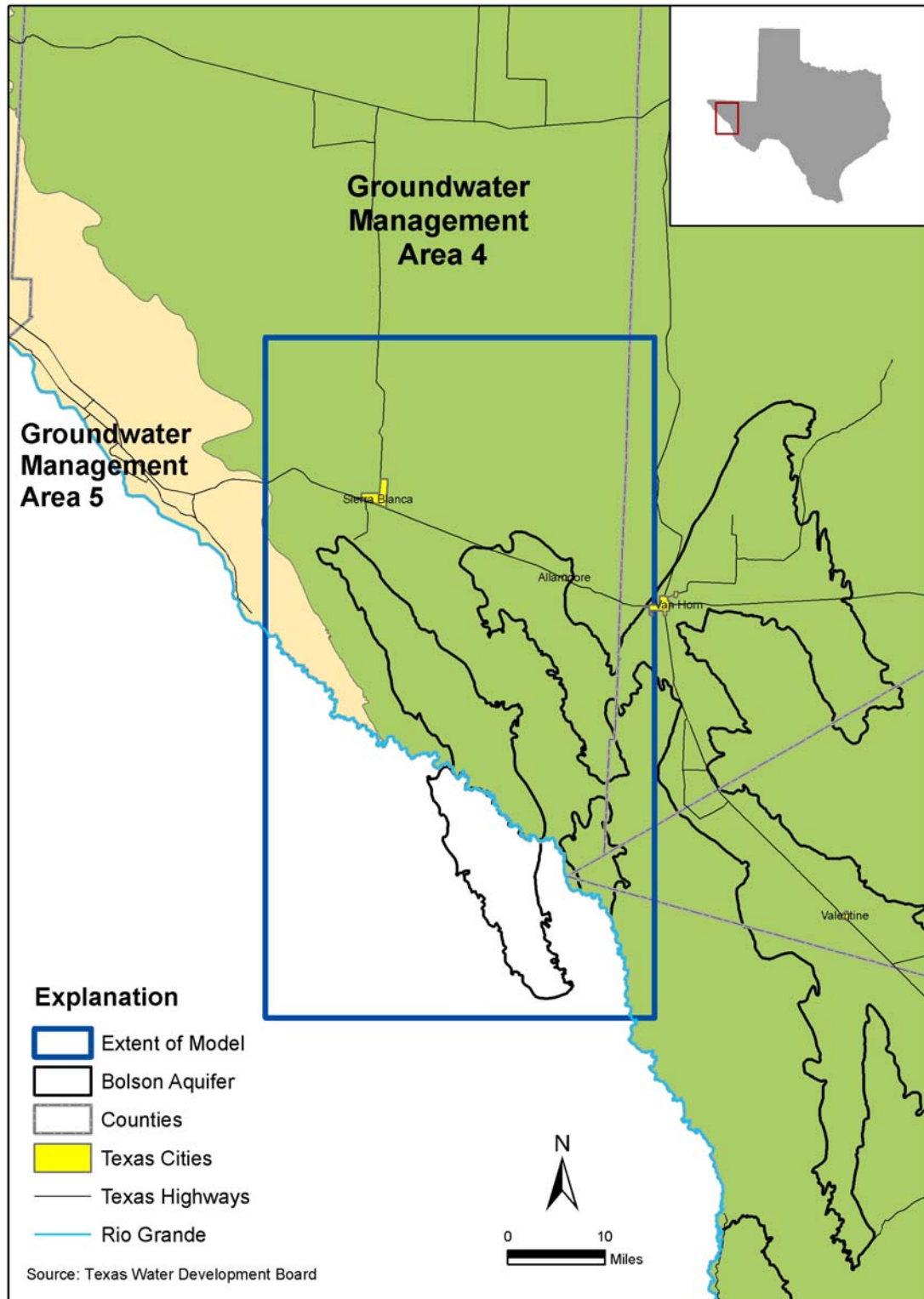


Figure 2.1.5 Groundwater Management Areas

2.2 Physiography

Regional Setting

Major land features within the Trans-Pecos region of Far West Texas are occupied by the topographically distinct area of North America known as the Basin and Range Physiographic Province (Fenneman, 1931; Thornbury, 1965). Figure 2.2.1 shows its two sub-sections, Sacramento and Mexican Highland. The Great Plains Province lies adjacent to the northeast. In Texas, the Trans-Pecos region is bounded on the north by New Mexico, on the south and west by the Rio Grande, and along the east by the Pecos River.

Traversed from north to south by an eastern range of the Rocky Mountains, the region contains all of Texas' true mountains with higher elevations and greater local relief than is characteristic of other areas of the state. Although the topography throughout most of Texas is generally flat and elevations are less than 2,500 feet above mean sea level (msl), the floors of most of the basins in West Texas are at elevations greater than 3,000 feet. Widely spaced mountain ranges rise from 1,000 to more than 4,000 feet above the lowlands. Fault-block basins separating the mountains are filled with sediments (bolson deposits) eroded from the surrounding highlands.

Local Setting

The topography of the WTBGAM area is dominated by long, narrow mountain ranges, intermontane basins (flats and draws), and gently sloping plateaus and is shown in Figure 2.2.2. The Northwest Eagle Flat basin is surrounded by the Diablo Plateau and Steeruwitz Hills to the north, by Devil Ridge and the Eagle Mountains to the west, and by Southeast Eagle Flat to the south. The floor of Northwest Eagle Flat slopes toward Grayton Lake, a topographically low desert playa that receives ephemeral runoff (Darling and others, 1994). Grayton Lake is dry for extended periods of time and water accumulates in the playa only after heavy rainfall.

The Southeast Eagle Flat basin is surrounded by the Carrizo Mountains to the northeast and the Van Horn Mountains on the southeast, by the Eagle and Indio Mountains on the west, and Green River Valley to the south. The floor of Southeast Eagle Flat slopes toward Scott's Crossing where surface drainage moves into the adjacent Wildhorse Flat area.

Red Light Draw is encompassed on the US side by the Eagle Mountains and Devil Ridge to the northeast, by the Quitman Mountains to the west, and by the Indio Mountains to the east. The Mexican part of Red Light Draw is bound by the Sierra de Pilares to the east and by the Sierra El Trozado to the west. The Rio Grande crosses the axis of the Red Light Draw basin (Figure 2.2.2). Surface flow in Red Light Draw is toward the Rio Grande. North of the Rio Grande, the floor of Red Light Draw slopes toward the southeast, decreasing over a distance of 30 mi from 4,500 feet above msl in the northern reaches of the basin to approximately 3,200 feet above msl along the Rio Grande (Hibbs and Darling, 2005). On the Mexican side, the floor of Red Light Draw slopes northwesterly toward the Rio Grande.

Green River Valley is bound to the northwest by the Indio Mountains and to the east by the Van Horn Mountains. Southeast Eagle Flat and the Rio Grande form Green River Valley's northern and southern boundaries, respectively. Surface flow in the northern part of Green River Valley merges with surface flow from Southeast Eagle Flat and discharges to the Rio Grande.

Sharp differences in relief are common throughout the area (Figure 2.2.2). The highest point is in the Eagle Mountains, at 7,510 feet. At opposite ends of Eagle Flat are the small settlements at Sierra Blanca and Allamoore, both at 4,500 feet. The Carrizo and Van Horn Mountains rise to more than 5,200 feet, and the Quitman Mountains are at least 6,200 feet.

Figure 2.2.3 shows the river basins and surface water features of the study area. The entire area is within the Rio Grande River basin, but the northern section (Eagle Flat) drains to a closed basin of the Rio Grande watershed. Red Light Draw and Green River Valley drain to the Rio Grande. With the exception of springs, the Rio Grande is the

only perennial stream in the study area. All other watercourses flow only after heavy rainfall. Grayton Lake (Figure 2.2.3), which lies in the center of the locally closed Eagle Flat at 4,270 feet, contains water only after heavy rainfall events. Along its southeasterly course, the elevation of the Rio Grande decreases from 3,300 feet near Indian Hot Springs to less than 3,200 feet at the southeastern corner of Green River Valley.

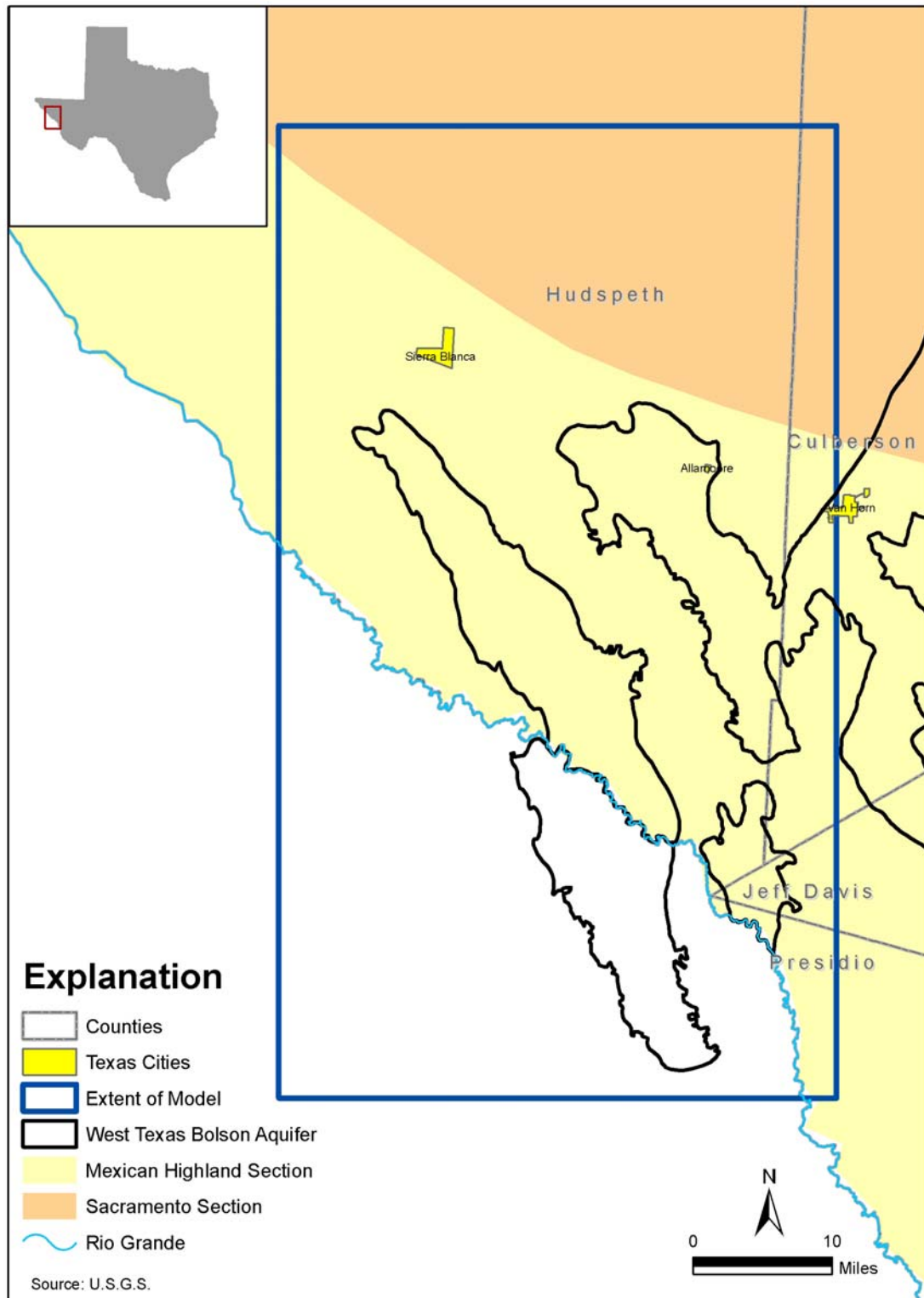


Figure 2.2.1 Sections Within the Basin and Range Physiographic Province

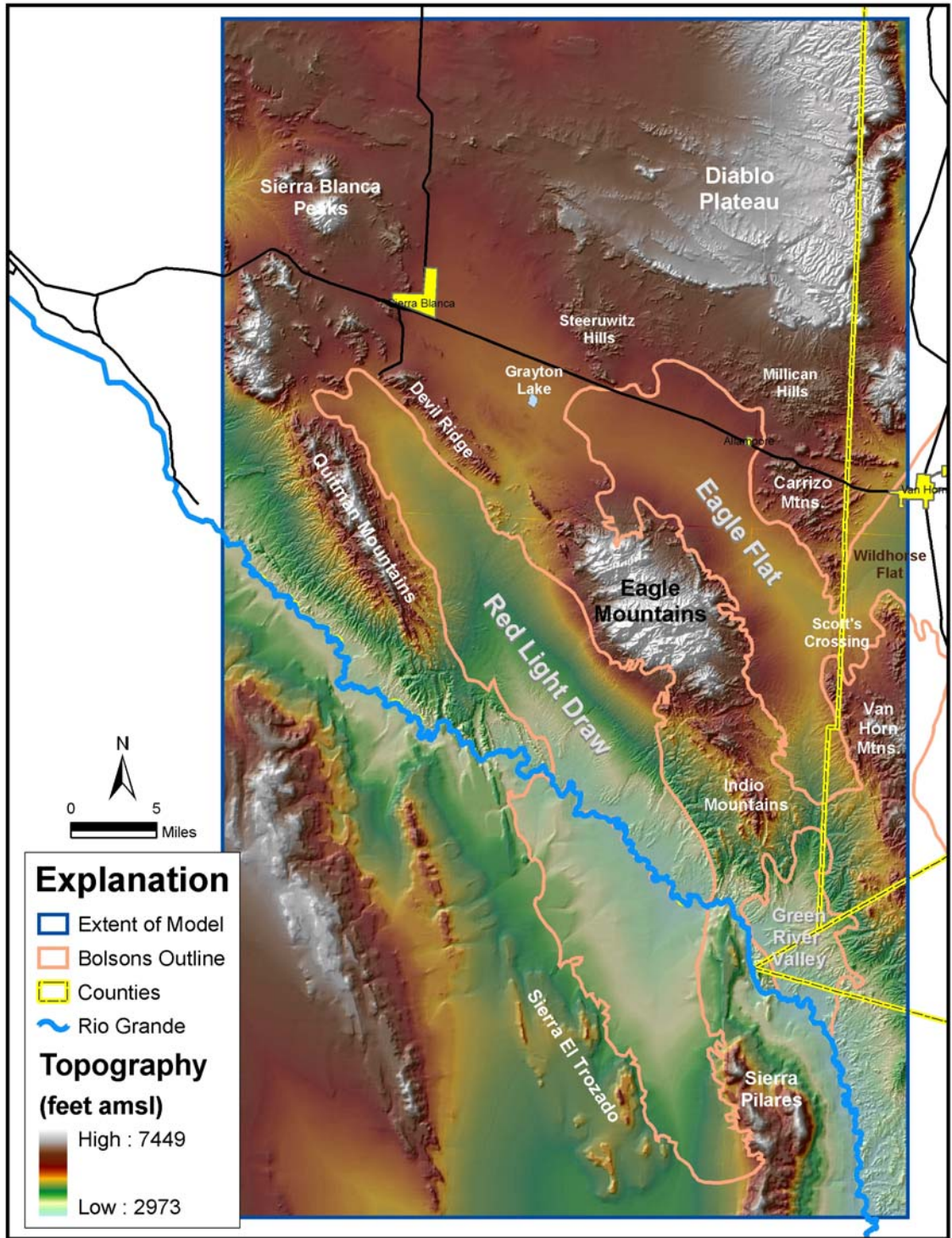


Figure 2.2.2 Topography

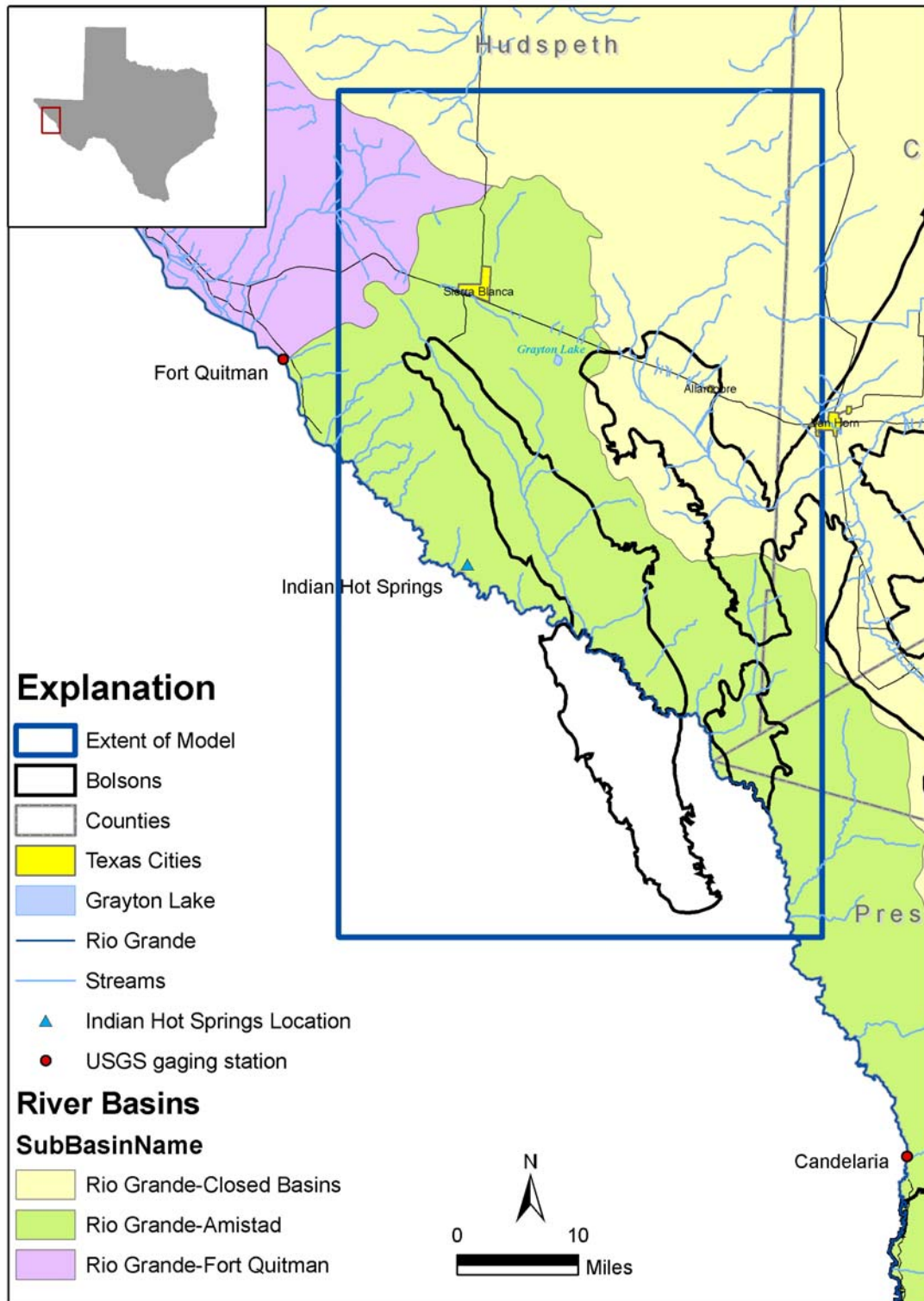


Figure 2.2.3 Major River Basins and Surface Water Features

2.3 Climate

The Chihuahuan Desert is described by the Larkin and Bomar (1983) as “subtropical arid” and is traversed by Mexico's two great mountain ranges - the Sierra Madre Oriental and the Sierra Madre Occidental. Figure 2.3.1 illustrates the Texas Climate Classification developed by Larkin and Bomar (1983). As warm moist air rises to move across these mountains, the air cools rapidly, and the cooling generates rainfall on the windward face of the mountains. This also creates a rain-shadow effect on the lee face of the mountain ranges and over the basins of the Chihuahuan Desert. While the other North American deserts have summer and winter rainy seasons (because of their location further to the west), rain typically comes to the Chihuahuan Desert between the months of June and October, during which as much as 90 percent of the annual rainfall takes place. This is often referred to as the monsoon season of the Southwest. In the Red Light Draw-Green River Valley groundwater availability model study area, an average of 74 percent of the annual rainfall takes place between June and October.

Rainfall between June and October is dominated by widely scattered thunderstorms (Larkin and Bomar, 1983; Nativ and Riggio, 1989 and 1990). Figure 2.3.2 shows the distribution of mean annual precipitation from 1971 to 2000 in the study area based on GIS interpolation of data from available weather statistics. Because of the convective nature of thunderstorms and the orographic lifting effect of mountainous areas, the amount of precipitation increases with elevation. The influence of orographic lifting on average annual rainfall is illustrated by the higher median precipitation areas centered over the Eagle Mountains and along the mountain ridge that borders the western side of the Salt Basin (e.g. Sierra Diablo). Within the Trans-Pecos region of the Chihuahuan Desert, only the highest elevations receive sufficient precipitation to be considered semi-arid, rather than true desert (Schmidt, 1995).

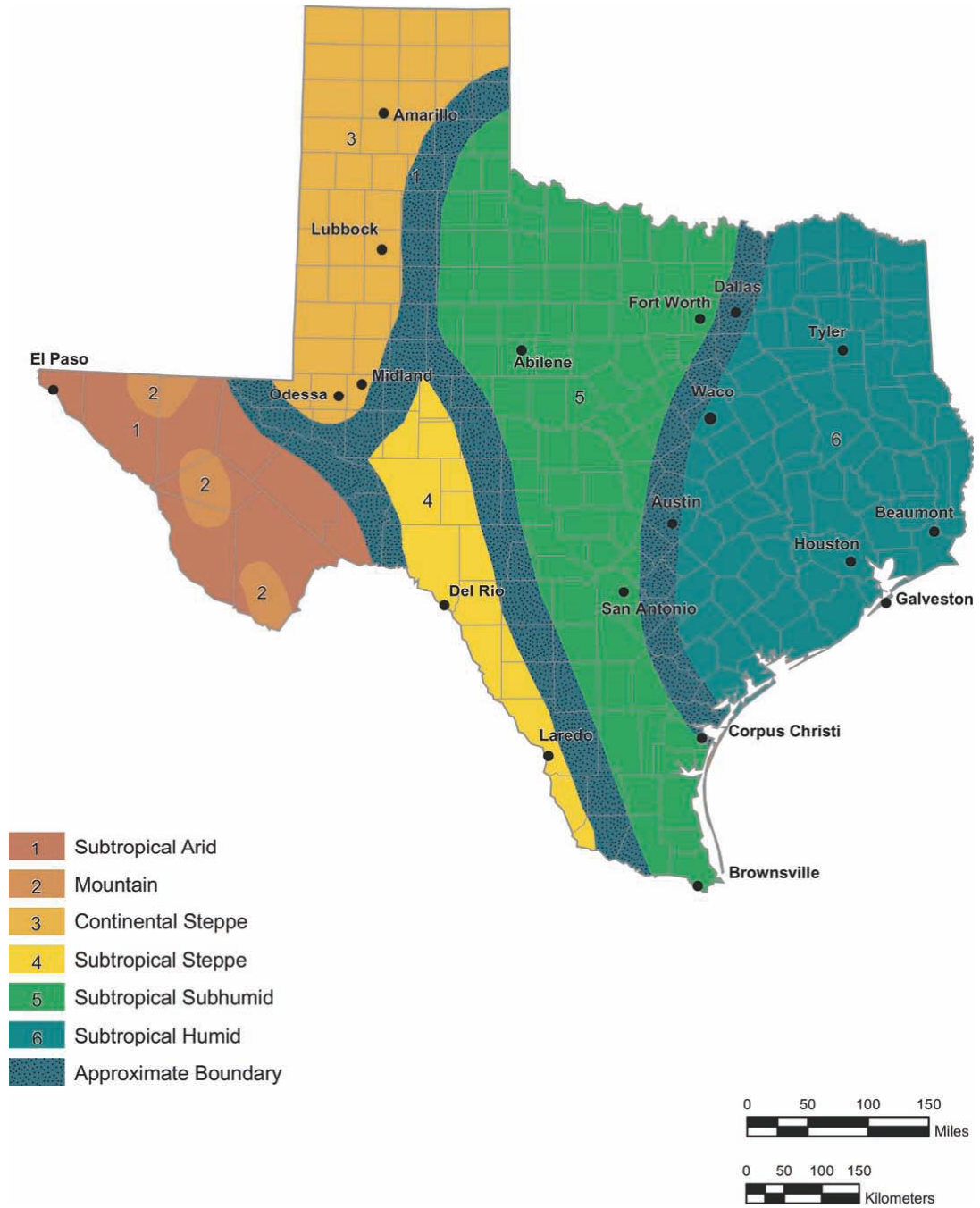


Figure 2.3.1 Texas Climate Classification (from Larkin and Bomar, 1983)

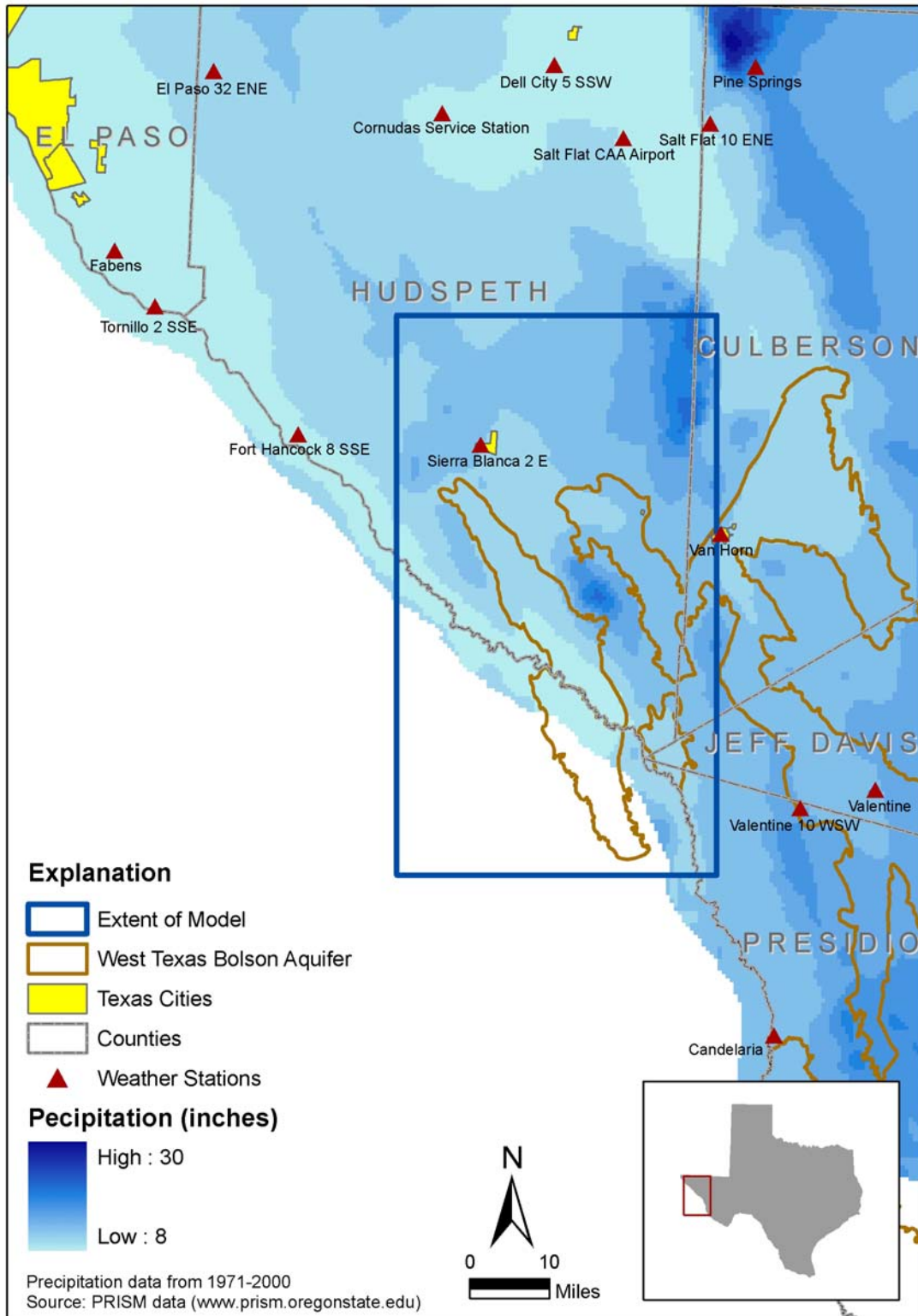


Figure 2.3.2 Mean Annual Precipitation and Weather Stations

Runoff-generating precipitation events occur several times a year in the study area. Throughout most of the study area, 24-hour precipitation event magnitude must exceed 0.67 inches to generate runoff (see Appendix B: Recharge Analysis). In some sub-basins of the study area, 24-hour precipitation event magnitude must exceed 1.58 inches to generate runoff. In the study area, precipitation events exceed 0.67 inches 4 times a year or less. Precipitation events exceed 1.58 inches once every other year. Finch and Armour (2001) estimated that runoff-generating precipitation events occurred only once every other year in Wild Horse Flat, just east of the study area, and LBG-Guyton Associates and others (2004) estimated that runoff-generating precipitation events occurred no more than 6 times a year in the highest elevations of the Davis Mountains.

Snowfall does occur in the study area, primarily in the higher elevations of the Eagle Mountains. Between 1939 and 2005, snowfall occurred once or twice a year at the Van Horn weather station. Recharge to the study area results from runoff-generating precipitation events and snowfall events, which occur several times a year (Section 4.4 Recharge).

The mean annual precipitation for the period of record 1950 to 2002 at Sierra Blanca 2 E weather station (elevation 4,554 feet amsl) is 11.45 inches (Figure 2.3.3). The mean annual precipitation for the period of record 1939 to 2005 at the Van Horn weather station (elevation 4,052 feet amsl) is 10.52 inches. Years with 3 or more months of missing data were omitted from the period of record. This represents a 0.95-inch difference in precipitation over a horizontal distance of 32 miles, and a vertical elevation change of 502 feet.

The mean annual evapotranspiration, calculated by the Utah Climate Center using COOP weather station temperature data and the Hargreaves equation, for the period of record 1893 to 1998 at Sierra Blanca 2 E weather station (elevation 4,554 feet amsl) is 61.27 inches. The mean annual evapotranspiration for the period of record 1943 to 2005 at the Van Horn weather station (elevation 4,052 feet amsl) is 62.15 inches. Years with 15 or more days of missing data were omitted from the period of record. This represents a 0.88-inch difference in evapotranspiration between the Sierra Blanca and Van Horn

Mountains over a horizontal distance of 32 miles, and a vertical elevation increase of 502 feet.

Figure 2.3.4 shows the average annual lake evaporation from 1954 through 2004 calculated for one-degree quadrangles by the Texas Water Development Board (<http://midgewater.twdb.state.tx.us/Evaporation/evap.html>). The average annual lake evaporation ranges from about 55 to 71 inches in the study area. Average monthly lake evaporation is 3 to 8 times the average monthly precipitation between June and October. Note, the period from 1954 to 2004 includes the Drought of Record (1947-1957) and therefore may represent a higher than normal evaporation average.

The mean annual temperature for the period of record 1950 to 2002 at Sierra Blanca 2 E weather station (elevation 4,554 feet amsl) is 60.7 °F. The mean annual temperature for the period of record 1939 to 2005 at the Van Horn weather station (elevation 4,052 feet amsl) is 62.6 °F. Years with 3 or more months of missing data were omitted from the period of record. This represents a 1.9 °F difference in mean annual temperature over a horizontal distance of 32 miles, and a vertical elevation change of 502 feet. Average annual temperature within the study area is shown in Figure 2.3.5. Maximum and minimum temperatures averaged from this period are 72 °F to 45 °F in the Eagle Mountains, and 78 °F to 45 °F at Red Light Draw (George and others, 2005).

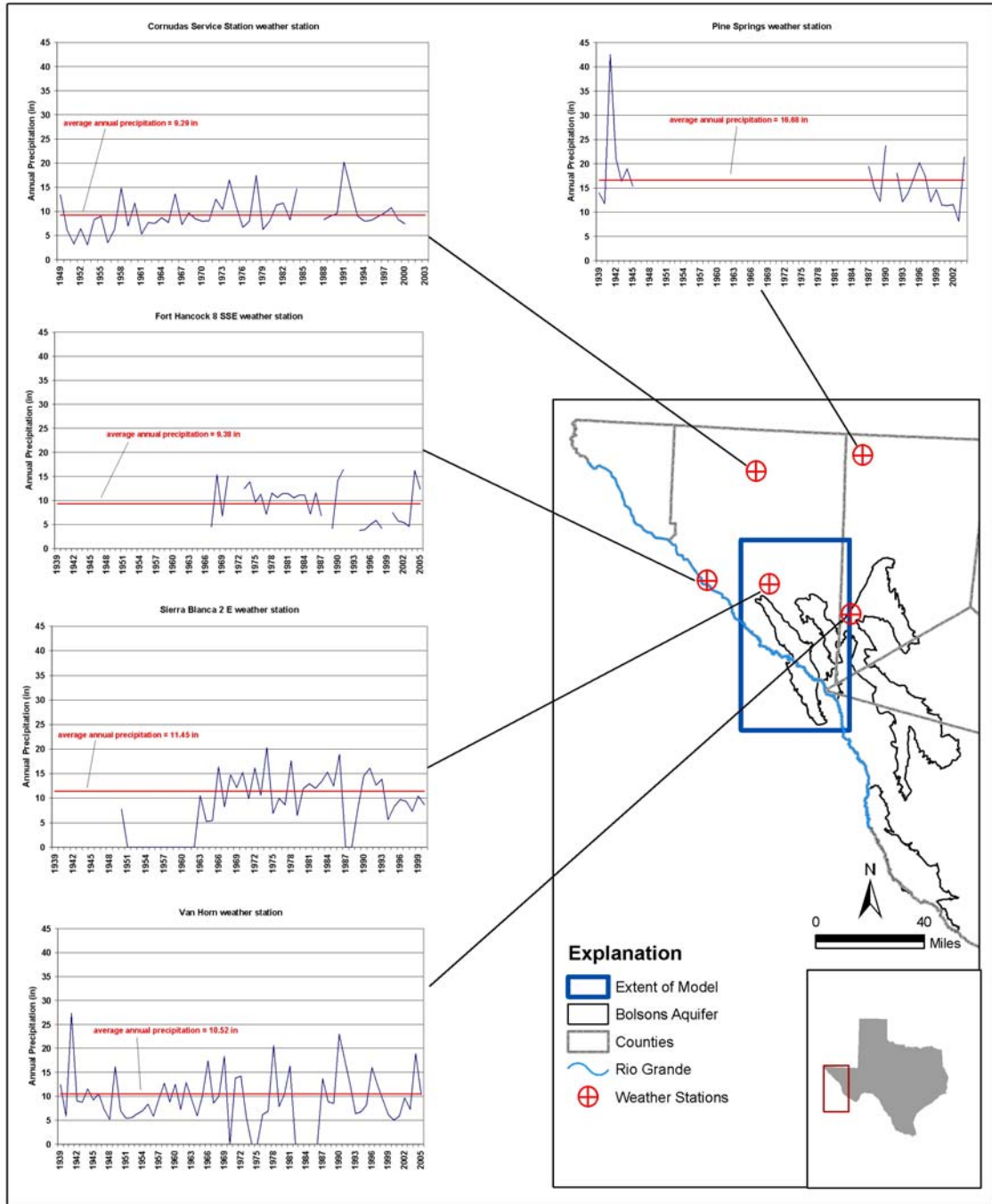


Figure 2.3.3 Selected weather stations with historic precipitation data

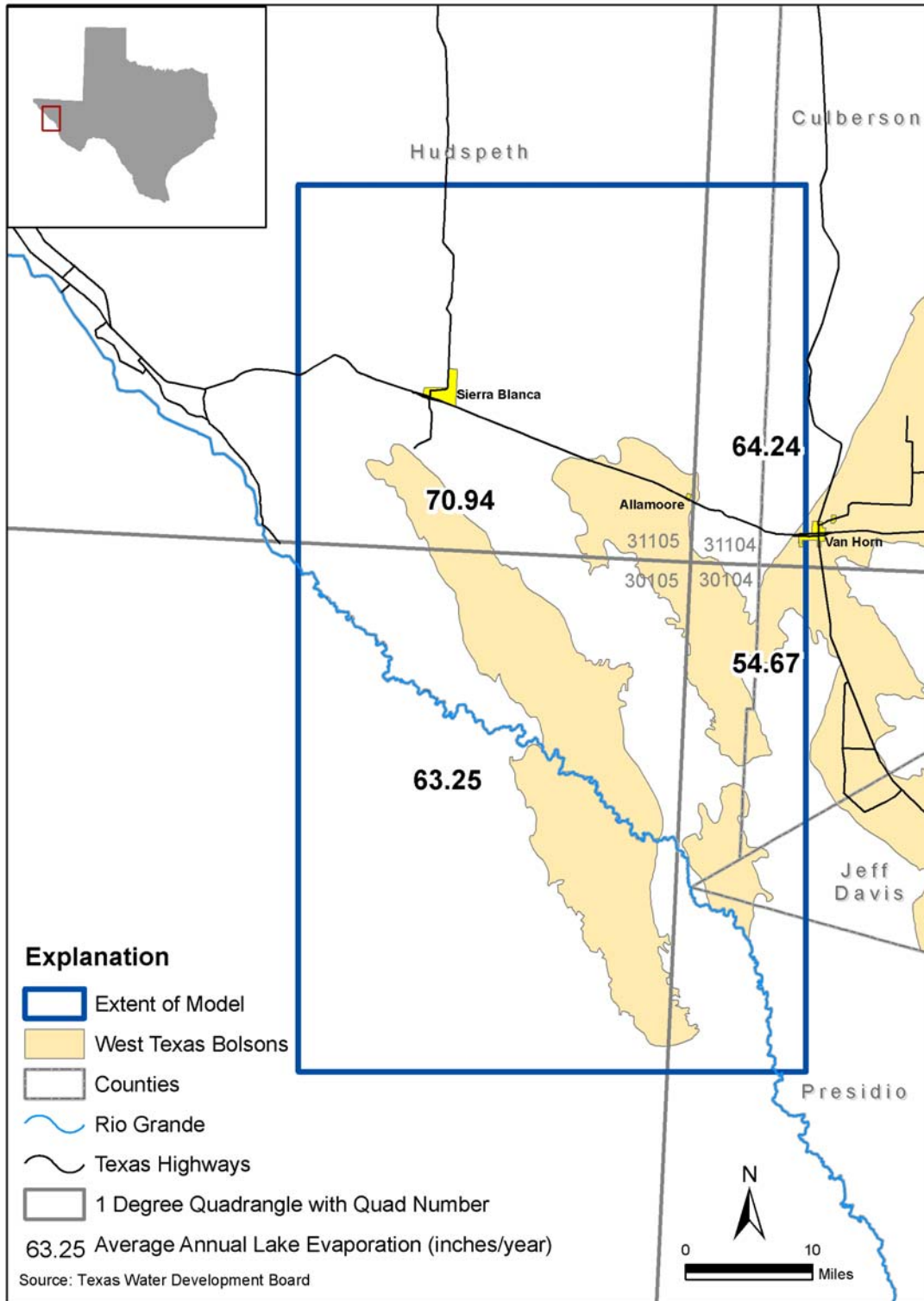


Figure 2.3.4 Average annual lake evaporation

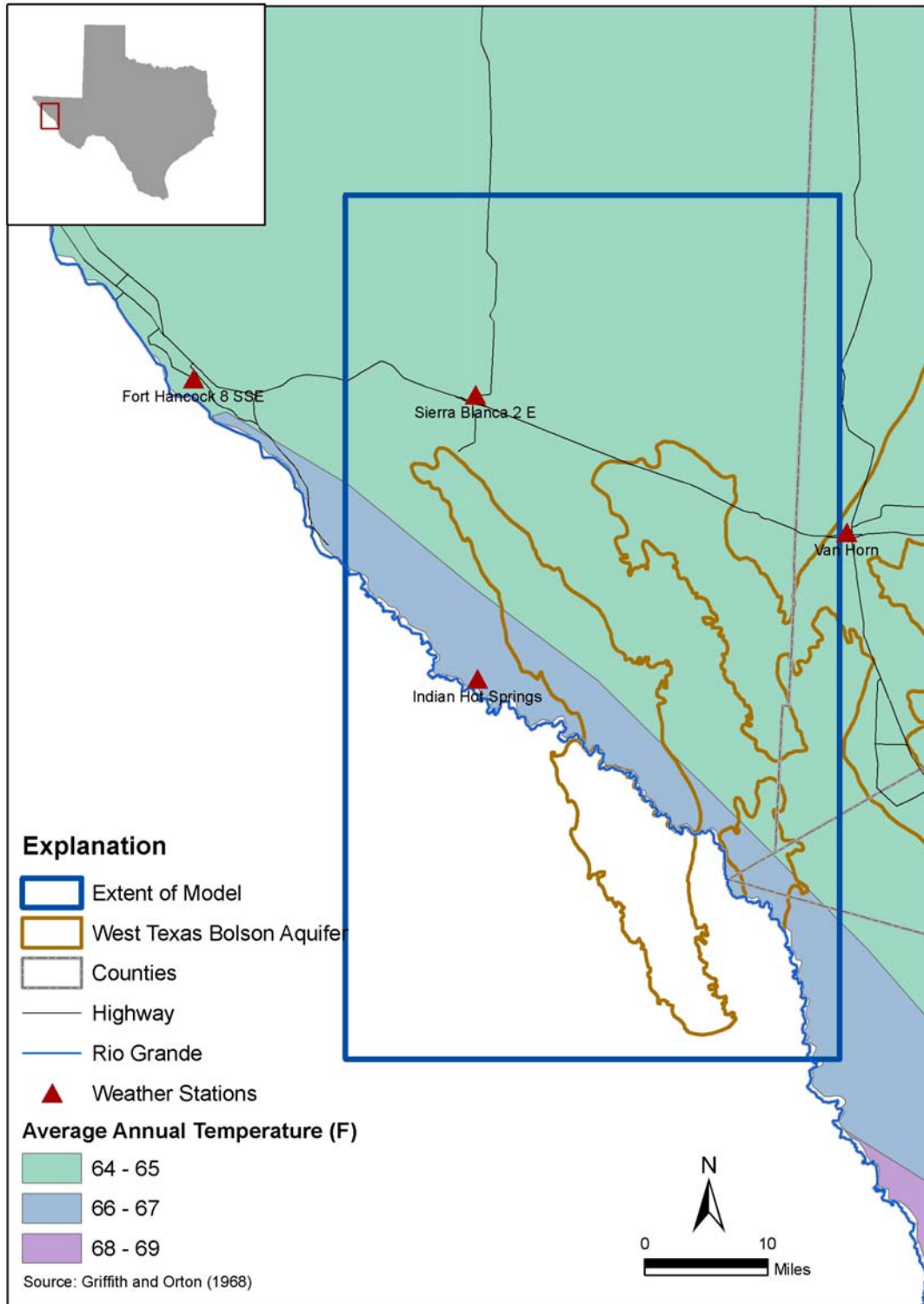


Figure 2.3.5 Average Annual Temperature

2.4 Vegetation and Land Use

Figure 2.4.1 shows the distribution of vegetation in the study area. The major climatic influence on natural vegetation in this region is the distribution of precipitation. Altitudinal differences, along with associated local temperature variations, are the major secondary controls. Desert shrub communities, particularly of creosote bush and mesquite, are most common in the region's western arid zones from the lowest altitudes to about 4,500 feet. The two plant indicators of the Chihuahuan Desert are lechuguilla (*Agave lechuguilla*) and sotol (*Dasylirion wheeleri*), which are generally found on the rough limestone slopes of the foothills. There are indications that xerophytic vegetation has been expanding upslope through the region for more than a century as a result of grassland disturbance from grazing, cultivation, introduction of non-native species, and drought (Schmidt, 1995).

Some of the semiarid portion of the study area supports short grassland. At higher elevations, the desert grassland grades into open woodland consisting of juniper and various species of oak, but this is limited to the highest elevations in the study area. Scattered through the region are smaller areas of riparian, holophytic, and other vegetation adapted to specific site conditions (Schmidt, 1995).

Most vegetation in this arid region of the State has adapted to the drier climate by developing means of storing water within the body of the plant. Evapotranspiration (ET) is significantly less from desert plants than from vegetation in wetter climates.

Figure 2.4.2 shows the land use and land cover distribution in the study area, with the vast majority of the land characterized as rangeland. The figure also shows the scattered agricultural areas within the study area. The extent of the urban areas associated with the Cities of Sierra Blanca and Van Horn are also shown, although Van Horn will not be included in the active part of the model.

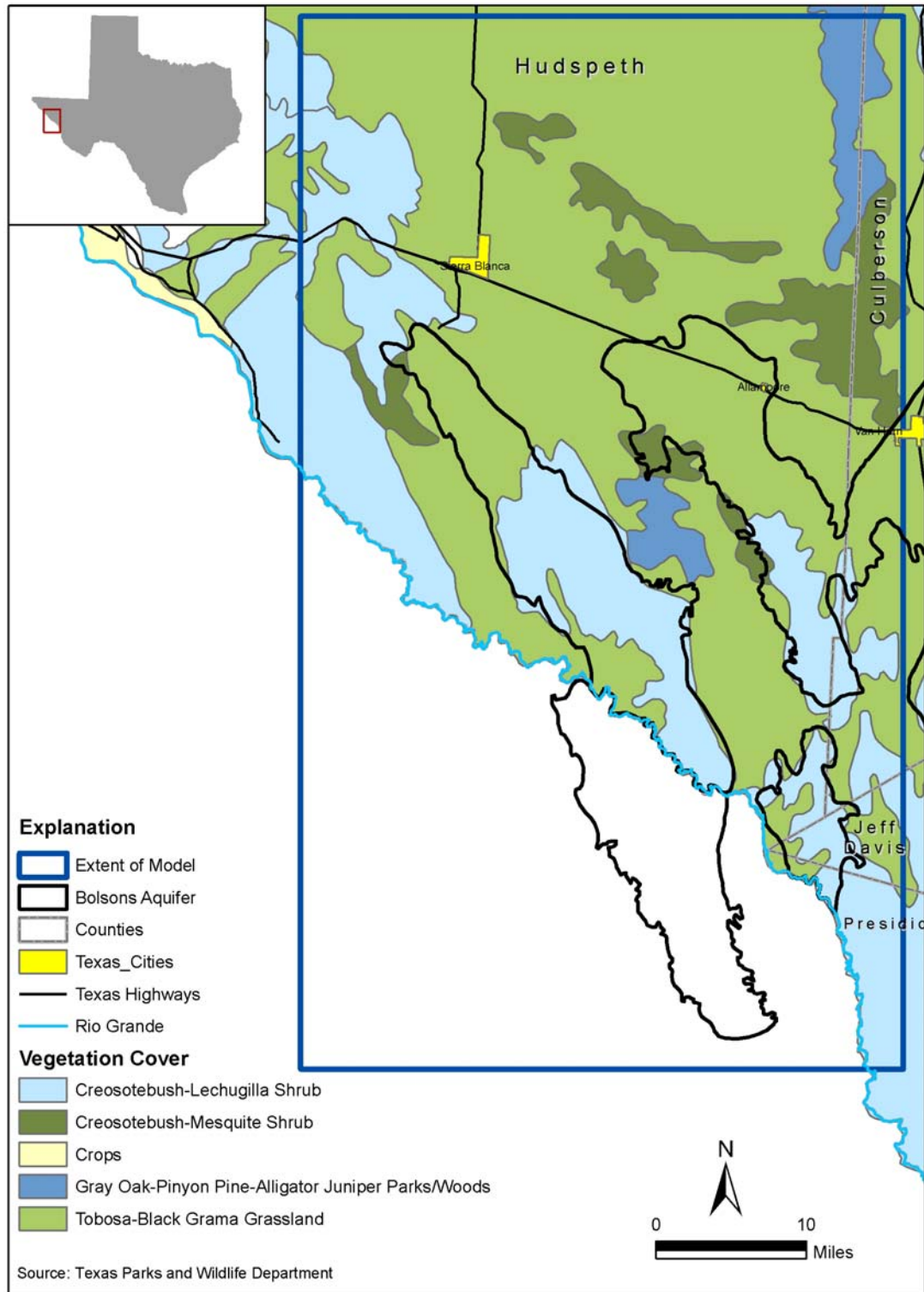


Figure 2.4.1 Distribution of Vegetation

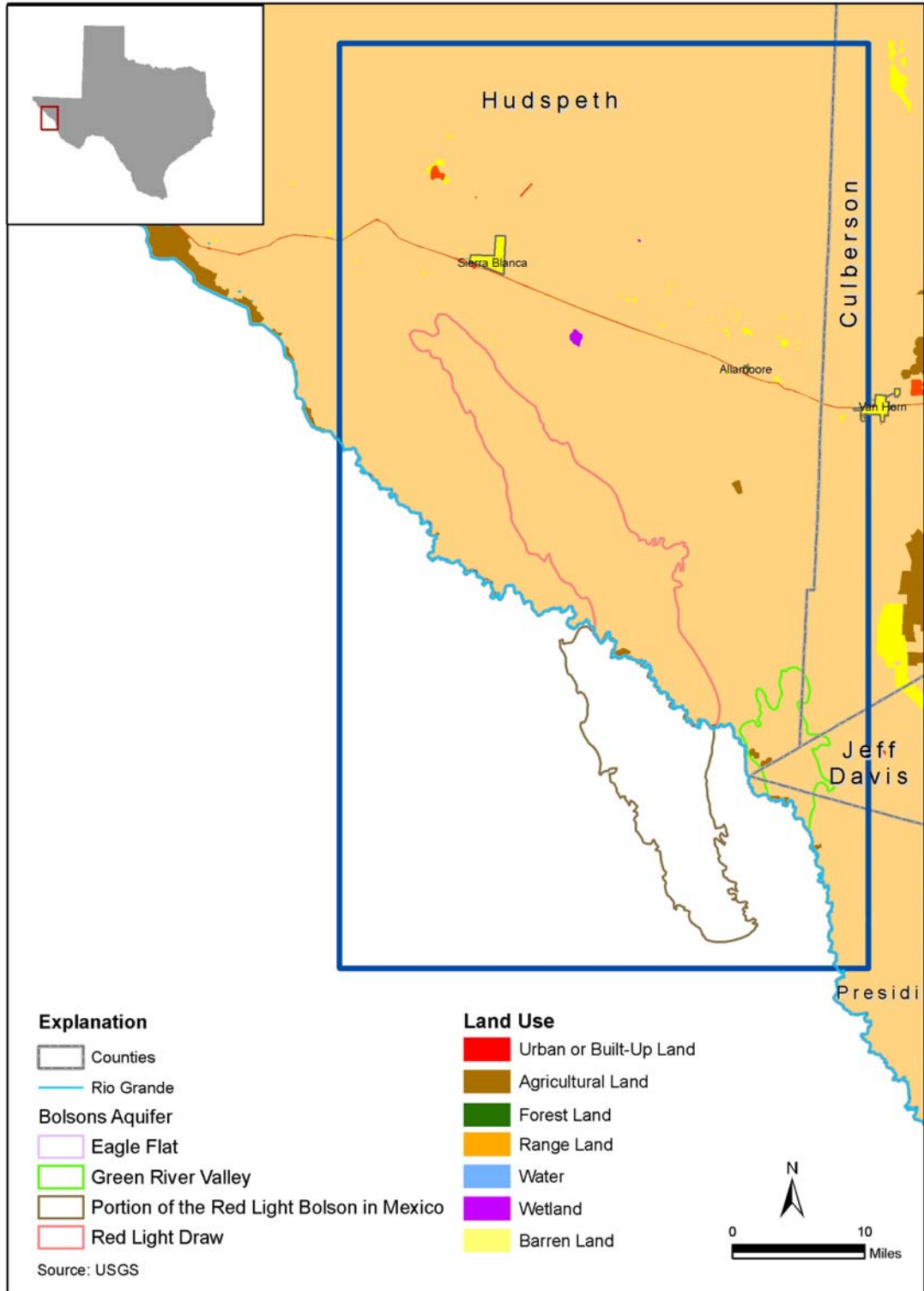


Figure 2.4.2 Land Use

2.5 Geology

The study area's geology, comprised of Precambrian, Permian, Cretaceous, and Cenozoic deposits, is simplified in Figure 2.5.1. Because this figure is a generalized representation of the geology in this area, a further detailed geologic map and unit descriptions are included in Appendix A. In general, the geology consists of basin-fill deposits of three Cenozoic intermontane basins (Red Light Draw, Green River Valley, and Eagle Flat) and bedrock of the adjacent mountain ranges and the southern part of the Diablo Plateau. The basins resulted from episodic normal faulting that probably occurred in the last 24 million years (Henry and Price, 1985, 1986) and subsequent basin-fill sedimentation. Bedrock of the mountain ranges and plateau record the long geologic history and major tectonic events that have occurred in the West Texas region since Precambrian time (Henry and Price, 1985; Muehlberger and Dickerson, 1989; Raney and Collins, 1993; Collins and Raney, 1994, 1997). Although the geology and geohydrology of the intermontane basins are primary interests for this study, the geology of the bedrock areas between and beneath Red Light Draw, Eagle Flat, and Green River Valley basins and knowledge of the tectonic history of the area also help define the area's geologic framework.

Precambrian rocks, the oldest rocks of the region, crop out in the northeastern and eastern parts of the study area (Figure 2.5.1) at the southeast Diablo Plateau and adjacent hills (Eagle Flat Mountain, Steerwitz, and Millican Hills), Carrizo Mountains, northeast flank of the Eagle Mountains, and the Van Horn Mountains (King and Flawn, 1953; Twiss, 1959, 1979; Underwood, 1963; King, 1965; Dietrich and others, 1983). Precambrian rocks throughout the region reveal a variety of geologic processes and events, including sedimentation, magmatism, metamorphism, and deformation, which occurred across the region before deposition of overlying Paleozoic strata. Although Precambrian rocks crop out in the mountain ranges and on the Diablo Plateau, they lie at depths in excess of 13,120 feet southwest of Ciudad Juarez in Chihuahua, Mexico (located west of the study area). Muehlberger (1980) related the deep burial of

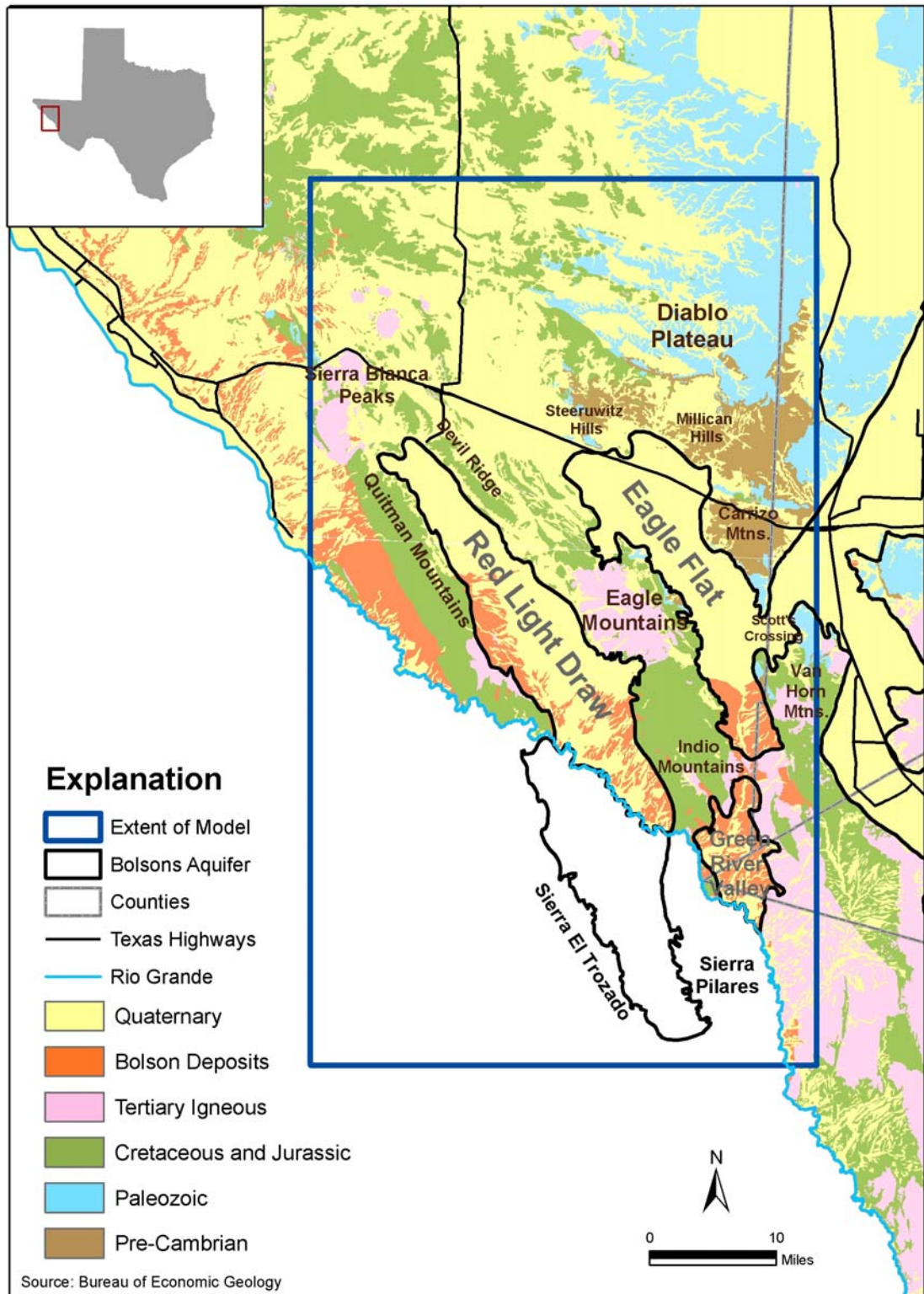








Figure 2.5.1 Surface Geology

Rock Unit Symbol Explanation	
	Quaternary Quaternary Alluvium Colluvium and Fans Windblown Sand
	Bolson Deposits
	Tertiary Igneous Bracks Rhyolite Buckshot Ignimbrite Chambers Tuff Colmena Tuff Garren Group Hogeye Tuff Intrusive Igneous Rocks Lower Rhyolite, Garren Group Pantera Trachyte Tarantula Gravel Trachyte porphery, Garren Group Upper Rhyolite, Garren Group Extrusive Igneous Rocks Vieja Group
	Cretaceous Cretaceous Rocks Benevides Formation Eagle Mountain Sandstone Bluff Mesa Formation Buda Limestone Campagrande Formation Comanchean rocks
	Cox Sandstone Etholean Conglomerate Espy Limestone, Benevides Formation, Finlay Limestone Eagle Mountain Sandstone Espy Limestone Finlay Limestone Loma Plata Limestone Ojinaga Formation San Carlos Sandstone Torcer Formation Yucca Formation
	Jurassic Malone Formation
	Paleozoic
	Permian - Briggs Formation - Bone Spring Limestone - Hueco Limestone - Victorio Peak Limestone Magdalena Formation
	Ordovician - El Paso Formation - Montoya Dolomite Bliss Sandstone
	Pre-Cambrian Allamore Formation Carrizo Mountain Meta-igneous rocks Carrizo Mountain Metasedimentary Rocks Lanoria Quartzite and Hazel Formation Van Horn Sandstone

* See Appendix E for complete Geologic map and definitions

Figure 2.5.1 Surface Geology (continued)

Precambrian rocks in Chihuahua to Precambrian rifting at about 1.45 billion years. He suggested this rifting developed a northwest-striking tectonic grain, referred to as the Texas Lineament Zone (Muehlberger, 1980; Muehlberger and Dickerson, 1989) that has influenced subsequent tectonic events. The northern part of the study area coincides with a portion of this northwest-trending regional tectonic zone.

Paleozoic limestones that overlie Precambrian rocks indicate marine sedimentation occurred across the area during the Paleozoic (Figure 2.5.1). Similar to the Precambrian rocks, Paleozoic limestones crop out in the northeastern and eastern parts of the study area (southeastern Diablo Plateau, Streeruwitz Hills, northeast flank of the Eagle Mountains, southern Carrizo Mountains and northern Van Horn Mountains). During the early and middle Paleozoic, the region was within a passive-margin setting (Horak, 1985). In the late Paleozoic the setting became more tectonically active. The Ouachita-Marathon orogenic event produced a belt of strongly deformed Paleozoic strata across the southeast edge of the west Texas region (southeast of the study area), and structural highs were uplifted in the foreland of the Ouachita-Marathon belt. Northwest-trending structures that were active during the late Paleozoic have been related to the Texas Lineament Zone (Muehlberger, 1980; Muehlberger and Dickerson, 1989).

Mesozoic-Era (includes Jurassic and Cretaceous formations) rocks exposed at the surface in the study area are dominantly marine Cretaceous limestones, sandstones, and shale (Figure 2.5.1) (Twiss, 1959, 1979; Underwood, 1963; Albritton and Smith, 1965; King, 1965; Dietrich and others, 1983; Jones and Reaser, 1970). Possible Jurassic evaporate deposits are exposed at the surface near the study area in the Malone Mountains (Albritton and Smith, 1965). These strata may also underlie Cretaceous strata in the western part of the study area. These Mesozoic rocks were deposited in the Chihuahua Trough, a deep northwest-trending sedimentary basin which developed during the Mesozoic in westernmost Texas and Chihuahua, Mexico (DeFord and Haenggi, 1971; Henry and Price, 1985). During the transition from the Mesozoic to the Cenozoic, the Laramide orogenic event caused a belt of compressional structures, including thrust faults, folds, and monoclines, to develop along the northeast margin of the Chihuahua Trough (Gries and Haenggi, 1971; Gries, 1980; Henry and Price, 1985). Major folding in

west Texas began no earlier than the Late Cretaceous, possibly about 80 million years ago (Wilson, 1970). Laramide thrust faulting and folding appear to have ceased by about 50 million years ago (Price and Henry, 1985) and Laramide compressive stress appears to have waned by about 30 million years ago (Price and Henry, 1984; Henry and Price, 1989). In the study area, southwest dipping thrust faults that cut Cretaceous rocks are common structural elements in the mountains bounding Red Light Draw (Quitman Mountains, Devil Ridge, and Eagle Mountains).

Cenozoic (also referred to as Tertiary) volcanic activity throughout the West Texas region occurred between 48 and 17 million years ago, with most of the activity occurring between 38 and 28 million years ago (Henry and Price, 1984, 1985; Price and Henry, 1984; Henry and McDowell, 1986; Henry and others, 1986). Extrusive and intrusive volcanic rocks of the study area consist of a wide variety of rock types, including tuff, rhyolite, trachyte, monzonite, granite, syenite, and basalt (Twiss, 1979; Dietrich and others, 1983). The volcanic rocks of the northern Quitman Mountains and central Eagle Mountains may be related to calderas (Price and others, 1986). Intrusive rocks within the study area occur as stocks, laccoliths, sills, and dikes. The areal extent of these features is relatively minor within the study area.

The regional stress regime across West Texas became extensional about 30 million years ago. By 24 million years ago normal faulting related to Basin and Range extension was well established (Henry and Price, 1985, 1986; Stevens and Stevens, 1985). This late Cenozoic normal faulting developed the basins and mountain ranges of the region, including the study area basins. Basin and Range faulting and related sedimentation in West Texas and southern New Mexico have been episodic, although the precise times of accelerated faulting and basin sedimentation for Red Light Draw, Green River Valley, and Eagle Flat basins are unknown (Seager and others, 1984; Henry and Price, 1985; Stevens and Stevens, 1985; Mack and Seager, 1990; Collins and Raney, 1997). In general, large amounts of sediment were shed from fault-bounded mountains into adjacent basins, partly filling them and constructing broad alluvial slopes, alluvial fans, and bajadas that now surround the mountain ranges. Even though many of the intermontane basins of West Texas do not currently exhibit internal drainage, the term

bolson is often used to describe the basins because they contain deposits that were deposited when the basins were internally drained. The history of the Rio Grande within the study area has not been studied in detail, although on the basis of studies upstream in the Hueco Bolson area located west of the Quitman Mountains, an ancestral river system breached a lacustrine bolson setting about 2.2 million years ago and the river was through going (Strain, 1966, 1971; Mack and others, 1998). Basin-fill deposition continued into the early Pleistocene. Since the early Pleistocene, periods of downcutting and backfilling deposition have occurred.

Cenozoic basin-fill within west Texas intermontane basins typically represents deposition in different settings, including alluvial fan, lacustrine, fluvial, and eolian deposits. Some basins also contain volcaniclastic deposits. Red Light Draw, also sometimes called Red Light Bolson, is about 56 miles long and 4 to 6 miles wide. It extends from Texas across the Rio Grande into Mexico. Red Light Draw is flanked on the west by the Quitman Mountains and on the east by Devil Ridge, Eagle and Indio Mountains, and Sierra de Pilares. Faults that moved during the Quaternary bound its eastern flank (Collins and Raney, 1997). Basin-fill of Red Light Draw is more than 2,000 feet thick in the southeast part of the basin (Gates and others, 1980; Collins and Raney, 1997). Akersten (1967) studied the upper 250 feet of basin-fill and proposed two formations: (1) a lower Pliocene Bramblett Formation composed of playa clay and silt, with associated sand and gravel facies, and (2) an overlying Pliocene-Quaternary Love Formation composed of alluvial fan and fluvial sand, gravel, and clay. Bedrock beneath Red Light Draw basin-fill and bedrock exposed at the surface in the adjacent mountains are mostly Cretaceous limestone, lesser sandstone and conglomerate, and minor shale of several formations, the Yucca, Bluff, Campagrande, Cox, Finley, and Benevides. These deposits dip southwestward and are cut by southwest-dipping thrust faults that have thickened this Cretaceous Section. Subsurface data are sparse for the area, but the Border Exploration-State "11" exploration test hole, located at the northeast margin of Red Light Draw near Devil Ridge (PSL, Section 11, Block 68½), is reported by Osburg and others (1985) to have penetrated well over 9,800 feet of Cretaceous deposits, including a large thrust fault. The distinct Cox sandstone was penetrated above and below the thrust fault. This test well also reportedly penetrated Precambrian rocks at a depth of about 14,300

feet. Another exploration test well, the Texaco-Emmet Unit No. 1 drilled at the southwest margin Red Light Draw near the Rio Grande (TMRR, Section 7, Block 3), is reported by Osburg and others (1985) to have penetrated more than 12,500 feet of Cretaceous deposits that compose the Yucca, Bluff, Cox, Finley, and Benevides Formations. This well also encountered Jurassic deposits beneath the Cretaceous rocks (Osburg and others, 1985).

Eagle Flat contains two structural basins. The relatively shallow northwest Eagle Flat Basin is mostly filled with less than 500 feet of Cenozoic gravel, sand, silt and clay (Gates and others, 1980; Jackson and Whitelaw, 1992; Jackson and others, 1993; Langford, 1993). Jackson and others (1993) reported these basin-fill sediments were deposited in fluvial, eolian, alluvial-fan, and local lacustrine or playa settings. Southeast Eagle Flat basin is about 26 miles long and 3 to 9 miles wide. Basin-fill deposits are as thick as 1,970 feet but most of the sediment section is buried and has not been described (Gates and others, 1980). Bedrock in the mountain and plateau areas east of the Eagle Flat structural basins contains Precambrian, Permian, and Cretaceous rocks. In general, depths to Precambrian rocks increase southwestward, although locally Precambrian rocks are exposed in the Eagle Mountains at the southwest margin of Eagle Flat. Permian and Cretaceous rocks dip gently toward the southwest. Precambrian strata include (a) meta-sedimentary and meta-igneous rocks of the Carrizo Mountain Group, (b) Allamoore Formation cherty limestone, limestone-pebble conglomerate, phyllite, and extrusive and intrusive igneous rock, and (c) Hazel Formation sandstone and conglomerate. Permian Hueco Limestone composed of limestone with minor conglomerate and sandstone overlies Precambrian rocks. Thickness of these Permian deposits in the Eagle Flat area probably range between 200 and 1,000 feet (Underwood, 1963; Dietrich and others, 1983). Cretaceous rocks beneath the northeastern margins of Eagle Flat, south of the Diablo Plateau, consist of less than 200 feet of sandstone, conglomerate, and limestone of the Cox, Bluff, and Campgrande Formations. Toward the southwest, the Cretaceous Section thickens to well over 6,500 feet in the Eagle Mountains area where Cretaceous limestone, sandstone, and shale compose the Yucca, Bluff, Cox, Finlay, Benevides, Espy, Eagle Mountains, Buda, and Chispa Summit Formations (Underwood, 1963).

Green River Valley basin lies south of Eagle Flat. It extends into Chihuahua, Mexico and is crossed by the Rio Grande. The deepest part of the Green River Valley Basin contains about 2000 feet of basin-fill but most of the section is not exposed and has not been described (Gates and others, 1980). Gravel, sand, and clay are exposed in surface outcrops and the Tertiary Tarantula gravel flanks the east margin of the basin (DeFord and Bridges, 1959). Bedrock at the mountain areas surrounding and probably beneath the Green River Valley Basin consists of Cretaceous limestone, sandstone, and conglomerate of the Yucca, Bluff, and Cox Formations. The southeast part of the basin is bound by Tertiary deposits of the Vieja Group (Twiss, 1979).

The stratigraphic chart in Table 2.1 is a listing of individual rock formations for each aquifer group and model Layer association which will be discussed in greater detail in Section 6. The youngest formations are Quaternary alluvial and bolson deposits. This Section includes maps of spatially distributed geologic information used in the modeling study, a map of the major structural and tectonic features in the area, and cross-sectional diagrams and their locations within the study area for reference to the vertical geologic structure of the model area.

The framework for the study area's hydrostratigraphy, discussed in detail in Section 4, is illustrated in a series of cross-sections shown in Figure 2.5.2. The cross-sections (Figures 2.5.3 through 2.5.8) compliment the surface geology map (Figure 2.5.1).

In general, northeast trending cross sections A-A', B-B', C-C', and D-D' (Figures 2.5.3 through 2.5.6) show a geologic section composed of four stratigraphic intervals: (1) alluvium and bolson-fill, (2) local Tertiary volcanic rocks, (3) Cretaceous and Paleozoic sedimentary rocks, and (4) Precambrian basement rocks. At the eastern part of the study area, Eagle Flat and Green River Valley are underlain by a relatively thin section of Paleozoic and Cretaceous rocks and structurally high Precambrian basement rocks. Red Light Draw, at the western part of the study area, is underlain by thick Cretaceous deposits. Cross sections E-E' and F-F' (Figures 2.5.7 and 2.5.8), along the axes of the basins as shown in Figure 2.5.2, illustrate bolson-fill is thicker in the southern parts of Red Light Draw and Eagle Flat. Laramide thrust faults with associated folds and

Cenozoic normal faults cut the bedrock throughout the area (Figures 2.5.3 through 2.5.6, and 2.5.8). Some normal faults also displace the bolson-fill deposits.

Structural faulting in the model area is shown in Figure 2.5.9. In this area, there is little or no faulting within the bolson aquifer basins that has been identified to date. Most fault systems in this area contain normal faulting striking northwest to southeast with the down-thrown side to the southwest. Northwest of the Red Light Draw lies the Caballo Fault system composing the Quitman Mountains. There is also extensive faulting to the north of the Eagle Flat basin responsible for the Steerwitz and Millican Hills. South of the Eagle Mountains lies a several fault systems that make up the Indio Mountain range separating the three major aquifer basins of the West Texas Bolsons. Finally, east of the southern tip of the Eagle Flat basin and Green River Valley lies the Van Horn fault system. Faulting in this area plays a major part in recharge as will be discussed later in Section 4.4.

Table 2.1 Generalized stratigraphic units

SYSTEM	STRATIGRAPHIC UNITS
Quaternary	Young Quaternary deposits
	Windblown sand
	Old Quaternary deposits
	Bolson deposits
Tertiary	Volcanic rocks undivided
	Intrusive Igneous rocks
	Chambers Tuff
	Garren Group
	Tarantula Gravel
	Hogeye Tuff
	Trachyte Porphyry
	Upper Rhyolite
	Pantera Trachyte
Cretaceous	Cretaceous undivided
	Buda Limestone
	Eagle Mountain Sandstone
	Espy Limestone
	Benevides Formation
	Finlay Limestone
	Cox Sandstone
	Bluff Mesa Formation
	Yucca Formation
	Etholean Conglomerate
	Torcer Formation
Jurassic	Malone Formation
Permian	Hueco Limestone
Cretaceous-Paleozoic	
Precambrian	Carrizo Mountain Group
	Precambrian bedrock undivided

Stratigraphic nomenclature from Univ. of Texas, BEG:
Van Horn-El Paso and Marfa Geologic Atlas Sheets.

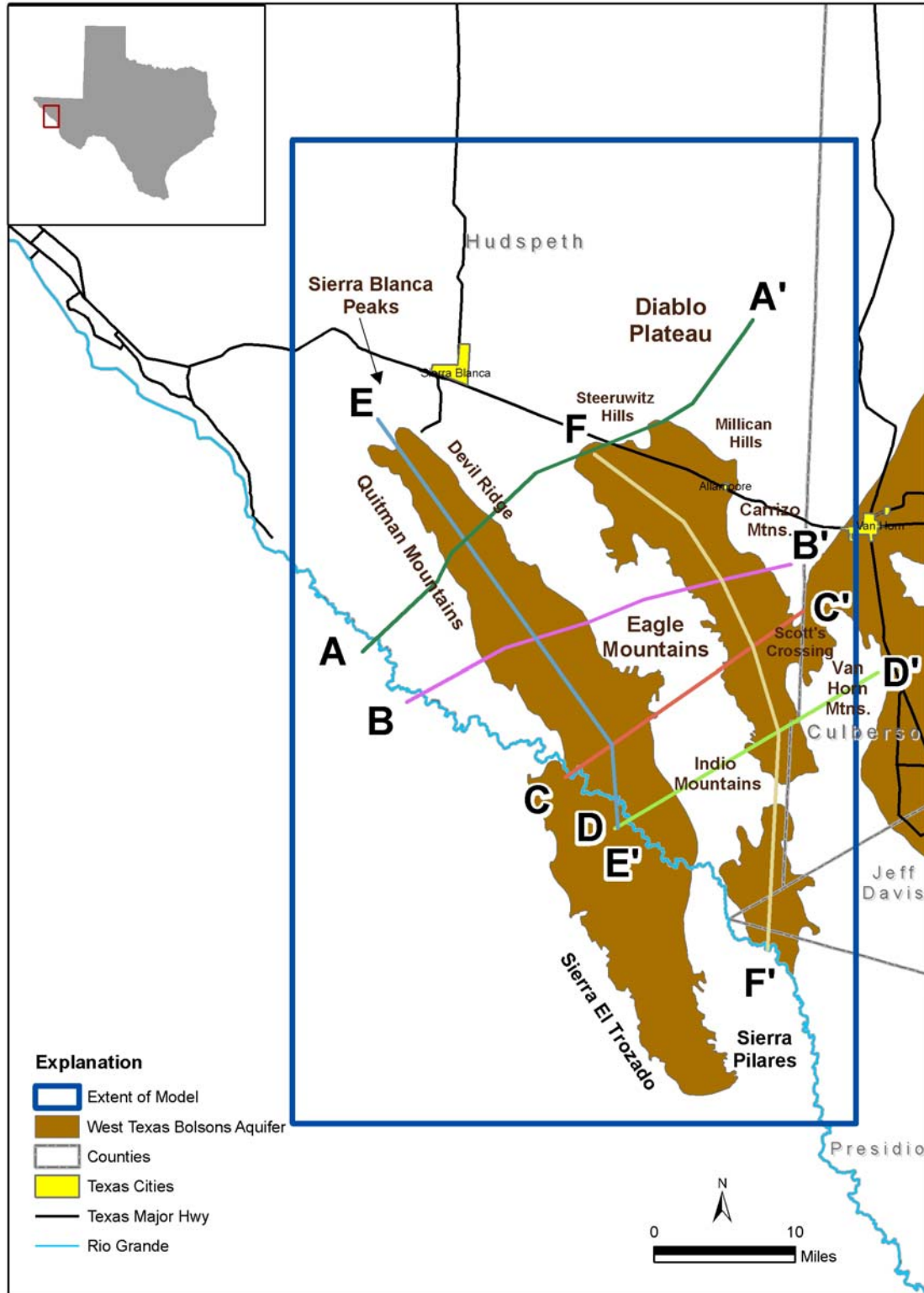


Figure 2.5.2 Location of Geologic Cross Sections

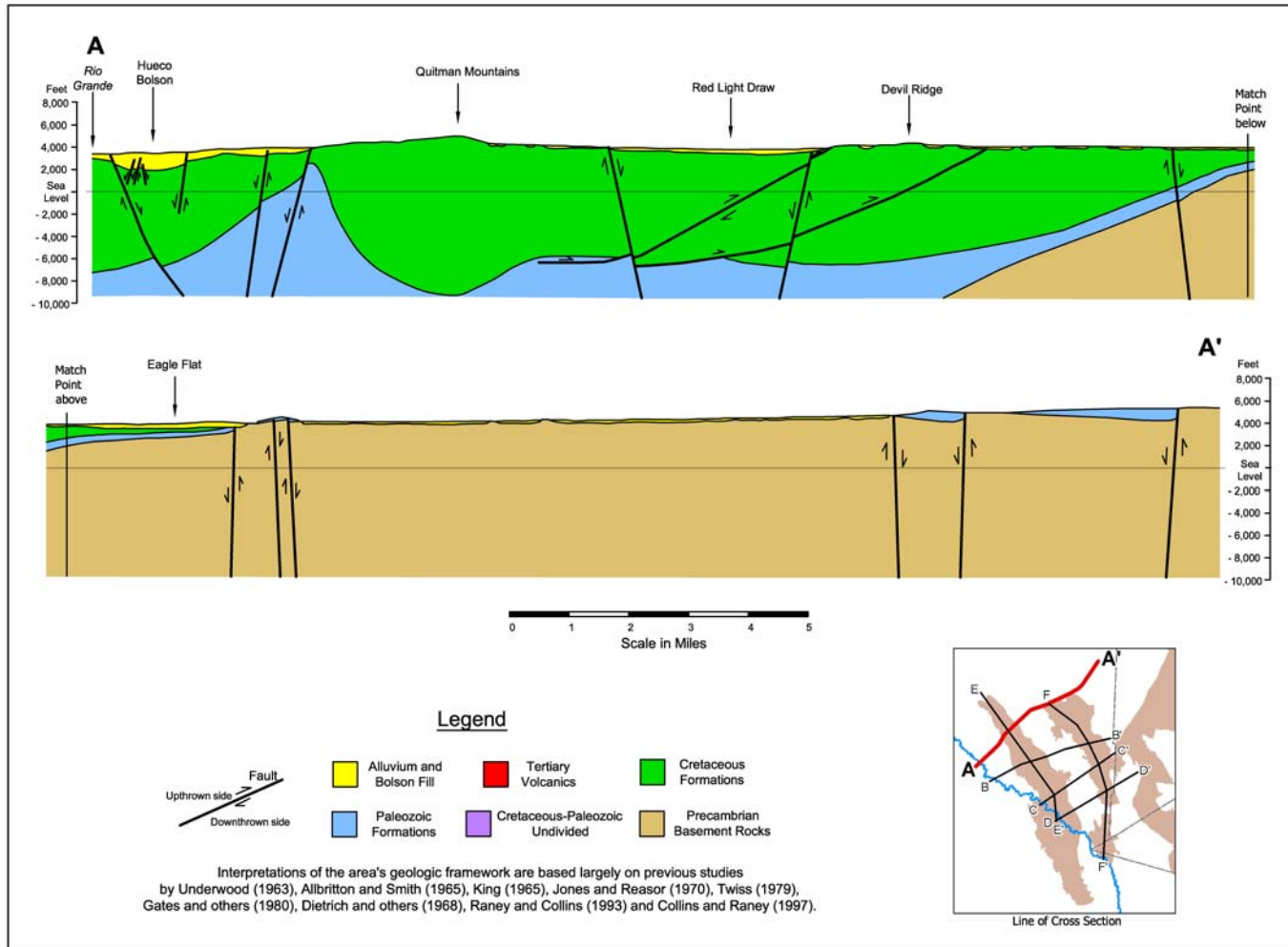


Figure 2.5.3 Geohydrologic Cross Section A-A'

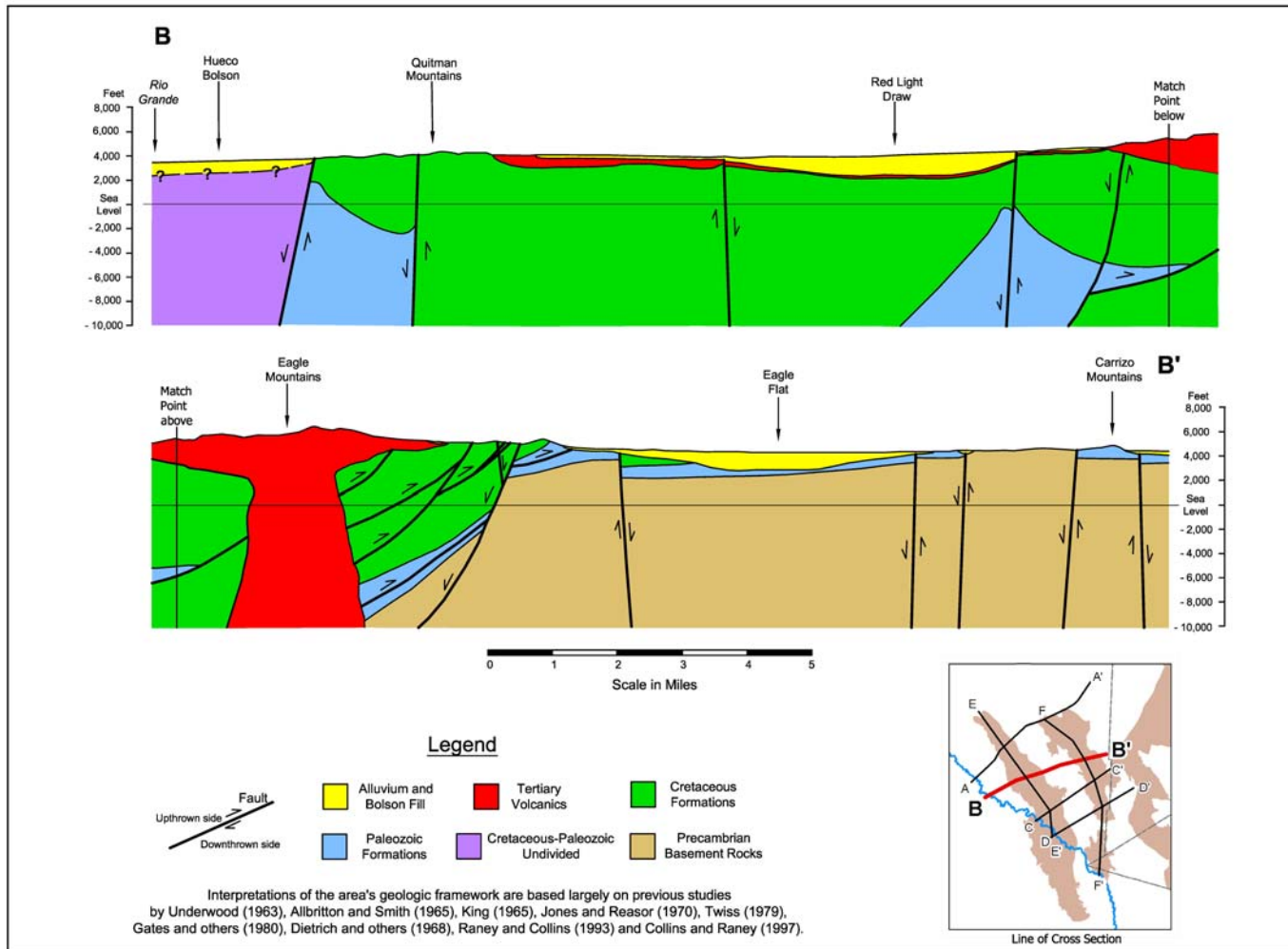


Figure 2.5.4 Geohydrologic Cross Section B-B'

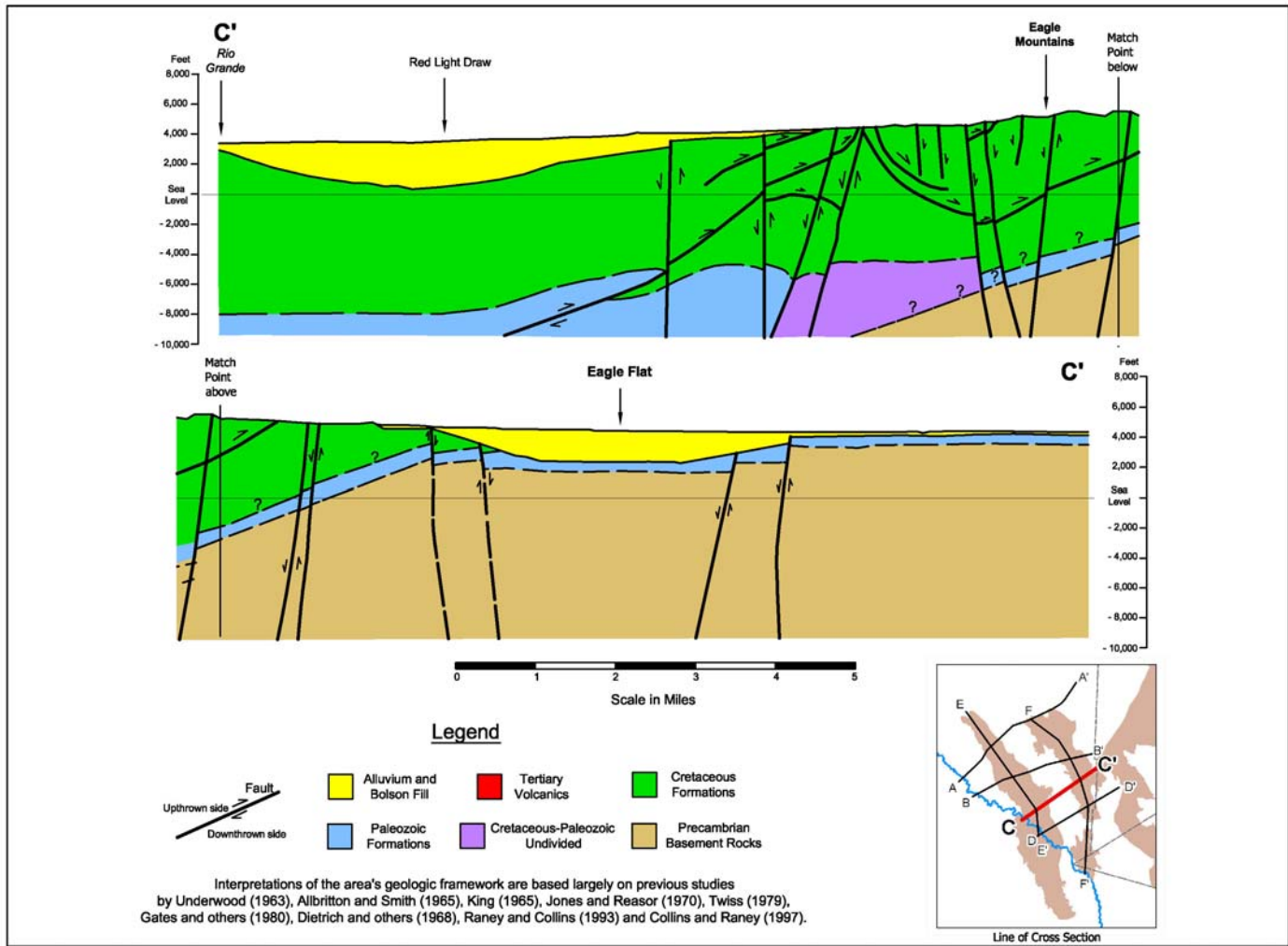


Figure 2.5.5 Geohydrologic Cross Section C-C'

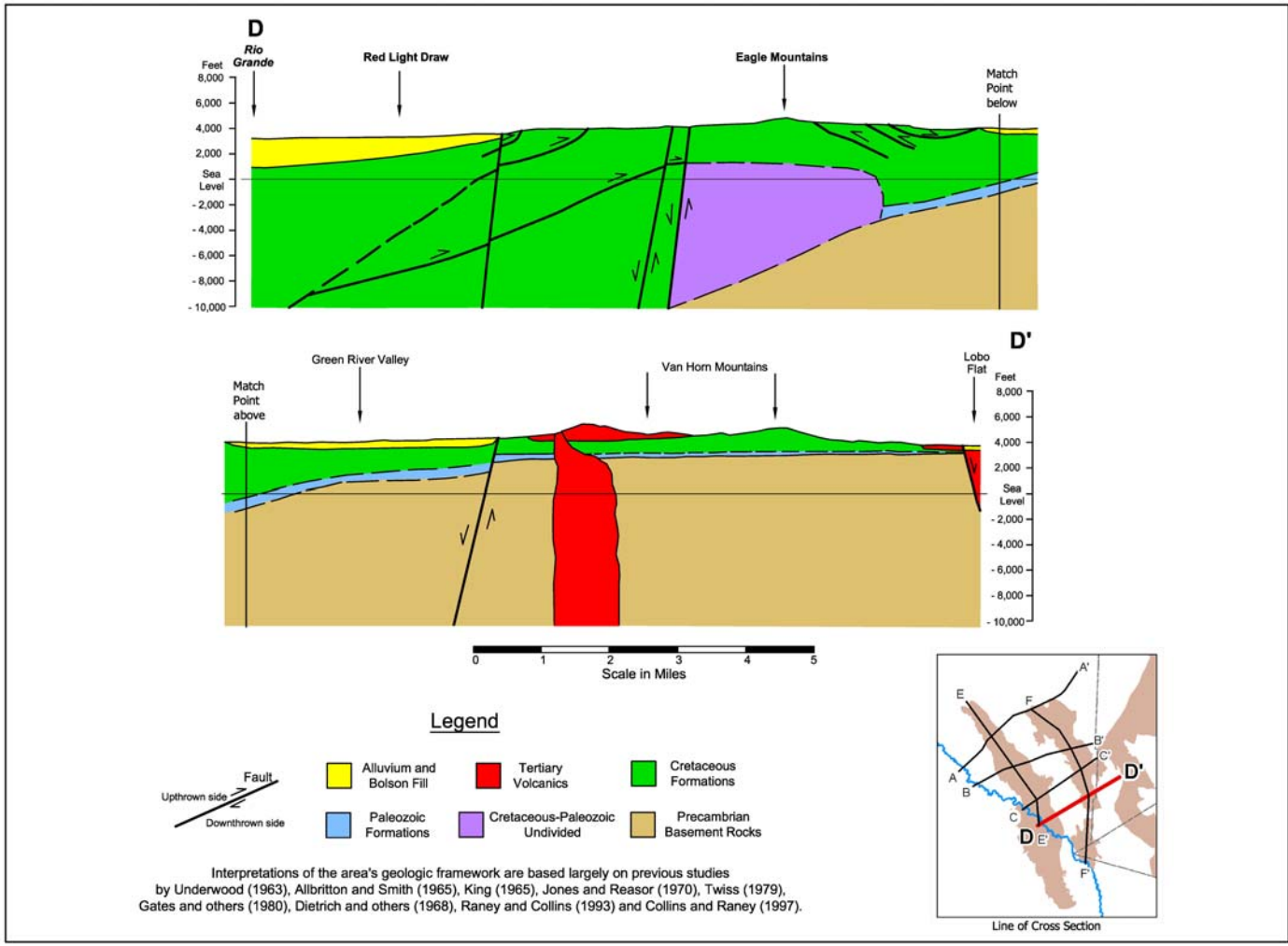


Figure 2.5.6 Geohydrologic Cross Section D-D'

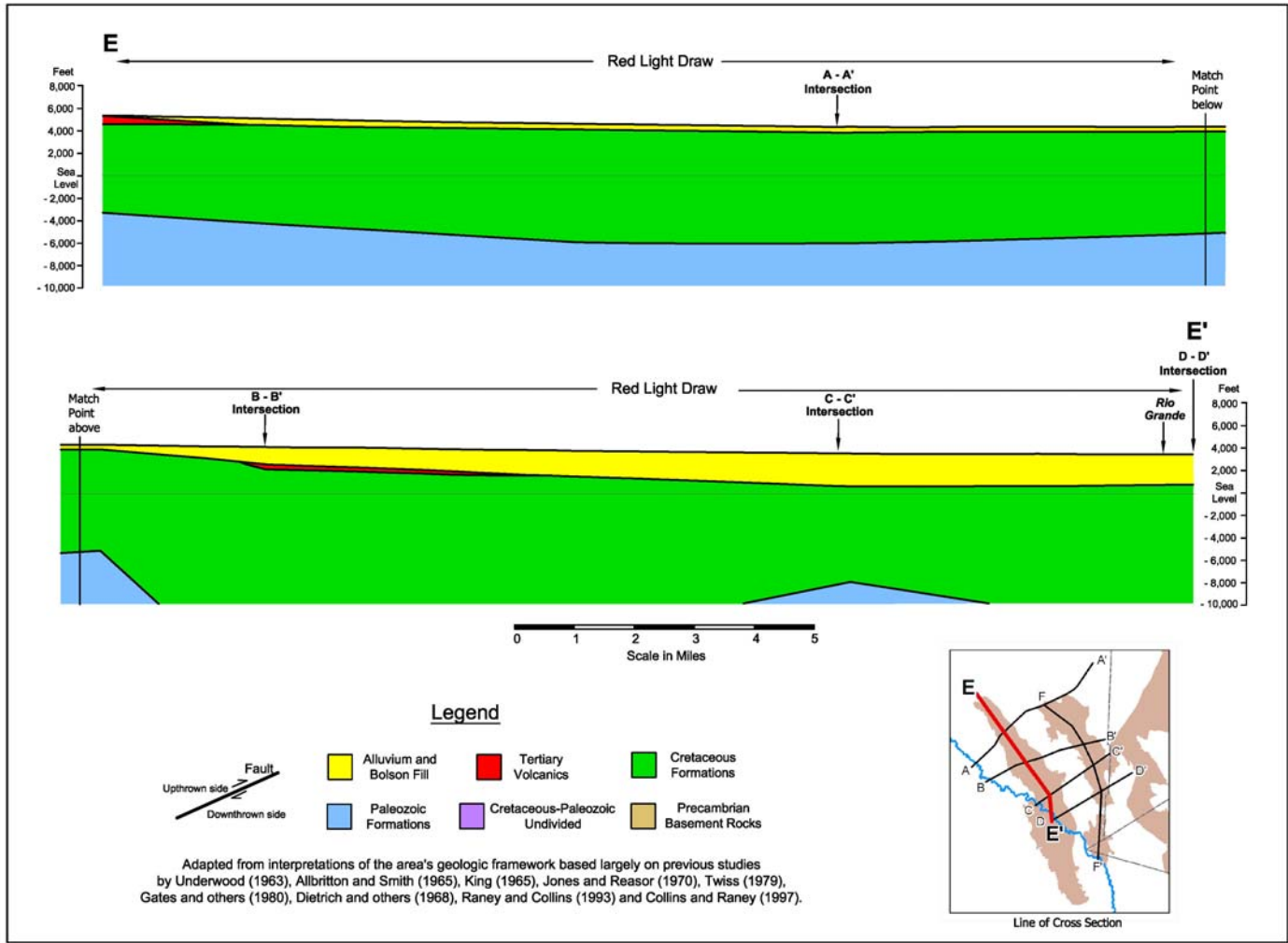


Figure 2.5.7 Geohydrologic Cross Section E-E'

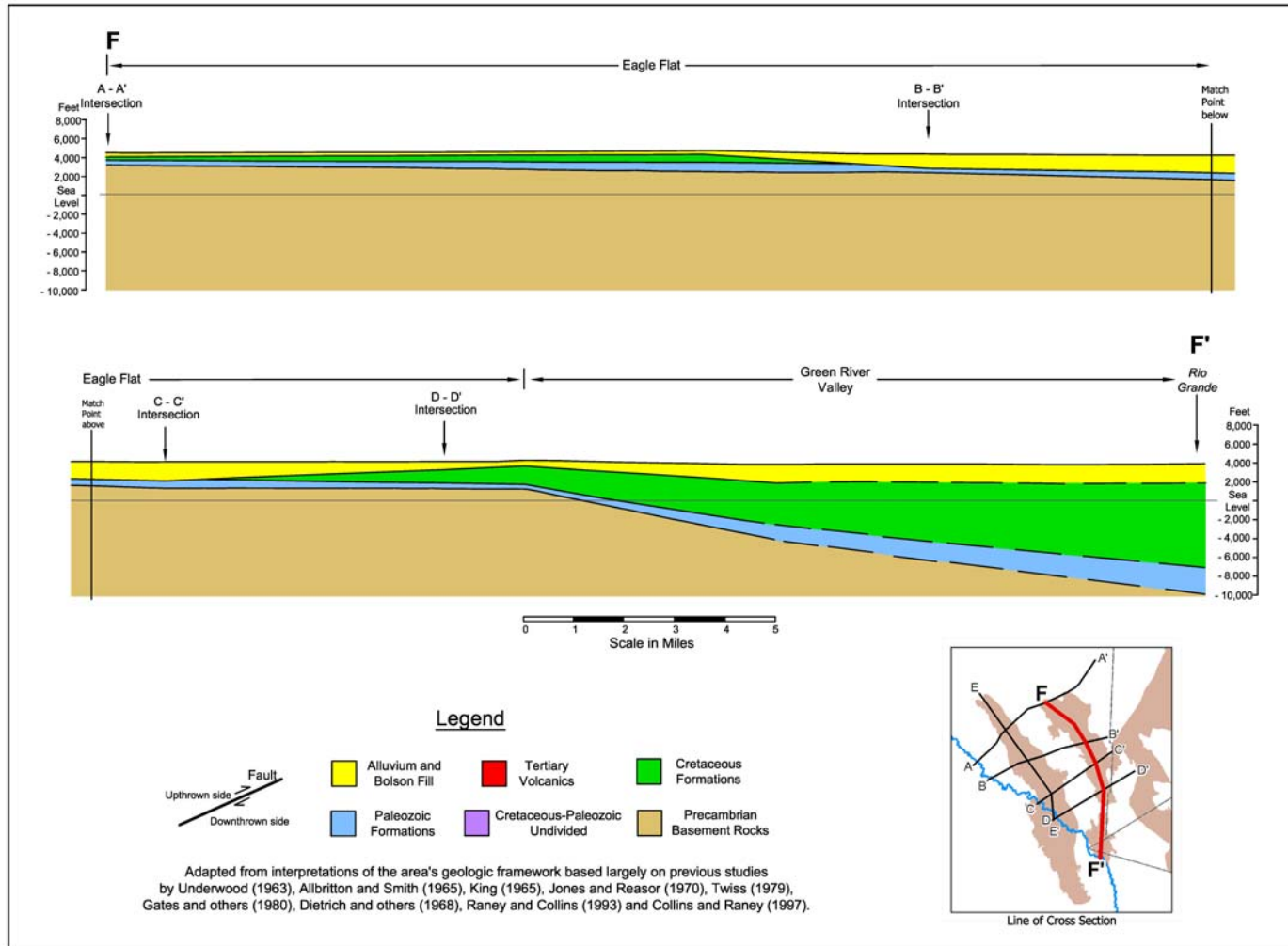


Figure 2.5.8 Geohydrologic Cross Section F- F'

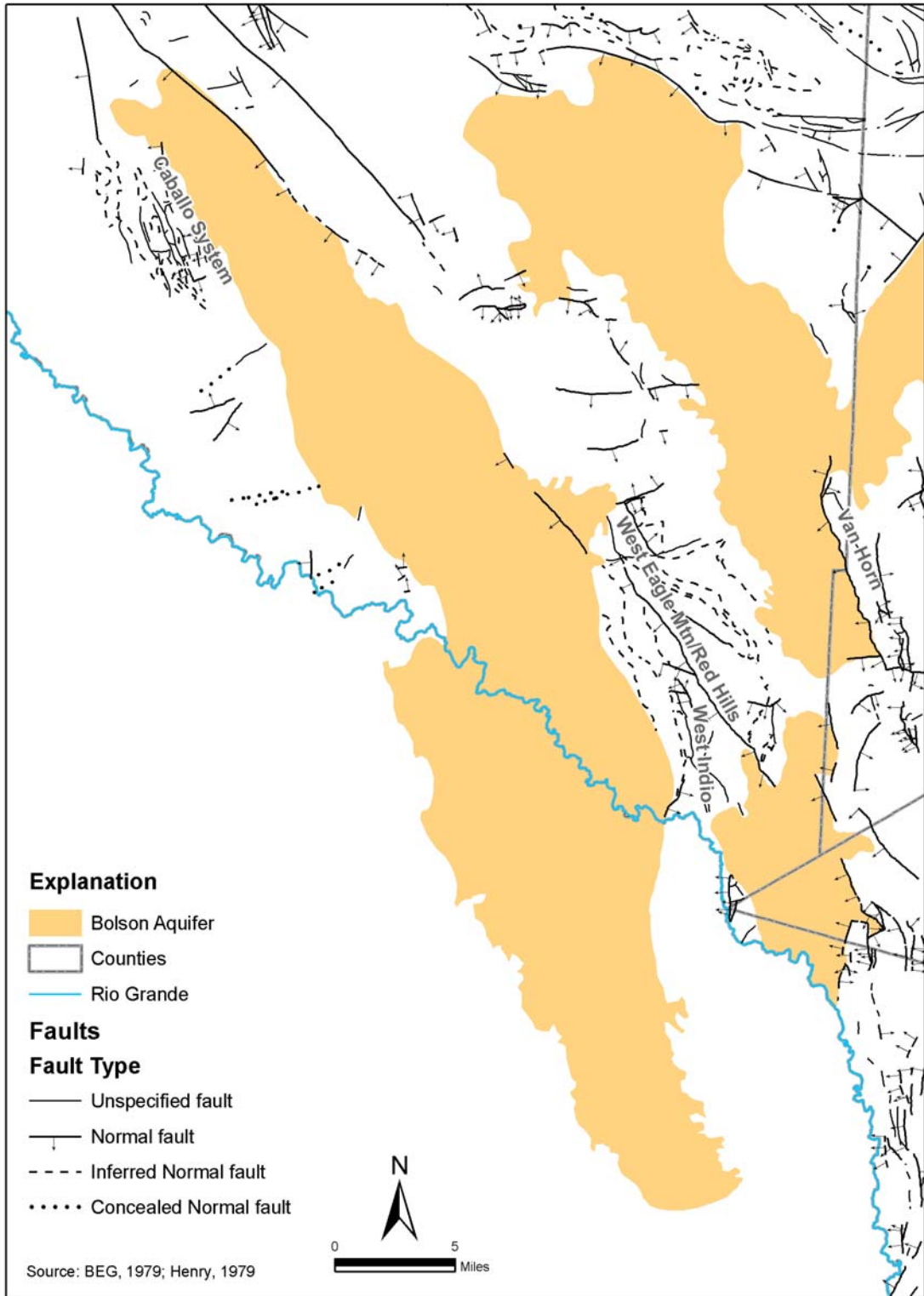


Figure 2.5.9 Structural Faulting

3.0 PREVIOUS WORK

3.1 Hydrogeologic Framework

The first comprehensive investigations of the hydrogeology of the study area were carried out by Gates and Smith (1975), Gates and White (1976), White and others (1980) and Gates and others (1980). Gates and Smith (1975) published a hydraulic head map for the Eagle Flat and Green River Valley basins showing groundwater movement from Southeast Eagle Flat beneath Scott's crossing into Wildhorse Flat. Gates and Smith (1975) and Gates and others (1980) speculated that groundwater in Northwest Eagle Flat might move out of the basin by discharge through Cretaceous rocks and other bedrock units toward the Rio Grande. Gates and White (1976) drilled test holes in Red Light Draw and in Southeast Eagle Flat, providing a suite of geophysical logs, vertical water quality samples, and geologic logs.

White and others (1980) developed a well inventory in the study area and collected water level data and water quality samples from many of the wells inventoried. Gates and others (1980) used these data and surface geophysical data (seismic reflection and earth resistivity) to develop water level contour maps, basin-fill thickness maps, and water quality maps. Reaser and others (1975) and Henry (1979) performed studies to determine the source of geothermal water in the Trans-Pecos region, including Red Light Draw and Eagle Flat.

Regional hydrogeologic investigations were performed in the 1980s and 1990s in Hudspeth County by the University of Texas Bureau of Economic Geology (BEG). Reconnaissance hydrogeologic studies covering parts of Northwest Eagle Flat and Red Light Draw were carried out by Kreitler and others (1987). They developed hydraulic head maps and water quality maps for much of Hudspeth County. Darling and others (1994) followed up the regional BEG studies with detailed investigations of the hydrogeology of Eagle Flat, Red Light Draw, and Green River Valley. They installed monitoring wells in Northwest Eagle Flat for aquifer test analysis and for groundwater sampling. Darling and others (1994) sampled these and many of the available livestock

and domestic wells in these basins for oxygen and deuterium isotopes, tritium, carbon-14, and halides.

Hibbs and others (1995) described groundwater movement out of the Northwest Eagle Flat basin by interbasin flow beneath local groundwater divides. Additional details on this conceptual model can be found in Darling and Hibbs (2001) and Hibbs and Darling (2005). The Bureau of Economic Geology initiated additional detailed investigations of the Eagle Flat aquifers in the mid to late 1990s. The proposed low-level radioactive waste site was denied a license and these studies were discontinued and never published.

More recently, hydrogeologic studies were carried out by LBG-Guyton Associates (1998) to evaluate potential impacts of biosolid disposal on water resources of Eagle Flat. This report included regional contour maps showing depth to groundwater. A regional report on the hydrogeology of Hudspeth County was recently published by the TWDB (George and others, 2005). George and others (2005) describe the hydrogeology of all of Hudspeth County and collates previous data collected in Eagle Flat, Red Light, and Green River Valley.

3.2 Groundwater Models

Darling, Hibbs and Dutton (1994) developed a cross-sectional MODFLOW model for Red Light Draw and used the model to estimate mountain and mountain front recharge rates and to assess regional flow patterns in Red Light Draw. The location of the 2-dimensional cross-sectional model is shown on Figure 3.2.1. The model was steady-state and was oriented northwest-southeast between the Diablo Plateau and the Rio Grande. Model-estimated residence times (as defined by particle-tracking) were constrained by groundwater age dates estimated with radioisotopes analysis. The model was used to estimate flowlines and groundwater velocity along the cross-section. This cross-sectional model was not intended to estimate groundwater availability and is not sufficient for groundwater availability assessments and impact analysis of various management strategies and plans.

Beach and others (2004) document a groundwater availability model that was developed for the four easternmost bolsons (Wild Horse Flat, Michigan Flat, Ryan Flat and Lobo Flat) of the TWDB designated West Texas Bolsons. This model also included the Igneous aquifer in the Davis Mountains region. The model was successfully calibrated to steady-state conditions and transient conditions between 1950 and 2000. The model simulated water level responses in the Bolson aquifer relatively well. The western extent of the easternmost bolson model is roughly the same as the eastern boundary of the model developed in this study. In addition, the current study bears a lot similarity with the easternmost bolson model in terms of aquifer property estimates, recharge estimates, and other hydrologic parameters.

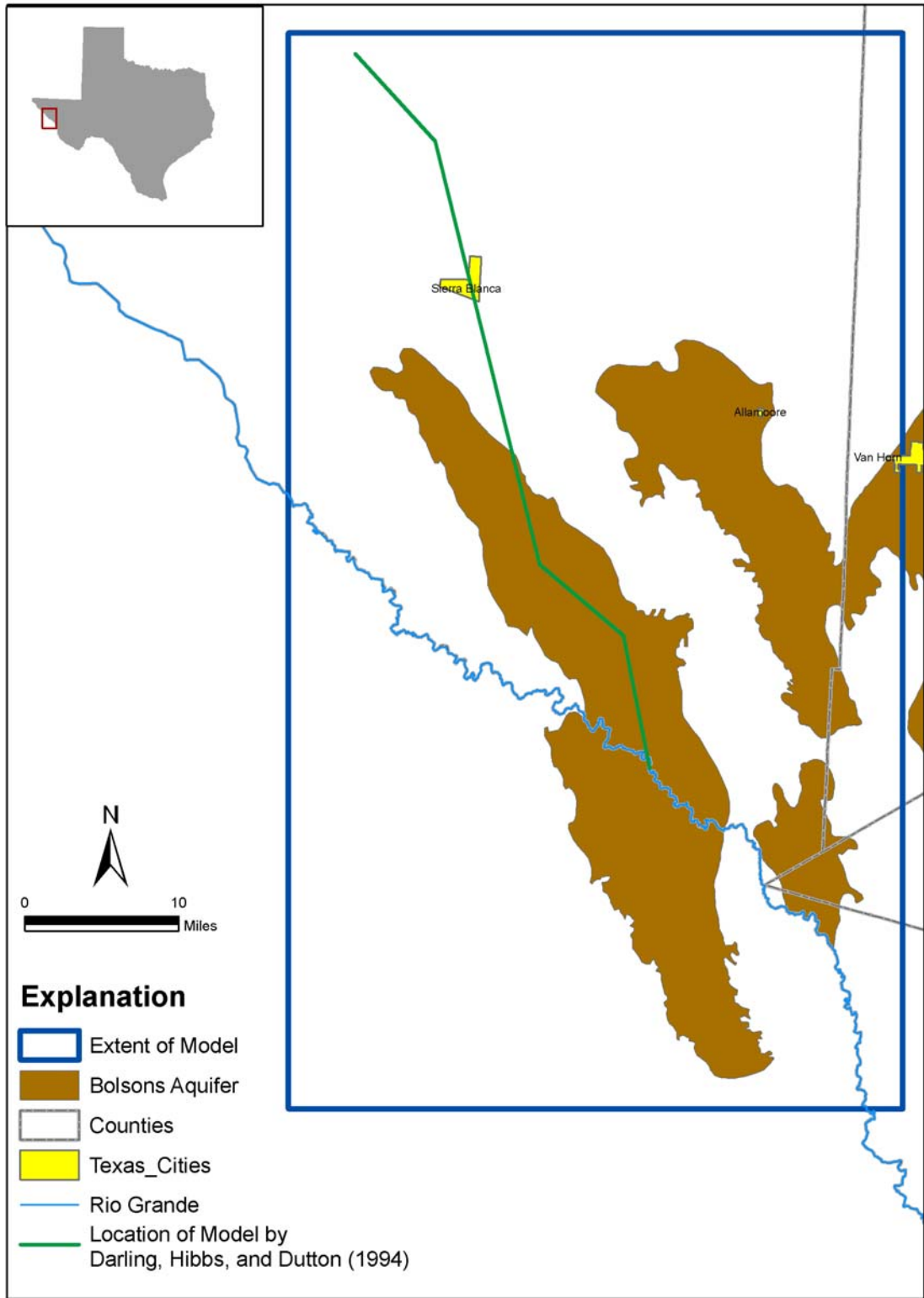


Figure 3.2.1 Location of previous modeling studies

4.0 HYDROLOGIC SETTING

Groundwater of variable quantity and quality occurs in the West Texas Bolsons. This Section details the major hydrogeologic components of this area and their significance to the GAM. Included is discussion of the hydrostratigraphy of the three major groundwater basins as well as the structure that defines them. The occurrence and flow of groundwater, recharge and discharge, and groundwater/surface water interaction are described in this Section.

4.1 Hydrostratigraphy

Discretization of hydrogeologic formations of this complex geologic system below alluvium and bolson deposits for the conceptual model was difficult because the elevation of the contacts between the conceptualized hydrogeologic units varies significantly over short distances. In addition, due to the faulting and complex geology, it is impossible to follow the Layering concepts used in the MODFLOW formulation without simplifying the hydrogeologic setting. Therefore, to facilitate the modeling process, the system was simplified for ease of presentation as hydrostratigraphic units and will be further discussed in Section 6.0 with the accompanying model Layer characteristics.

All alluvium and bolson deposits represent the West Texas Bolson aquifer. Cretaceous, Paleozoic, Tertiary, Permian and other units are jointly represented in the model area because of the previously mentioned hydrogeologic complexity and the uncertainty regarding precise elevations of geologic contacts and hydraulic properties of various hydrogeologic units. The top of the Precambrian basement rocks are assumed to form the lower no-flow boundary for the model except in the area northeast of Eagle Flat where the Precambrian rocks form part of the shallow aquifer near the ground surface. In that area, the joint representation of underlying, water-bearing units mentioned above incorporates the upper portion of the Precambrian basement rocks.

4.1.1 Red Light Draw

Hydrostratigraphic boundaries of the Red Light Draw include the Eagle Mountains and Devil Ridge to the north, the Quitman Mountains to the west, the Indio Mountains to the east, and the Sierra de Pilares and Sierra El Trozado to the south (Figures 2.5.1 through 2.5.8). A segment of Red Light Draw extends southward into Mexico. The Rio Grande establishes the boundary between the U.S. and Mexican portions of the basin.

Some minor water-bearing/contributing units surround the major basin area. Shallow water-bearing rocks in the Eagle Mountains consist mostly of Tertiary intrusive and extrusive rocks, and Cretaceous carbonate and clastic rocks. Permian carbonate rocks and Precambrian metamorphic rocks are exposed at the Eagle Mountains. Devil Ridge consists mostly of Cretaceous carbonate and clastic rocks. The northern Quitman Range consists of Tertiary volcanic rocks, and the southern Quitman Mountains consist mostly of Cretaceous carbonate and clastic rocks with minor Tertiary volcanics. The Indio Mountains consist of carbonate and clastic rocks of Cretaceous age. In Mexico, the Sierra de Pilares and Sierra El Trozado contain primarily Cretaceous carbonate rocks and some tertiary volcanic rocks.

Basin-fill material is Tertiary and Quaternary alluvium, with some mixed volcanoclastic rocks intercalated with the lower basin-fill. Basin-fill thickness increases to the south along the draw, from about 500 feet in the northwestern part of the basin to as much as 3,000 feet in the southeastern half of the basin (Gates and others, 1980). Relatively coarse-textured deposits are found at shallow depths in the upper and middle portions of the Red Light Draw basin. Along the Rio Grande the basin-fill is often fine-textured, commonly of the playa-lacustrine variety. The USGS drilled a test hole to a depth of 1,100 feet along the central portion of the basin, between the Quitman and Indio Mountains (Gates and White, 1976). Coarse textured alluvial fan material was penetrated throughout most of the depth of the test hole, until volcanic flow units were encountered at the bottom of the test hole.

In Red Light Draw, wells produce water from the Cretaceous bedrock units and basin-fill. Cretaceous rocks are the primary water-bearing units in the northern half of

the basin. Wells in the central and southern parts of Red Light Draw produce water from the thicker basin-fill material.

4.1.2 Northwest Eagle Flat

The Northwest Eagle Flat basin is surrounded by the Diablo Plateau and Steeruwitz Hills to the north, by Devil Ridge and the Eagle Mountains to the south, and by Southeast Eagle Flat to the east. A groundwater divide separates northwest Eagle Flat and Southeast Eagle Flat. The floor of Northwest Eagle Flat slopes toward Grayton Lake, a vadose playa that receives surface runoff within the basin (Hibbs and Darling, 2005). Water wells in the southern part of the Diablo Plateau derive water mostly from Cretaceous carbonate and clastic rocks. These Cretaceous rocks are underlain by Permian rocks that are highly prolific where they are exposed in the northern Diablo Plateau. Basin-fill thickness usually varies from about 200 to 500 feet in Northwest Eagle Flat (Gates and others, 1980); however, one test hole drilled by the BEG near Sierra Blanca penetrated 700 feet of basin-fill material (Darling and others, 1994). This is an anomalous basin-fill thickness, probably controlled by local faulting.

Basin-fill in Northwest Eagle Flat is mostly Tertiary and Quaternary alluvium. Basin-fill is usually not saturated in Northwest Eagle Flat because depth to groundwater is usually greater than 600 feet along the basin floor. The Cox Sandstone is an important water-bearing unit in northwest Eagle Flat, especially north of Interstate 10 (Albritton and Smith, 1965). Outcrop exposures of Cox Sandstone are generally fine-to-coarse grained, yellowish gray, quartzitic, and cross-laminated. The Cox Sandstone contains interbeds of silt, shale, and medium-gray limestone with shell fragments and chert pebbles (Underwood, 1963; Albritton and Smith, 1965). South of Interstate 10, two monitoring wells drilled by the BEG produce water from the Finlay Limestone (Darling and others, 1994). Exposures of the Finlay in the Sierra Blanca area range from massive beds of gray, fossiliferous limestone to thin bedded, finely crystalline and nodular limestone bedded with thin layers of shale, siltstone, and fine-grained quartz sandstone (Underwood, 1963; Albritton and Smith, 1965). Further south of Interstate 10, a well drilled on the northeast side of Devil Ridge produces water from either the Bluff Mesa

Formation or the Yucca Formation. Fractures in bedrock units in Northwest Eagle Flat in many cases account for much of the aquifer's permeability (Hibbs and Darling, 2005).

4.1.3 Southeast Eagle Flat

The Southeast Eagle Flat basin is surrounded by the Millican Hills to the north, the Carrizo Mountains to the east, the Eagle Mountains and Green River Valley to the south, and by a groundwater divide separating Eagle Flat into its northwestern and southeastern segments (Figures 2.5.1, 2.5.2 through 2.5.5, and 2.5.7). The floor of Southeast Eagle Flat slopes toward Scott's Crossing where most surface drainage moves into the adjacent Wildhorse Flat area.

Shallow water-bearing rocks in the Millican Hills and Carrizo Mountains consist mostly of Precambrian metamorphic rocks. Precambrian rocks in the Allamoore area are also the principal water bearing strata, where aprons of alluvial pediment are too thin to contain much groundwater. From the northern part of the basin extending to just south of Allamoore, well depths range from 80 to 480 feet with water depths of 20 to 230 feet (Darling and others, 1994). South of Allamoore, extending across the basin-bounding faults, wells as deep as 1,000 feet produce water from basin-fill.

Along the axis of Southeast Eagle Flat, the basin-fill thickness increases from nearly 700 feet at the western groundwater divide to over 2,000 feet near Scott's Crossing (Gates and others, 1980). Basin-fill is mostly Tertiary and Quaternary alluvium, with some mixed volcanoclastic rocks and volcanic flows. Basin-fill is coarse grained near the Eagle Mountains, becoming more fine-textured toward the axis of Southeast Eagle Flat (Gates and others, 1980). Along the axis of the basin, the USGS Davis No. 1 test hole penetrated 2,012 feet of basin-fill, consisting mostly of brown clay with thin beds of sand and gravel (Gates and White, 1976). Bedrock was never penetrated at this test hole.

4.1.4 Green River Valley

Green River Valley is bound to the northwest by the Indio Mountains and to the east by the Van Horn Mountains, which are composed mostly of Cretaceous limestone

and sandstone, and some Tertiary volcanic and intrusive rocks (Figures 2.5.1 and 2.5.7). Tertiary intrusive rocks are exposed approximately 7 miles north of the Rio Grande, just northeast of the axis along Green River Valley. At one time the Tertiary intrusive rocks formed the drainage limits of Green River Valley, but the ephemeral river has extended northward through headward erosion up into Southeast Eagle Flat (Gates and others, 1980). Green River Valley now captures a small portion of the drainage of Southeast Eagle Flat. The Tertiary intrusives are only 2 miles south of the groundwater divide separating the Green River Valley aquifer from the Southeast Eagle Flat aquifer.

South of the intrusive rocks exposed along the Green River Valley axis, basin-fill increases from only a few feet thick to more than 2,000 feet thick near the Rio Grande (Gates and others, 1980). Basin-fill is coarse textured near the intrusive rocks along the Valley axis and along parts of the Indio and Van Horn Mountains, but is finer textured along the axis of the basin at distances from the Tertiary intrusive rocks and flanking alluvial fans. The sections of basin-fill near the volcanic intrusive rocks most likely include interbeds of volcanoclastic rocks, especially at depth. The basin-fill near the Rio Grande is primarily fine-grained material of the playa-lacustrine variety (Gates and others, 1980).

4.2 Structure

This Section describes the elevation of the top and bottom of each of the hydrostratigraphic units. Due to the lack of detailed structural information and data regarding the structural surfaces between each unit, the structure below the bolson deposits were lumped together. A discussion of how this structure was subdivided for modeling purposes (including Layer thickness maps) can be found in Section 6.2.

4.2.1 Data Sources

The land surface elevation in the model was estimated using the National Elevation Database (NED) data. The grid spacing for the NED data is 30 meters. The topography of the model area is shown in Figure 2.2.2. The land surface elevation will be used as the top of all the Layers in outcrop areas.

Section 2.5 discusses the development of the hydrogeologic cross-sections shown in Figures 2.5.2 through 2.5.8. In addition to the hydrogeologic cross-sections, structural contours were also developed based on the geophysical and well data available at the time. These hand-drawn structural contours were digitized during this study and used as a basis for determining the thickness of the bolsons and underlying units, therefore no control points are necessary for the figures. The thickness of the bolson aquifers was based on structure contours developed by Eddie Collins at the Bureau of Economic Geology in 1997 (personal communication with Eddie Collins).

4.2.2 Construction of the Structural Surfaces

To develop a raster dataset for the structural surfaces from the hand-drawn contour maps developed by Eddie Collins, the following steps were completed.

1. The image of each contour map was scanned.
2. Each image was georeferenced.
3. Contour lines were digitized.
4. Each contour line was assigned the appropriate elevation attribute.
5. Using the ESRI Spatial Analyst `topo_to_raster` algorithm, the contour lines were used to create a raster dataset with 500-foot grid spacing.
6. Raster data were used to reproduce contour lines for comparison to digitized contour lines.
7. If reproduced contour lines did not match the digitized contour lines, additional contour lines and/or point data coverages were developed to help constrain the algorithm and thus reproduce the digitized contour lines. Additional points and/or lines were added to the constraining shapefile until digitized contour lines were reasonably reproduced.

4.2.3 Discussion of Structure

Figure 4.2.1 shows the estimated thickness of the bolson aquifers in the study area. In Red Light Draw, basin-fill thickness increases to the south along the draw, from about 500 feet in the northwestern part of the basin to as much as 3,000 feet in the southeastern half of the basin. These estimates are consistent with those of Gates and others (1980).

The estimated thickness of Red Light draw in Mexico was extrapolated from the data available north of the Rio Grande. The purpose of extending the model into Mexico is to avoid incorporating a no-flow boundary condition at the Rio Grande. By extending the bolson model Layer into Mexico, the model can be used to appropriately simulate the impact of pumping near the Mexico border without an adverse impact from the boundary. Therefore, uncertainty in extrapolation of the bolson thickness south of the Rio Grande should have a minimal impact on groundwater availability estimates on the north side of the River.

The thickness of deposits in Eagle Flat ranges from less than 50 feet in the northern most extent of the TWDB mapped aquifer to over 2,000 feet in Southeast Eagle Flat between the Carrizo and Eagle Mountains. The minimum thickness indicated on the map is 50 feet because calculated values less than 50 feet were assigned a thickness of 50 feet inside the TWDB designated aquifer boundaries. The bolson deposit thickness in Green River Valley is the smallest of the three basins and ranges from about 50 to almost 1,500 feet. Figure 4.2.2 illustrates the base elevation of bolson deposits in the model area.

The importance of the deep systems underlying the bolson deposits is minimal to the groundwater availability from the Bolsons in the next 50 years. However, the steady-state simulation of the deeper regional flow systems is important to the overall model calibration effort. For this reason, the thickness and base elevation of the post Cambrian rocks, which is consistent with top elevation of the Cambrian basement rocks, and are shown in Figure 4.2.3.

Figure 4.2.3 indicates that the thickness of the underlying units increases very quickly from the northeast to the southwest due to the affect of the Rio Grande rift. In the southwest corner of the model area, a question mark indicates the uncertain nature of the estimates in that area. In fact, the reduced thickness of the underlying units is likely an artifact of the interpolation because we have no information in that area. The thickness of the underlying rocks varies from zero between the Carrizo mountains and the Diablo Plateau where Precambrian rocks outcrop to over 15,000 feet below the Rio

Grande. The contact between the underlying Precambrian basement and this complex regional flow system is shown in Figure 4.2.4 as the base elevation of these lumped units.

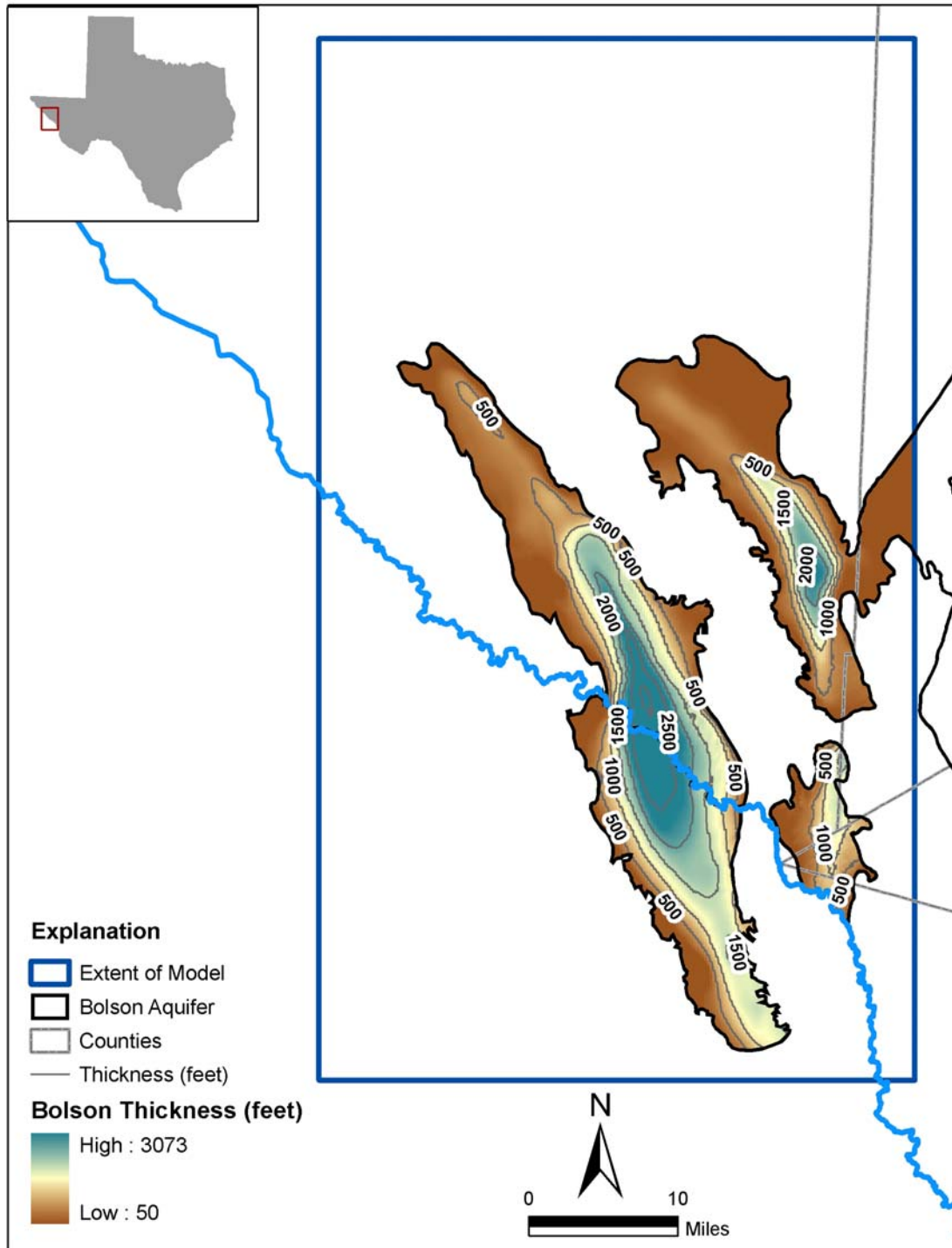


Figure 4.2.1 Thickness of West Texas Bolson Aquifer

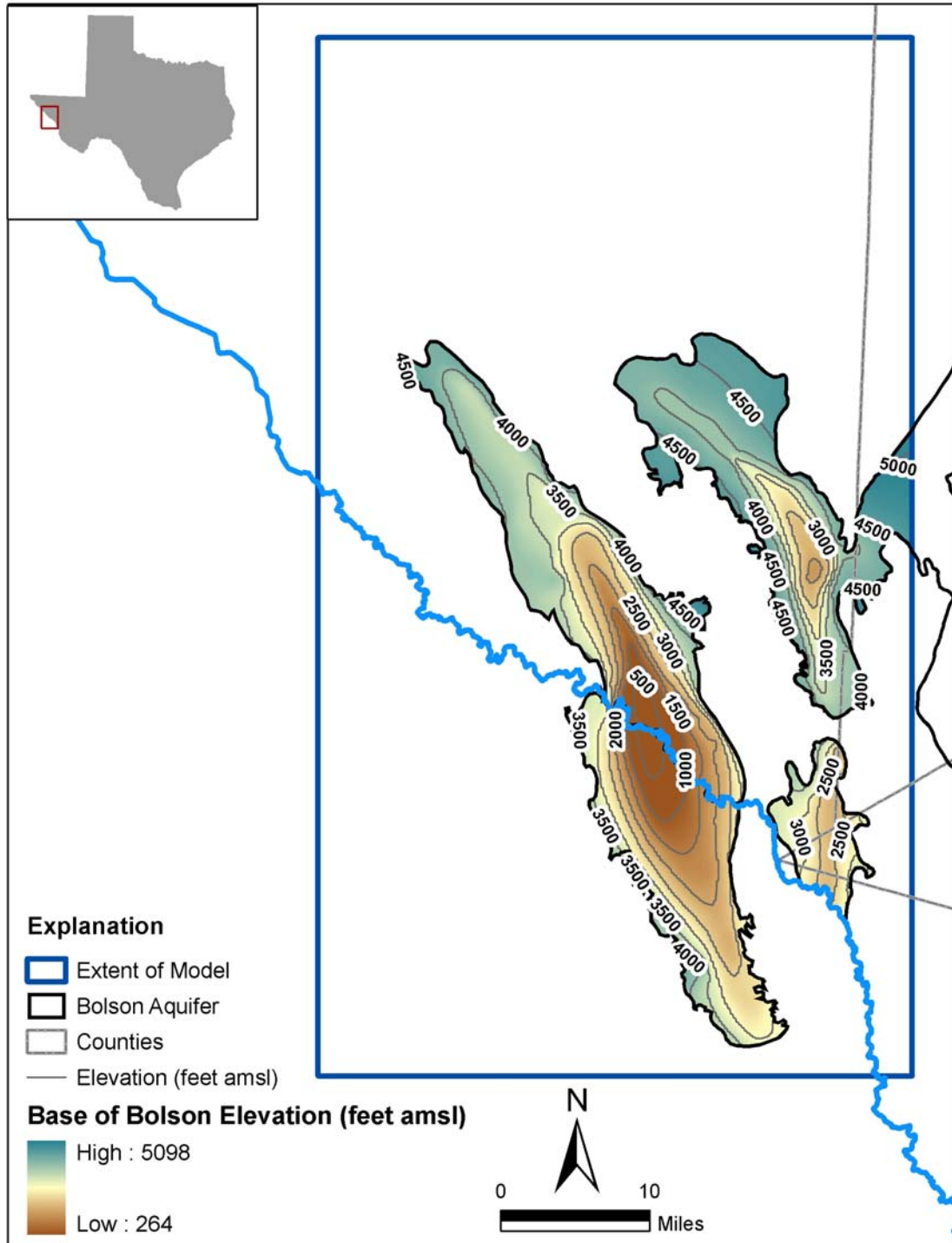


Figure 4.2.2 Elevation of the base of the West Texas Bolsons Aquifer

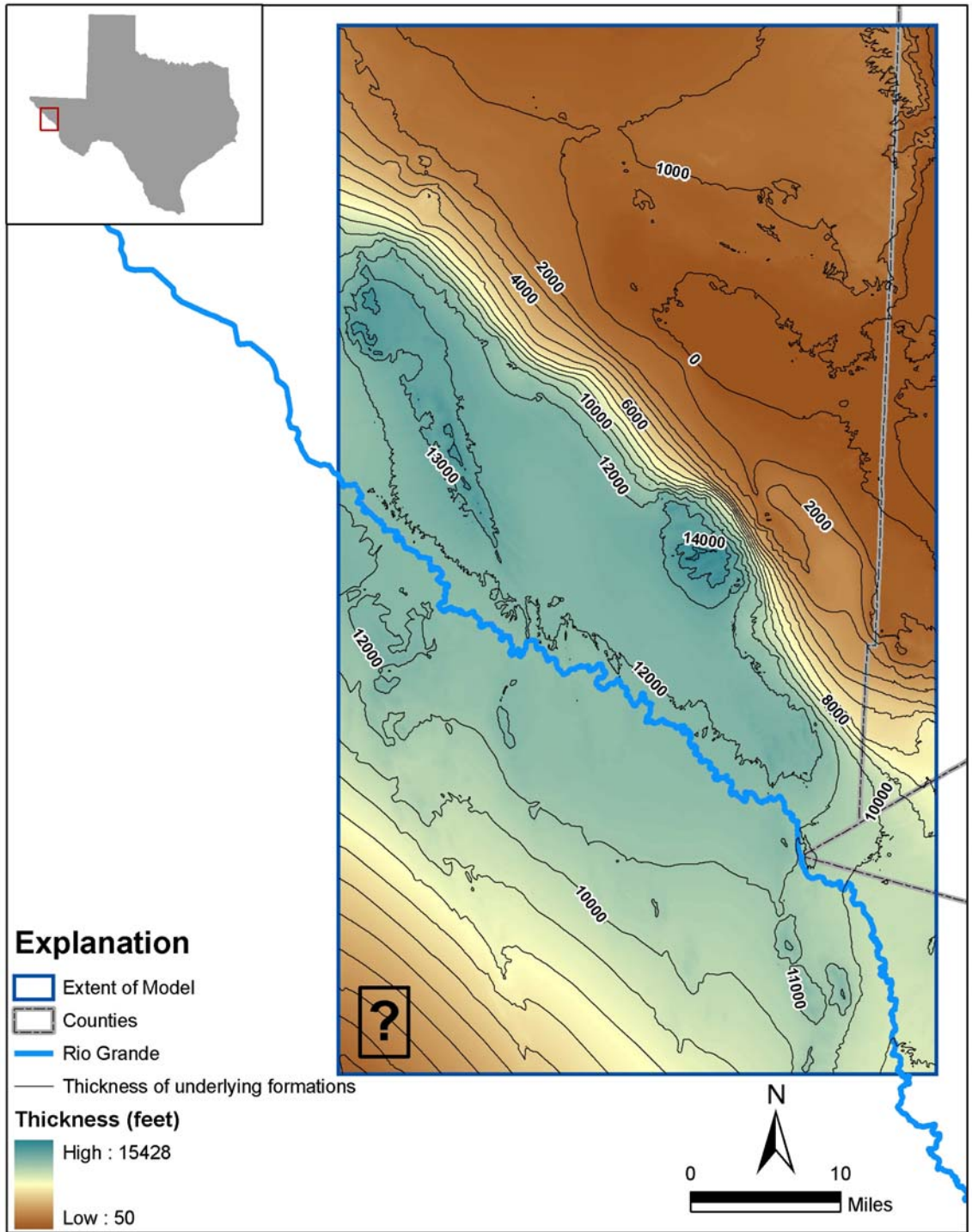


Figure 4.2.3 Thickness of the underlying units

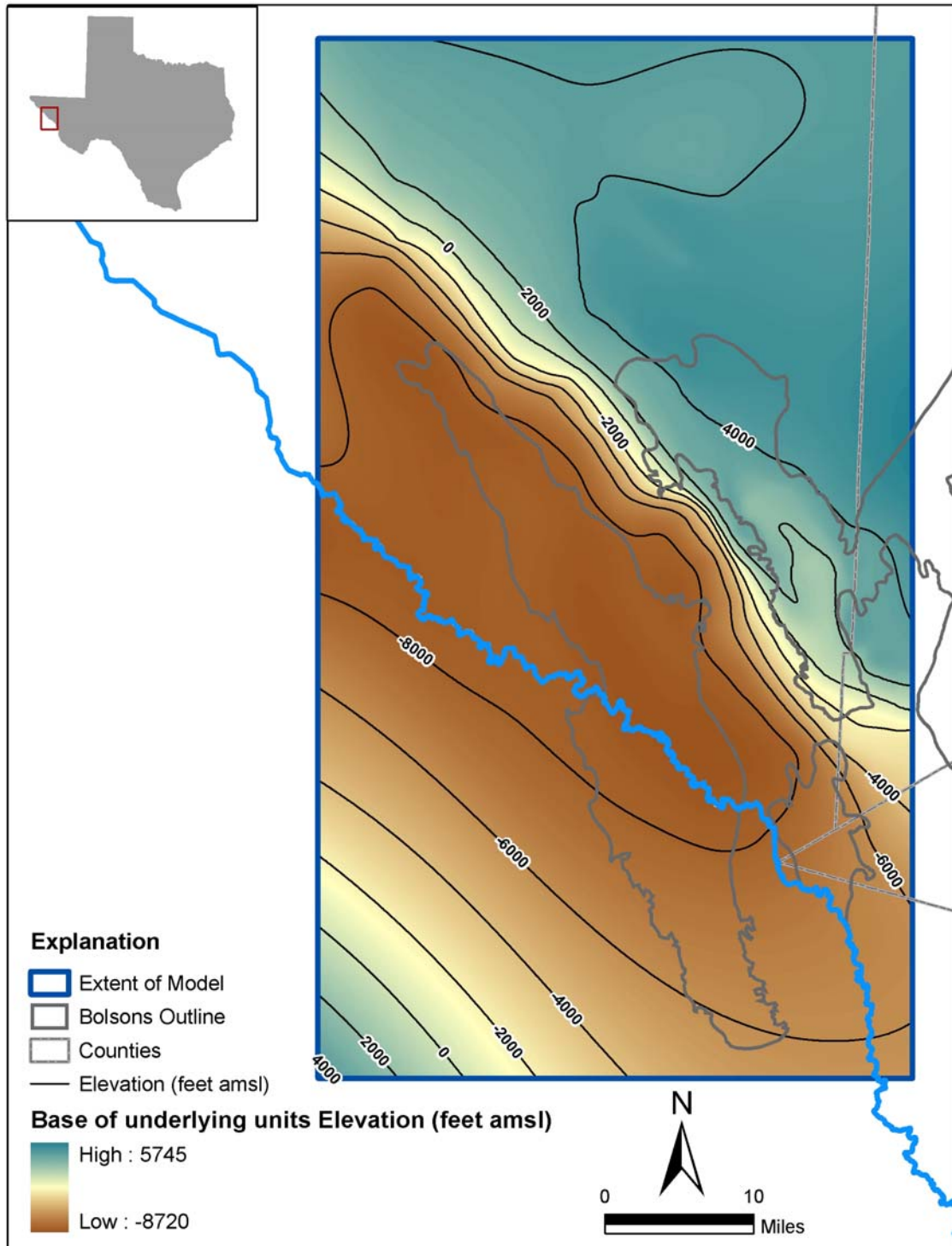


Figure 4.2.4 Elevation of the base of underlying units

4.3 Water Levels and Regional Groundwater Flow

Either the Texas Department of Water Resources (TDWR) – the predecessor agency of the Texas Water Development Board – or the University of Texas at Austin - Bureau of Economic Geology (BEG) has made nearly all of the recorded measurements of the depth to groundwater in the Eagle Flat area since 1957. Most of the depth measurements reported by the above agencies were made in the 1972-74 and 1992-93 time periods (Figure 4.3.1). Measurements from the period 1972-74 were made by or for the TDWR. The latter group of depth measurements was made by BEG. Prior to the first group of measurements, there were insufficient data to support the construction of a potentiometric map.

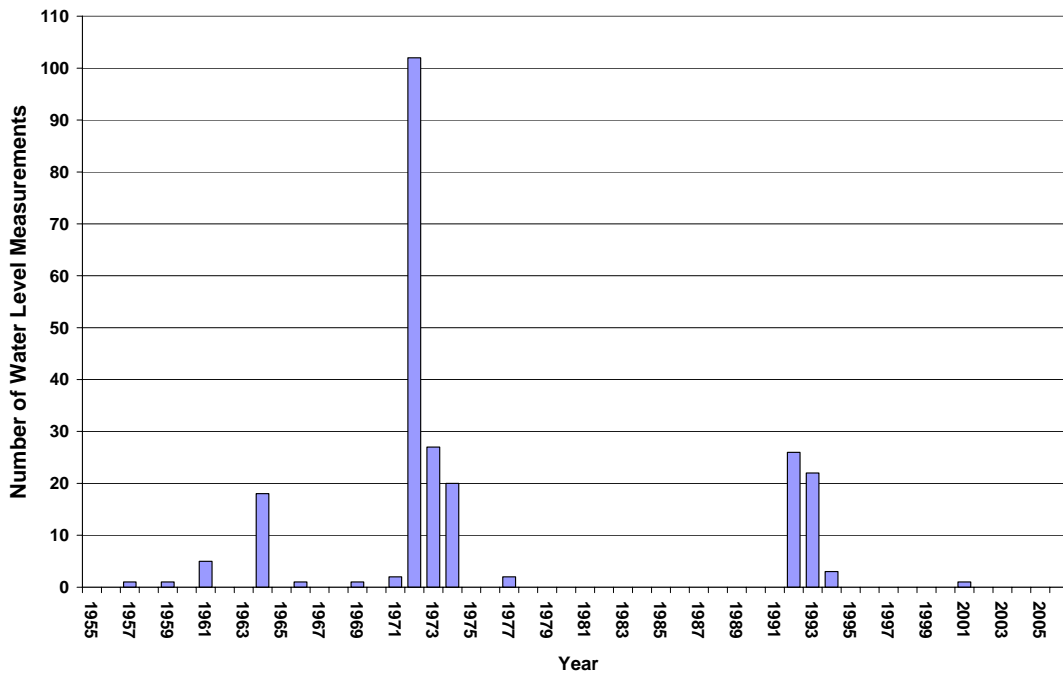


Figure 4.3.1 Histogram showing the number of water level measurements in each year

4.3.1 Hydrographs

Hydrographs based on measurements from wells in alluvium, and the Red Light, Green River and Eagle Flat Bolsons (Figure 4.3.2) indicate only small changes in hydraulic head over a 25-to-30 year period. There is no consistent pattern of increasing or decreasing heads for all areas. Wells in the alluvium show a slight tendency for increasing head, but this is probably related to the cessation of pumpage for irrigation after about 1980.

4.3.2 Groundwater Flow

Darling (1997) observed that when water-level elevations are plotted against land-surface elevations, the water-level measurements could be divided into two groups. Figure 4.3.3, which contains all the water level information available for this study, confirms this conclusion. Group 1 consists of points which lie along an upward sloping line, and Group 2 is made up of points that form an approximate horizontal line. Group 1 covers a wider range of elevations of the land and potentiometric surfaces than Group 2. For Group 1, the elevation of the land surface ranges from 3,152 to 5,900 ft above mean sea level (msl), and the median elevation is 4,300 ft above msl. The potentiometric surface is 3,121 ft to 5,709 ft above msl, and the median elevation is 4,252 ft. The median depth to the potentiometric surface is 142 ft.

Darling (1997) reported the following least-squares equation for Group 1:

$$PSG_1 = 195 + 0.92 * LSG_1$$

where:

PSG_1 = the estimated elevation of the Group 1 potentiometric surface, and
 LSG_1 = the reported Group 1 land surface elevation.

Pearson's correlation coefficient (r), based on the above least-squares model, is 0.98, and the coefficient of determination (r^2) is 0.97.

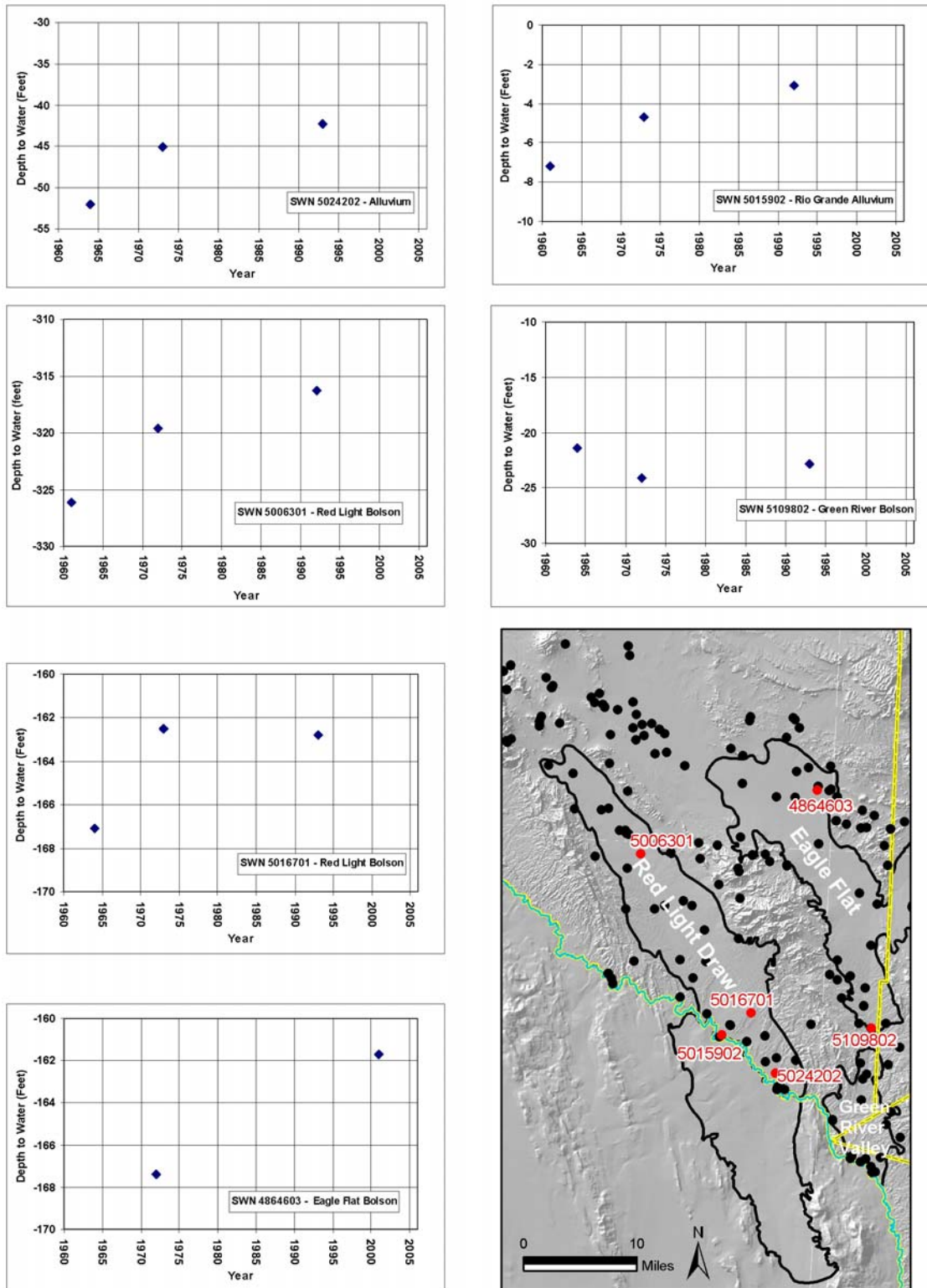


Figure 4.3.2 Hydrographs for Wells in Eagle Flat, Red Light Draw, Green River Valley and Rio Grande Alluvium

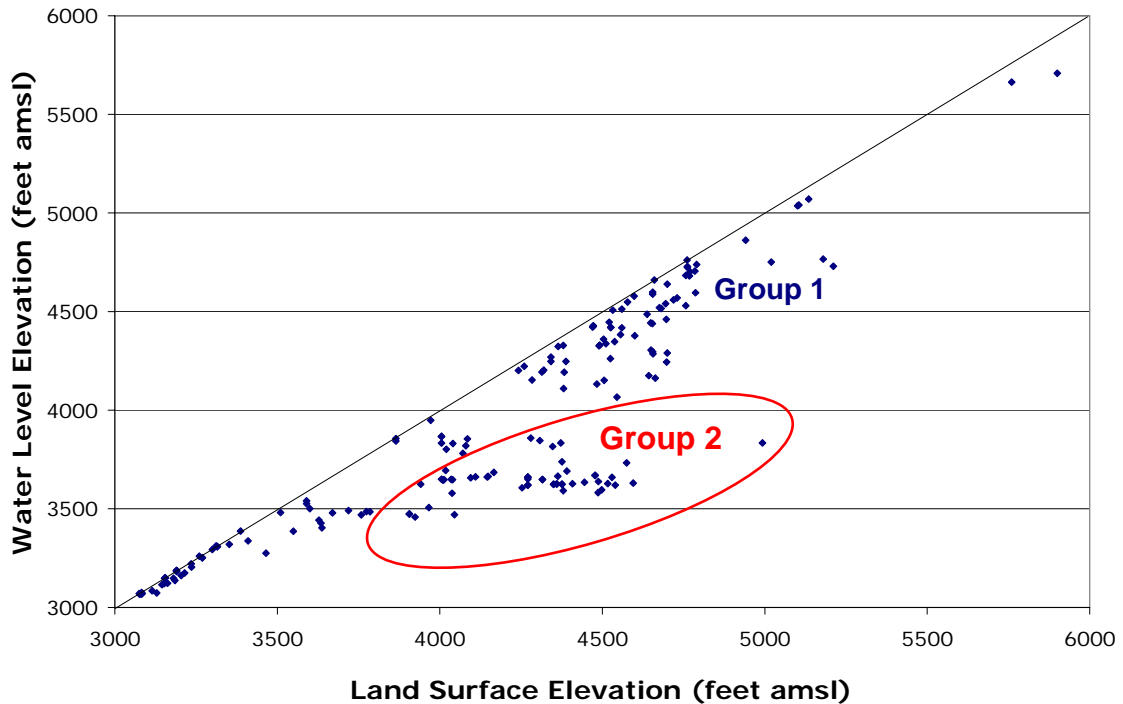


Figure 4.3.3 Water level elevation versus land surface elevation

With regard to Group 2, Darling (1997) reported that the land surface elevation ranges from 3,906 ft and 4,993 ft above msl, with a median elevation of 4,376 ft. The range of the potentiometric surface is from 3,459 ft to 3,859 ft above msl, with a median elevation of 3,638 ft. The least-squares equation for the second group is:

$$PSG_2 = 3,257 + 0.09 * LSG_2$$

where: PSG_2 = the estimated elevation of the Group 2 potentiometric surface, and LSG_2 = the reported Group 2 land surface elevation.

For the Group 2 regression, r is 0.27 and r^2 is 0.06.

Darling (1997) observed that the value of r^2 associated with Group 1 indicates a more pronounced correlation between the elevations of the land and potentiometric surfaces than for Group 2. More specifically, the value of r^2 for Group 1 (0.97) indicates that 97 percent of the variability of the potentiometric surface is accounted for by a regression model which uses the elevation of the land surface as the independent variable. The value of r^2 for Group 2 (0.06) indicates that only 6 percent of the variability of the

potentiometric surface can be explained by associated land-surface elevations. Darling (1997) interpreted this to denote the occurrence of at least two hydrogeologic systems. The first, represented by points belonging to Group 1, consists of shallow groundwater for which the configuration of the potentiometric surface mimics local topography. The second, represented by points that make up Group 2, consists of groundwater that is sufficiently deep that the potentiometric surface does not reflect variations in local topography.

To further illustrate the difference between the two systems, Figure 4.3.4 shows the color shaded contour map representing the depth to water in this area. This data is consistent with the interpretation made by Darling (1997). For the Eagle Flat Basin, the depth to the potentiometric surface is generally less than 200 ft beneath the hills and mountains surrounding the basin. The depth to water varies from 200 to 600 ft beneath the topographically lowest areas of the basin, and increases to more than 1,000 ft well north of the northernmost reaches of Eagle Flat. Within the northern and central areas of the Red Light Basin, the depth to the potentiometric increases from less than 200 ft beneath the Eagle Mountains and the Quitman Mountains to more than 400 ft beneath the floor of the basin. In the southern areas of the Red Light Basin, the depth to the potentiometric surface decreases in the direction of the Rio Grande. In the Green River Basin, the depth to the potentiometric surface increases to 400 ft or more in the northern and central areas of the basin and then decreases in the direction of the Rio Grande.

Darling (1997) also observed that the increasing depth to the potentiometric surface between the highlands and the topographically lowest areas of the Eagle Flat Basin and the northern and central areas of the Red Light and Green River basins is the inverse of the expected association between topography and the depth to groundwater for most flow systems. He noted that points representative of Group 1 occur along the margins and highlands of all of the basins. Points belonging to Group 1 are also found in the southern areas of the Red Light and Green River basins, where the depth to the potentiometric surface decreases in the direction of the river. Points belonging to Group 2 are all within the topographically lowest reaches of Eagle Flat and beneath the floors of the northern and central areas of the Red Light Basin and the Green River Basin.

Darling (1997) concluded that the least-squares equations and the contour map of the depth to the potentiometric surface indicate that local topography is a reliable guide for developing a contour map of the potentiometric surface in areas with points representative of Group 1. He also observed that the association with topography is less reliable in areas with points from Group 2, such that the potentiometric surface would likely be flatter than inferred for areas with points belonging to Group 1.

4.3.3 Potentiometric Map

Figure 4.3.5 shows a composite contour map of the potentiometric surface. The map was constructed from all water level measurements made in 1972-74 and 1992-93. Because the hydrographs do not show a consistent trend or significant variability, it is assumed that using all of the water level measurements is a reasonable approach for obtaining a better geographic coverage of wells to estimate a potentiometric surface. Marked on the map are four groundwater divides which act as boundaries for three distinct flow systems. The potentiometric surface developed here is consistent with Darling (1997), and the location of the groundwater divides and the interpretation regarding the divides is based on Darling (1997).

The first divide, which is traced by the northwest-oriented rim of the Diablo Plateau, separates groundwater of the Diablo Plateau to the north from groundwater of the Hueco Bolson and the Eagle Flat Basin to the south. This hydrologic barrier is referred to as the Plateau groundwater divide. The second extends north-northeastward from the Eagle Mountains to an area slightly to west of the Carrizo Mountains to form a saddle in the potentiometric surface of Eagle Flat. This feature is the Eagle Flat groundwater divide. The third extends from beneath the Eagle Mountains eastward to the Van Horn Mountains to form a broad low-relief saddle beneath the valley floor between the two mountains. This is the Green River groundwater divide. The fourth is projected toward the northwest from the Eagle Mountains, beneath the Devil Ridge. This hydrologic barrier is the Devil Ridge groundwater divide.

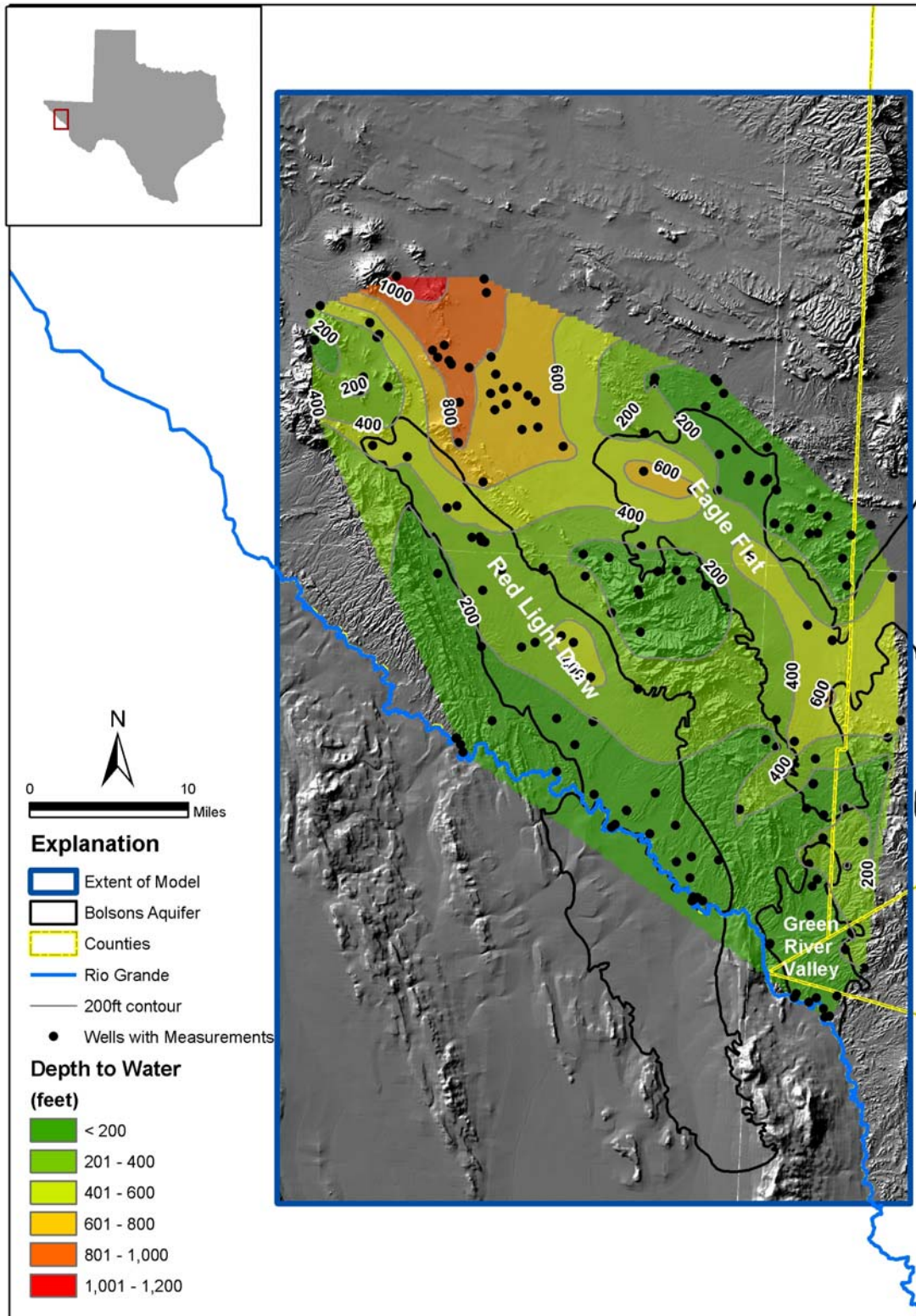


Figure 4.3.4 Depth to Water

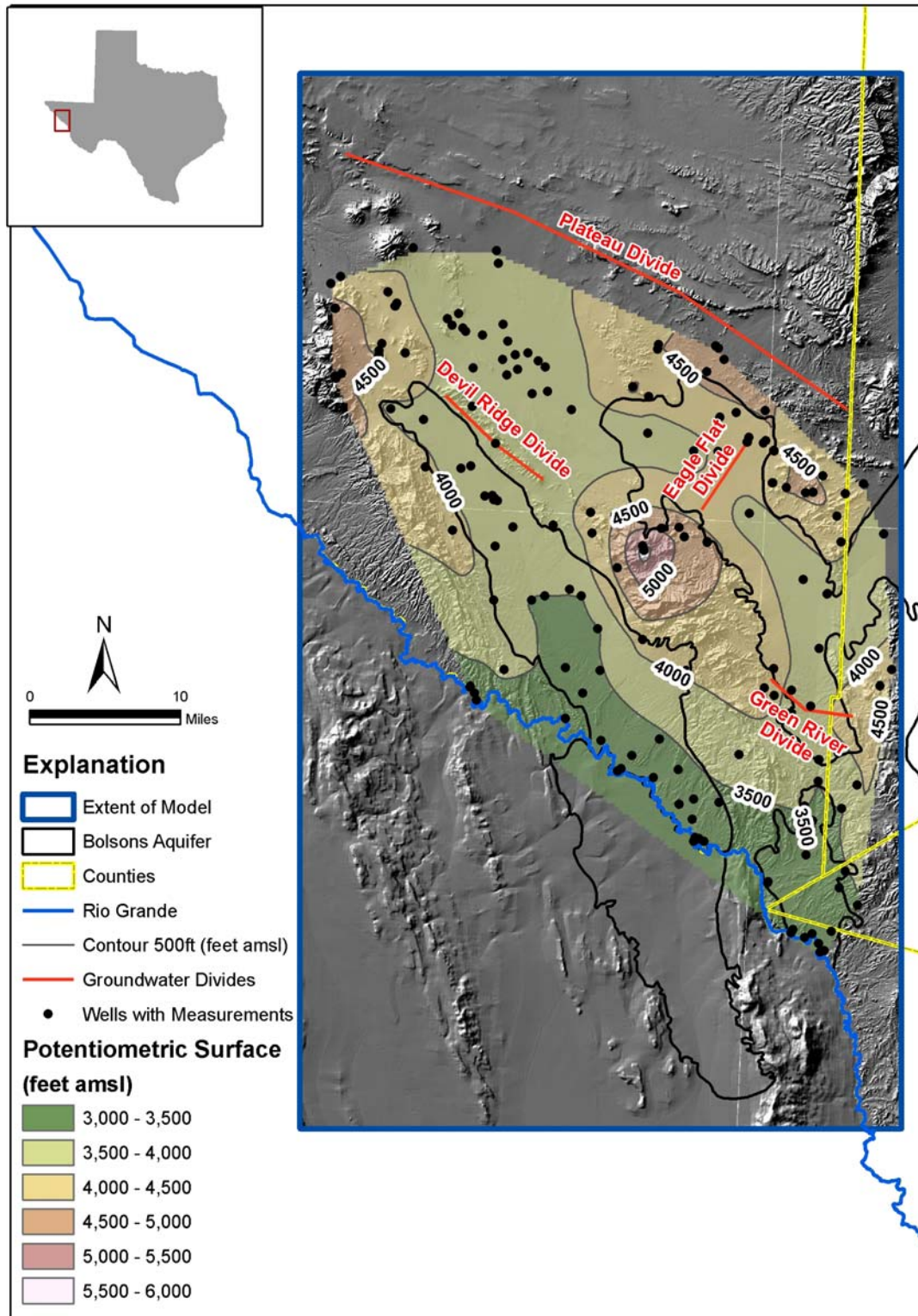


Figure 4.3.5 Steady-state potentiometric surface based on all available measurements

4.3.4 Flow Systems

Groundwater flowing northeastward from the Eagle Mountains converges, beneath the floor of Eagle Flat, with groundwater flowing toward the southwest from the Precambrian rocks of the Bean and Millican Hills and the Carrizo Mountains. The convergence forms the Eagle Flat groundwater divide. This hydrologic barrier creates two flow systems within the Eagle Flat Basin – the Allamoore flow system, which lies to the east of the divide, and the Sierra Blanca flow system, which lies to the west of the divide. The Allamoore and Sierra Blanca systems are bounded along the north by the Plateau groundwater divide, and the Sierra Blanca system is also bounded along the southwest by the Devil Ridge divide. The southern boundary of the Allamoore system is the Green River groundwater divide. The Green River flow system lies to the south of the Green River groundwater divide. The Red Light flow system lies entirely within the boundaries of the overlying Red Light Basin. The Devil Ridge divide separates the Red Light system from the Sierra Blanca system to the north.

4.3.4.1 Allamoore Flow System

Figure 4.3.6 illustrates the regional flow patterns that can be discerned from the potentiometric surface if one assumes two-dimensional flow in a homogeneous and isotropic aquifer system. Of course, those assumptions are not necessarily valid in this system. The “D” symbols on the map indicate locations of closed contours or areas where it is assumed that significant downward flow is occurring.

The regional potentiometric map indicates that groundwater of the Allamoore system flows eastward toward Lobo Valley. The depth to groundwater increases from less than 100 ft in the surrounding highlands to between 400 and 600 ft near Scott’s Crossing, the pass between the Carrizo Mountains to the north and Van Horn Mountains to the south. This contour pattern is controlled partially by water-level measurements from Lobo Valley, where the potentiometric surface immediately to the east of Scott’s Crossing is slightly lower than that of the Allamoore system (Darling, 1997). Flow within the Allamoore system occurs in Precambrian rocks and in Tertiary basin fill. There is no

known production of groundwater from Cretaceous rocks in the system. Darling (1997) observed that, although the overlying watershed is open to the east through Scott's Crossing, the presence of a thick unsaturated zone and the lack of a surficial discharge feature such as a playa or a gaining axial stream underscore the strong similarity of the system to the topographically closed by drained valleys of the Great Basin, as described by Snyder (1962). He further commented that if bedrock formations are both porous and permeable, then the lower hydrologic potential in Lobo Valley should establish both necessary and sufficient conditions for flow toward the east.

4.3.4.2 Red Light and Green River Flow Systems

Groundwaters of the Red Light and Green River systems converge beneath the floors of their respective watersheds and then flow southward toward the Rio Grande. In each system, the depth to the potentiometric surface decreases with proximity to the river, and the flow paths inferred from the potentiometric map suggest the river as the probable discharge zone. On the basis of this interpretation, Darling (1997) commented that the Red Light and Green River systems appear to be similar to the topographically open and drained valleys of the Great Basin (based on Snyder, 1962). Cretaceous rocks are known to be significant hydrostratigraphic formations in the northern areas of the Red Light Basin. Tertiary basin fill and Quaternary alluvium predominate in the central to southern areas of the basin. Quaternary alluvium and Tertiary volcanics are the principal water-bearing rocks of the Green River Basin. Only a few wells are thought to produce water from Cretaceous rocks.

4.3.4.3 Sierra Blanca Flow System

The greatest depths to groundwater are within the central part of the flow system (Figure 4.3.4). The potentiometric map (Figures 4.3.5 and 4.3.6) reveals two areas where the equipotentials are closed at elevations as low as 3,600 ft above msl. Darling (1997) assigned most wells of the wells that define the Sierra Blanca system to Group 2. Wells in this area produce water from Cretaceous rocks. The overlying Tertiary basin fill is unsaturated.

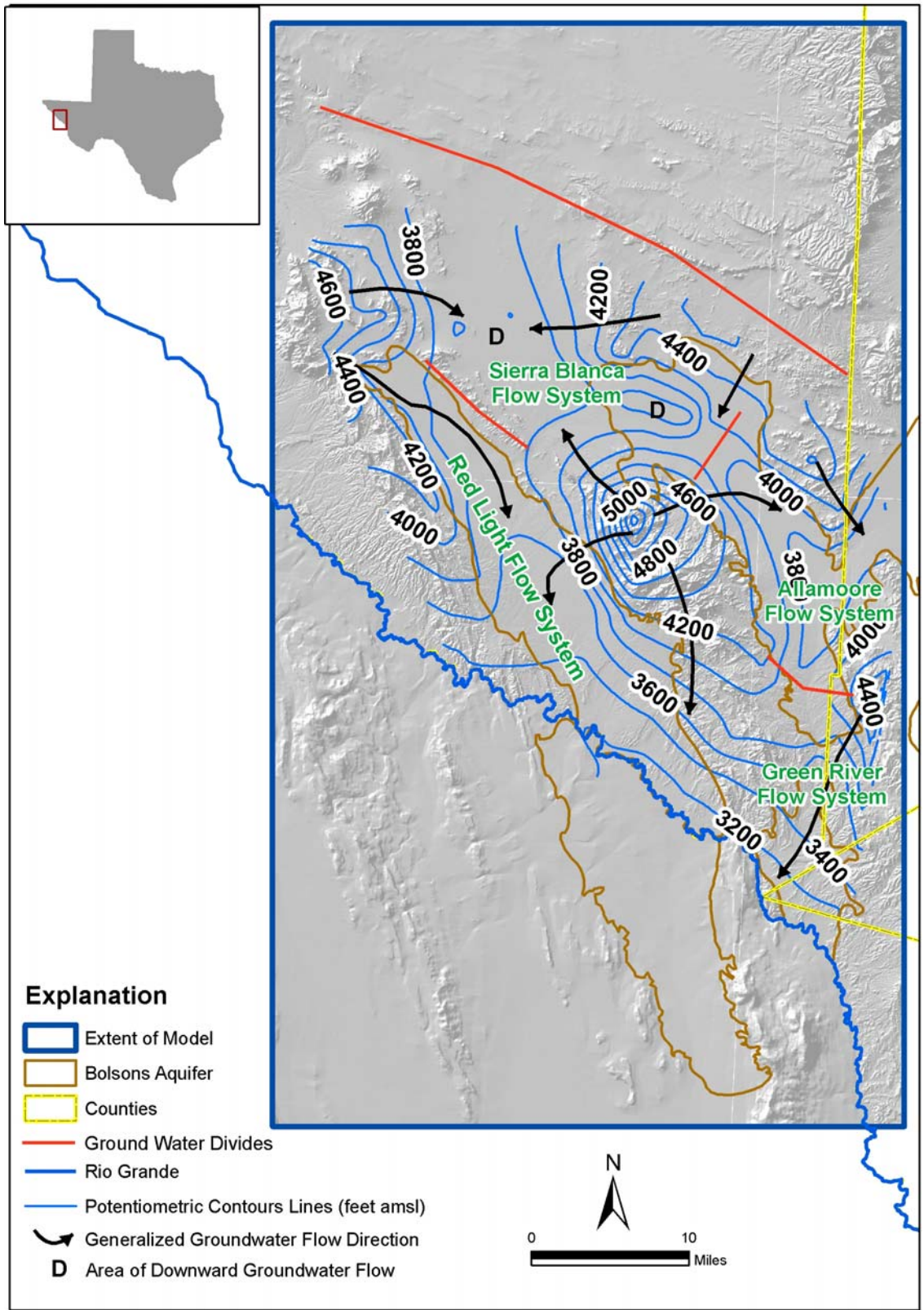


Figure 4.3.6 Regional groundwater flow patterns

Darling (1997) surmised that the combination of topographic and hydrogeologic closure is similar to the closed and undrained valleys of the Great Basin (as described by Snyder, 1962). In a closed and undrained valley, groundwater would be expected to discharge to a playa; however, Darling (1997) noted that the great depth to the static water level in the Eagle Flat Basin precludes that possibility.

Darling (1997) commented that all of the water level measurements on any potentiometric map of the area are representative of conditions only near the top of the zone of regional saturation. As such, the measurements provide no data on hydraulic gradients in deeper rocks. Hence, a two-dimensional representation such as Figure 4.3.6 is inadequate to show with certainty where groundwater leaves a flow system, especially if more porous and permeable rocks lie at depths not penetrated by wells in the basin (Freeze and Witherspoon, 1967; Maxey and Mifflin, 1966; Mifflin, 1968).

4.3.5 Vertical Flow

Darling (1997) surmised that the Eagle Flat and Devil Ridge groundwater divides limit direct lateral flow from the Sierra Blanca system to the Allamore and Red Light systems. He hypothesized that the most likely avenue for the movement of groundwater from the Sierra Blanca system is along vertical pathways to more porous and permeable rocks beneath the Cretaceous bedrock aquifer. Darling (1997) cited, as a basis for the vertical flow hypothesis, the widespread occurrence of Group 2 wells in the Eagle Flat Basin and the closed potentiometric contours, which suggest the influence of leakage to deeper rocks. He noted that vertical drainage could account for the unsaturated basin fill in the western and northwestern areas of the Eagle Flat Basin.

Darling (1997) cited the record of an abandoned core test as support for the occurrence of higher permeability in rocks beneath the Cretaceous bedrock aquifer. In 1965, Texaco drilled a 1,700-ft core test (Capitan Drilling Company, No. 1 Espy Ranch) in the Eagle Flat Basin. White and others (1980) listed the well as 48-63-602, but did not report an associated water-level measurement. The surface elevation at the well was reported to be 4,368 ft above msl. According to the drilling record on file at the TWDB,

the bore hole penetrated 240 ft of basin fill before encountering carbonate rocks. The record also reports lost circulation in carbonate rocks between depths of 1,590 ft and 1,700 ft, with inability to regain circulation.

That No. 1 Espy Ranch core test is one of the deepest documented penetrations of bedrock in the Eagle Flat Basin. The lost circulation reported for the test occurred at an elevation of 2,778 ft above msl – or between 900 ft and 1,000 ft below the potentiometric surface in this part of the Sierra Blanca flow system. Darling (1997) commented that the loss of circulation suggests that a higher permeability pathway might lie beneath the uppermost part of the zone of regional saturation to provide an effective zone for flow to deeper rocks. In this setting, groundwater in the less permeable Cretaceous rocks might drain to deeper, more transmissive rocks. Darling (1997) noted that this type of hydrogeologic communication was suggested by Winograd (1962) and Winograd and Thodarson (1975) in studies of regional (interbasin) flow systems in the Great Basin of Nevada.

The closed contours of the Sierra Blanca system indicate leakage of groundwater to deeper and more permeable rocks, but the direction of flow from the system is not apparent because of the closed equipotentials. Darling (1997), however, postulated two possible flow directions: eastward flow beneath the Allamoore system; or southward flow beneath the Red Light system. He concluded that the most probable direction of flow is toward the south, beneath the Devil Ridge groundwater divide and the thick deposits of Tertiary basin fill of the Red Light Basin. The potential for flow toward the east might be limited by the higher hydraulic head of the Allamoore system, compared with the lower average head of the Red Light system.

4.4 Recharge

4.4.1 Recharge Areas

In the West Texas Bolsons groundwater availability model study area, groundwater recharge primarily occurs as 1) direct recharge from infiltration of precipitation on the mountain block (i.e. Quitman Mountains, Eagle Mountains, Carrizo Mountains, and Van Horn Mountains), and 2) as bolson-fringe recharge (also termed mountain front) from infiltration of storm-water runoff along channels of ephemeral streams on alluvial fans along the bolson perimeter (Gates and others, 1980; Scanlon and others 2001; Finch and Armour, 2001). Due to climatic characteristics (high evapotranspiration and low precipitation), little to no recharge occurs directly to the bolson. This recharge concept is depicted in Appendix B, Figure B.1.

There are two types of bolsons in the study area as defined by Hibbs and Darling (2005):

1. Topographically open and through-flowing basins, where surface-water runoff and groundwater flow out of the basin. The Red Light Draw, Green River Valley, and Southeast Eagle Flat Bolsons fall into this category.
2. Topographically closed drained basins, where surface water is confined to the watershed and flows to the basin center, and groundwater drains by inter-basin flow through a deep regional system. The Northwest Eagle Flat (Sierra Blanca-Grayton Lake area) falls into this category.

Some evidence suggests recharge is captured and conveyed by regional fault systems in the study area (Figure 2.5.9). Some precipitation that infiltrates in the Eagle Mountains may be channeled along the West Eagle Mountains-Red Hills Fault (Collins and Raney, 1997). Some precipitation that infiltrates in the Indio Mountains may be channeled along the West Indio Mountains Fault and Indio Fault (Collins and Raney, 1997). Also, precipitation that infiltrates in the Van Horn Mountains may be channeled along the West Van Horn Mountains Fault (Collins and Raney, 1997). Groundwater

moving along these faults does not discharge at hot springs, as is the case with the Caballo Fault Zone on the western flank of the Quitman Mountains (Henry, 1979; Hibbs and Darling, 2005), but instead discharges to the bolson aquifers, Cretaceous-age aquifers, and the Rio Grande.

The remainder of the precipitation that infiltrates in the mountains infiltrates Cretaceous-age sandstone and limestone rocks. These rocks are known to be productive aquifers in the Sierra Blanca area.

4.4.2 Recharge Estimates from Previous Work

Previous investigators have made estimates of recharge to the bolsons in the Red Light Draw-Green River Valley groundwater availability model study area based on a percentage of precipitation (Gates and others, 1980), radioactive isotope analysis and cross-sectional numerical flow modeling (Darling, 1997), storm runoff and infiltration, and watershed analysis (Table 4.1). The USGS recharge study (Gates and others, 1980) assumed one percent of the average annual precipitation as the rate of recharge, and estimated average annual recharge as high as 2,000 acre-feet per year (ac-ft/yr) in Red Light Draw, 1,000 ac-ft/yr in Green River Valley, and 3,000 ac-ft/yr in Eagle Flat. This method did not take into account watershed characteristics, rock type, the feasibility of surface water to enter the groundwater system, or inter-basin flow.

Based on analysis of radioactive isotopes carbon-14 and tritium, and cross-sectional numerical flow modeling, Darling (1997) concluded that recharge in Red Light Draw occurs only along the higher elevations, and not along the middle to lower elevation alluvial fans. Darling (1997) estimated average annual recharge as low as 280 ac-ft/yr in Red Light Draw, 120 ac-ft/yr in Green River Valley, and 430 ac-ft/yr in Eagle Flat (Table 4.1).

Table 4.1 Comparison of Recharge Estimated for West Texas Bolsons by Other Researchers

Method	Estimated recharge, ac-ft/yr			Comments
	Red Light Draw	Green River Valley	Eagle Flat Draw	
One-percent rule (Gates and others, 1980)	2,000	1,000	3,000	Does not consider watershed or geologic variability
Radioactive isotopes (Darling, 1997)	280	120	430	
Modified one-percent rule (LBG-Guyton Assoc. and others, 2001)	700	700	1,000	
Storm-runoff infiltration (Finch and Armour, 2001)	-	-	4,119	Does not consider aerial (direct) recharge at higher elevations or geology
Runoff redistribution (Beach and others, 2004)	-	-	3,036	Accounts for watershed characteristics and distribution of recharge from storm water runoff

Using a modification of the USGS approach, in which one percent of average annual precipitation in the higher elevations was assumed to be available as recharge, LBG-Guyton Associates and others (2001) estimated average annual recharge of 700 ac-ft/yr in Red Light Draw, 700 ac-ft/yr in Green River Valley, and 1,000 ac-ft/yr in the southeastern part of Eagle Flat.

Based on watershed topographic analysis, the assumption that a runoff-generating storm event occurs only once every two years, and 35 percent of runoff becomes recharge, Finch and Armour (2001) estimated average annual recharge of 4,119 ac-ft/yr in Eagle Flat.

Based on watershed topographic analysis, and a modified version of the runoff redistribution method of Stone and others (2001), Beach and others (2004) estimated average annual recharge of 3,036 ac-ft/yr in Eagle Flat.

4.4.3 Summary of Recharge Method

In the current study, the method selected to calculate initial recharge estimates for the study area was based on previous studies completed by Nichols (2000), Stone and others (2001), Bennett and Finch (2002), and Beach and others (2004). This approach to determining recharge and distribution of recharge takes into account climate, watershed, and geologic characteristics for each sub-basin defined in the study area. The method includes the following analyses:

1. Delineating mountain and bolson sub-basins within the study area, and their hydrologic characteristics;
2. Calculating topographic statistics for each sub-basin;
3. Estimating potential recharge (corrected for elevation zones and evaporation) for each sub-basin;
4. Determining runoff from each sub-basin by analyzing the magnitude of precipitation events that result in runoff (scaled to elevation);
5. Determining the amount of runoff that leaves mountain sub-basins, and is thus removed from potential recharge to mountain sub-basins; and,
6. Determining the amount of runoff that enters the bolson, and is thus available as recharge to the bolson.

Details regarding the recharge methodology and analysis are provided in Appendix B. The assumptions made for calculating recharge and recharge distribution include the following:

1. Direct precipitation on the bolson does not infiltrate and become recharge;
2. Precipitation increases with elevation as defined by existing data;
3. There is no potential recharge for areas with less than 12 inches per year average precipitation (this correlates to < 4,700 feet amsl);
4. Dry soil conditions are used for estimating the runoff curve number; and,
5. Approximately 30 percent of the runoff infiltrates at the alluvial fan and the remaining 70 percent evaporates or flows out of the model domain.

The first step in determining potential recharge is to develop a relationship between precipitation and elevation for weather stations within and surrounding the study area (Figure 2.3.2). Average annual and daily precipitation data for the period of record were collected for 14 weather stations throughout the entire bolson region (Table B.2, Appendix B) (Utah State University Climate Center, 2006). For each weather station, we determined the frequency of 24-hour precipitation events of specified magnitudes that could potentially generate storm-water runoff. We used the linear relationship between elevation and frequency of runoff events at the weather stations to calculate runoff for each sub-basin in the study area. Calculated runoff was subtracted from potential recharge in the mountain (topographically up-gradient) sub-basins and added to potential recharge in the bolsons.

It is important that the effects of evapotranspiration and other losses be considered when estimating potential recharge; otherwise the potential recharge values for the sub-basins are overestimated. Figure 2.3.4 presents average annual lake evaporation in the study area. To account for these losses, the potential recharge was estimated from empirical relationships (coefficients; Nichols, 2000) developed for similar basins in Nevada and modified to represent Trans-Pecos climate conditions (Bennett and Finch, 2002). The coefficients used to estimate potential recharge are summarized in Table 4.2. The percent of total precipitation becoming potential recharge ranges from 0 to 7 percent, increasing with increasing elevation.

Table 4.2 Summary of coefficients used to estimate potential recharge, and corresponding elevation, average annual precipitation, and potential recharge

Average annual precipitation, in/yr	Potential recharge coefficient	Potential recharge, in/yr	Elevation, feet amsl
12	0.000	0.00	3,000
14	0.018	0.25	3,870
16	0.035	0.56	4,740
18	0.052	0.94	5,600
20	0.070	1.40	6,475

4.4.4 Recharge Estimates

The results of the recharge analysis are illustrated on Figures 4.4.1 and 4.4.2, and compared in Table 4.3. Total recharge to the study area is estimated at 5,214 ac-ft/yr, which is about 0.7 percent of the total precipitation. Most of the potential recharge to the bolsons is from infiltration of storm-water runoff in the mountain sub-basins where they adjoin the bolsons (alluvial fans are typically present at this interface), and from cross-formational groundwater flow between the Cretaceous-age aquifer and the bolson aquifers.

Table 4.3 Summary of Recharge Estimates for Red Light Draw-Green River Valley Groundwater Availability Model Study Area

Parameter	Unit	Red Light Draw	Green River Valley	Eagle Flat Draw	Blanca Draw	Eagle Canyon	Total
Area	acres	227,430	103,210	200,850	131,380	9,530	672,400
Total precipitation	ac-ft/yr	203,640	87,780	209,740	125,130	7,070	633,360
Estimated directed recharge to mountain block	ac-ft/yr	1,190	80	2,380	130	0	3,780
Runoff from mountain block	ac-ft/yr	1,470	560	1,630	1,030	90	4,780
Estimated recharge along bolson fringe ^a	ac-ft/yr	441	168	489	309	27	1,434
Total estimated recharge to watershed area encompassing bolsons	ac-ft/yr	1,631	248	2,869	439	27	5,214
	in/yr	0.09	0.03	0.17	0.04	0.03	0.09
Total precipitation that becomes recharge	percent	0.8	0.3	1.4	0.4	0.4	0.8

^a30 percent of runoff from mountain block

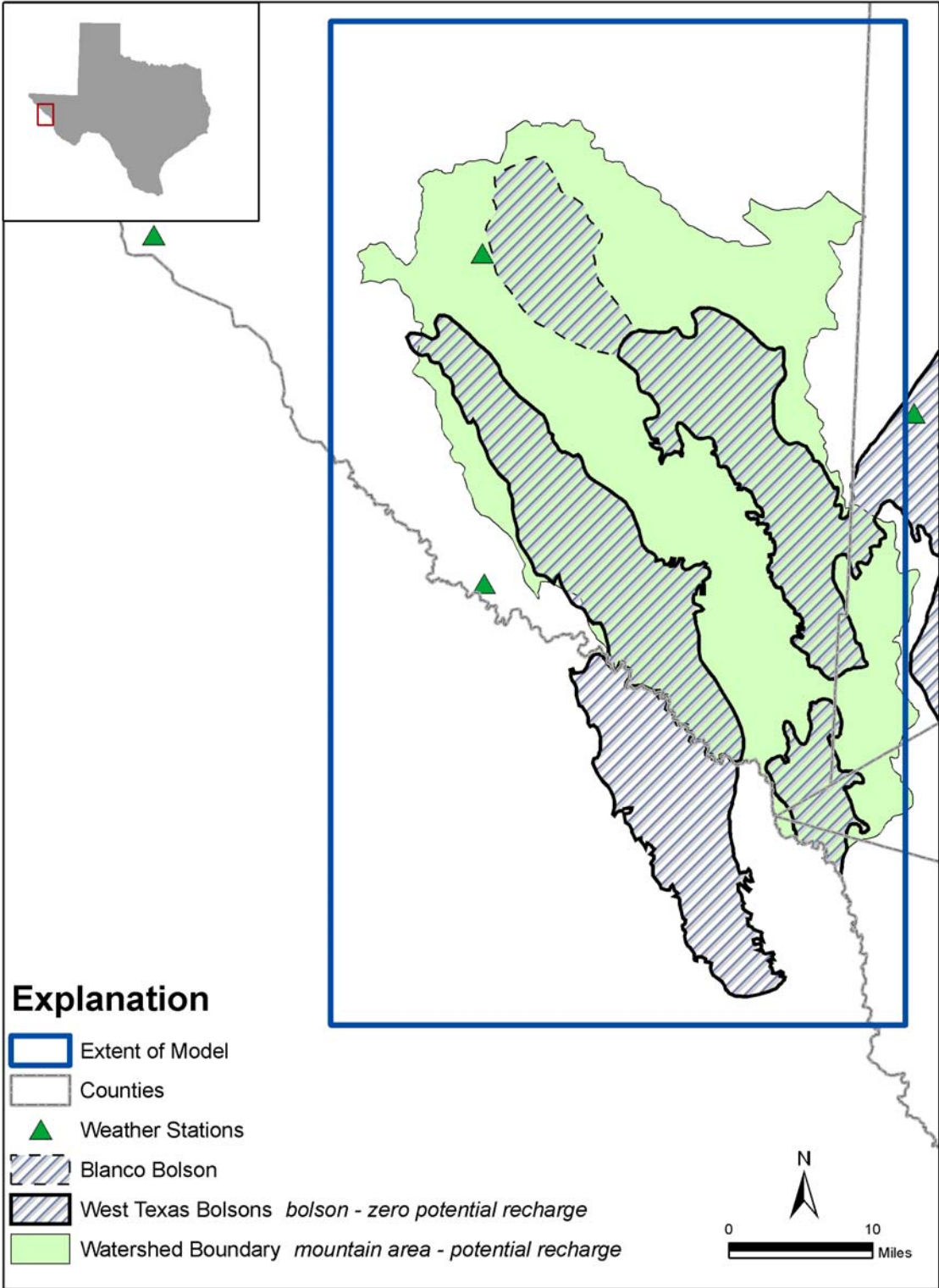


Figure 4.4.1 Distribution of potential recharge

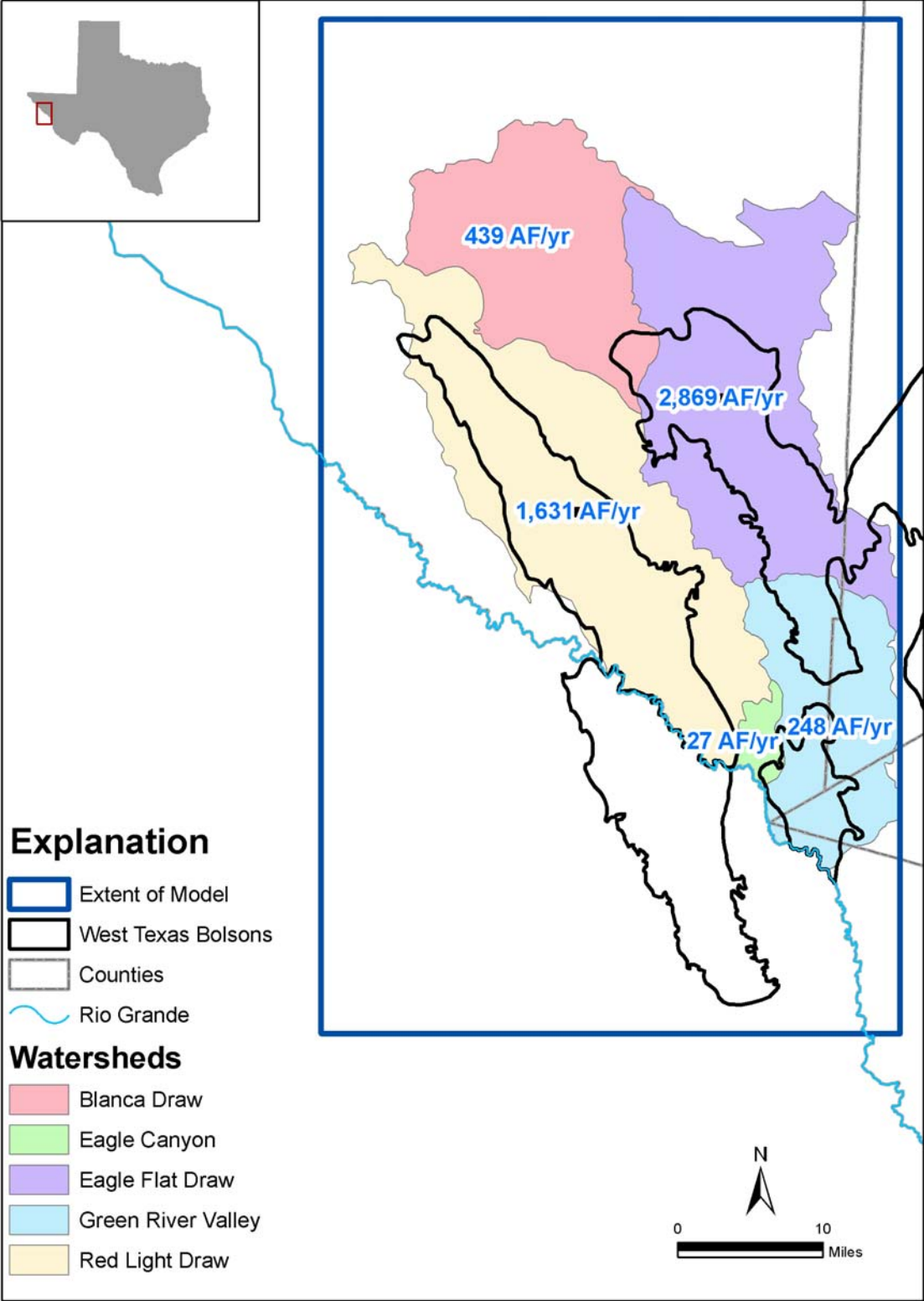


Figure 4.4.2 Average annual recharge estimates in five watersheds

A comparison of other recharge methods with the re-distribution method is provided for the study area in Table 4.4. The runoff-redistribution method appears to be an appropriate method for the West Texas Bolsons groundwater availability model study area because it considers the runoff characteristics of each sub-basin and the variable precipitation received by each sub-basin. Previous recharge estimates using a flat percentage of the precipitation (Gates and others, 1980; Meyer, 1976) do not consider components of the conceptual model, such as geologic characteristics for infiltration and areas on the bolsons where recharge does not likely occur. Therefore, the runoff-redistribution method provides constraints on a sensitive model parameter consistent with the conceptual model, and helps minimize the inherent non-uniqueness associated with parameterization in numerical models.

Table 4.4 Comparison of Recharge Methods for Red Light Draw-Green River Valley Groundwater Availability Model Study Area

Method	Estimated recharge, ac-ft/yr		
	Red Light Draw	Green River Valley	Eagle Flat Draw
Previous work (Table 4.1)	280 to 2,000	120 to 1,000	430 to 4,119
Darcy flux check (this study)	915 to 4,576 ^a	1,365 to 6,823 ^a	53 to 266 ^a
Modified runoff redistribution (this study)	1,631	248	2,869

^a considers cross-sectional area of bolsons and low and high range of hydraulic conductivity value of 1 and 5 feet per day, respectively.

ac-ft/yr = acre-feet per year

Groundwater flow models are sensitive to prescribed recharge and recharge distribution, and given the uncertainties in recharge estimates for the study area, the runoff-redistribution method provides an approximation to recharge distribution and quantity that would otherwise be difficult or impossible to obtain.

Beach and others (2004) found that the recharge estimates from the runoff-redistribution approach for regional model of the Igneous and Bolson aquifers to the east was higher than those obtained from final model calibration. The USGS Española Basin model prepared by McAda and Wasiolek (1988) calibrated to 9,600 ac-ft/yr of recharge for selected drainages along the western side of the Sangre de Cristo Mountains. A very detailed recharge analysis of the same area by the USGS (Wasiolek, 1995) resulted in an estimate of average recharge of 14,700 ac-ft/yr; the model-calibrated recharge resulted in approximately 66 percent of the estimated recharge. Similar results have been realized from recent studies of the Tularosa Basin in southern New Mexico, where the estimated recharge (Waltemeyer, 2001) was approximately 60 percent of the model-calibrated recharge (Huff, 2004), and of the Mimbres Basin in southwestern New Mexico, where the estimated recharge was 69 percent of the model-calibrated recharge (Finch and others 2005, JSAI 2006).

There is likely some rejected recharge that is not accounted for in the recharge estimates that causes the model-calibrated recharge to be less than the estimated recharge. One example of rejected recharge would be recharge to a perched groundwater system that is discharged to a spring or by evapotranspiration. Other possibilities for the recharge discrepancy may be related to the lack of long-term climate data (i.e. comparing 20 years of climate data to a regional hydrologic system that takes thousands of years for water to be recharged and ultimately discharged), and the lack of detail in the regional model to account for conveyance of all the estimated recharge through the groundwater system.

4.5 Rivers, Streams, Springs and Lakes

Figure 2.2.3 shows the river basins and surface water features of the study area. The entire area is within the Rio Grande River basin, but the northern section (Eagle Flat) drains to a closed basin of the Rio Grande watershed. With the exception of springs, the Rio Grande is the only perennial stream in the study area. Along its southeasterly course, the elevation of the Rio Grande decreases from 3,300 feet near Indian Hot Springs to less than 3,200 feet at the southeastern corner of Green River Valley. All other watercourses flow only after heavy rainfall.

The only two stream gauging stations near the study area are on the Rio Grande. One gauge is located to the west (upstream) of the study area at Fort Quitman and the other is located east (downstream) of the study area at Candelaria. Figure 4.5.1 shows the monthly mean flow at each gauge located in Figure 2.2.3. The period of record for each gauge varies, but the gauges indicate that the largest mean monthly flows occur in late summer and early fall. Flows in the Rio Grande have been regulated by Elephant Butte, which started filling in 1915, and other upstream irrigation operations for many years, so the graphs are more representative of managed flows in this portion of the river.

Stream conductance information for this section of the Rio Grande was not available. Because there is no gain/loss information for this section, streamflow depths will not be routed with the model. The streambed top is assumed equal to the average ground surface elevation for the model gridblocks in the river and stream depth is assumed to be one foot. Channel width and slope, and Manning's roughness coefficient are not required if stream depth is not estimated by the model.

Red Light Draw and Green River Valley drain to the Rio Grande. Grayton Lake (Figure 2.2.3), which lies just northwest of the locally closed Eagle Flat at 4,270 feet, contains water only after heavy rainfall events.

Figure 4.5.2 shows the location of springs in the study area based on data compiled by the USGS (2003) and Brune (1975 and 1981). The largest of these are Indian Hot Springs and Mesquite Springs, each producing over 100 gallons of water per minute. The

most notable of these two major springs is Indian Hot Springs, located near the Rio Grande west of Red Light Draw. Indian Hot Springs is a thermal spring that is likely sourced by both deep and shallow groundwater systems. Other springs in the area are classified as small by Brune (1981) and are more likely sourced by shallower groundwater systems.

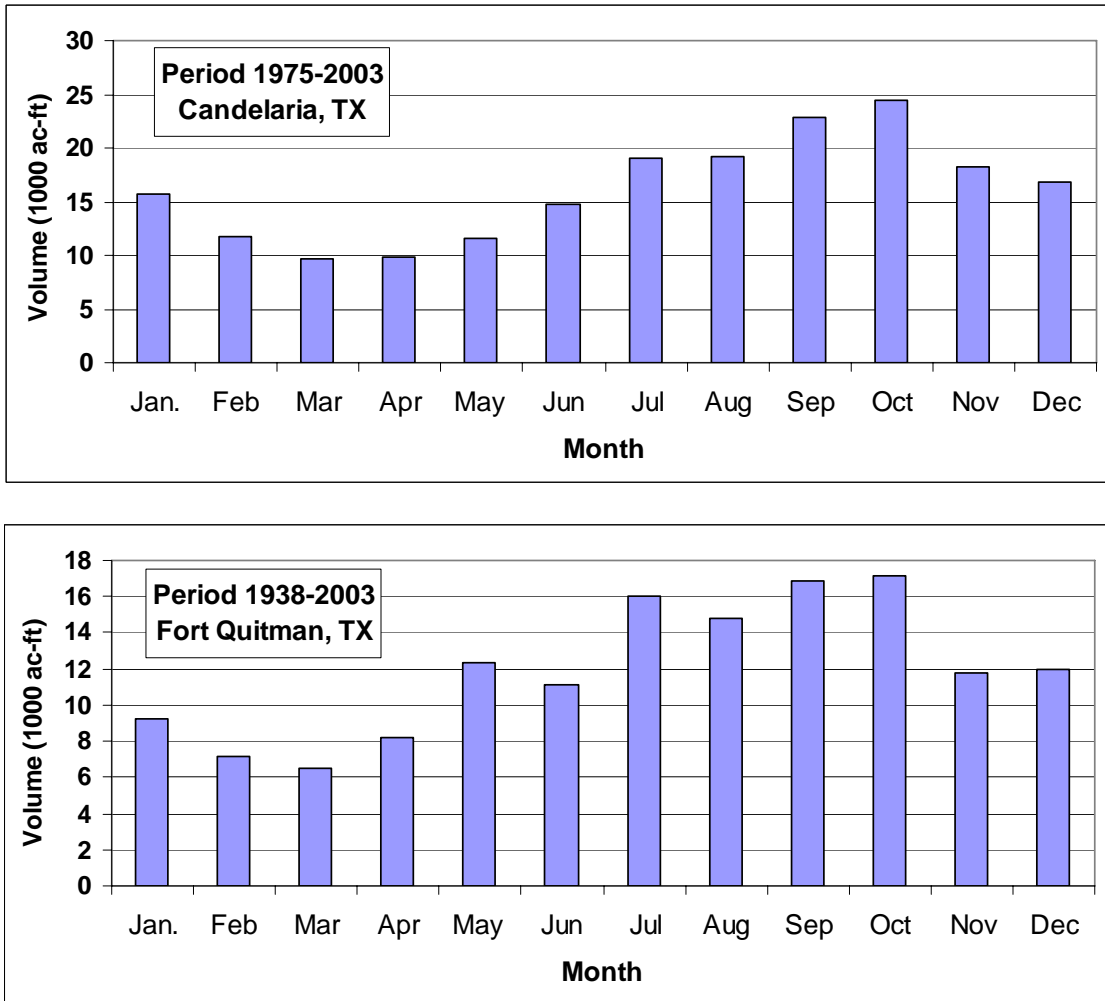


Figure 4.5.1 Monthly Mean Streamflow at Candelaria and Fort Quitman

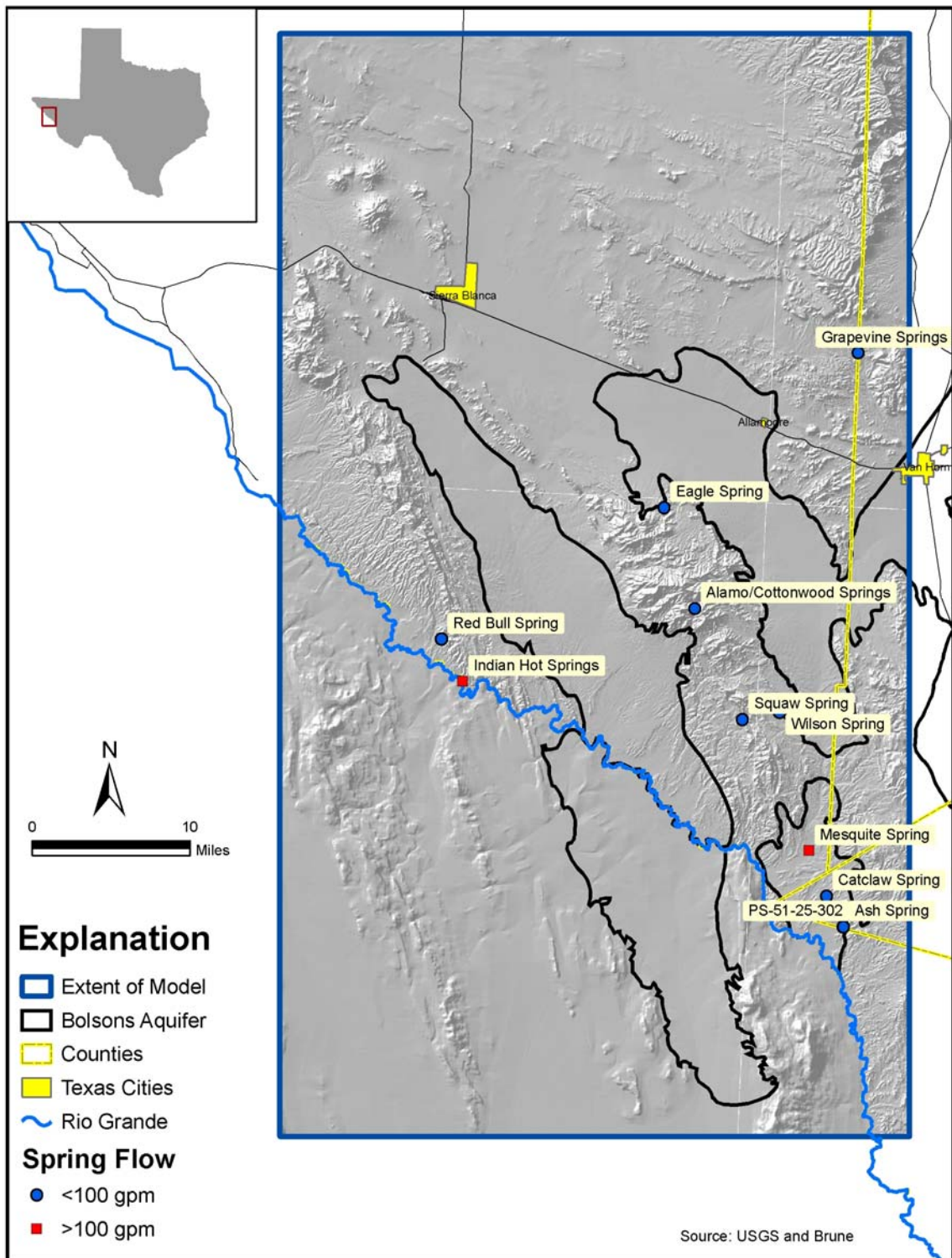


Figure 4.5.2 Location of Springs

4.6 Hydraulic Properties

4.6.1 Hydraulic Conductivity

Very little testing data exists in the model area to provide for an assessment of the hydraulic properties of either the bolsons or the Cretaceous aquifers. The data set evaluated in this report consists of 11 tests on wells completed in the Cretaceous, and one test on a well completed in the Eagle Flat Bolson. All of the wells in the data set are in the northern half of the model area. The data set was prepared from TWDB well records and tests reported in Darling, and others (1994). Estimated hydraulic conductivities for each well test are presented in Table 4.5 and located in Figure 4.6.1.

The Cretaceous well test data consists of six tests of specific capacity in TWDB records and five pumping or slug tests for which a transmissivity was calculated in Darling and others (1994). Transmissivities were estimated for the wells with specific capacity data using the approximated relationships for specific capacity and transmissivity in confined and unconfined aquifers described in Appendix 16.D of Driscoll (1986). Specifically, Driscoll describes the specific capacity as being directly proportional to the transmissivity for confined and unconfined aquifers in the following manner:

$$\text{specific capacity (gpm/ft)} = \text{transmissivity(gpd/ft)}/2000 \quad [\text{confined}]$$

$$\text{specific capacity (gpm/ft)} = \text{transmissivity(gpd/ft)}/1500 \quad [\text{unconfined}]$$

These relationships are approximate because they are based on assumed values in the log term of the modified nonequilibrium equation of Cooper and Jacob (1946). Taking the logarithm of these assumed values tends to mute inaccuracies in the assumptions, leading to the approximations above.

Very little pumping test data is available in the model area with calculated transmissivity, so a more site- or formation-specific empirical relationship between specific capacity and transmissivity has not been attempted.

Wells completed in the Cretaceous in the northwest Eagle Flat area (state well numbers 48-53-801, 48-53-802, and 48-53-803) were assumed to be unconfined. The other wells completed in the Cretaceous were assumed to be confined. Hydraulic conductivities were estimated from transmissivity and thickness. The thickness of the aquifer was assumed to be equal to the screened interval of the well.

The transmissivities calculated or estimated from specific capacity data ranged from 2 to 5,013 ft²/day. The estimated hydraulic conductivities ranged from 0.01 to 279 ft/day. A histogram of the estimated hydraulic conductivities in the wells completed in the Cretaceous is presented in Figure 4.6.2. The median value of hydraulic conductivity is about one foot per day.

There is no information concerning vertical hydraulic conductivity in the model area. Vertical anisotropy will be adjusted based on professional judgment and the results of the calibration process.

As mentioned above, only one test is available for the bolsons in the study area. The pumping test result is reported in Darling, and others (1994) for a well completed in the Eagle Flat Bolson. This test gave a calculated transmissivity of 217 ft²/day and an estimated hydraulic conductivity of 0.54 ft/day.

4.6.2 Storage Properties

A single test in the data set was conducted with an observation well. This test was conducted on a well completed in the Cretaceous (state well number 48-54-902) in June 1997, and a storativity of 4×10^{-3} was derived from the observation well data.

Freeze and Cherry (1979) indicate that the storativity in confined aquifers usually range in value from 0.005 to 0.00005, and that porosity in fractured rocks may vary from zero to 0.10. The specific yields of unconfined aquifers are much higher than the storativity of confined aquifers, and generally range from 0.01 to 0.30 (Freeze and Cherry, 1979).

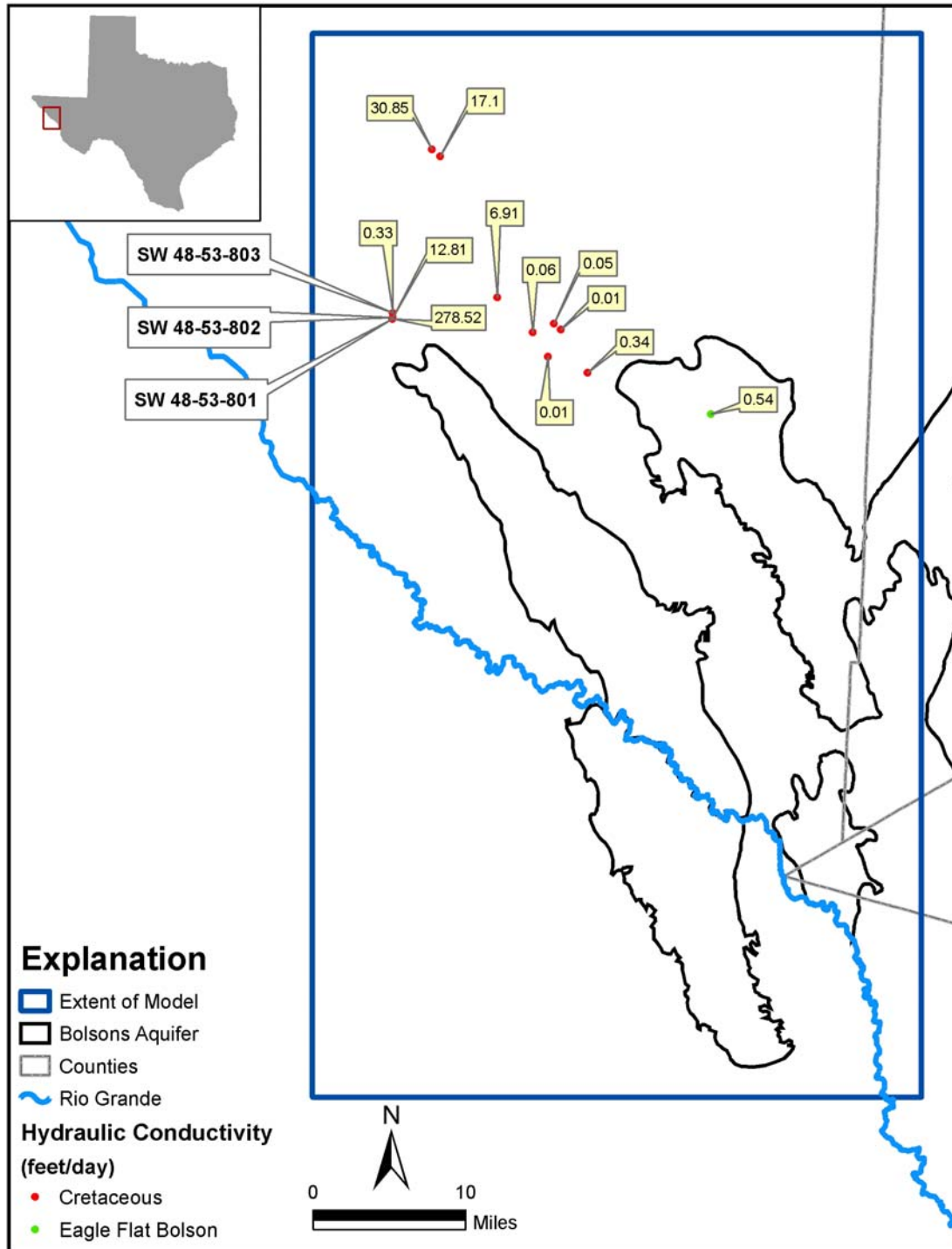


Figure 4.6.1 Hydraulic conductivity data in the model area

Table 4.5 Hydraulic property data from pumping tests

State Well Number	Layer	Reported Yield (gpm)	Test Yield (gpm)	Drawdown (ft)	Specific Capacity (g/m/ft)	Transmissivity (g/d/ft)	Aquifer Thickness (ft)	Hydraulic Conductivity (ft/d)	Data Source
4845602	Creataceous	210	300	11	15.00	30,000	130	30.85	TWDB GWDB
4845603	Creataceous		516	45	11.46	22,900	179	17.10	TWDB GWDB
4853801	Creataceous		75	3	25.00	37,500	18	278.52	TWDB GWDB
4853802	Creataceous		100	13	7.69	11,500	120	12.81	TWDB records
4853803	Creataceous	13	60	180	0.33	500	200	0.33	TWDB GWDB
4854503	Creataceous		200	29	6.90	13,800	267	6.91	TWDB GWDB
4854902	Creataceous		18	50	0.36	71	200	0.05	Darling Dissertation
4854903	Creataceous					77	160	0.06	Darling Dissertation
4854904	Creataceous					20	200	0.01	Darling Dissertation
4862301	Creataceous					18	200	0.01	Darling Dissertation
4863101	Creataceous					508	200	0.34	Darling Dissertation
4864502	Bolson					1,620	400	0.54	Darling Dissertation

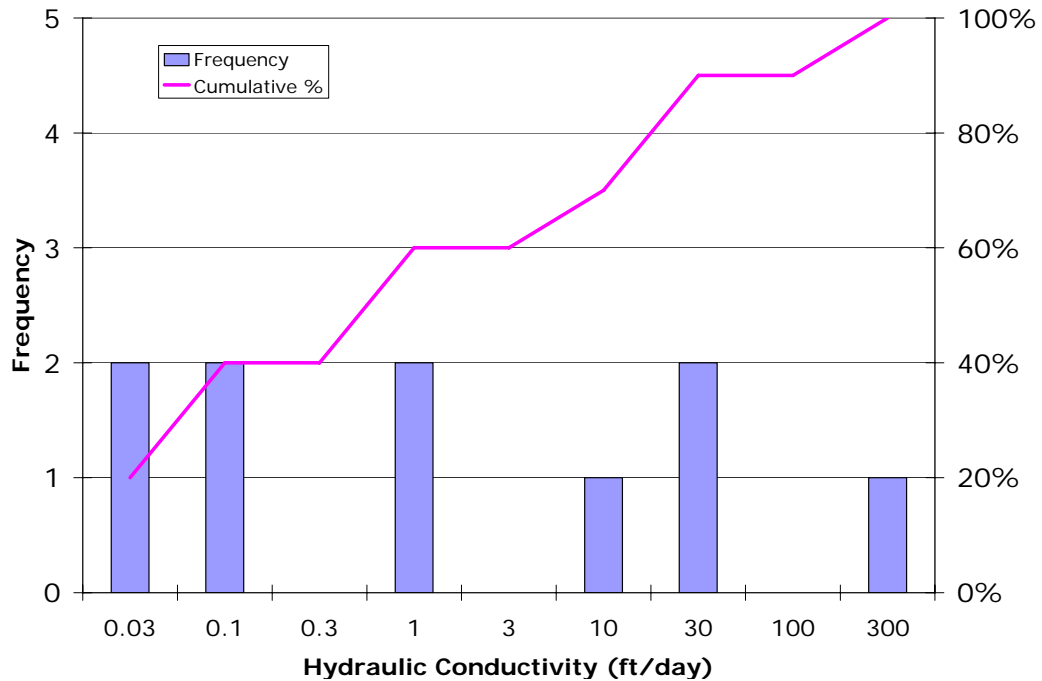


Figure 4.6.2 Histograms of hydraulic conductivity in the West Texas Bolsons Aquifer

4.7 Discharge

In Texas, total historical pumping, groundwater withdrawals by aquifer, and groundwater withdrawals by county are illustrated in Figures 4.7.1 through 4.7.3, respectively. Table 4.6 provides a summary of historical pumping by user group for each county in the model area.

In Figures 4.7.1 and 4.7.2, elevated levels of pumping in between 1980 and 1983 are attributed to above average irrigation activity in Hudspeth County. The trend of irrigation in Hudspeth County from 1980 to 1984 was because the irrigation survey showed surface water/groundwater mixed use in Red Light and Green River Valley in 1974 and 1979. However, the following survey in 1984 indicated farming had stopped in the study area. It is unknown what year farming ceased between 1979 and 1984. Rural-domestic pumping is proportionally distributed by rural population density (Figure 4.7.4).

Groundwater usage within the study area in Hudspeth County changed dramatically in the early 1980s. Irrigated agriculture accounts for approximately 64 percent of the total groundwater withdrawal between 1980 and 1997. Figure 4.7.5 indicates that during 1989 and 1994, there was no irrigated agriculture documented by TWDB. As can be seen in Figure 4.7.3, between 1980 and 1983, 85 percent of the total groundwater withdrawal within Hudspeth County was for irrigated agriculture. Irrigated agriculture ceased in the area after 1983. Between 1980 and 1997, irrigated agriculture in Presidio County accounted for approximately 1,000 acre-feet of pumping from within the extreme western portion of the county that lies within the study area, near the Rio Grande. No irrigated agriculture contributed to groundwater withdrawals in Jeff Davis or Culberson County within the study area.

Non-agricultural pumping is divided into municipal, livestock, manufacturing, and rural-domestic uses. The distribution of non-agricultural pumping between the major pumping types has remained fairly consistent for Hudspeth, Culberson, Jeff Davis, and Presidio Counties. Stock pumping accounts for approximately 60 percent of groundwater

withdrawals between 1984 and 1997 and rural-domestic pumping accounts for 31 percent of groundwater withdrawals between 1984 and 1997.

Livestock pumping accounts for 51 percent of total groundwater withdrawal in Culberson County, 99 percent in Jeff Davis County and 36 percent of groundwater withdrawals in Presidio County between 1980 and 1997. Livestock pumping accounts for approximately 10 percent of the groundwater withdrawals in Hudspeth County between the agriculturally irrigated period from 1980 to 1983. Between 1984 and 1997, livestock pumping accounts for approximately 57 percent of groundwater withdrawals in Hudspeth County.

In 1980, the city of Sierra Blanca pumped 74 acre-feet of groundwater for municipal use. After 1980, the city began receiving their water from Culberson County. Hudspeth County manufacturing pumping totaled approximately 23 acre-feet between 1980 and 1997.

Rural-domestic pumping accounts for 49 percent of total groundwater withdrawal in Culberson County, less than 1 percent in Jeff Davis County and 2 percent of groundwater withdrawals in Presidio County between 1980 and 1997. Rural-domestic pumping accounts for approximately 4 percent of the groundwater withdrawals in Hudspeth County between the agriculturally irrigated period from 1980 to 1983. Between 1984 and 1997, rural-domestic pumping accounts for approximately 43 percent of groundwater withdrawals in Hudspeth County.

Pumping estimates of groundwater withdrawals were determined from the historical water use inventories provided by the TWDB. The spatial distribution of the water use inventories was determined by land use and well locations.

There is no information available regarding the quantity of cross-formational flow or baseflow to streams. Discharge to springs was discussed in Section 4.7, but we did not locate any information regarding the variability of springflow.

In an effort to assess irrigation pumping in Mexico south of Red Light Draw, we reviewed the pumping permit database from the Comisión Nacional del Agua (CONAGUA).

(<http://siga.cna.gob.mx/ArcIMS/Website/REPDA/Localizador/viewer.htm>) Several permits were found in the model area but the accuracy of the data could not be verified and the clarity of the units for the pumping rates was uncertain. In addition, it was uncertain whether the amount permitted by the Mexican government was actually pumped from each well. There is also little data on well completion in this area. In order to perform a proper calibration in this area, good estimates of production and transient water levels would be required, and because neither of these were available, the pumping data from Mexico was not incorporated into the model.

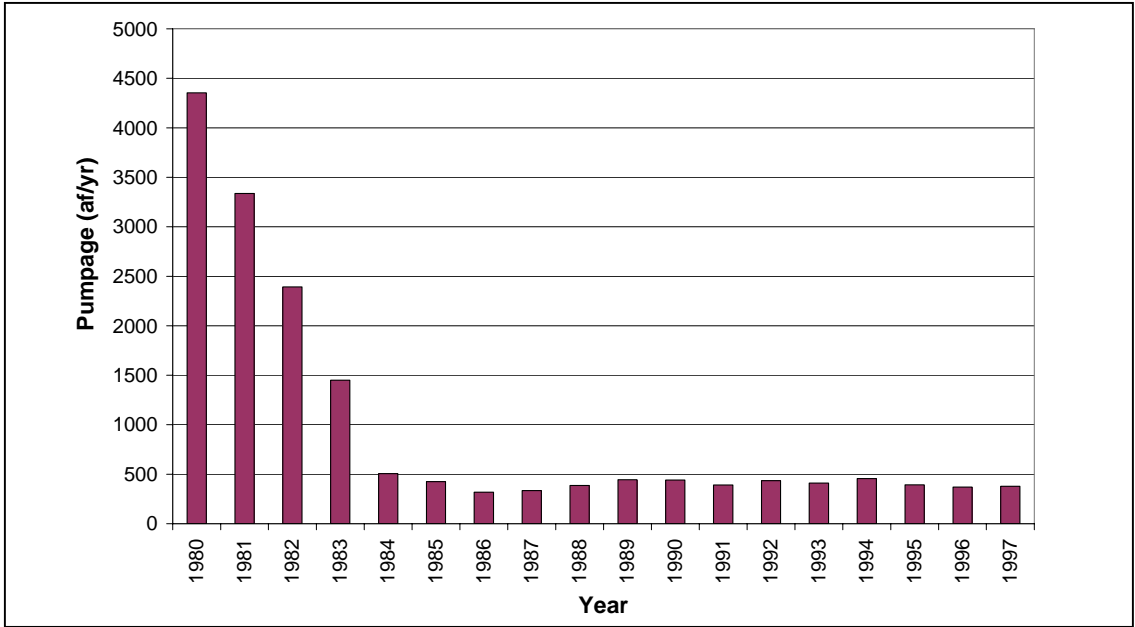


Figure 4.7.1 Total pumping in the study area

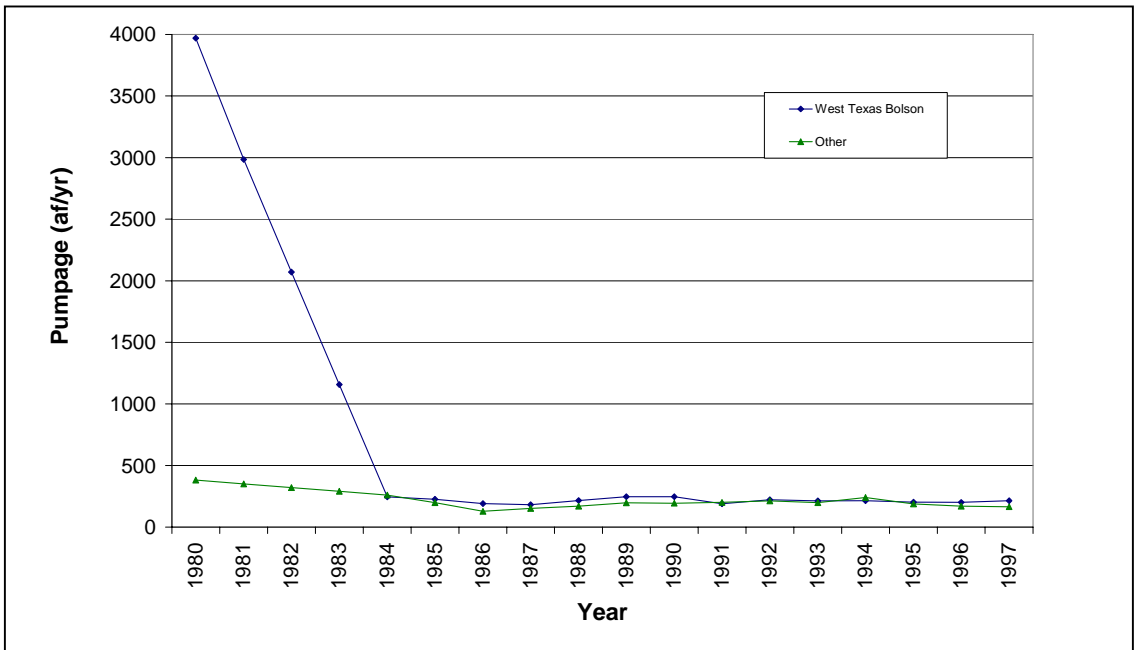


Figure 4.7.2 Total pumping by aquifer

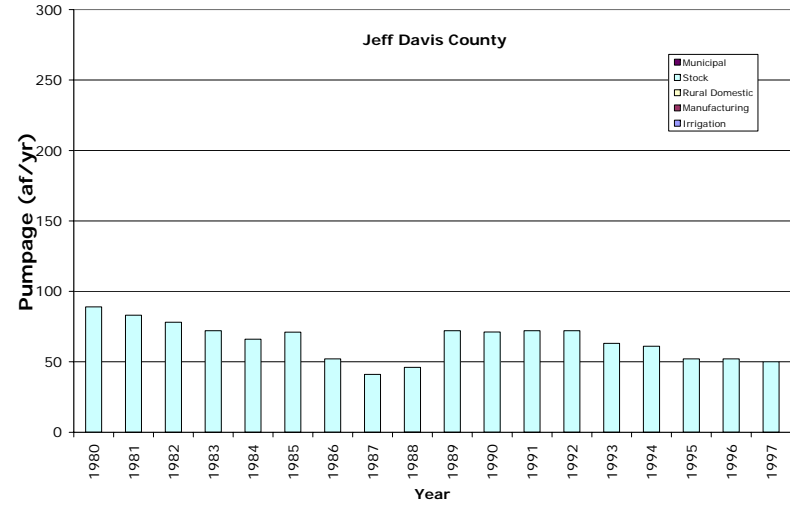
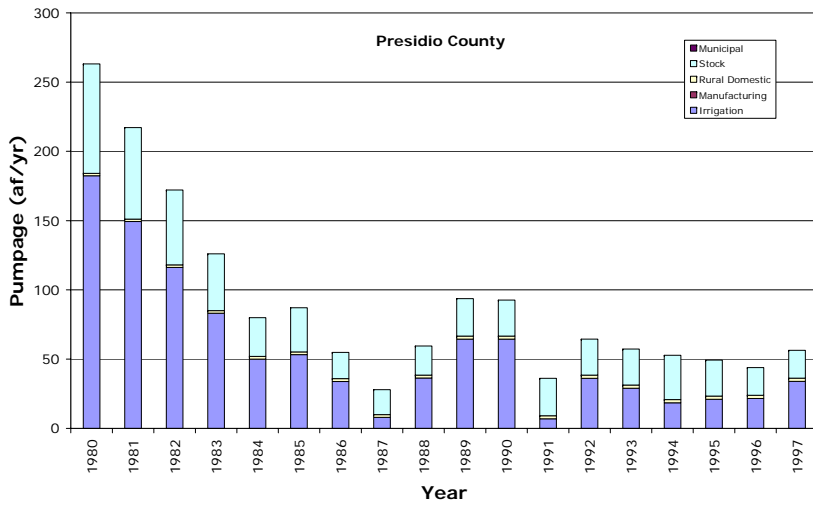
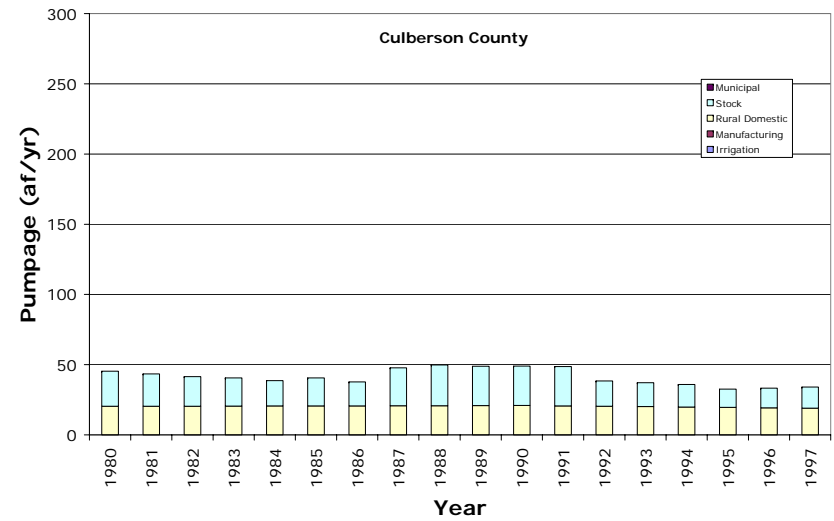
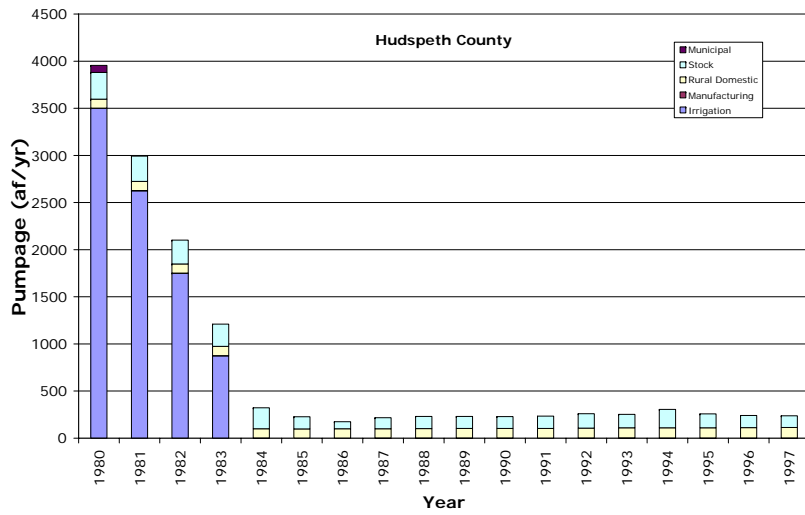


Figure 4.7.3 Total pumping for portion of the county in the study area by county and type

Table 4.6 Historical pumping by user group and county

County	Type	1980	1981	1982	1983	1984	1985	1986	1987	1988	1989	1990	1991	1992	1993	1994	1995	1996	1997	
CULBERSON	Irrigation	0	0	0	0	0	0	0	0	0	0	0	0	0	0	0	0	0	0	
	Manufacturing	0	0	0	0	0	0	0	0	0	0	0	0	0	0	0	0	0	0	
	Rural Domestic	20	20	20	21	21	21	21	21	21	21	21	21	21	20	20	20	20	19	19
	Stock	25	23	21	20	18	20	17	27	29	28	28	28	18	17	16	13	14	14	15
	Municipal	0	0	0	0	0	0	0	0	0	0	0	0	0	0	0	0	0	0	0
	TOTAL		45	43	41	41	39	41	38	48	50	49	49	49	38	37	36	33	33	34
HUDSPETH	Irrigation	3500	2625	1750	875	0	0	0	0	0	0	0	0	0	0	0	0	0	0	
	Manufacturing	1	3	1	1	1			1	1	1	1	0	3	3	2	2	1	1	
	Rural Domestic	96	96	97	98	98	99	100	100	101	102	102	104	105	107	108	110	111	113	
	Stock	283	268	253	237	222	128	75	117	130	128	126	130	152	144	196	147	129	125	
	Municipal	74	0	0	0	0	0	0	0	0	0	0	0	0	0	0	0	0	0	
	TOTAL		3954	2992	2101	1211	321	227	175	218	232	231	229	234	260	254	306	259	241	239
JEFF DAVIS	Irrigation	0	0	0	0	0	0	0	0	0	0	0	0	0	0	0	0	0	0	
	Manufacturing	0	0	0	0	0	0	0	0	0	0	0	0	0	0	0	0	0	0	
	Rural Domestic	0	0	0	0	0	0	0	0	0	0	0	0	0	0	0	0	0	0	
	Stock	89	83	78	72	66	71	52	41	46	72	71	72	72	63	61	52	52	50	
	Municipal	0	0	0	0	0	0	0	0	0	0	0	0	0	0	0	0	0	0	
	TOTAL		89	83	78	72	66	71	52	41	46	72	71	72	72	63	61	52	52	50
PRESIDIO	Irrigation	182	149	116	83	50	53	34	8	36	64	64	7	36	29	18	21	22	34	
	Manufacturing	0	0	0	0	0	0	0	0	0	0	0	0	0	0	0	0	0	0	
	Rural Domestic	2	2	2	2	2	2	2	2	2	2	2	2	2	2	2	2	2	2	
	Stock	79	66	54	41	28	32	19	18	21	27	26	27	26	26	32	26	20	20	
	Municipal	0	0	0	0	0	0	0	0	0	0	0	0	0	0	0	0	0	0	
	TOTAL		263	217	172	126	80	87	55	28	59	94	93	36	64	57	53	49	44	56

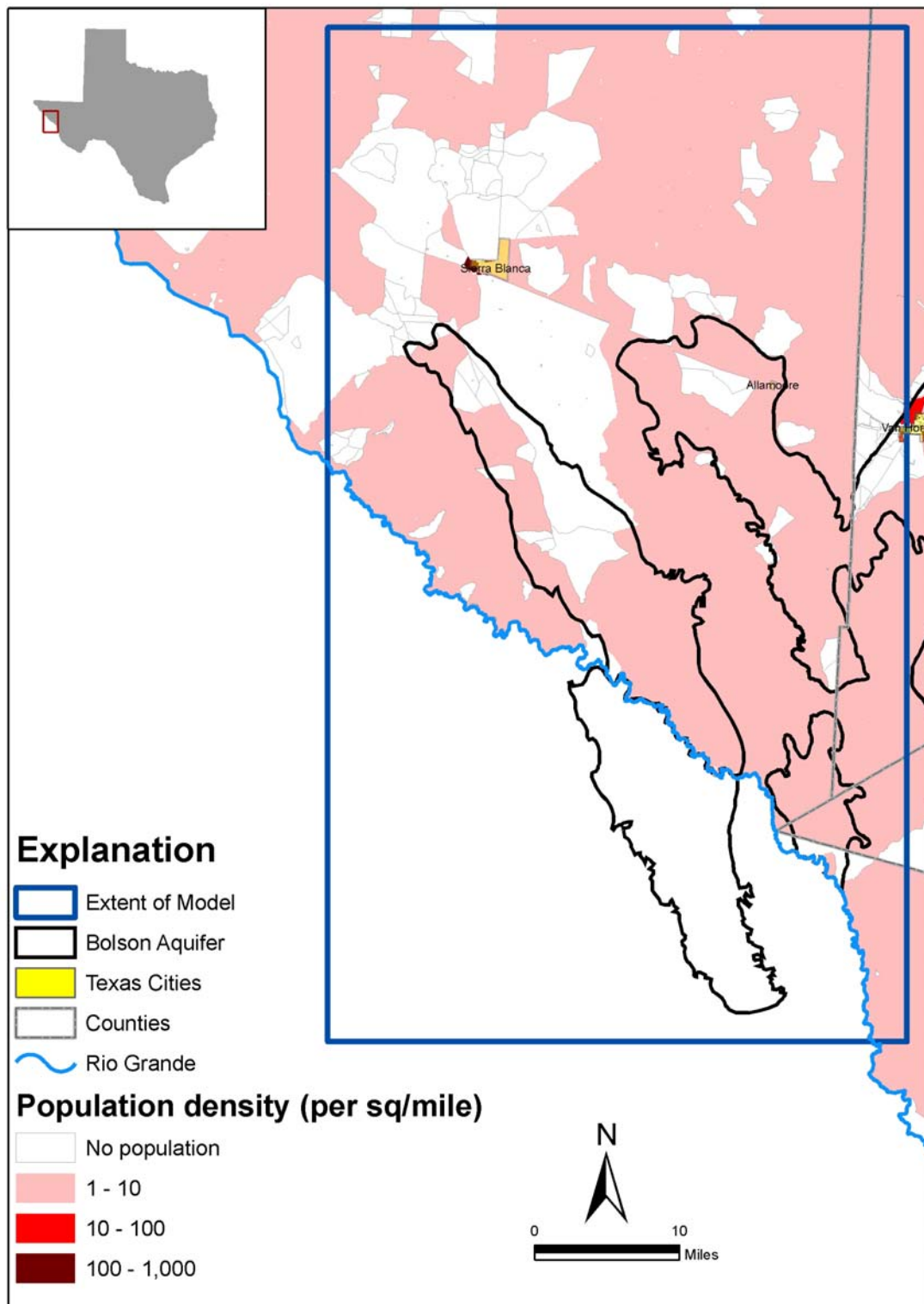


Figure 4.7.4 Population density in 1990 and 2000

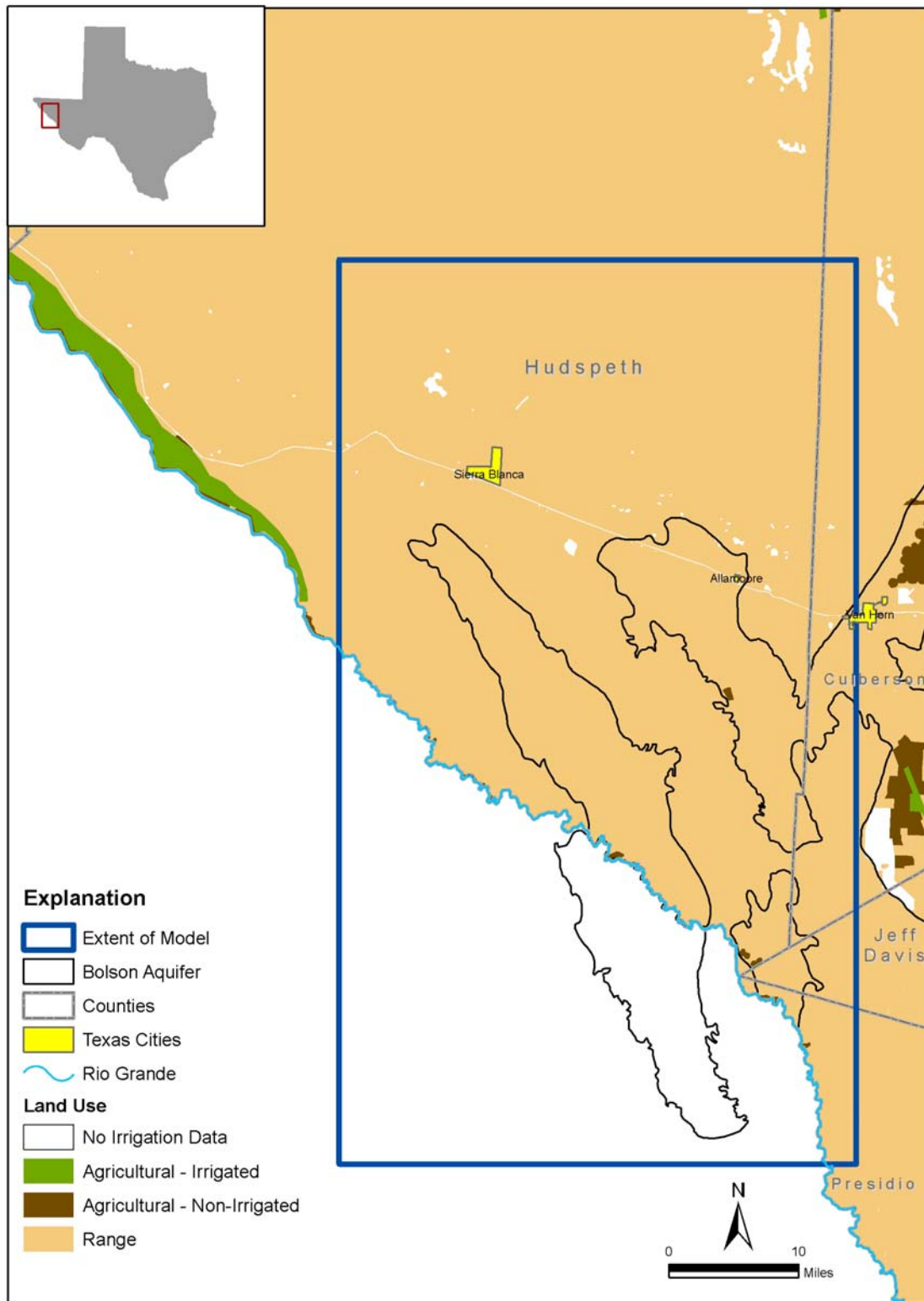


Figure 4.7.5 Irrigated land in 1989 and 1994

4.8 Water Quality

The quality of groundwater in the West Texas Bolsons aquifer was evaluated to help potential users of the model assess the quality of available groundwater. Water-quality data was compiled from the TWDB groundwater database and the Texas Commission on Environmental Quality (TCEQ) public water-supply well database. The main parameter of interest for this study is total dissolved solids (TDS). Several other parameters may be of interest from the standpoint of water quality for drinking-water supplies, including nitrate. A summary of the available data for these parameters is included below.

TDS is a measure of the salinity of groundwater, and is the sum of the concentrations of all of the dissolved ions, mainly sodium, calcium, magnesium, potassium, chloride, sulfate, and bicarbonate. The TWDB has defined aquifer water quality in terms of dissolved-solids concentrations expressed in milligrams per liter (mg/L) and has classified water into four broad categories:

- fresh (less than 1,000 mg/L);
- slightly saline (1,000 - 3,000 mg/L);
- moderately saline (3,000 - 10,000 mg/L); and
- very saline (10,000 - 35,000 mg/L).

Based on these broad categories, the groundwater from the wells in the model area is generally classified as fresh to slightly saline. The groundwater in this area is generally fresh, but over one third of samples contain TDS measurements greater than 1000 mg/L. Figure 4.8.1 illustrates the distribution of TDS in wells, and indicates that most of the West Texas Bolsons aquifer water is fresh, with TDS less than 1,000 mg/L. Circles indicate the wells that are screened in bolson aquifers and the wells screened in other aquifers are indicated by triangles. The color of the symbol indicates the TDS measurement in the well. The highest TDS concentrations occur along the Rio Grande and in the northwestern area of the Eagle Flat Bolson.

A total of 134 water sample results were assimilated for the analysis of groundwater quality. A summary of the available data for parameters of interest from a standpoint of

drinking water quality and irrigation is included in Table 4.7. This table includes parameters and screening levels for primary and secondary maximum contaminant levels (MCL) as well as irrigation hazards. The table indicates that there are several results that exceed the MCL screening level, including 38% of nitrate results, and one of nine results for arsenic (11%), 33% of the sulfate results, and 37% of the results for TDS.

Iron also exceeds the secondary MCLs for about one third of the results. Fluoride is also above the secondary MCL in 43% of the 46 samples that have been analyzed.

With regard to guidance on irrigation water, 22% of the results are at the medium screening level for the sodium adsorption ratio (SAR) and 9% are very high. Chloride concentrations exceed the irrigation guidance standard of 1000 mg/L in 16% of the samples analyzed.

Table 4.7 Water quality constituents and MCLs

Constituent	Type of Standard*	Screening Level	Units	Number of Results	Number of Results Exceeding Screening Level	Percent of Results Exceeding Screening Level
Fluoride	Primary MCL ¹	4	mg/L	46	1	2%
Nitrate	Primary MCL ¹	10	mg/L as N	48	18	38%
Arsenic	Primary MCL ¹	10	µg/L	9	1	11%
pH	Secondary MCL ¹ (lower bound)	7		59	50	85%
Chloride	Secondary MCL ¹	300	mg/L	58	16	28%
Fluoride	Secondary MCL ¹	2	mg/L	46	20	43%
Sulfate	Secondary MCL ¹	300	mg/L	58	19	33%
Manganese	Secondary MCL ¹	300	µg/L	9	0	0%
Iron	Secondary MCL ¹	50	µg/L	16	5	31%
TDS	Secondary MCL ¹	1000	mg/L	54	20	37%
SAR	Irrig. Sodium Hazard - Medium ²	10		54	12	22%
SAR	Irrig. Sodium Hazard - High ²	18		54	8	15%
SAR	Irrig. Sodium Hazard - Very High ²	26		54	5	9%
Specific Conductance	Irrig. Salinity Hazard - High ²	750	µmhos/cm	37	25	68%
Specific Conductance	Irrig. Salinity Hazard - Very High ²	2250	µmhos/cm	37	13	35%
Chloride	Irrig. Hazard ³	1000	mg/L	58	9	16%

1. 30 TAC Section 290 SubSection F
2. United States Salinity Laboratory (1954)
3. Tanji (1990)

Darling (1997) conducted a detailed analysis of the geochemistry of groundwaters of the Eagle Flat, Red Light, and Green River Bolsons. He identified four major hydrochemical facies – three of which are traceable to the reaction of groundwater with carbonate rocks and silicates such as albite, pyroxene, or amphibole, and to cation exchange reactions. Darling attributed the evolution of the fourth facies to the dissolution of gypsum and halite. Darling described the four facies as follows:

Type 1: calcium-bicarbonate and mixed-cation-bicarbonate;

Type 2: sodium-mixed-anion to mixed-cation-mixed-anion;

Type 3: sodium-bicarbonate; and

Type 4: sodium-chloride to sodium-sulfate and mixed-cation-sulfate.

The different facies above are summarized below with respect to TDS ranges and median TDS concentrations (Darling, 1997) in Table 4.8.

Table 4.8 Groundwater facies (after Darling, 1997)

Groundwater Facies	TDS Range (mg/L)	Median TDS (mg/L)
Type 1	374 to 782	561
Type 2	603 to 1,452	816
Type 3	259 to 1,203	423
Type 4	1,072 to 16,174	3,913

Except in the alluvium and from thermal springs discharging where the Rio Grande truncates the southernmost Quitman Mountains, the Red Light system is characterized primarily by Types 1 through 3. Type 4 groundwater is the norm for the shallow wells and springs near the river. Type 3 is typical of the Allamoore and Green River systems, and Types 1 and 2 are found in the Precambrian rocks which lie to the north of the Eagle Flat groundwater divide. West of that divide, groundwater of the Sierra Blanca system is dominantly Type 4.

5.0 CONCEPTUAL MODEL OF FLOW IN WEST TEXAS BOLSONS AQUIFER

5.1 Conceptual model

Sections 2 through 4 document and summarize available hydrologic and hydrogeologic data for the study area. While it is evident that there is still much to learn about the aquifer system, the assimilated data provide a foundation for developing a more quantitative understanding of the aquifers and a numerical model that can be improved as more data become available.

A groundwater conceptual model of an aquifer represents the foundation for the numerical model. The conceptual model describes the basic structure of the flow system, the hydrologic processes that are important to the water budget of the system, the occurrence and movement of groundwater, and the inflow and outflow components. Anderson and Woessner (1992) describe a conceptual model as “a pictorial representation of the groundwater flow system, frequently in the form of a block diagram or a cross section.” The conceptual model for the West Texas Bolsons aquifer system provides a regional perspective of the aquifer system dynamics, which is consistent with the objectives of the WTBGAM.

Figure 5.1.1 provides a schematic of the conceptual model for the WTBGAM. The diagram shows the relationship between the three major hydrostratigraphic units in the aquifer system in a block-form schematic. The diagram shows the geologic units that are a part of the flow system: the bolson aquifers, which are designated as Layer 1, and the underlying water-bearing units, including the Cretaceous and Paleozoic age rocks, as well as the Tertiary Igneous intrusions and other units. Because of the geologic complexity of the area caused by faulting and igneous intrusions, it is difficult to identify and isolate distinct hydrogeologic Layers that extend across the model area. For this reason, the stratigraphy has been lumped or combined for all of the underlying rocks and then divided into two Layers (model Layers 2 and 3) during model construction.

All of the hydrostratigraphic units are connected and under natural conditions, the combination of the driving force caused by higher heads in recharge areas, variable hydraulic properties, and the location of discharge areas determines groundwater movement. Aquifer pumping does not affect flow patterns significantly in the basin.

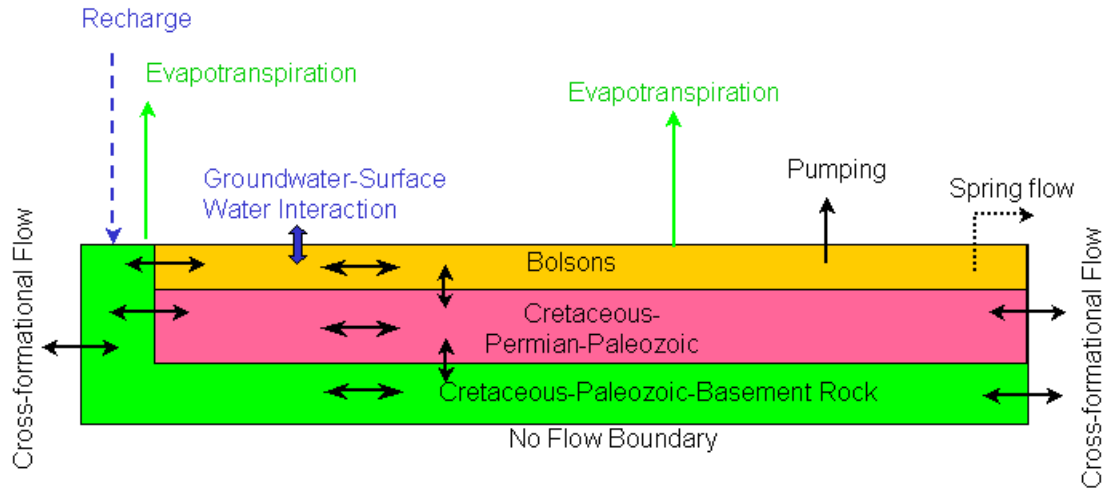


Figure 5.1.1 Schematic of conceptual model for the WTBGAM

The assessment of recharge in the study area is based on the distribution of recharge and the understanding of groundwater flow between the various hydrostratigraphic units. Direct recharge to the higher elevation areas moves downward through Cretaceous and Permian rocks until it reaches a lower permeability Layer. The combination of lower permeability units and perennial recharge is evidenced by the higher water levels in the mountainous areas. A small amount of the water that recharges the mountainous areas is lost from the aquifer system as evapotranspiration, streamflow, and pumping (where wells exist). A portion of the recharge moves laterally, and some of it discharges as groundwater underflow to the bolson aquifers, to other rocks of higher permeability, or as spring flow outside the model area.

Direct recharge to the higher elevation areas constitutes a significant portion of the recharge to the study area and contributes to deep circulation of groundwater through

regional Cretaceous and Permian aquifers. Infiltration of storm-water runoff occasionally occurs in streambed alluvium and on alluvial fans along the perimeter of the bolsons.

The hydraulic properties and the variability of these properties throughout the system also play a role in determining the movement of groundwater. In addition, the hydrogeologic structural controls in the system help determine both regional and local flow components and natural discharge locations (springs and streams).

Evapotranspiration is a major force in the hydrologic system and mainly impacts the water budget of the unsaturated zone (above the water table) and functions to limit recharge to a small percentage of precipitation. However, groundwater evapotranspiration is very limited due to depth of the water table and vegetation. In a few areas where the water table is close to land surface, direct evapotranspiration from the water table may be a factor in the saturated zone water budget on a local level. There has not been enough pumping in the model area to provide insight into long-term aquifer responses.

6.0 MODEL DESIGN

A numerical groundwater flow model uses a computer code to simulate groundwater flow based on data developed for the conceptual model. Design of the numerical model consists of choosing a computer modeling code, developing a model grid (horizontal extent and vertical Layers), assigning model parameters and stresses, and determining boundary conditions, types and values in the model grid. Each of these components of model design and their implementation are described in this Section.

6.1 Code and Processor

The TWDB selected the MODFLOW-2000 (Hill, Banta, and Harbaugh, 2000) to be used for the West Texas Bolson GAM. MODFLOW-2000 is a multi-dimensional, finite-difference, block-centered, saturated groundwater flow code that is supported by a variety of boundary condition packages to handle recharge, streams, drainage, ET, and wells. Some of the benefits of using MODFLOW are (1) MODFLOW is the most widely accepted groundwater flow code in use today, (2) MODFLOW was written and is supported by the United States Geological Survey (USGS) and is public domain, (3) MODFLOW is well documented (McDonald and Harbaugh, 1988; Harbaugh and McDonald, 1996), (4) there are several graphical user interface programs written for use with MODFLOW, and (5) MODFLOW has a large user group.

Groundwater Vistas (Version 5, Rumbaugh and Rumbaugh, 2007) was used to develop the MODFLOW datasets. The model was developed and executed on x86 compatible (i.e. Pentium class) computers equipped with the Windows XP operating system. The type of computer and memory required to use the model will vary depending on the type of operating system and pre- and post-processing software that is used. For this model, the GMG linear equation solver package was used (Wilson and Naff, 2004) for the final models.

6.2 Model Layers and Grid

Based on the conceptual hydrostratigraphy described in Section 4 and the conceptual flow model detailed in Section 5, three model Layers were used to simulate regional flow in the West Texas Bolson GAM. This conceptualization is consistent with that of the GAM for the Igneous and Bolson aquifers located just east of the model area, as shown in Figure 2.1.2 and described by Beach and others (2004). Vertical discretization of this complex system was difficult because the elevation of the contacts between the conceptualized hydrogeologic units varies significantly over short distances and across the modeled area. In addition, due to the faulting and complex geology, it was impossible to follow the Layering concepts used in the MODFLOW formulation without simplifying the hydrogeologic setting. Each of the model Layers is described below in the order which MODFLOW numbers the model Layers, which is from top (nearest to ground surface) to bottom.

Figure 6.2.1 schematically depicts how the complex geology was simplified for the MODFLOW model. Layer 1 represents the bolson aquifer and is only active in those areas where the bolson deposits are present. Layers 2 and 3 represent the Cretaceous, Paleozoic, Tertiary, Permian and other units in the model area (green, blue, and red formations in Figure 6.2.1). Because of the complexity of the hydrogeology and the uncertainty regarding exact elevations of geologic contacts and hydraulic properties of various hydrogeologic units throughout the model area, the total thickness of the underlying rocks was split between Layer 2 and 3. The dashed line in Figure 6.2.1 shows the approximate division between the Layer 2 and 3.

The base elevation and thickness of the bolson deposits in west Texas as well as the base of the sub-bolson units were discussed in Section 2.5 and Section 4 (Figures 4.2.1 through 4.2.3) to illustrate the geology and hydrostratigraphy of this aquifer system. As mentioned in these previous Sections, thickness and contact elevations of each hydrostratigraphic unit were taken directly from contour maps that were developed from geophysical data, so no control points were used.

Figures 6.2.2 and 6.2.3 show the total thickness and elevation of the base of Layer 2, respectively. Layers 2 and 3 represent all of the formations underlying the bolson deposits above the Precambrian basement rock. The thickness of Layer 3 is shown in Figure 6.2.4, and as discussed above, the base elevation of Layer 3 is shown in Figure 4.2.3. As can be seen in Figures 6.2.2 and 6.2.4, the maximum thickness of both Layers 2 and 3 is about 7,500 feet. As previously mentioned, these two figures indicate that the thickness of the underlying units increases very quickly from the northeast to the southwest due to the affect of the Rio Grande rift. Figure 6.2.3 shows the elevation at which these two Layers were divided which is now the base of Layer 2. Table 6.1 illustrates how Layers 2 and 3 represent the Tertiary, Cretaceous, Jurassic, Permian and the undivided Cretaceous-Paleozoic units at different locations in the model area.

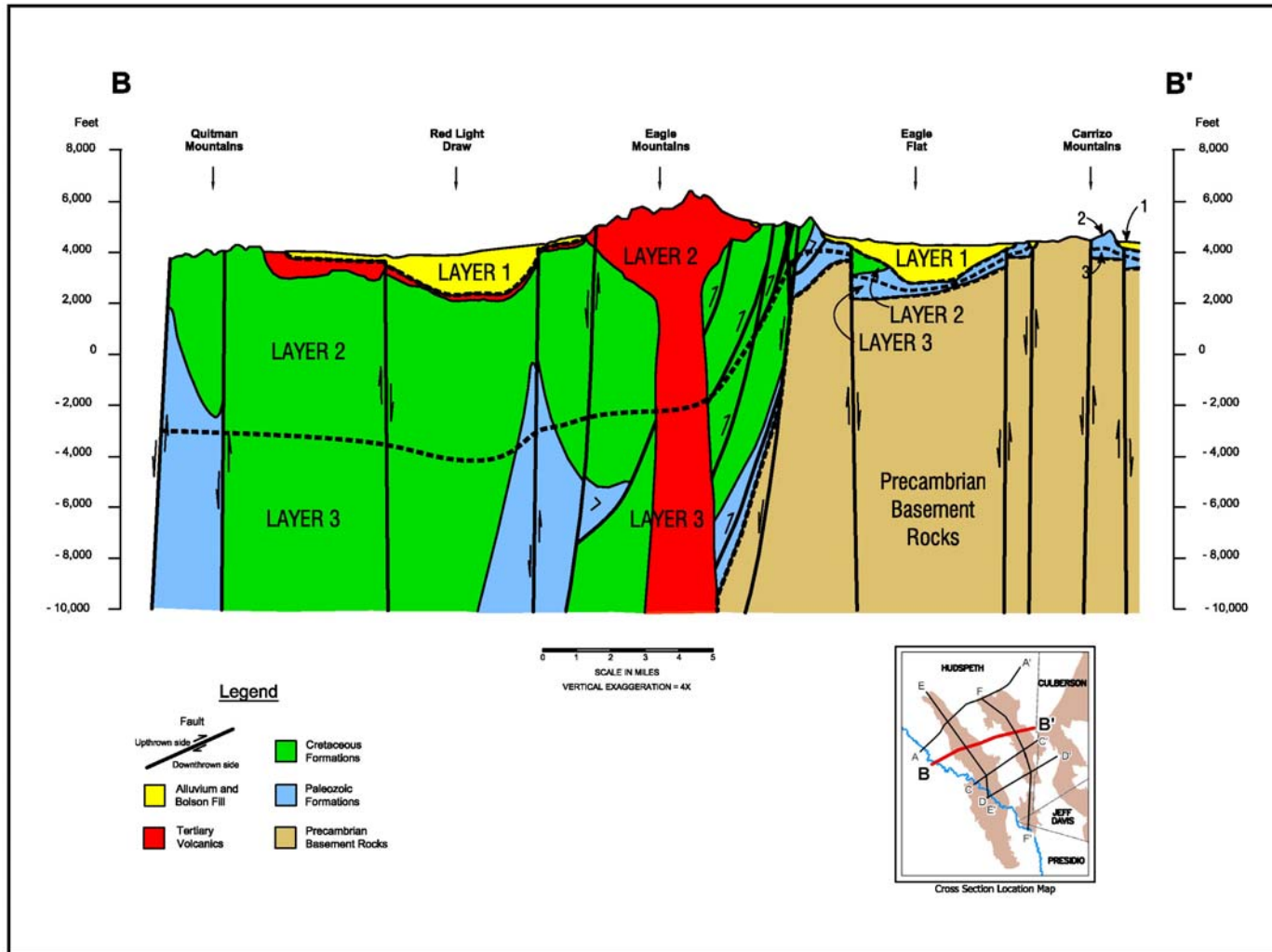


Figure 6.2.1 Model schematic and Layer representation

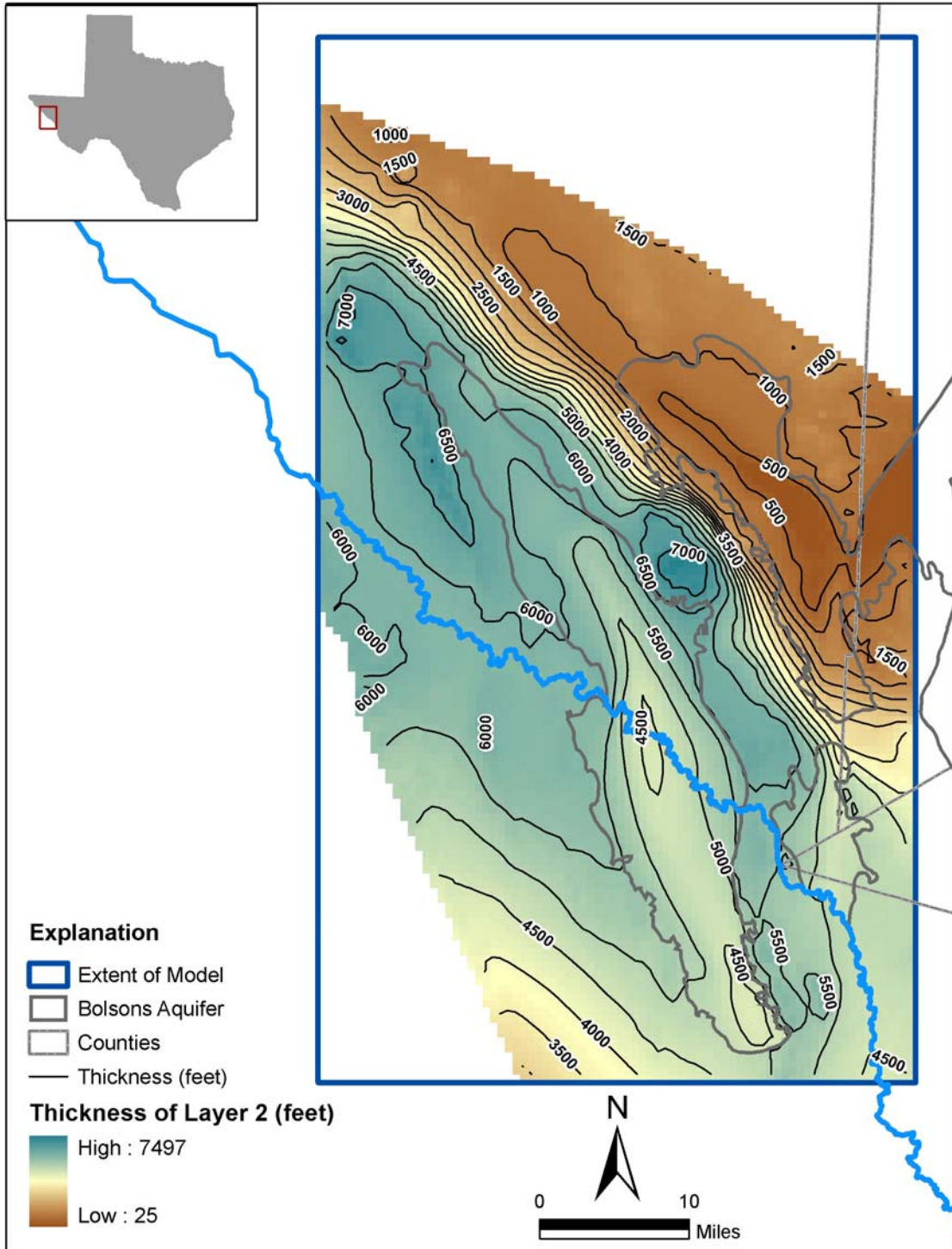


Figure 6.2.2 Thickness of Layer 2

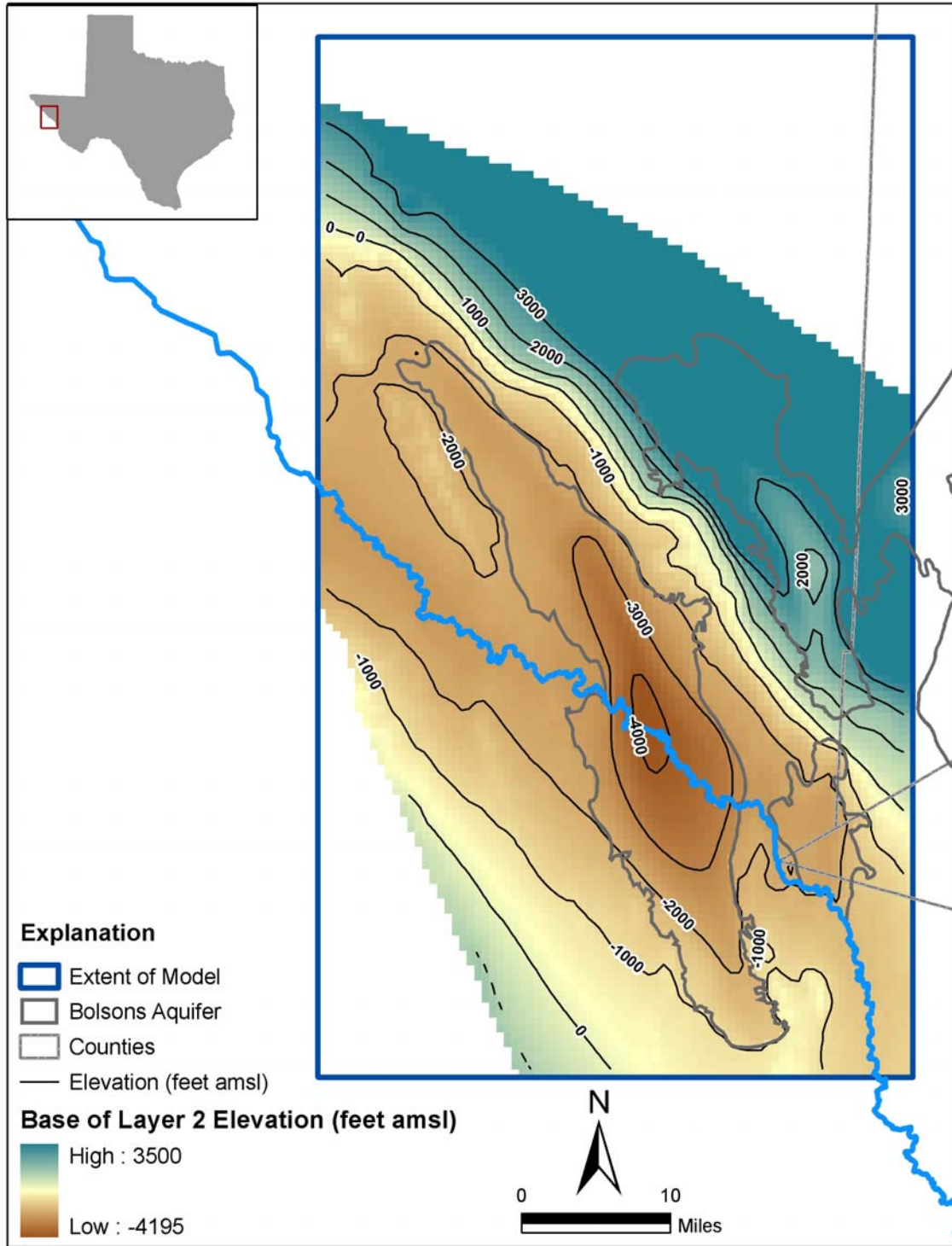


Figure 6.2.3 Elevation of the base of Layer 2

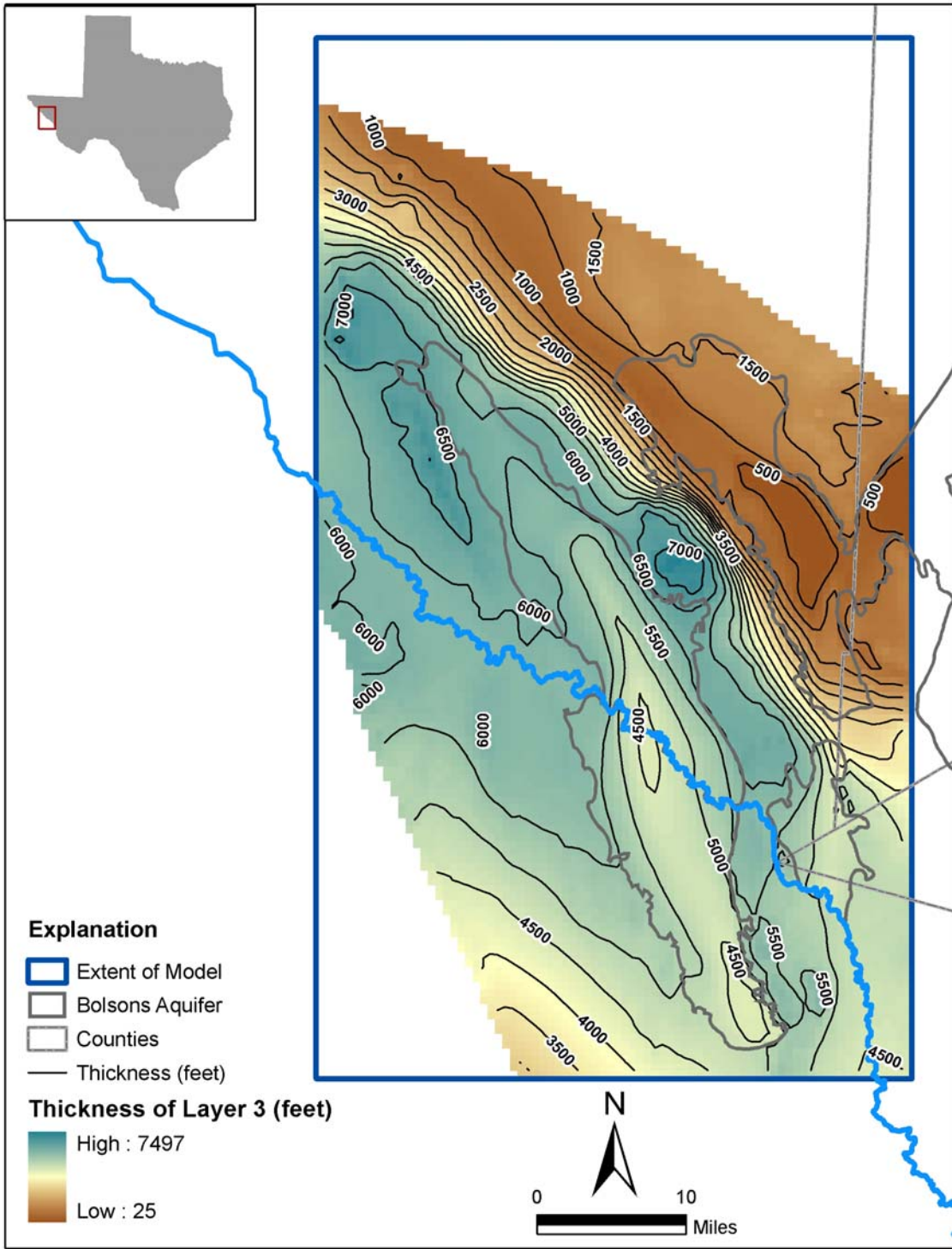


Figure 6.2.4 Thickness of Layer 3

Table 6.1 Generalized stratigraphic units

SYSTEM	STRATIGRAPHIC UNITS	MODEL LAYER	
Quaternary	Young Quaternary deposits	1	
	Windblown sand		
	Old Quaternary deposits		
	Bolson deposits		
Tertiary	Volcanic rocks undivided	2	
	Intrusive Igneous rocks		
	Chambers Tuff		
	Garren Group		
	Tarantula Gravel		
	Hogeye Tuff		
	Trachyte Porphyry		
	Upper Rhyolite		
	Pantera Trachyte		
	Cretaceous		Cretaceous undivided
Buda Limestone			
Eagle Mountain Sandstone			
Espy Limestone			
Benevides Formation			
Finlay Limestone			
Cox Sandstone			
Bluff Mesa Formation			
Yucca Formation			
Etholean Conglomerate			
Torcer Formation			
Jurassic		Malone Formation	
Permian		Hueco Limestone	
Cretaceous-Paleozoic			
Precambrian	Carrizo Mountain Group	Not included	
	Precambrian bedrock undivided		

Stratigraphic nomenclature from Univ. of Texas, Bureau of Economic Geology: Van Horn-El Paso and Marfa Geologic Atlas Sheets.

As shown in Figure 6.2.5, a rectangular grid covers the model area. The model area extends laterally on the north to the Diablo Plateau. The southern boundary of the model is roughly defined by the southern extent of the bolson deposits across the Rio Grande from Red Light Draw. This area was included in the model to insure that the model could appropriately represent groundwater flow beneath the Rio Grande if the model is used to simulate large groundwater withdrawals on either side of the Rio Grande.

Flow models are generally aligned so that one axis of the model grid is parallel to the primary direction of groundwater flow. Because of the radial flow from the highest elevations in the Eagle Mountains and the variations in the orientation of the bolson aquifers, this was difficult to do for this model. Therefore, the model grid was oriented in the north-south direction with no rotation. The model grid origin (the lower left-hand corner of the grid) is located at GAM Coordinates (3195300,19417000).

The grid cells are square with a uniform dimension of ½-mile on each side and contain ¼ square mile or 160 acres. The model has 140 rows and 80 columns, totaling 11,200 grid cells per Layer. Only those cells overlaying part of the aquifer that the Layer represents have to be active cells. Layers 1, 2, and 3 contain 1331, 8289, and 8289 active cells, respectively, totaling 17909 active cells for the entire model.

Active cells in Layer 1 do not extend to the full extent of the bolson aquifer in some areas because some of the cells near the boundaries of each of the basins have a relatively small saturated thickness (generally less than 50 feet). It is helpful to note that the general outline of the aquifers as designated by TWDB was based largely on surface geology. Therefore, it is not surprising that some areas of the bolsons are either unsaturated or have a very thin saturated thickness. The cells with small saturated thickness continually caused problems during model calibration because they would cause instabilities for the MODFLOW solvers, resulting in mass balance errors in or near these cells. Therefore, to alleviate this problem, many of the cells with small saturated thickness were inactivated.

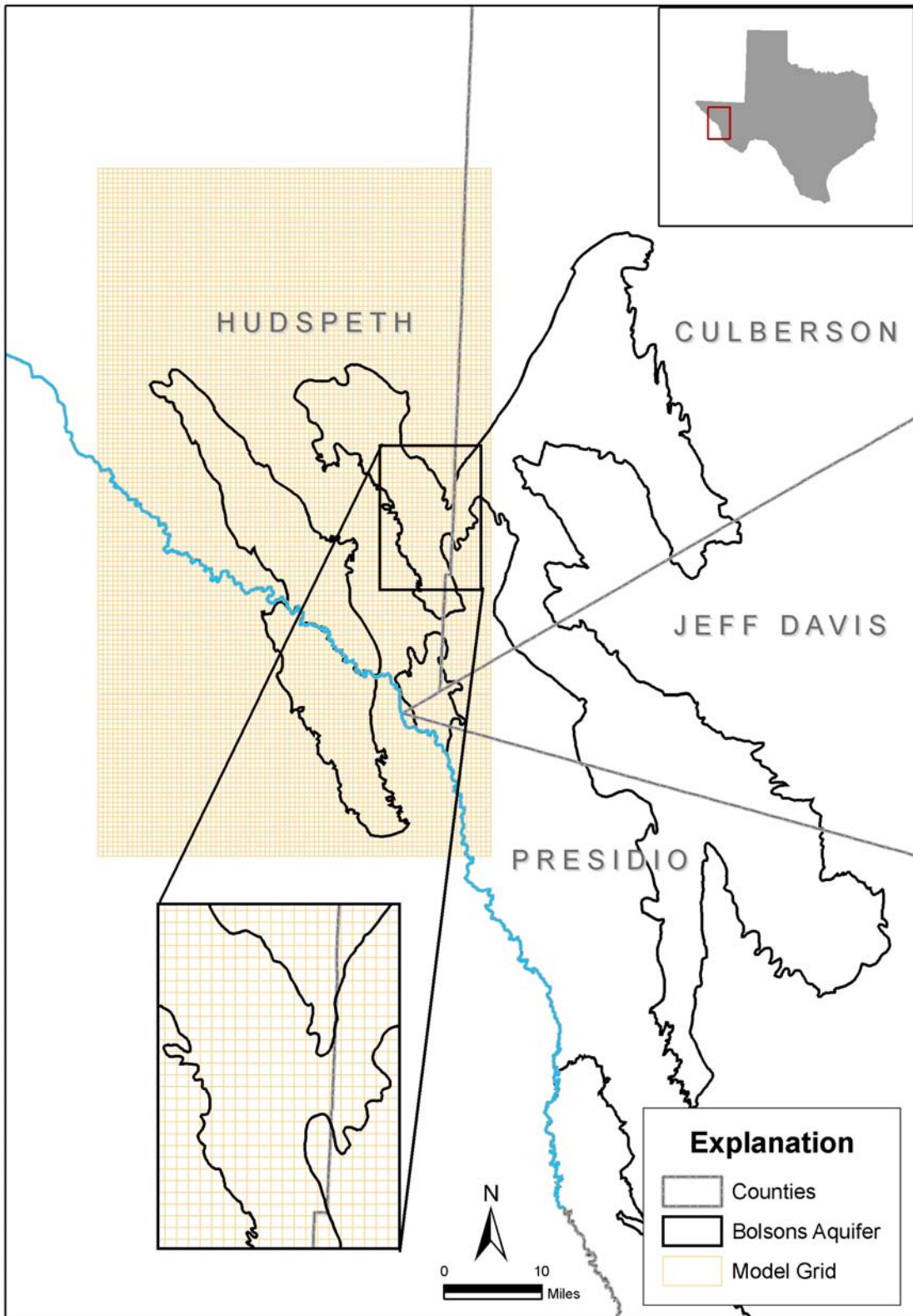


Figure 6.2.5 Model grid

6.3 Model Parameters

Model parameters include the hydraulic properties of the aquifer(s) modeled. These parameters provide information about the characteristics of the aquifer that determine how water moves through it. Hydraulic conductivity is one of the most important parameters to be estimated and distributed across the model because in part, it determines how fast water will flow in the system and how much groundwater wells can produce. The storage coefficient is important in determining the volume of water in storage and the rate of water level change when the aquifer is pumped.

6.3.1 Hydraulic Conductivity

As discussed in Section 4.6, there are only a small number of hydraulic conductivity estimates in the model area and only one in the bolson aquifer. The bolson estimate is located in northwest Eagle Flat and is most likely more representative of the underlying rocks than of the alluvium fill. In determining the utility of locally determined hydraulic conductivity estimates (generally, from pump and specific capacity tests), it is important to consider the nature of the aquifer and the type of rocks which make up the aquifer. Although a pumping test can be used to estimate local scale hydraulic conductivity, it is still small in scale by comparison to the regional flow system. The effective hydraulic conductivity that is incorporated into the model depends on the geometry, hydraulic conductivity, and the scale at which variations in hydraulic conductivity occurs.

In the model development process, it was assumed that the available hydraulic conductivity and transmissivity estimates typically represent the highest permeability porous media tested and that these estimates could be used as a guide for estimating effective model hydraulic conductivity. However, direct estimates of vertical hydraulic conductivity meaningful to the general modeling process are almost never available, and that is true for this study. The distribution and estimated values of vertical hydraulic conductivity for the model, while guided by available data, are usually determined mainly through the model calibration process. This can lead to non-unique parameterization and introduces a degree of uncertainty into the model results. The type and amount of

available calibration data (water level measurements and discharges) and the degree to which it is implemented usually determine the degree of success in reducing this uncertainty. For this study, there was very little information regarding vertical head differences in the different aquifers being simulated. This lack of data is not uncommon, but it does limit the calibration process with respect to the level of certainty in model parameters.

This aquifer is a complex fractured and Layered system. Hydraulic conductivity estimates from short duration pumping tests are very helpful in estimating local scale hydraulic conductivity, but the estimates are likely to be biased toward high values for several reasons. First, pumping tests are not performed in “dry boreholes”. Second, pumping tests are usually not performed in wells which don’t produce much water. These biases are enough to skew the estimates of hydraulic conductivity. In addition, the connection of the fracture network on a regional basis is unknown, and many surface water and groundwater interactions are controlled by more local hydrogeologic structures. These local structures may not be represented in the data or the conceptual model, nor can they be incorporated into the numerical model at the regional scale. Therefore, estimates of hydraulic conductivity in the Cretaceous rocks north of Red Light Draw are biased toward high values and were generally decreased in the model. The initial hydraulic conductivity estimates throughout the entire model were 1 foot/day.

6.3.2 Storage Coefficients

As discussed in Section 4.6.2, only one test was conducted within the study area having an observation well. This data is useful as a reference for assuming reasonable estimates of confined storage. The specific storage was assumed to be 1×10^{-5} feet⁻¹ for all Layers, which resulted in a confined storage coefficient (storativity) that varies with aquifer thickness because storativity is defined as the specific storage times the aquifer thickness.

The specific yield in the bolson aquifers was assumed to be 0.06 and the specific yield estimate for rocks in Layers 2 and 3 was assumed to be 0.01, which are the calibrated estimates for the Salt Basin Bolsons (Beach and others, 2004). The rocks in

Layer 2 and 3 include mainly Tertiary volcanics (tuff, rhyolite, and basalt), Cretaceous formations (limestones, sandstones, shales, et al.) and Paleozoic formations (for example, limestones).

6.4 Model Boundaries

Boundary conditions constrain a model by representing physical components in the system such as evapotranspiration, streams, or cross-formational flow. Boundary conditions are also used to permit the interaction between the active simulation grid domain (modeled area) and the hydrologically connected system surrounding the model area. Anderson and Woessner (1992) identify three general types of boundary conditions; specified flow, specified head, and head-dependent flow. Boundaries can be steady or transient. Based on the level of data available in the model area, all boundary conditions were assumed to be steady-state.

6.4.1 Lateral Boundaries

Figure 6.4.1 shows active cells and boundary conditions in Layer 1. The black lines represent the outer extent of the bolson deposits as defined by the TWDB. The red line indicates the estimated extent of saturation within the bolsons based on water level measurements and the base elevation of the bolsons. In other words, it is the approximate location where the water table intersects the base of the bolson deposits. The red line does not extend into Mexico because we had no water level measurements in Mexico. The gray areas represent inactive (no-flow) gridblocks where the bolson deposits were estimated to be dry or where the model consistently simulated dry zones during the calibration runs. Due to the added difficulty of simulating gridblocks with very small saturated thickness, some of the gridblocks inside the red line in the north end of Red Light Draw were inactivated, as well as other gridblocks on the periphery of other bolsons.

Based on the conceptual model developed for the West Texas Bolsons aquifer, the only lateral boundary required was the General Head Boundary (GHB) in Layer 2 simulating the hydrogeologic connection to Salt Basin Bolson east of the Eagle Flat

Bolson. Based on measured water levels in the area, heads at this boundary were assumed to be 3700 feet above mean sea level. The GHB was placed in Layer 2 to avoid potential dry cell problems in Layer 1 near the edge of the bolson, but groundwater moves from all three Layers out of this boundary.

As shown in Figure 6.4.1 and 6.4.2, stream cells were included in Layers 1 and 2 and the MODFLOW stream package was implemented to simulate groundwater-surface water interaction along the Rio Grande. Figure 6.4.3 shows active cells and boundary conditions in Layer 3. The lack of active boundaries in Layer 3 ensure that groundwater moving through this Layer will not enter or leave laterally, but rather must go through Layer 2 prior to moving in or out of the model. This assumption was made incorporated due to lack of information regarding deep flow systems in this area. Due to the relatively small storage volumes and low transmissivity of Layer 3, this assumption is not expected to significantly affect groundwater availability in the bolsons.

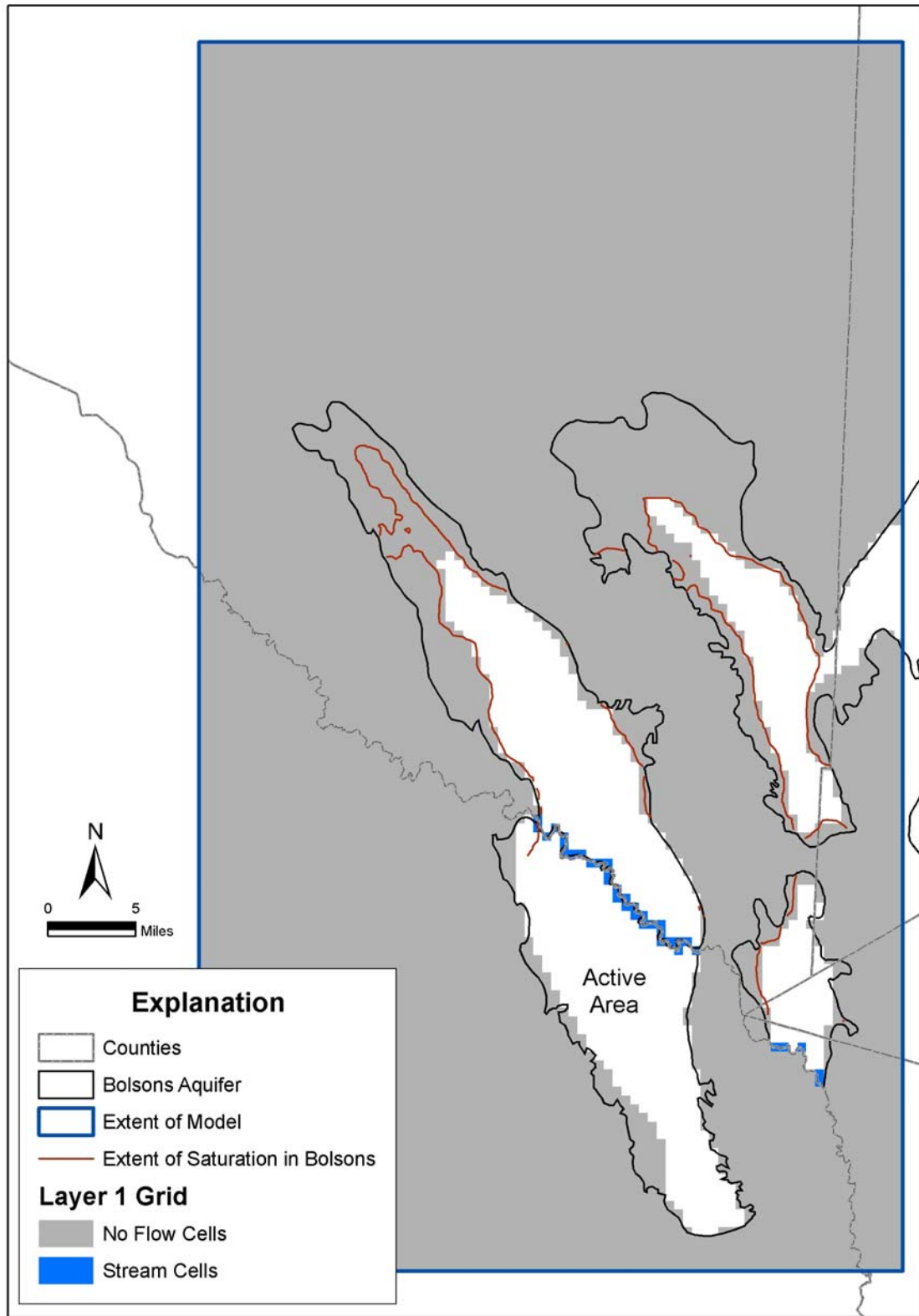


Figure 6.4.1 Active cells and boundary conditions in Layer 1

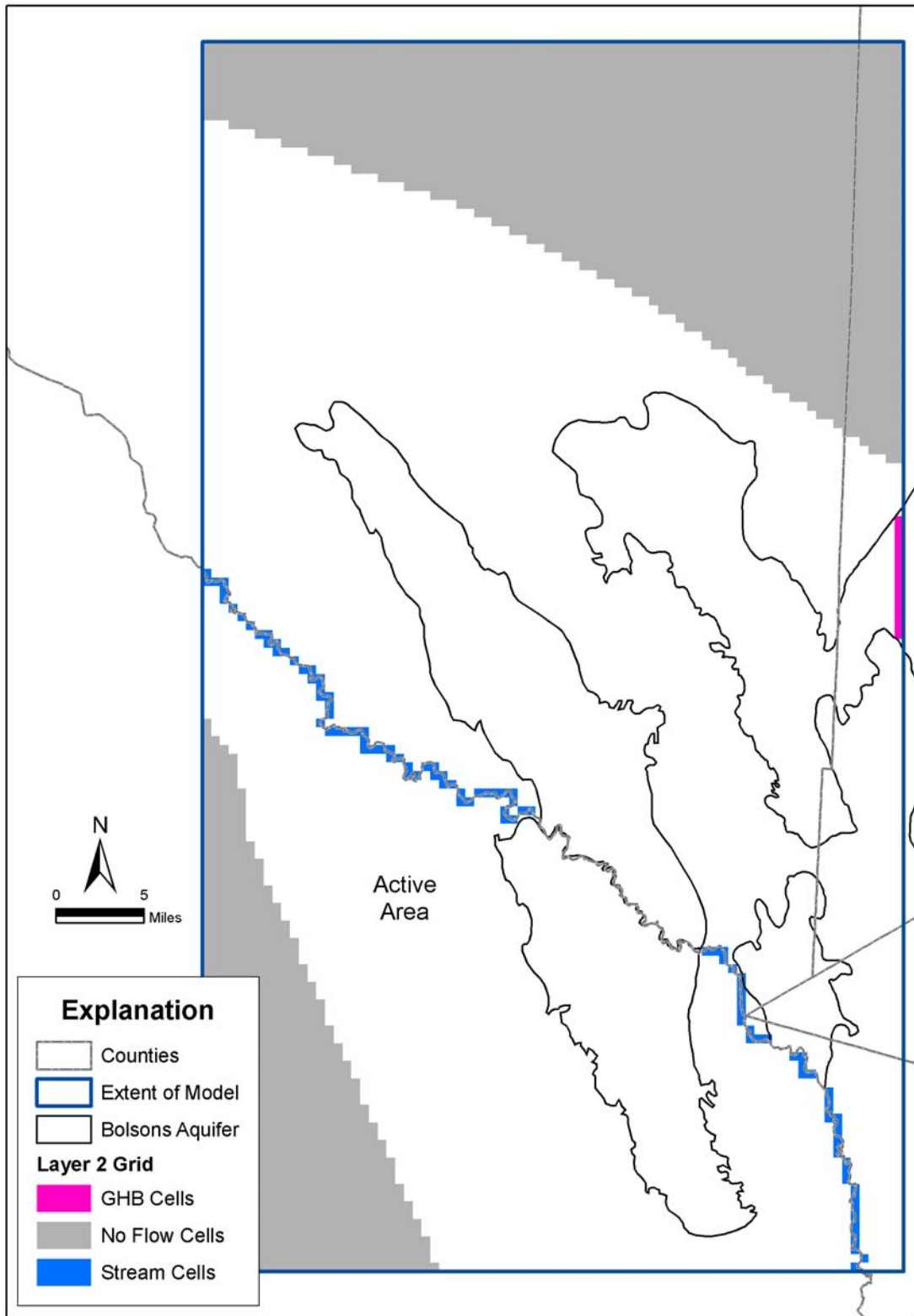


Figure 6.4.2 Active cells and boundary conditions in Layer 2

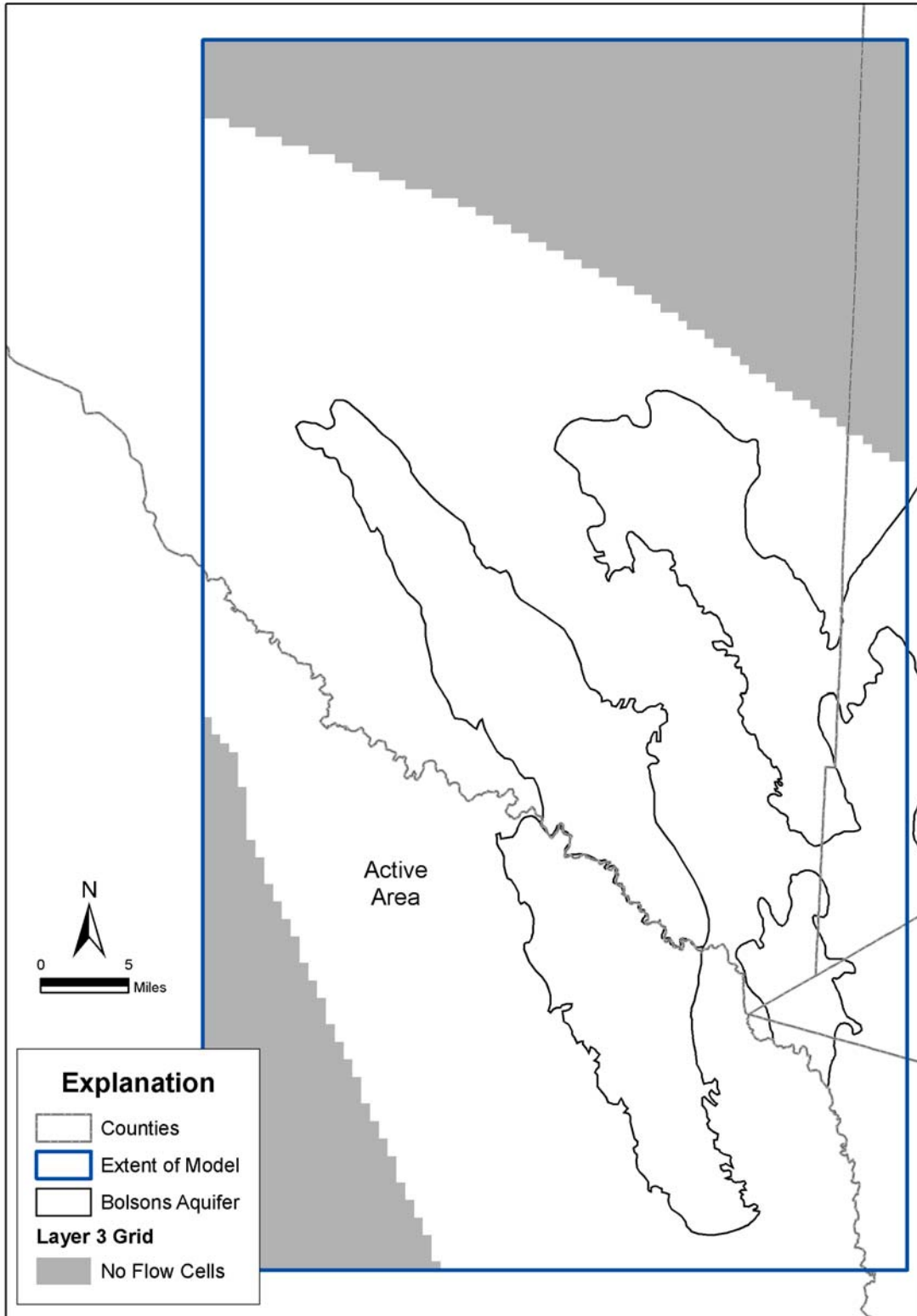


Figure 6.4.3 Active cells and boundary conditions in Layer 3

6.4.2 Vertical Boundaries

A no-flow boundary is assumed for the base of Layer 3. This is consistent with the conceptual model, which assumes that the amount of flow across the bottom of the aquifers is insignificant.

6.4.3 Streams and Springs

Although it is relatively dry in the model area, the Rio Grande bisects the Red Light Bolson and intersects the south side of Green River Valley (discussed in Section 4.5). The MODFLOW stream package is used to represent groundwater-surface water interaction between model Layers 1 and 2 and the Rio Grande. Stream boundaries are a head-dependant boundary condition allowing flow to and from the aquifer according to head levels and surface water availability.

6.4.4 Recharge and Evapotranspiration

As discussed in Section 4, initial estimates of recharge were based on the results of a runoff redistribution analysis that is detailed in Appendix B. In general, recharge estimates (using methods similar to the runoff redistribution) for regional modeling studies have resulted in recharge values slightly greater than those obtained from final model calibration. Similar applications of this methodology to arid settings have resulted in over-predicting model recharge. However, because of lack of other constraining data for the model (such as hydraulic conductivity distribution), the spatial distribution and the estimated rate of recharge was not modified from the original assessment during model calibration.

Evapotranspiration studies or data within the model area was not identified for this study. Because of the relatively sparse vegetative cover over most of the model area, even near the Rio Grande, it was assumed that the potential evapotranspiration was relatively small. Evapotranspiration was simulated by incorporating a potential evapotranspiration rate of 5 inches per year across the model area with an extinction depth of 10 feet. The estimate for extinction depth was based on reported maximum

rooting depths of shrubs and grasses similar to those found in the model area. The estimated evapotranspiration rate is lower than the 10 inches per year that was assumed by Beach and others (2004) for the Igneous and Bolson GAM in the Salt Basin. However, because the gridblocks were ½-mile wide and the vegetation is only thick in a very narrow corridor near the river, the reduced rate was considered appropriate.

6.4.5 Pumping Discharge

As documented in Section 4.7, discharge from well production in the model area is limited. Because the steady-state model represents predevelopment conditions, discharge from pumping was not incorporated into the steady-state model.

As documented in Figure 4.3.2, only a few wells in the model area contain more than one or two water level measurements. The wells that do contain more than two water level measurements indicate that there has not been a significant change in water levels during the period of record, including the transient calibration period prescribed by TWDB, which is 1980 to 1997. The lack of calibration data and the lack of significant pumping in the active model area were the reason that TWDB did not require a transient calibration for the model.

7.0 MODELING APPROACH

Calibration of a groundwater flow model is the process of adjusting model parameters until the model reproduces field-measured values of water levels (heads) and flow rates. Successful calibration of a flow model to observed heads and flow conditions is usually a prerequisite to using the model for prediction of future groundwater availability. Parameters that are typically adjusted during model calibration are hydraulic conductivity, storativity, and recharge. Model calibration typically includes completion of a sensitivity analysis and a verification analysis. Sensitivity analysis entails running the model with a systematic variation of the parameters and stresses in order to determine which parameter variations produce the most change in the model results. Those parameters that change the simulated aquifer heads and discharges the most are generally considered important parameters to the calibration. The sensitivity analysis guides the process of model calibration by identifying potentially important parameters but does not in itself produce a calibrated model. Model verification is another approach used to determine if the model is suitable for use as a predictive tool. Verification is using the model to predict aquifer conditions during a time period that contains different observed data than was used for the model calibration.

7.1 Calibration

7.1.1 Approach

Groundwater models are inherently non-unique. Non-uniqueness refers to the characteristic of a model that allows many combinations of hydraulic parameters and aquifer stresses to reproduce measured aquifer water levels. To reduce the impact of non-uniqueness on model results, several approaches were used. Where possible, the model incorporated parameter values (i.e., hydraulic conductivity, storativity, recharge) that were consistent with measured values. In addition, a relatively long calibration period was selected to incorporate a wide range of hydrologic conditions and the verification period entailed simulation of different time periods. Finally, to the degree

possible, two different calibration performance measures, hydraulic heads, and aquifer flowrate, were used to reduce non-uniqueness in the model.

Measured hydraulic conductivity and storativity data were initially incorporated into the model based on the data described in Section 4. In areas where measured data were not available, estimates were incorporated from similar aquifers for which data exist. As mentioned in Section 6, there are no available measurements of vertical hydraulic conductivity. Therefore, vertical hydraulic conductivity was estimated based on the observed flow directions, the conceptual model, and professional judgment.

Model parameters were held to within reasonable ranges during calibration based on available data and relevant literature. As a general rule, parameters that have few measurements were adjusted preferentially as compared to parameters that have a good supporting database.

The model was calibrated for only steady-state hydrologic conditions. There is very little, if any transient water-level and hydrographs in this area show no significant movement over time. For this reason, steady-state calibration targets were developed using the maximum water level measurements in the historical record.

7.1.2 Calibration Targets and Measures

In order to calibrate a model, targets and calibration measures were developed. The primary type of calibration target was hydraulic head (water level). Table 7.1 summarizes the available water level measurements for the steady-state model period.

Table 7.1 Summary of the steady-state calibration targets

Layer	Number of steady-state targets
1 - Bolson	40
2 - Cretaceous-Permian	94
3 - Basement Rocks	38

To address the issue of non-uniqueness, it is best to use as many types of calibration targets as possible, such as stream gain and loss information. However, no such data exist for the Rio Grande in the model area. Therefore, average stream-flow estimates were incorporated into stream package and appropriate estimates of stream conductance were used to ensure that reasonable gains and losses were simulated in the river.

Model calibration is judged by quantitatively analyzing the difference (or residual) between observed and model computed (i.e., simulated) values. Several graphical and statistical methods are used to assess the model calibration. These statistics and methods are described in detail in Anderson and Woessner (1992). The mean error is defined as:

$$ME = \frac{1}{n} \sum_{i=1}^n (h_m - h_s)_i \quad 7.1$$

where:

h_m is measured hydraulic head, and

h_s is simulated hydraulic head, and

$(h_m - h_s)$ is known as the head error or residual.

A positive mean error (ME) indicates that the model has systematically underestimated heads, and a negative error, the reverse. It is possible to have a mean error near zero and still have considerable errors in the model (i.e., errors of +50 and -50 give the same mean residual as +1 and -1). Thus two additional measures, the mean absolute error and the root mean square of the errors, are also used to quantify model goodness of fit. The mean absolute error is defined as:

$$MAE = \frac{1}{n} \sum_{i=1}^n |(h_m - h_s)_i| \quad 7.2$$

and is the mean of the absolute value of the errors. Root mean squared (RMS) error is defined as:

$$\text{RMS} = \left[\frac{1}{n} \sum_{i=1}^n (h_m - h_s)_i^2 \right]^{0.5} \quad 7.3$$

A large RMS means that there is wide scattering of errors around the mean error.

These statistics were calculated for the calibration period. In addition, the distribution of residuals was evaluated to determine if they are randomly distributed over the model grid and not spatially biased. Head residuals were plotted on the simulated water-level maps to check for spatial bias. Scatter plots were used to determine if the head residuals are biased as compared to the observed head surface.

The model mass balanced was also used to as another criteria to ensure the validity of the solution and model results. MODFLOW calculates a water budget for the overall model. The percentage error of the total inflow and outflow should be small if the model equations are solved correctly. The TWDB specifications require the difference between the total simulated inflow and the total simulated outflow less than one percent and ideally less than 0.1 percent. The mass balance error for the WTBGAM steady-state model was 0.005%.

7.1.3 Calibration Target Uncertainty

Groundwater elevation measurements have an inherent error component due to several factors, including measurement error, instrument error, sampling scale limitations, and recording errors. In order to know when the model calibration is acceptable, a level of reasonable uncertainty in the observed head data should be recognized and estimated. This uncertainty in observed data provides some guidance regarding setting calibration goals to avoid over-calibrating the model. Over-calibration of a model occurs when parameters are modified too much in order to match observed conditions.

The TWDB GAM standard for calibration criteria for head is an MAE less than or equal to 10% of head variation within the aquifer being modeled. Head differences

across the Salt Basin Bolson aquifer are about 800 feet. Head differences across the Igneous aquifer are about 2600 feet. This leads to an acceptable MAE of about 260 feet for the entire model, and about 80 feet for the bolsons. This MAE can be compared to an estimate of the head target errors to consider what level of calibration the underlying head targets can support.

7.2 Sensitivity Analyses

A sensitivity analysis was performed on the calibrated model to determine how changes in a calibrated parameter affect the results of the calibrated model. The sensitivity analysis was completed such that each of the hydraulic parameters or stresses was adjusted from its calibrated value by a small factor while all other hydraulic parameters were held at their calibrated values. The parameters include horizontal hydraulic conductivity, vertical hydraulic conductivity, confined storativity, specific yield, recharge, pumping, hydraulic head assigned at any constant head and general head boundaries and conductance values for drains, streams, and general head boundaries. The model parameters were adjusted plus and minus 10 and 50 percent from calibrated values. The sensitivity of the model parameters were evaluated by calculating the average head change at the calibration points in the calibrated model.

8.0 STEADY-STATE MODEL

The calibration of the steady-state model involved adjusting some of the model input parameters in order to get a good fit to the observed target data. The WTBGAM was calibrated with an iterative trial-and-error approach based mainly on the groundwater conceptual model and professional judgment. Automated parameter estimation techniques were generally not effective because of the lack of constraint on the system. This Section describes the final steady-state calibration results.

8.1 Calibration

8.1.1 Calibration Targets

Figure 8.1.1 shows the locations of the wells with water levels that were used for the steady-state calibration. As discussed in Section 7 and shown in Table 7.1, a total of 40 water level measurements were available in the bolson aquifer for steady-state calibration; 94 wells are completed in Layer 2 and 38 in Layer 3.

8.1.2 Horizontal and Vertical Hydraulic Conductivities

The initial distribution of hydraulic conductivity was based on the measured data as discussed in Section 4, Table 4.5. The distribution of the hydraulic conductivity was zonal and the zones were generally consistent with the major water producing areas of the bolsons (i.e., Red Light Draw, Eagle Flat, and Green River Valley). Initial hydraulic conductivity values were adjusted during the calibration period of the steady-state and transient model. Table 8.1 summarizes the range of calibrated hydraulic conductivity values used in each Layer.

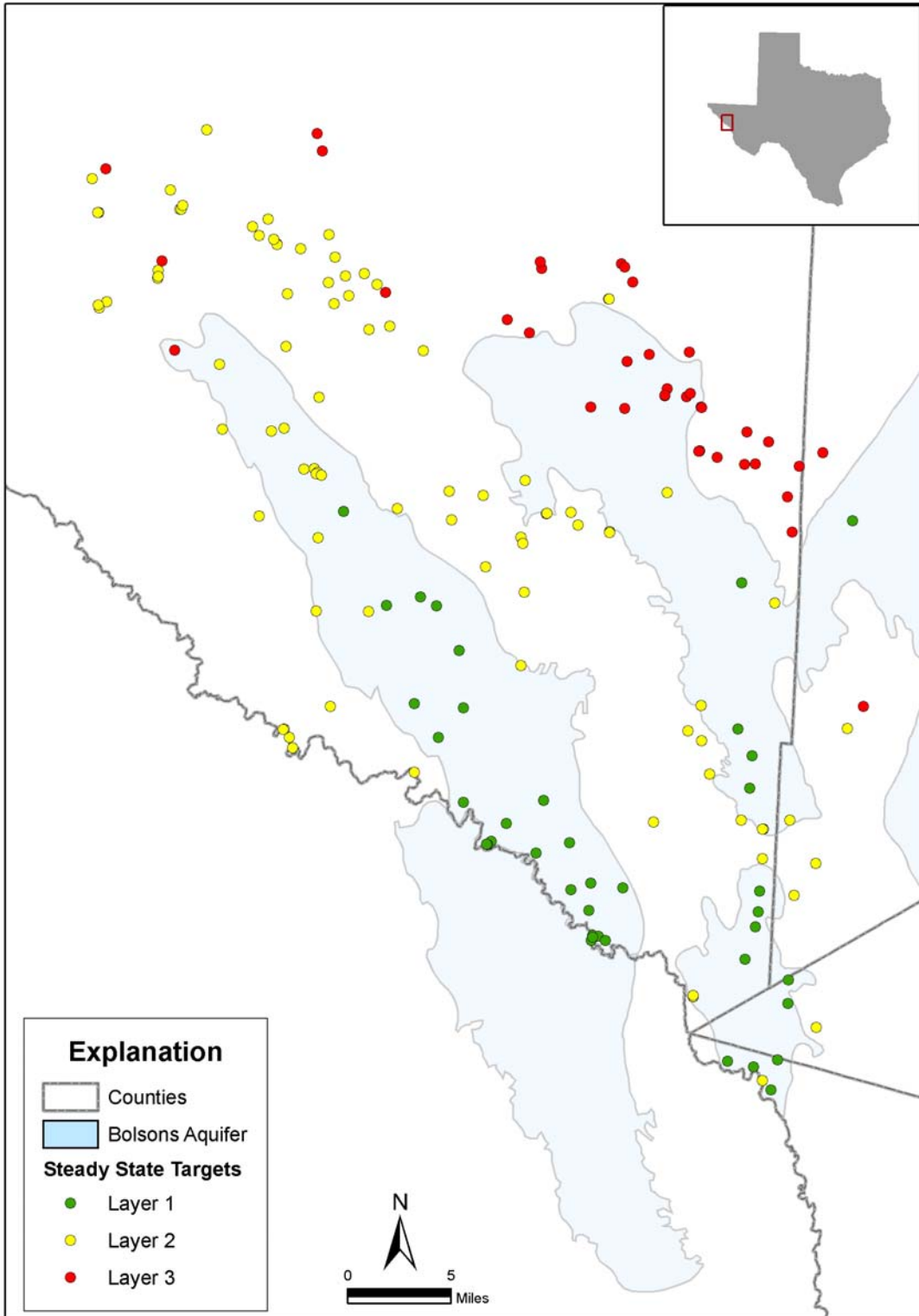


Figure 8.1.1 Location of Wells Used for Steady-State Calibration Targets (Including Layer Designation)

Table 8.1 Summary of hydraulic properties used in model

Layer	Horizontal Hydraulic Conductivity (ft/day)	Vertical Hydraulic Conductivity (ft/day)	Specific yield (-)	Specific Storage (feet⁻¹)
1	0.001- 1	0.0001 - 0.5	0.06	---
2	0.001 – .3	0.00005 - 0.3	0.01	1x10 ⁻⁵
3	0.001 - .3	0.00005 - 0.3	0.01	1x10 ⁻⁵

The final distribution of hydraulic conductivity values for Layers 1, 2, and 3 are shown in Figures 8.1.2, 8.1.3, and 8.1.4, respectively. Also shown on each figure is the ratio of horizontal to vertical hydraulic conductivity for each zone.

The distribution of hydraulic conductivity in Layer 1 is illustrated in Figure 8.1.2. Hydraulic conductivity in the West Texas Bolsons aquifer varies from 0.001 to 1 ft/day. The Red Light Bolson was assigned a hydraulic conductivity of 0.2 ft/day, Eagle Flat was assigned a hydraulic conductivity of 1 ft/day in the north and 0.5 ft/day in the southernmost reach, and the Green River Valley was assigned a hydraulic conductivity of 0.001 ft/day. These estimates were based on compiled estimates from similar aquifers, previous modeling studies, sensitivity analysis, and the hydraulic conductivity values that were required to reproduce the observed heads during the calibration process.

The spatial pattern of vertical hydraulic conductivity zones was consistent with the pattern used for the horizontal hydraulic conductivity. The vertical hydraulic conductivity estimates are used to estimate a vertical conductance between model Layers. It is often easier to gain an understanding to the vertical hydraulic conductivity of an aquifer by looking at its anisotropy ratio (K_h/K_v). The anisotropy ratio is relatively low throughout the model area. One reason that anisotropy exists on a small scale is the orientation of thin clays and silts in unconsolidated sediments. Generally, the low

anisotropy ratios in the model were required to match observed heads, which may indicate that groundwater flows vertically with relative ease between the underlying aquifers and the bolsons.

Figure 8.1.3 illustrates the distribution of hydraulic conductivity in Layer 2. As expected, the hydraulic conductivity and anisotropy required to match observed water levels in the Eagle Mountains was generally lower than in the areas to the northwest of Eagle Flat. The area north of Red Light Draw was assigned the highest hydraulic conductivity in Layer 2. This is based on the transmissivity estimates in that area. In addition, the low anisotropy (1.0) in the area is consistent with the conceptual model and water level measurements in the region that indicate the potential for downward flow, as discussed in 4.3. The hydraulic conductivity beneath the bolsons is generally higher than in other areas. This is based on the theory that a deeper groundwater flow path exists between the area north of Red Light Draw and the Rio Grande, which is the regional sink in the model area.

Figure 8.1.4 illustrates the final distribution of hydraulic conductivity in Layer 3. Similar hydraulic conductivity patterns were incorporated in Layer 3 as in Layer 2 for generally the same reasons. Layer 3 represents the very deep flow system beneath the bolsons and while flow through the deep system is relatively small, it is assumed that the flow patterns mimic those of the rocks directly below the bolsons.

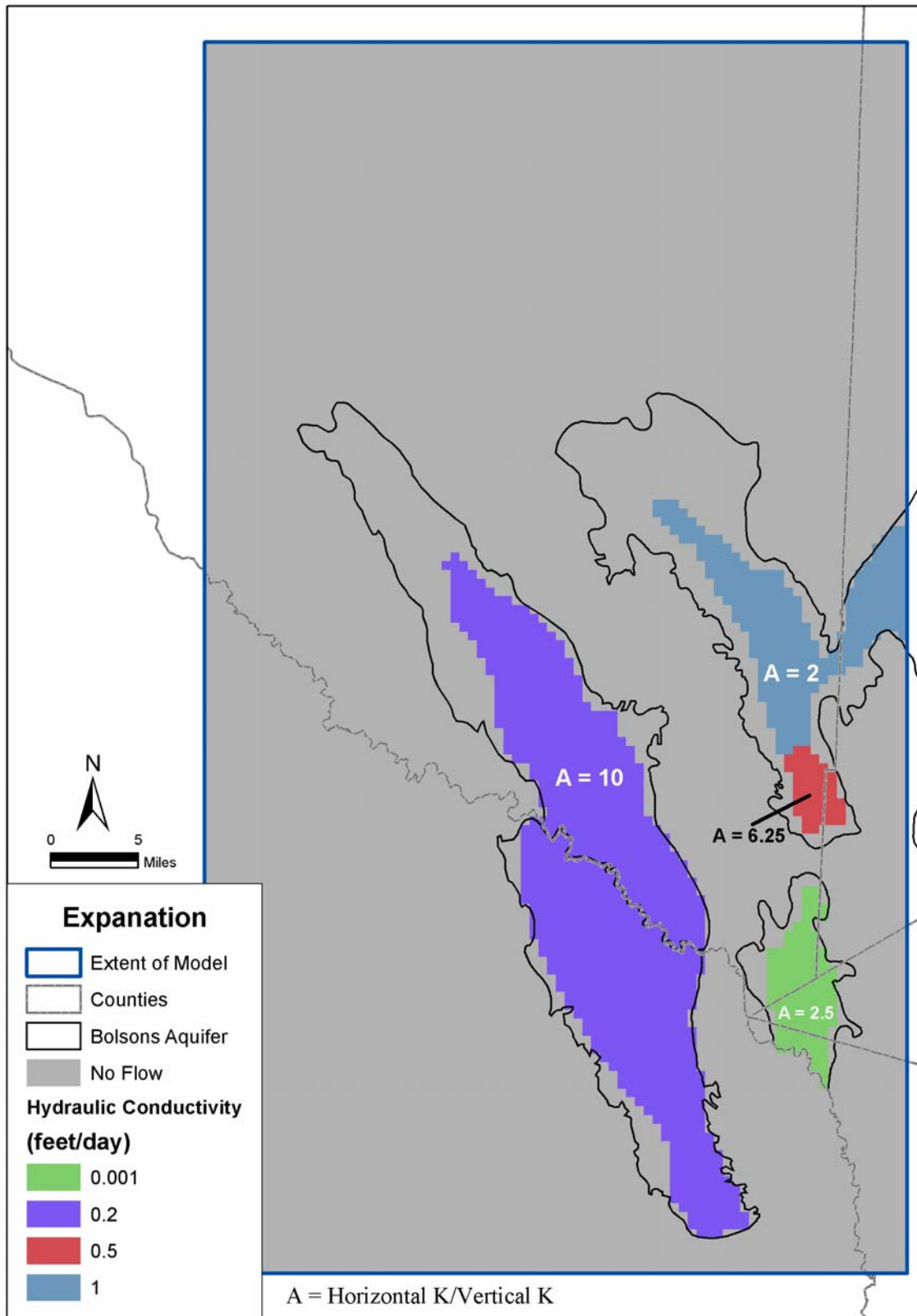


Figure 8.1.2 Final distribution of hydraulic conductivity in Layer 1

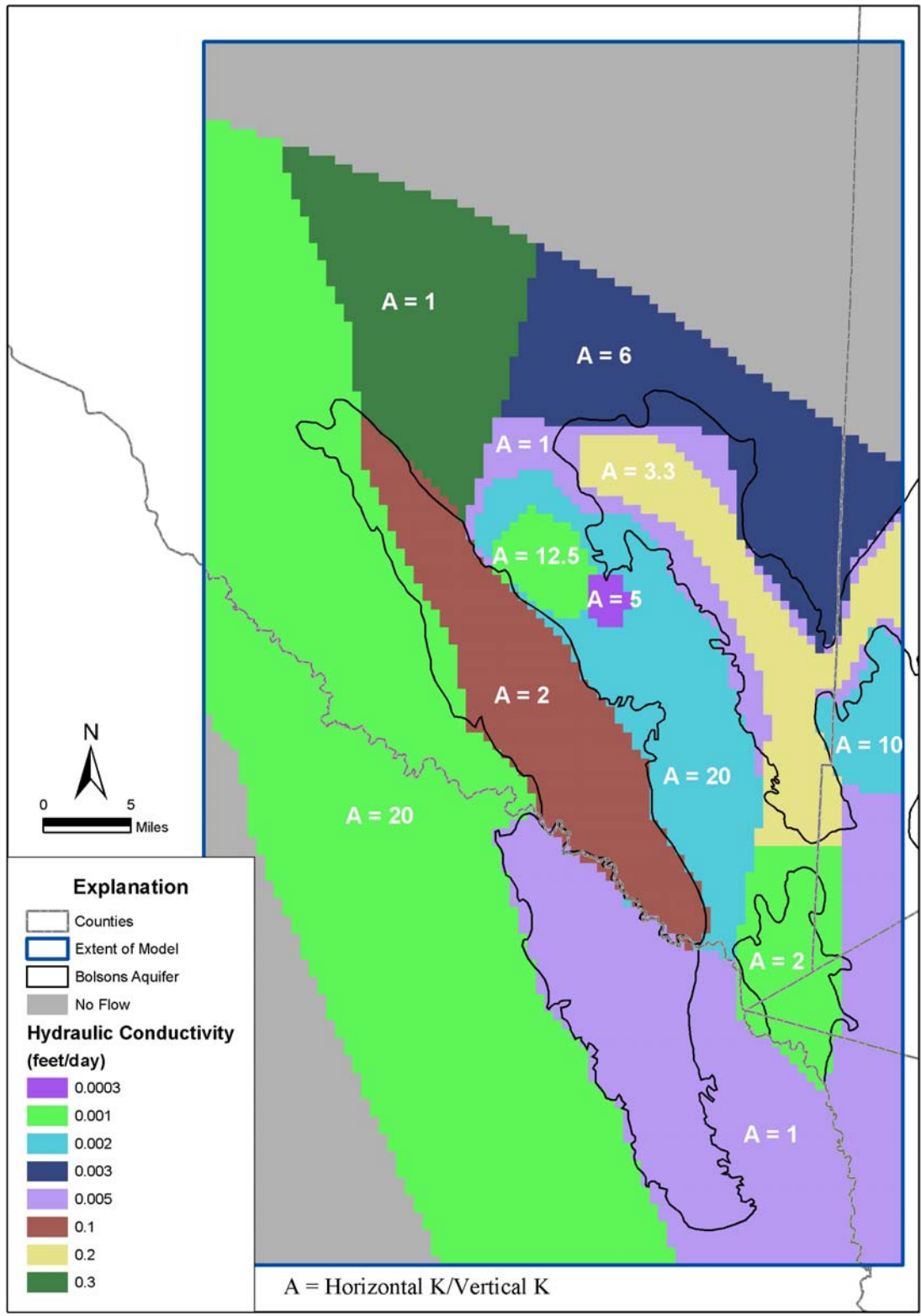


Figure 8.1.3 Final distribution of hydraulic conductivity in Layer 2

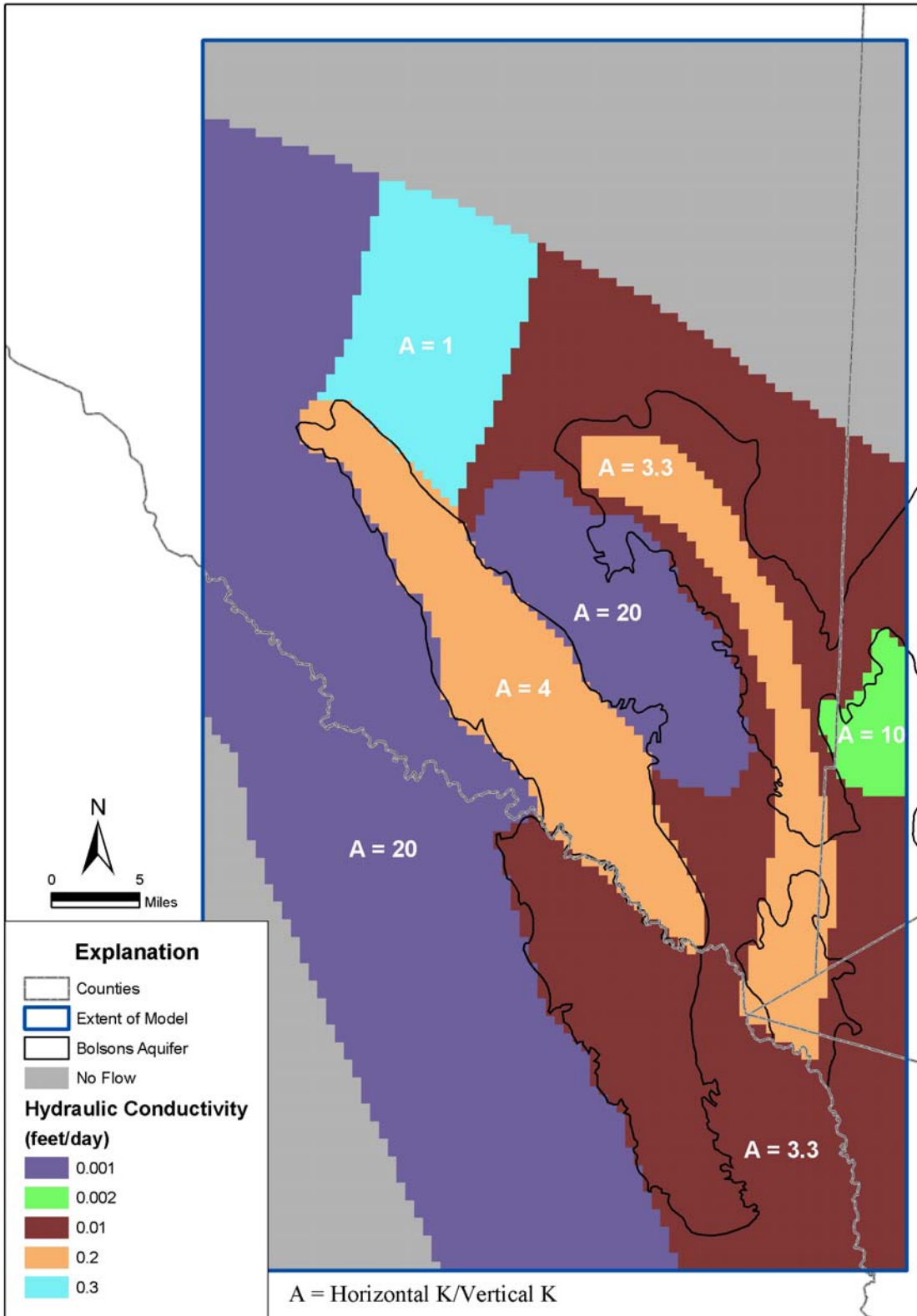


Figure 8.1.4 Final distribution of hydraulic conductivity in Layer 3

8.1.3 Recharge

As discussed in Sections 4.4 and 6.4, initial estimates of recharge were based on the results of a runoff-redistribution analysis that is detailed in Appendix B. Those Sections address the assumptions regarding recharge estimates and the application of the results to the model.

For the steady-state period, average recharge estimates were incorporated into the model and no adjustments were made from the estimates shown in Section 4.4. The spatial distribution of calibrated recharge in the steady-state model is shown in Figure 8.1.5. Direct recharge from precipitation is not assigned to the bolsons, and assumed to be zero. The recharge estimates range from zero in the bolsons to about 0.9 inches/yr in the mountain regions.

8.1.4 Groundwater Evapotranspiration

It was assumed that the evapotranspiration extinction depth of 10 feet was appropriate across the model area. Simulated evapotranspiration rates in the steady-state calibrated model are shown in Figure 8.1.6. There are only a few areas where the water levels are within 10 feet of land surface, and therefore, evapotranspiration directly from the water table is not active over most of the model area.

8.1.5 General Head Boundaries

As discussed in Section 6.4, GHB cells were included along the model boundary to hydraulically connect Eagle Flat and the Salt Basin Bolson aquifers to the east. The GHB heads were adjusted slightly during the calibration to reduce water levels in that area.

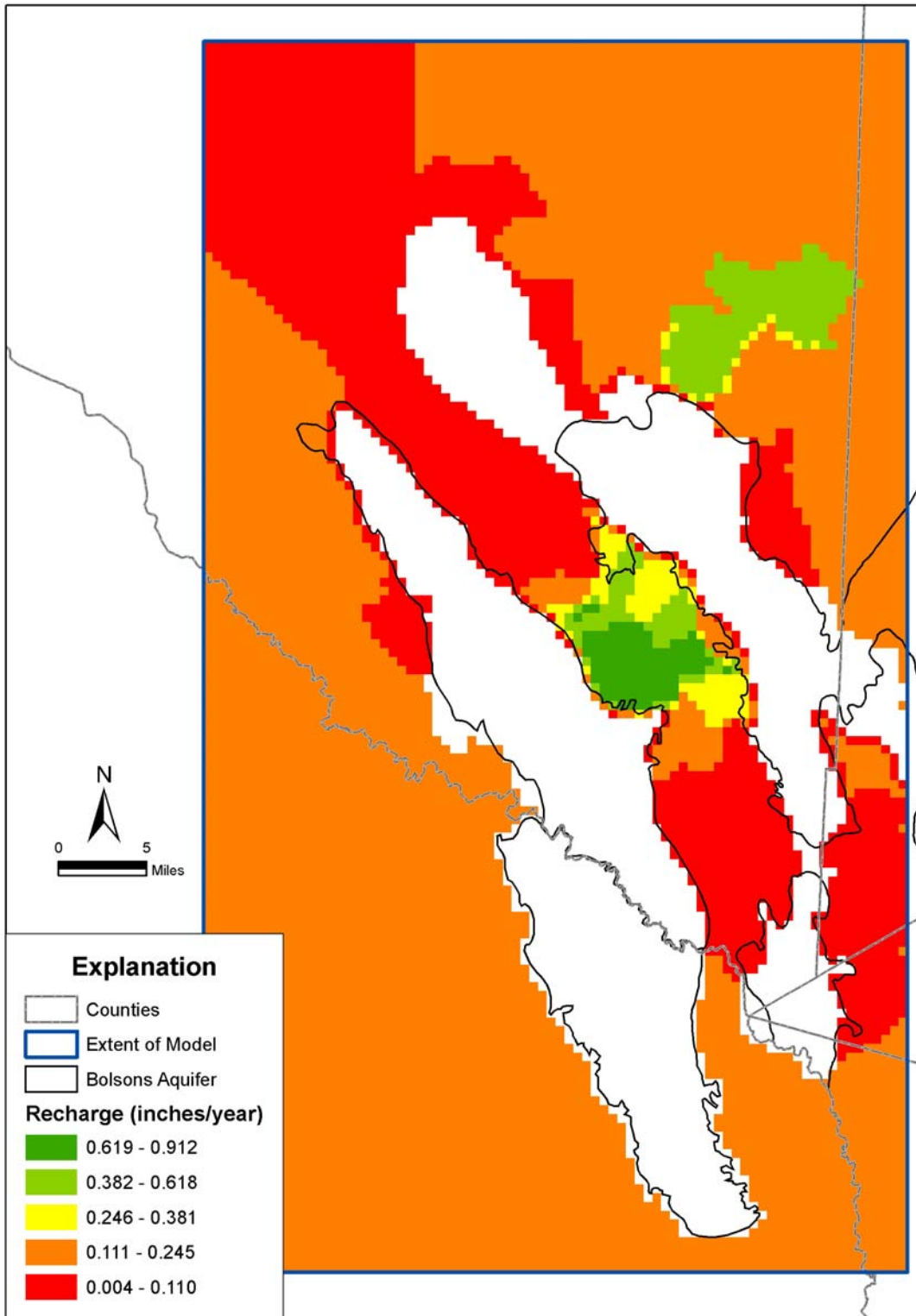


Figure 8.1.5 Final distribution of recharge rate in the steady-state model

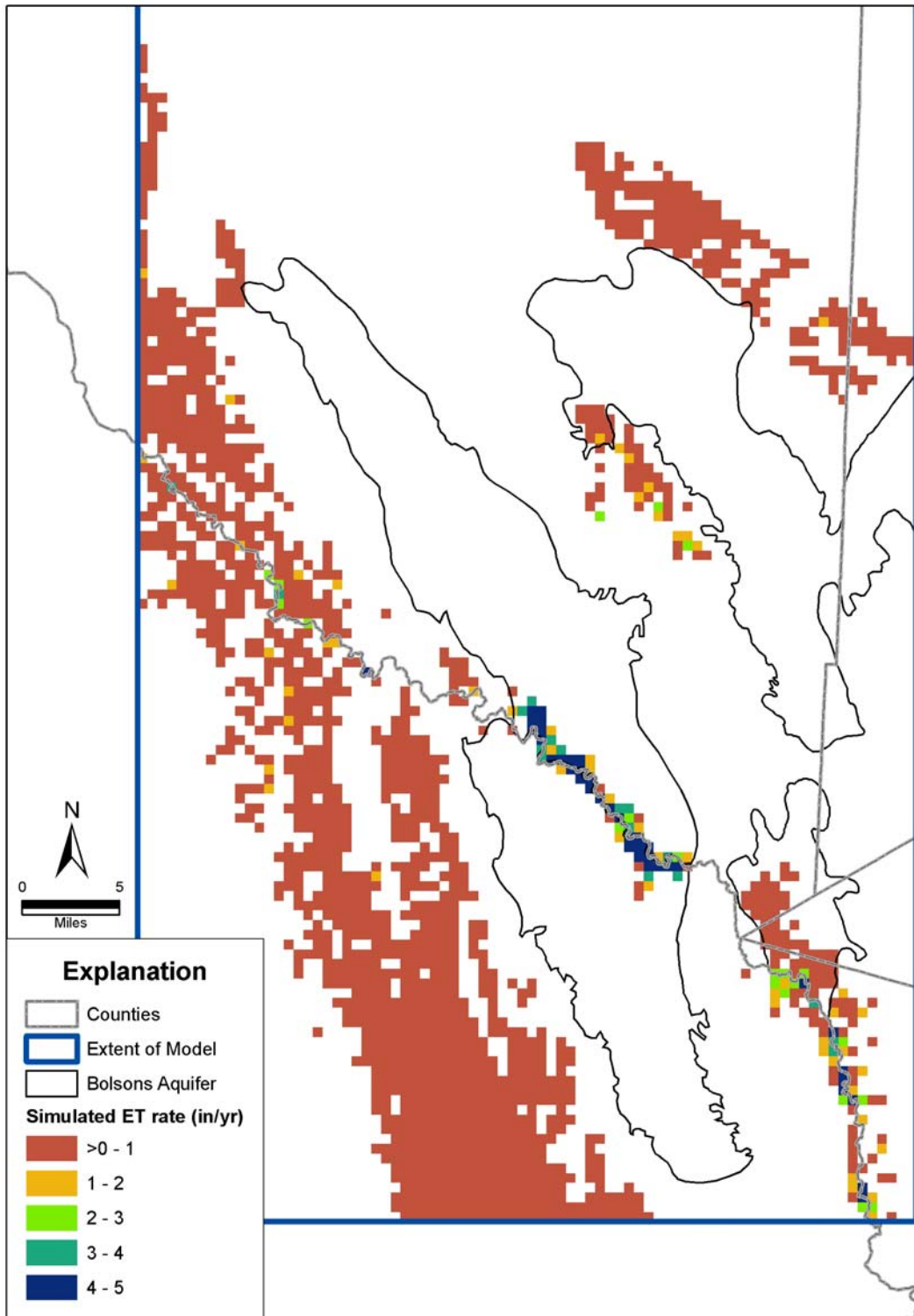


Figure 8.1.6 Simulated evapotranspiration rates in the steady-state model

8.1.6 Calibration Results and Statistics

The steady-state model was calibrated using water level measurements collected 1900 to 2006, which were assumed to represent predevelopment conditions since pumping in this area is scarce and has not affected the aquifer water levels significantly. This Section describes some of the observations that were made during the calibration of the model and presents results of the calibration of the steady-state portion of the model.

Steady-state conditions were simulated using a long transient stress period for the calibration model. A 10,000,000-day stress period was incorporated to simulate “steady-state” conditions. This approach was used because incorporating a steady-state stress period in the model during the calibration runs usually resulted in the PCG and GMG solvers not converging appropriately or not yielding a solution that maintained good mass balance.

The MODFLOW rewetting option was used, but some cells near the edge of the bolson aquifers still went dry during the steady-state calibration simulations. The model solution is sensitive to the rewetting and GMG solver settings, and the mass balance should always be checked carefully to ensure that instability in the solution has not caused significant mass balance errors. The total flow through the model is relatively small due to limited recharge, so even a few cells that have mass balance errors can cause significant errors in the model budget. Experience with the model indicates that these cells are typically close to the edge of the bolsons, and that is why the gridblocks that had small saturated thickness were inactivated (i.e., no flow cells). It was very difficult too achieve a good solution with good mass balance with a lot of cells that were oscillating between wet and dry conditions. It should also be noted that it is possible to have a good overall mass balance for the whole model but have significant but offsetting errors in different Layers.

Dry cells in MODFLOW can be indicative of model instability during solver iterations or may indicate that the Layer has a small saturated thickness or is dry. As can be seen in Figure 8.1.9, dry cells are located along the edge of Layer outcrops, where cell

thickness is low. The model currently uses a GMG solver. Using a PCG solver instead would result in similar pattern of distribution of dry cells. Both are indicative of dry cells being actual dry zones or areas where the saturated thickness is so small that the flow in the cells is relatively insignificant to the overall flow dynamics.

Table 8.2 summarizes the calibration statistics for the steady-state model. The mean absolute error (MAE) of the steady-state calibration targets for the bolsons is 56 feet over a range of 800 feet, resulting in a MAE/range ratio of 7.0%. For Layer 2, MAE was 99 feet over a range of 2638 feet resulting in a ratio of 3.8% and Layer 3 has a MAE of 119 feet over a range of 1106 feet for a ratio of 10.8%. Over the entire model, MAE was 93 feet over a range of 2641 feet, resulting in a 3.5% ratio.

Table 8.2 Summary of steady-state head calibration statistics

Layer	# of Target Wells	ME (feet)	MAE (feet)	Range (feet)	MAE/Range (%)
Layer 1	40	20	56	800	7.0
Layer 2	94	28	99	2638	3.8
Layer 3	38	10	119	1106	10.8
All	172	22	93	2641	3.5

8.1.7 Hydraulic Heads

Figure 8.1.7 shows a crossplot of the observed heads versus the simulated heads for the steady-state model. The figure indicates that there is relatively good agreement in most areas of the model. Figure 8.1.8 plots the residuals against the steady-state observed heads. The plot indicates that there are no significant trends in the residuals across the model domain. Figure 8.1.9 shows a map of the simulated hydraulic head results from the calibrated steady-state model for the bolsons (Layer 1) as well as residuals for Layer 1 targets. As indicated in this figure, the flow direction and gradients are very similar to those shown in Figure 4.3.6. Also shown in Figure 8.1.9 are the dry cells (shown as brown gridblocks) that are simulated by the model. As a comparison, the

PCG solver was also used with the calibrated steady-state model, and the distribution of dry cells was very similar to the solution when using the GMG solver.

Figure 8.1.10 shows head residuals for all Layers in the steady-state model. The positive and negative residuals are scattered throughout the model area, indicating that there is no significant geographical bias to the residuals. However, it is evident that measured water levels in Eagle Flat are not very well replicated by the model. The reason for this is not known. However, there is significant lack of data regarding the structure and hydraulic properties in this area, and these unknowns in conjunction with the geologic complexity probably result in hydrogeologic flow system that is difficult to simulate with a simplified model. Many of the wells in this area are also completed across several water-bearing zones, and therefore the water level measurements may not be indicative of any particular hydrogeologic unit or model Layer.

Figure 8.1.11 illustrates the simulated steady-state heads and target residuals in Layer 2. Water level elevations in the Eagle Mountains and in the areas to the north of Red Light Draw follow the same trends that are seen in Figure 4.3.5. The contours north of Red Light Draw mimic those in Figure 4.3.5, indicating that the flow patterns are similar and that there is downward flow from Layer 2 to Layer 3 in the area.

Figure 8.1.12 shows the simulated water levels and target residuals in Layer 3. According to calibration data available for Layer 3, the general flow directions in the aquifer mimic the regional flow patterns that were discussed in Section 4.3.4. Most of the targets in Layer 3 are located in the northeast part of the model area (northeast of Eagle Flat) because that is where the Precambrian basement rocks are relatively shallow. Therefore, some of the deeper wells in that area are screened in model Layer 3.

Comparison of Figures 8.1.2, 8.1.3, and 8.1.4 to the available hydraulic conductivity data (Section 4.6) will confirm that significant liberty has been taken in the assignment of hydraulic property values and their distribution. In the absence of good hydraulic property data, the assignment of horizontal and vertical hydraulic conductivity data was based largely on the conceptual model and the insight gained during the iterative calibration process. While more effort could have been expended to employ more

sophisticated parameter estimation methods, the lack of hydraulic property data and water level measurements would have likely resulted in similar results. Specifically, in the absence of real hydraulic property data, automated calibration methods require significant guidance regarding the range and distribution of hydraulic conductivity estimates. Because this range and distribution of hydraulic properties would be largely driven by the intuition gained from the hydrogeologic conceptual model and refined by the water level measurements, the calibration process would have been similar in either case. Obviously, from a statistical standpoint, there are many potential advantages of automated parameter estimation methods (Doherty, 2002). But the non-uniqueness of the hydraulic property values and distribution cannot be eliminated in a system with very limited data.

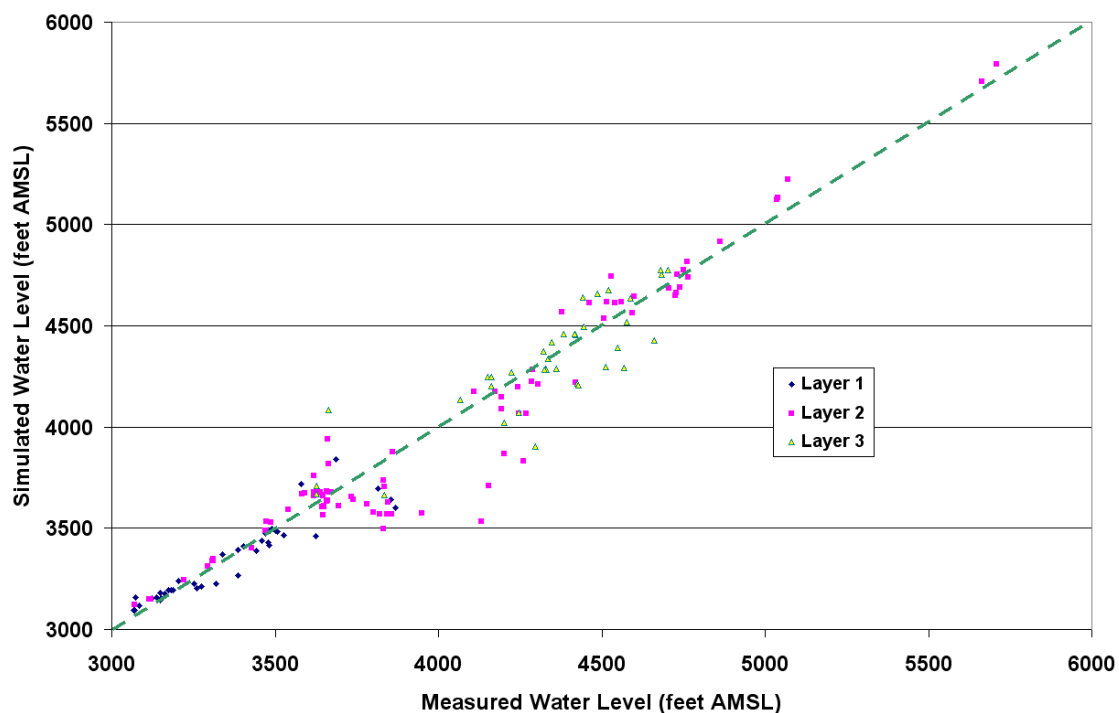


Figure 8.1.7 Crossplot of simulated versus observed heads in the steady-state model

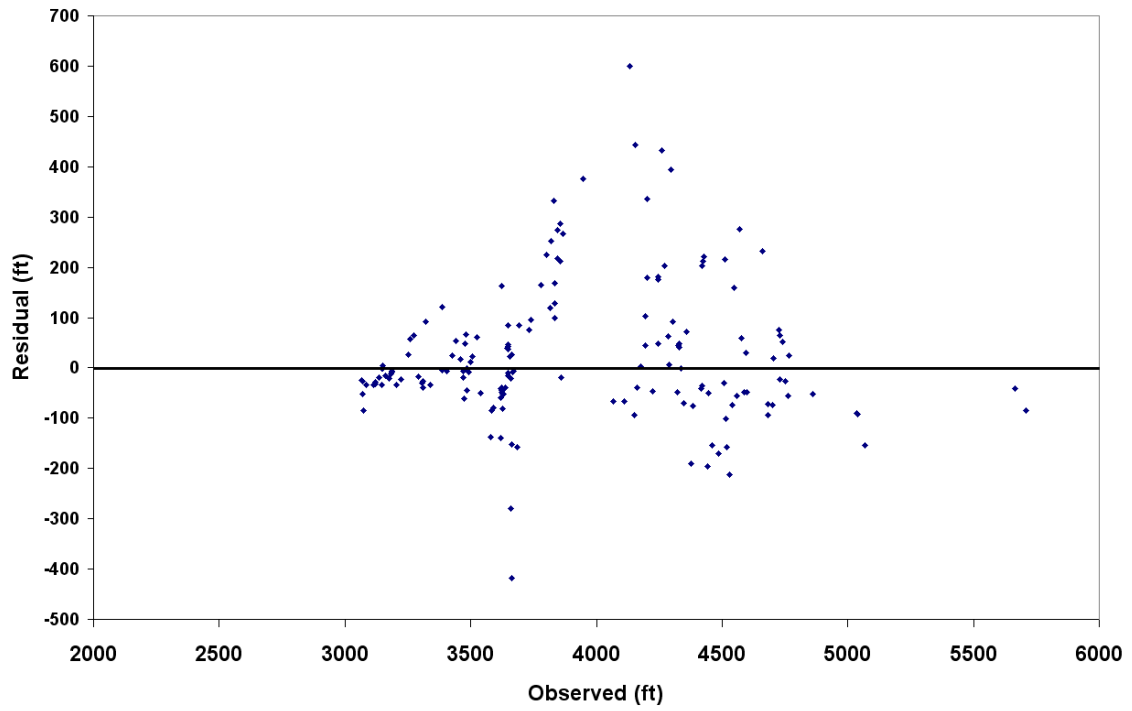


Figure 8.1.8 Plot of residuals versus observed heads in the steady-state model

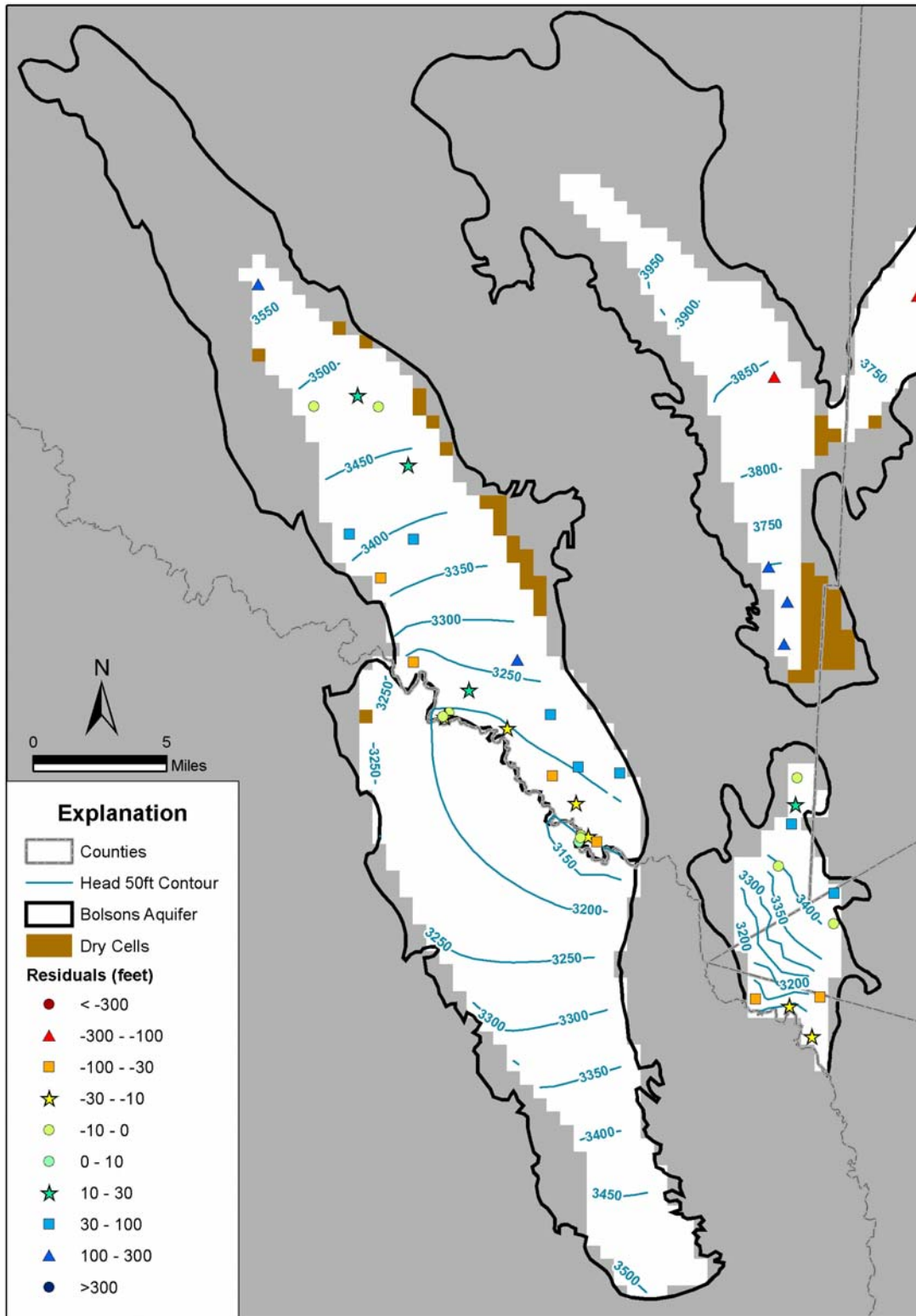


Figure 8.1.9 Simulated steady-state hydraulic heads and residuals in Layer 1

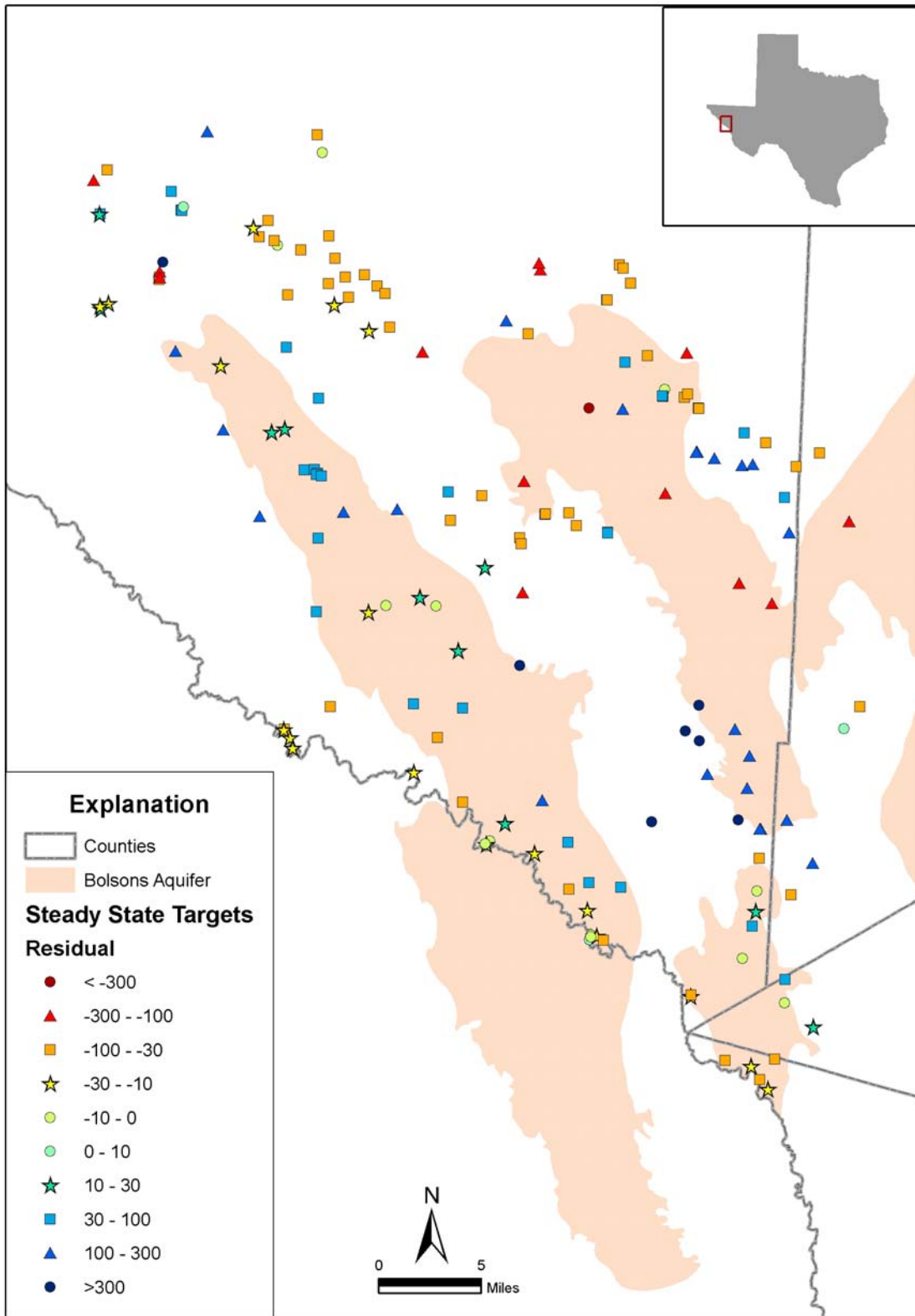


Figure 8.1.10 Residuals in the steady-state model (all Layers)

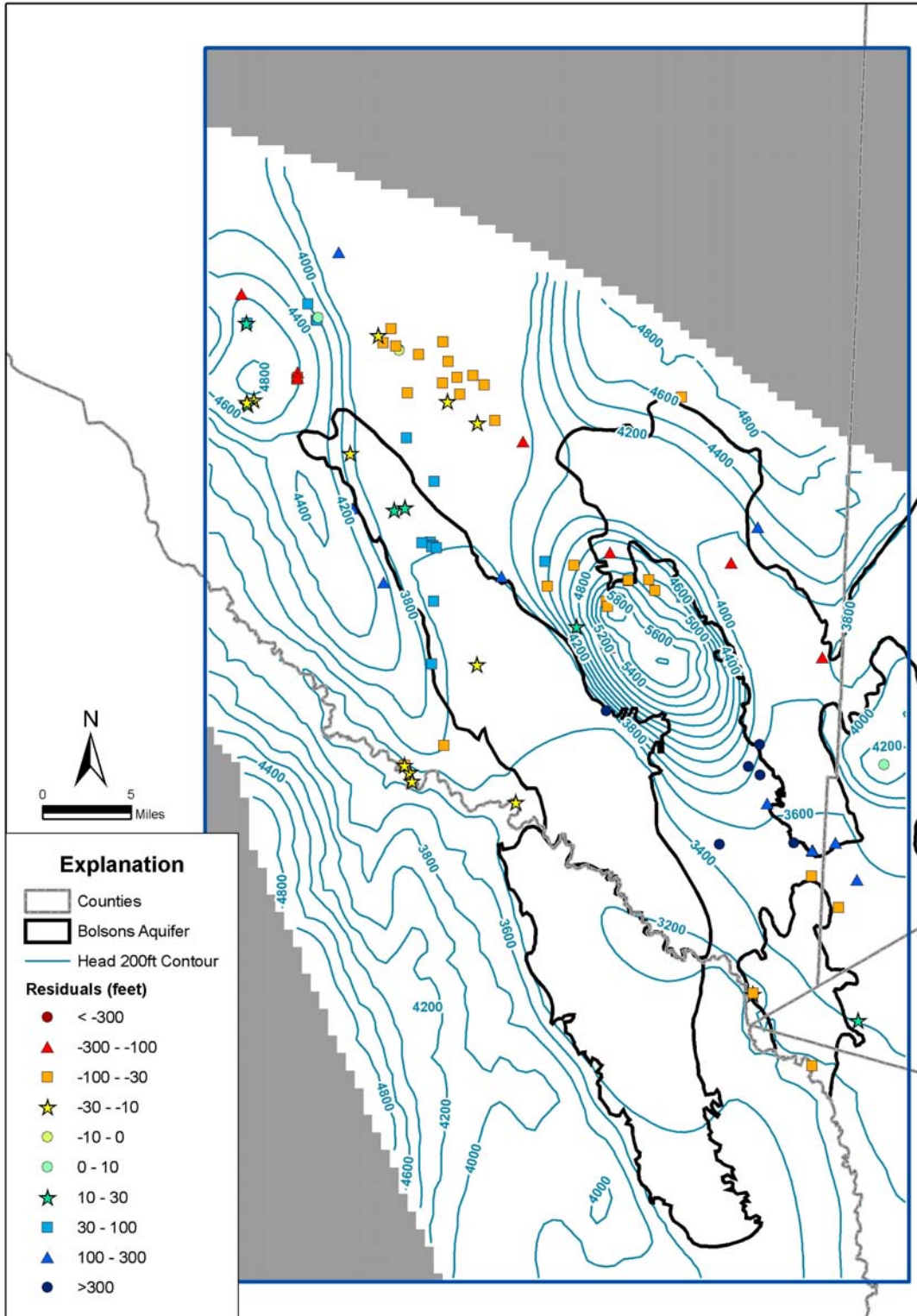


Figure 8.1.11 Simulated steady-state hydraulic heads and residuals in Layer 2

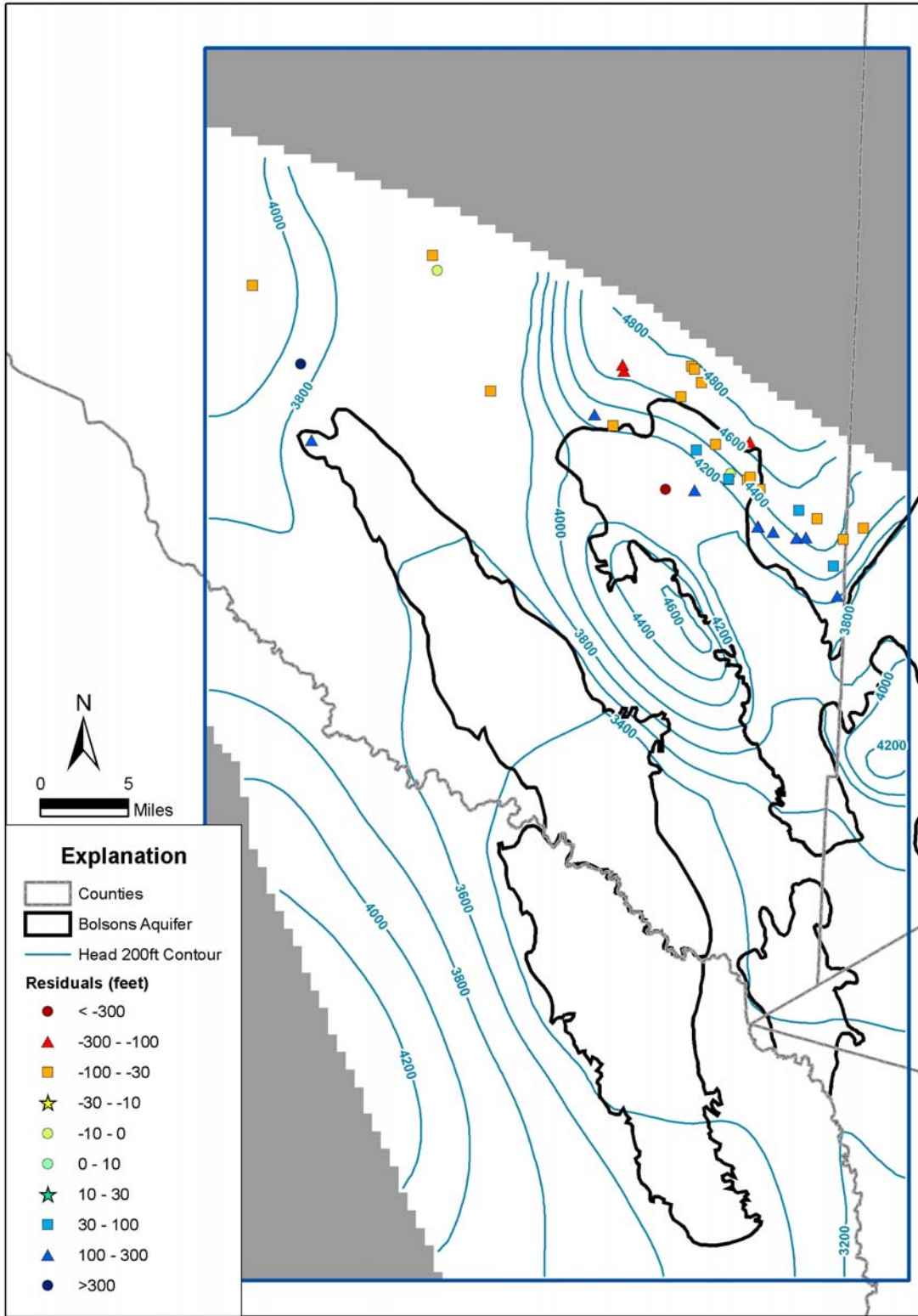


Figure 8.1.12 Simulated steady-state hydraulic heads and residuals in Layer 3

8.1.8 Water Budget

Table 8.3 provides a Layer-by-Layer summary of the steady-state water budget for the model. Figure 8.1.13 illustrates the steady-state budget components for each Layer in graphical form. Under steady-state conditions, the model estimates that about 11,160 acre-feet per year of the 13,455 acre-feet per year of recharge are lost to evapotranspiration. About 387 af/yr exits the Eagle Flat through the GHBs on the east side of the model and flow into the bolson deposits Culberson County. The Rio Grande is a net sink in the model area, and gains about 855 af/yr from the aquifers.

Table 8.3 Summary of steady-state water budget components

	Layer	Top	Bottom	GHB	Stream	Recharge	ET
IN	1	0	4,258	0	320	178	0
	2	873	3,650	0	738	12,218	0
	3	3,649	0	0	0	0	0
	Sum			0	1,059	12,396	0
OUT	1	0	873	0	838	0	3,045
	2	4,258	3,649	387	1,075	0	8,114
	3	3,650	0	0	0	0	0
	Sum			387	1,914	0	11,160
All units in acre-feet per year							

The Layer-by-Layer water budget for each county in the model is presented in Appendix D.

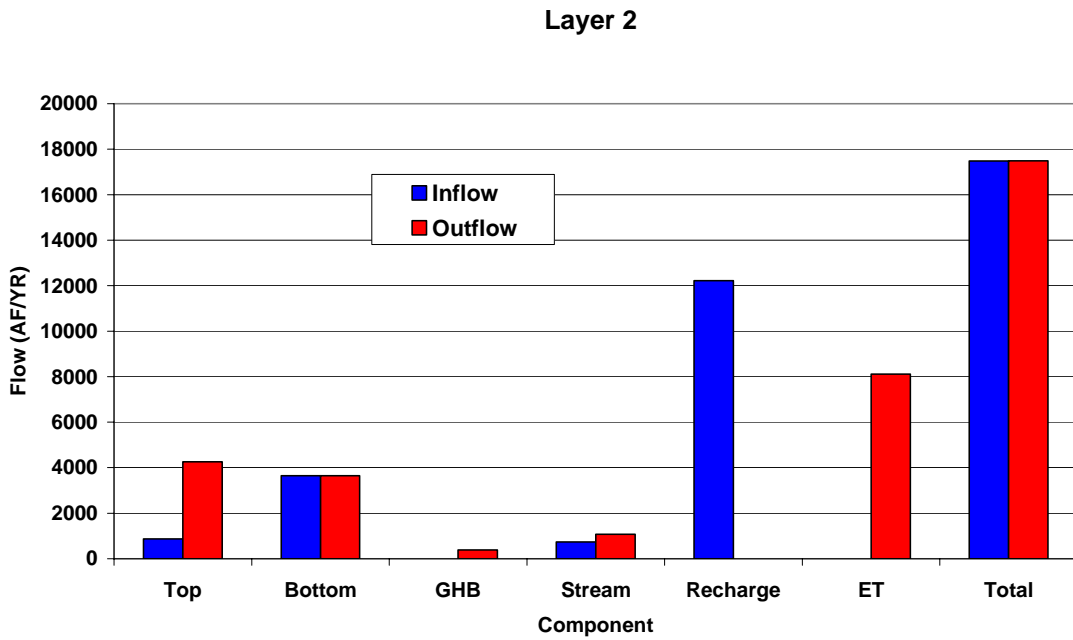
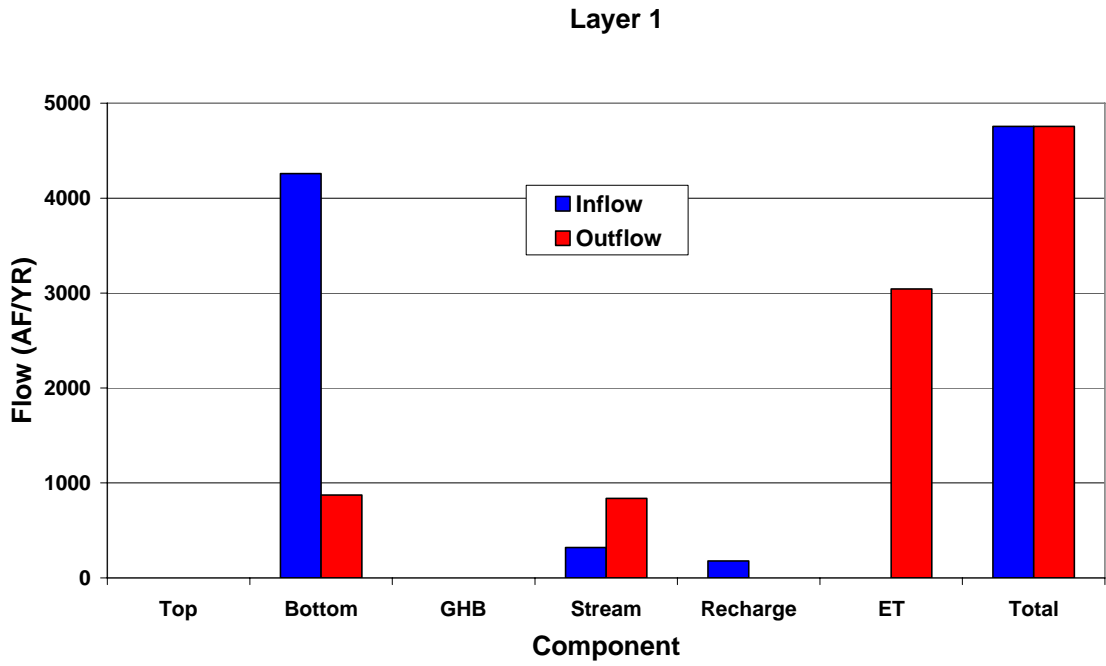


Figure 8.1.13 Water budget components in the steady-state model

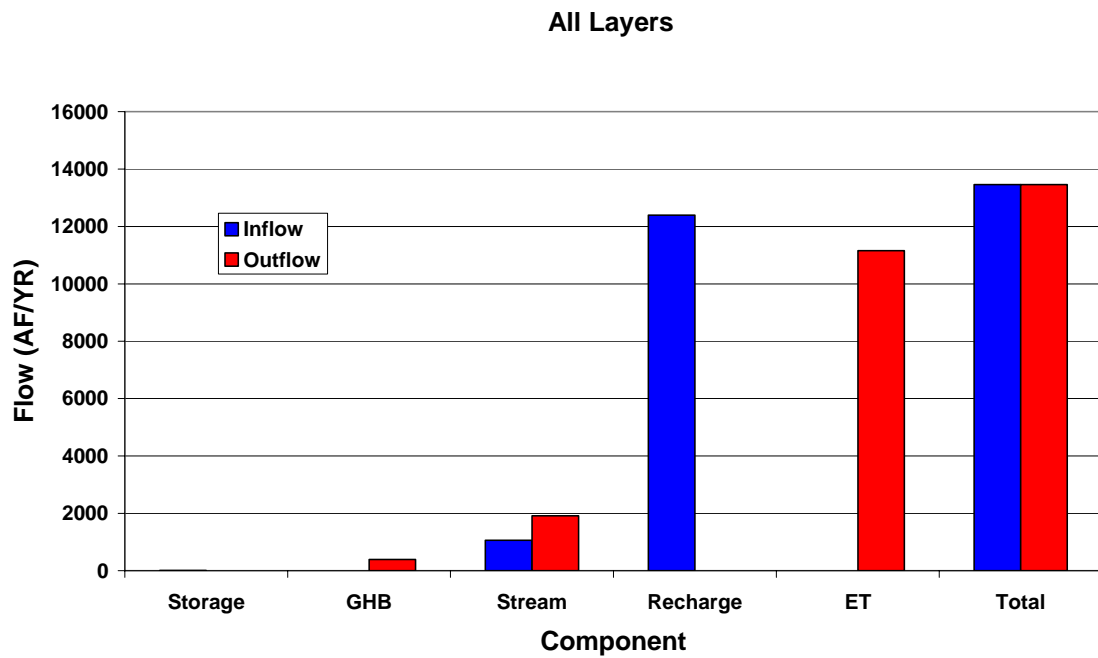
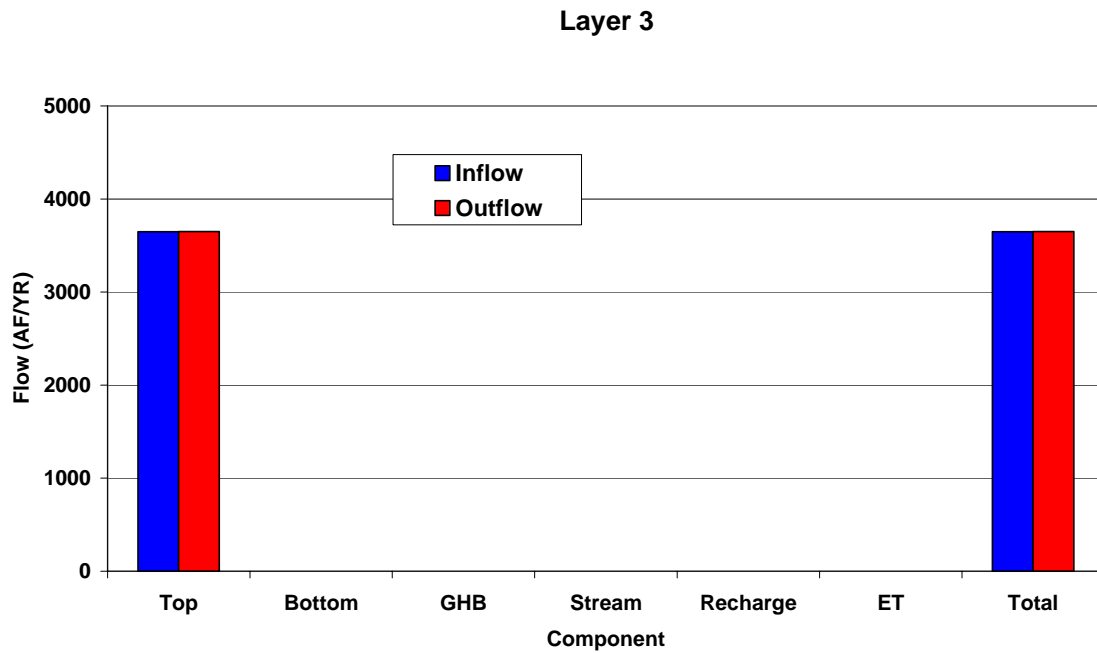


Figure 8.1.13 Water budget components in the steady-state model (continued)

8.2 Sensitivity Analysis

A sensitivity analysis was completed for the calibrated steady-state model. One purpose of the sensitivity analysis was to quantify the impact on the model results when input parameters are varied. For this evaluation, hydraulic parameters were systematically increased and decreased from their calibrated values while the average change in head was calculated for each Layer and also for the entire model. For each parameter that was varied, four simulations were completed. The sensitivity factors were 0.5, 0.9, 1.1, and 1.5. For the steady-state analysis, the sensitivity of eight parameters was evaluated. The eight parameters are:

1. Evapotranspiration
2. Stream conductivity
3. Vertical hydraulic conductivity
4. Bolson horizontal hydraulic conductivity
5. Layers 2 and 3 horizontal hydraulic conductivity
6. Recharge
7. General head boundary conductance (GHB-C)
8. General head boundary heads (GHB-Head)

Figures 8.2.1 to 8.2.4 show the sensitivity of water level to changes in the eight parameters for each Layer and the whole model. The Figures indicate that when horizontal hydraulic conductivity is decreased, average head in each Layer increases, showing a negative correlation. Changing the horizontal hydraulic conductivity in Layers 2 and 3 has similar but more pronounced affect on water levels for each Layer as does changing horizontal hydraulic conductivity in Layer 1. Other parameters that exhibit a slight negative correlation to average bolson head are evapotranspiration, and stream conductance. The most sensitive positively correlated parameter is recharge, followed by GHB heads. The model is not sensitive to changes in GHB conductance. The vertical hydraulic conductivity shows a positive correlation in Layer 3 but negative correlation in other cases.

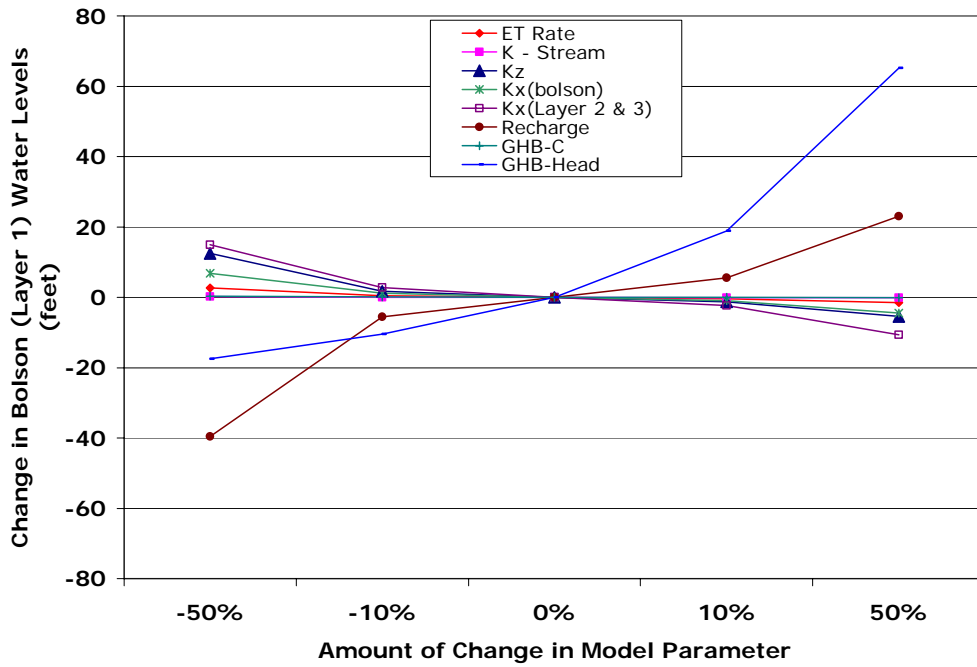


Figure 8.2.1 Steady-state sensitivity results for the Bolsons (Layer 1)

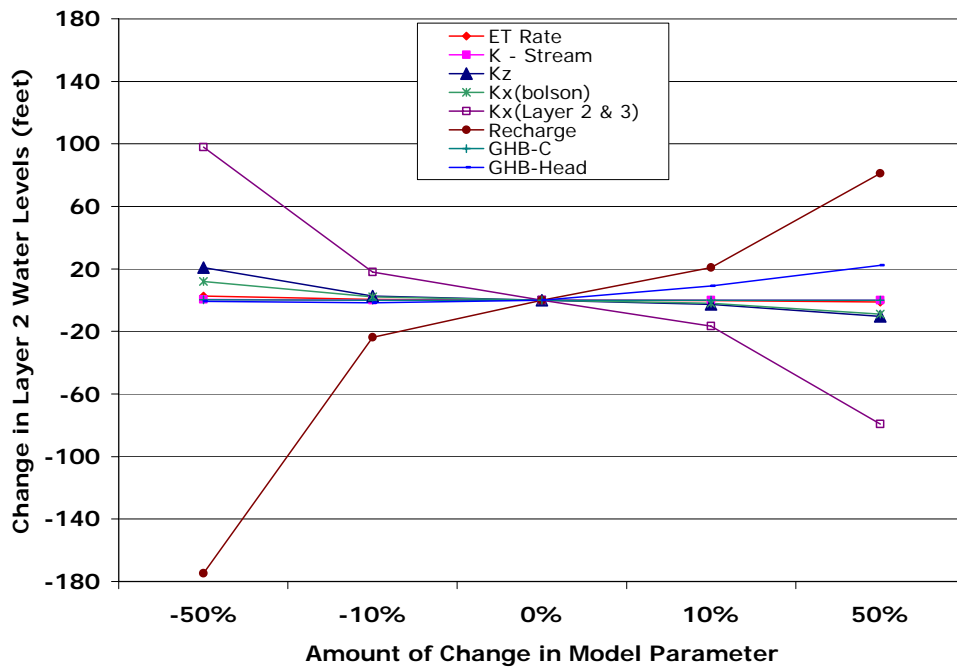


Figure 8.2.2 Steady-state sensitivity results for Layer 2

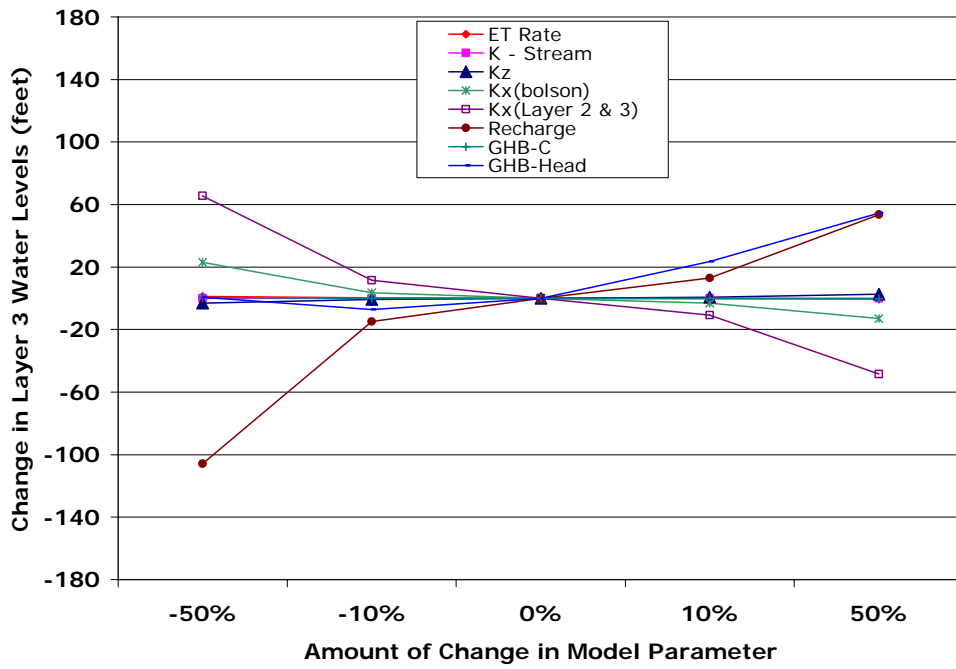


Figure 8.2.3 Steady-state sensitivity results for Layer 3

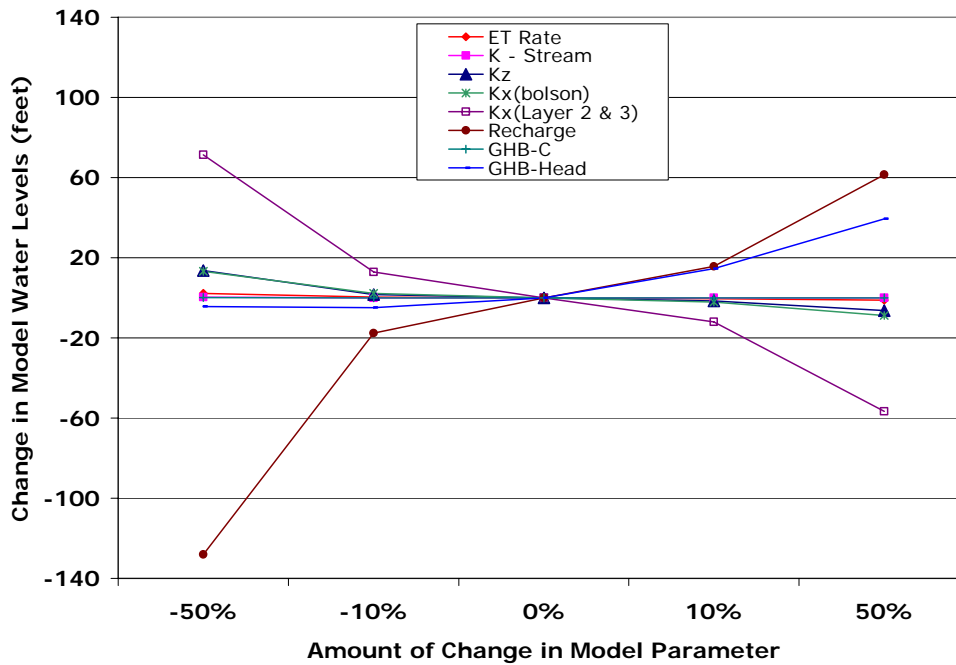


Figure 8.2.4 Steady-state sensitivity results for all Layers

9.0 TRANSIENT MODEL

As documented in Figure 4.3.2, only a few wells in the model area contain more than one or two water level measurements. The wells that do contain three water level measurements indicate that there has not been a significant change in water levels during the period of record, including the transient calibration period prescribed by TWDB, which is 1980 to 1997. In addition, as indicated in Section 4.7, the estimate of total pumping from the entire model area from 1984 through 1997 was less than 500 af/yr. For these reasons, the TWDB did not want to perform a transient model calibration. However, because the model may be used in the future to assess the impacts of production from the bolson or Cretaceous aquifers, the TWDB did want to ensure that reasonable storage properties were incorporated into the model and that reasonable results could be obtained from transient simulations. This was accomplished by completing a transient simulation and a sensitivity analysis for the storage properties and pumping values.

9.1 Transient Simulation

As discussed in Section 6.3, specific yield estimates for the model were based on the calibrated estimate for the Igneous and Bolson GAM (Beach and others, 2004). The storativity values were based on the one estimate obtained from the pumping test in Eagle Flat, as discussed in Section 4.6.2.

To test the ability of the model to perform transient simulations, we developed a transient scenario that incorporated 9,700 acre-feet per year of production from Red Light Draw over a 30-year period. The pumping was allocated equally to 12 wells. The well locations and water levels after 30 years of pumping are shown in Figure 9.1.1. As indicated in the plot, two of the gridblocks containing wells go dry during the 30-year simulation. Both of these gridblocks are located in areas where the saturated thickness is relatively small, and therefore the model predicts that those wells will go dry. In reality, it may mean either that the well goes dry, or that water levels would decline to a level where the well would need to be operated at a reduced rate.

Figure 9.1.2 illustrates the drawdown after a 30-year period and Figure 9.1.3 shows the water level hydrograph in one well of the wellfield during the 30 years production period. The well is located at (115365.6, 149093.4). These model results indicate that the simulated water level declines were reasonable and generally comparable to the response of the bolsons in the Salt Basin that have experienced a similar level of production.

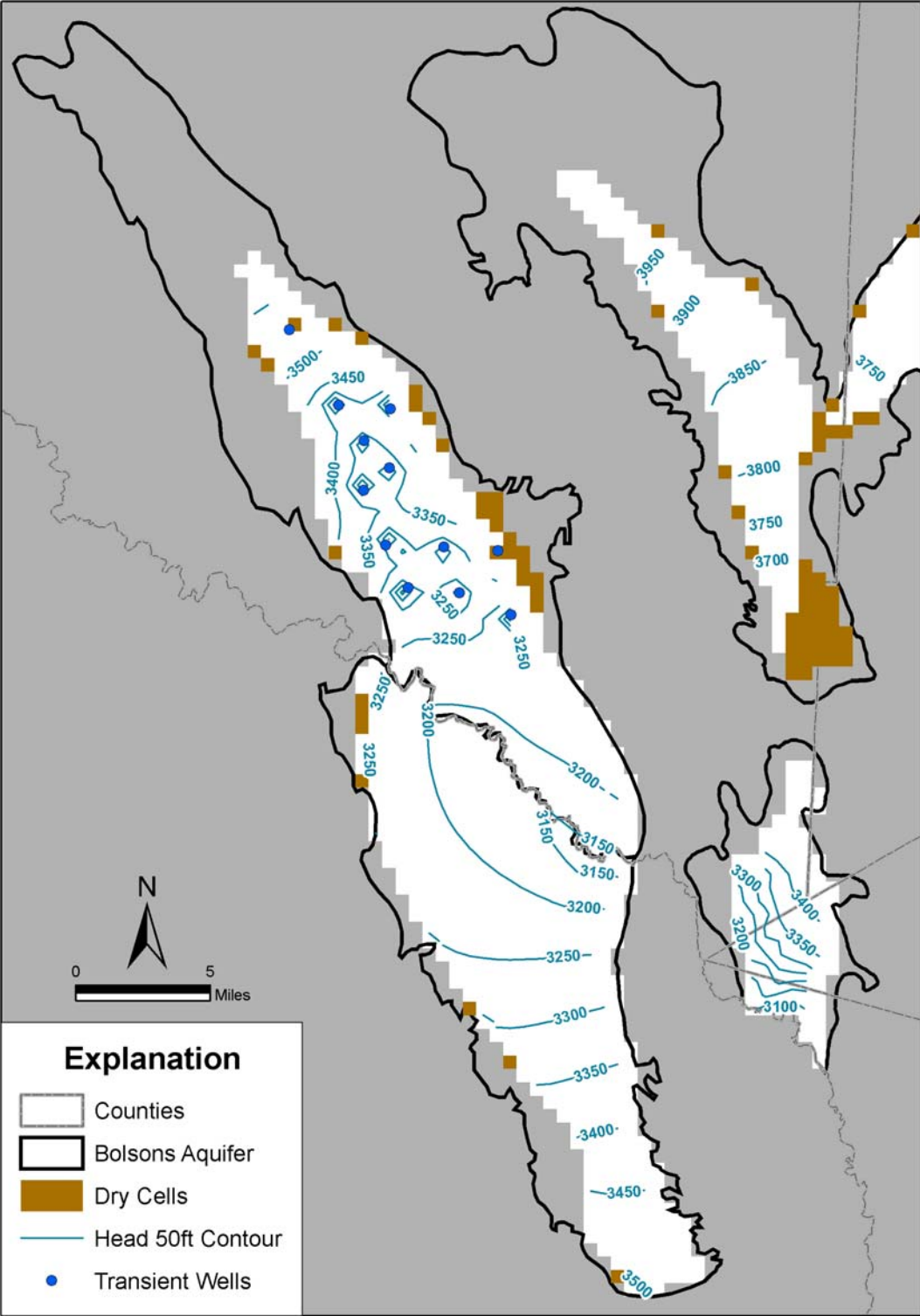


Figure 9.1.1 Well locations and water levels after 30 years with production of 9700 af/yr

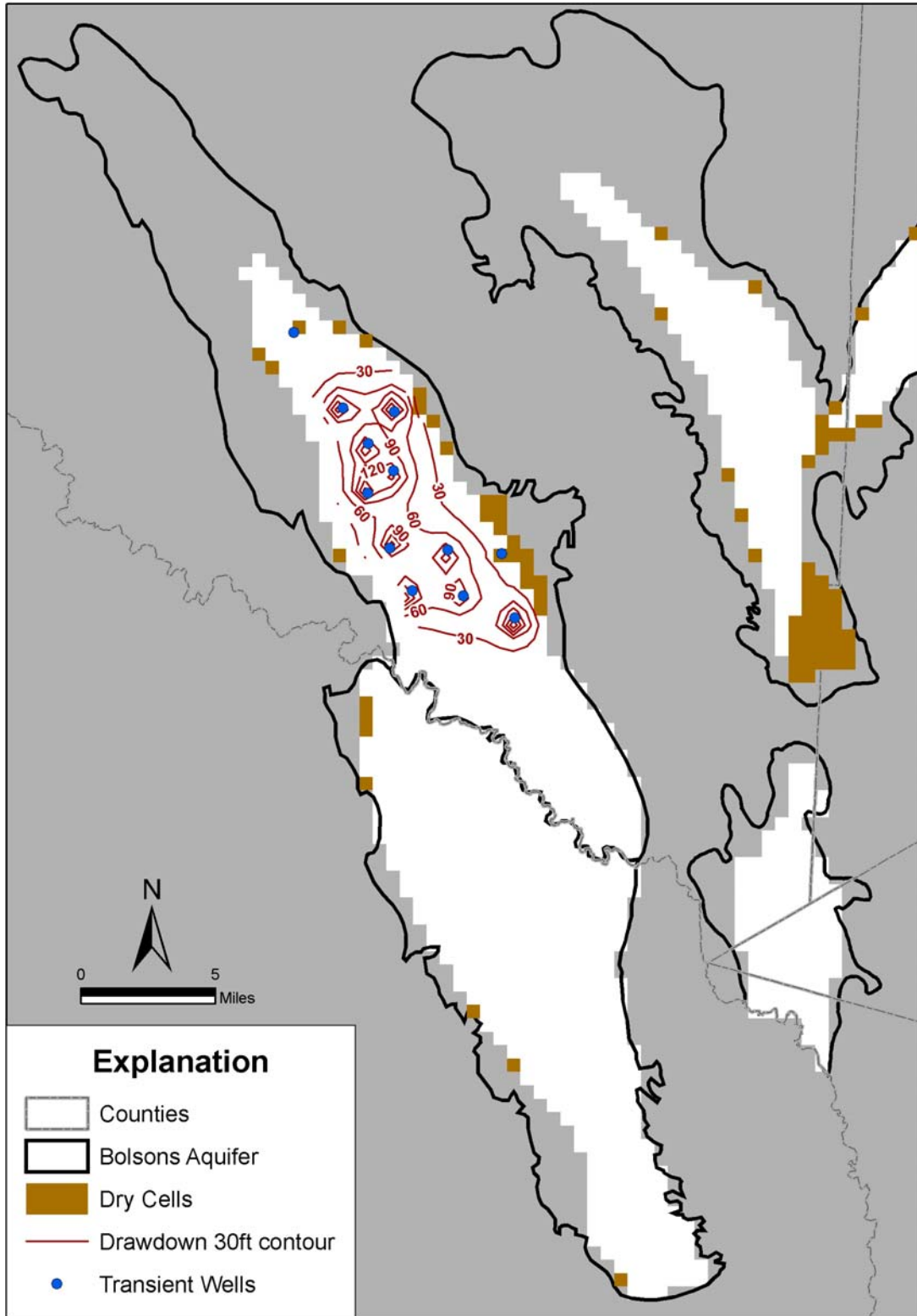


Figure 9.1.2 Water level decline after 30 years with production of 9700 af/yr

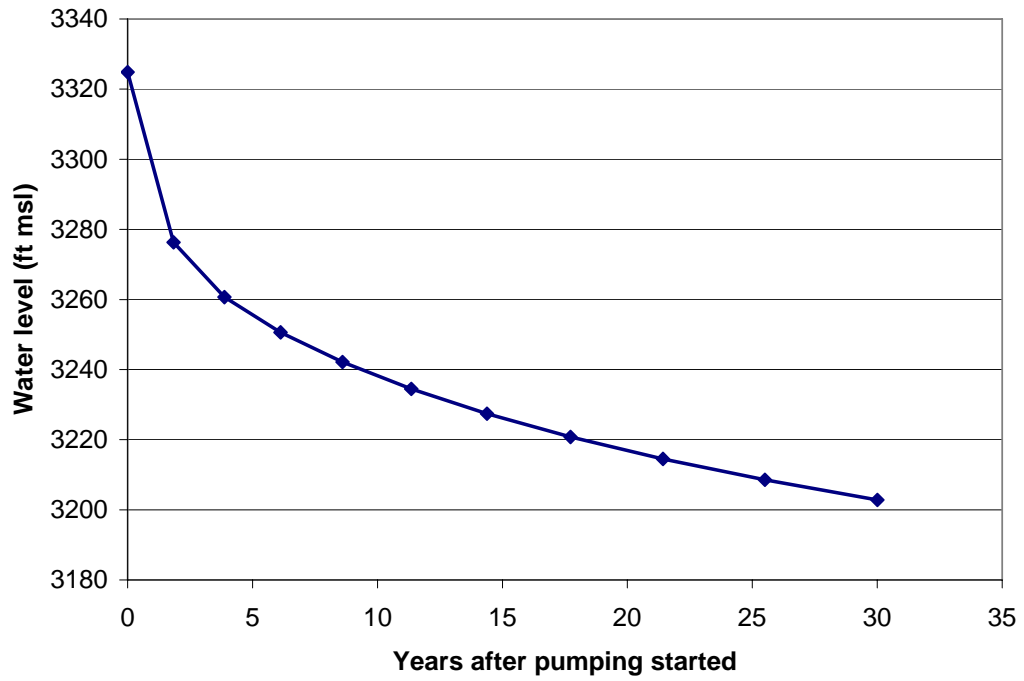


Figure 9.1.3 Water level decline during 30-year period with production of 9700 af/yr

9.2 Sensitivity Analysis

The sensitivity of the simulated water levels to storativity values and the pumping at the 12 well locations is shown in Figure 9.2.1. As expected, the plot indicates that the water levels are inversely related and very sensitive to pumping stress. Increasing the amount of pumping by 50% reduced the average water level at pumping wells more than 80 feet. Because the production occurred in the bolson, the model is also more sensitive to specific yield than to the specific storage. The water level change is around 10 to 20 feet at pumping wells if the calibrated specific yield changes 50%.

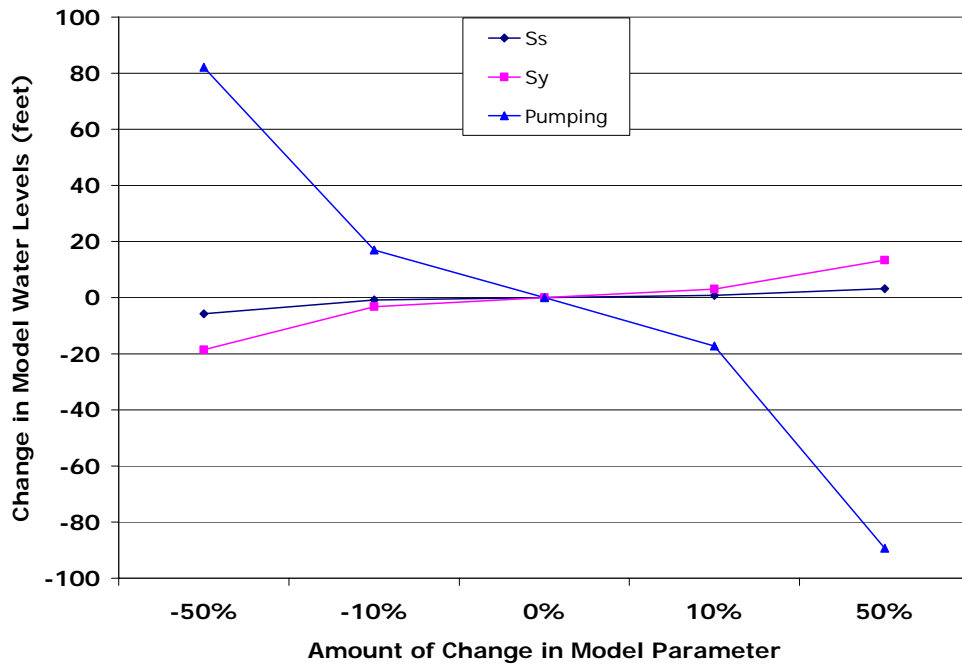


Figure 9.2.1 Transient sensitivity of the model to storage properties and pumping

10.0 LIMITATIONS OF THE MODEL

10.1 Limitations of Supporting Data

A groundwater model simulates aquifer dynamics and responses to hydrologic stresses such as groundwater withdrawals and change in recharge conditions. The accuracy to which a model can simulate this phenomenon is directly related to the reliability of aquifer data that are input into the model. The WTBGAM attempts to simulate groundwater flow in adjacent but hydrogeologically distinct aquifers that are hydrologically connected. Although the model simulates the observed regional radial flow pattern in the Eagle Mountains and the general water levels observed in the aquifers to a degree, it should be recognized that the model assumes a single, although heterogeneous, hydrogeologic unit, which is a greatly simplified model of reality.

Because the rock units that make up the modeled aquifers are a complex and heterogeneous system, there is a significant lack of data to quantitatively define the system. This is a limitation when developing a groundwater flow model, even at the regional scale. Some examples of data shortages include the lack of:

- sufficient deep wells,
- sufficient long-term water-level trends,
- aquifer transmissivity and saturated thickness data,
- location and extent of fracture zones and associated hydraulic characteristics,
- definition and characterization of distinct water bearing zones within the Cretaceous and Paleozoic units,
- precipitation, evapotranspiration, and recharge data,
- structural control, and
- gain-loss studies to determine stream-aquifer interaction.

10.2 Limiting Assumptions

The flow system in the study area contains several complexities that have been simplified for modeling purposes. A single model Layer in the conceptual and numerical

models represents each of the major aquifer units in the model area. In reality, each aquifer consists of many different zones that are hydraulically connected in varying degrees. The Cretaceous and Paleozoic rocks contain many potential water-bearing zones which transmit groundwater, but because there is a lack of data to characterize these units, the bolson and underlying aquifers have been lumped together into a single Layer in the model. While this conceptualization is consistent with the current understanding of the aquifer, it should be recognized that it is a great simplification of a very complex hydrogeologic system.

Cross-formational flow from the Cretaceous and Paleozoic rocks to the bolson aquifers is controlled by several factors that have not been fully characterized, including the hydraulic conductivity and connection between the aquifers. Additionally, the significance of any interaction with underlying units has not been established.

MODFLOW is formulated to simulate flow in continuous porous media like sand and gravel aquifers. Flow in the Cretaceous and Paleozoic rocks occurs largely in fractures, fissures, and through the porous matrix. MODFLOW has been used in other studies to simulate flow in fractured flow systems, but simulating flow in such a complex system with MODFLOW offers significant limitations under some conditions. However, there are limits to the applications for the model.

10.3 Limits for Model Applicability

The Cretaceous and Paleozoic aquifers were included in the WTBGAM mainly because of the recognition that it is a part of the regional flow system in the study area and provides recharge to the bolson aquifers. In general the model does a reasonable job simulating steady-state conditions in the Cretaceous and Paleozoic rocks and is helpful for gaining insight into the regional conditions in the aquifer and the regional impact of proposed strategies. However, the model is probably not a reasonable tool to assess spring flow in the mountainous areas of the model, stream-aquifer interaction, or assessment of localized water level conditions or aquifer dynamics in the Cretaceous and Paleozoic aquifers. These types of aquifer dynamics and interactions are controlled by many complex and local factors that were not and could not have been incorporated into

the simplified conceptual, data, or numerical model developed for this study. For instance, using the model to do particle tracking or capture zone analysis in Layer 2 or 3 would not be prudent due to the limitations discussed above. Performing such analysis in the bolsons (Layer 1) might be reasonable as a preliminary evaluation. In addition, the Cretaceous and Paleozoic portion of this model should be used with caution when attempting to simulate individual well dynamics, and possibly even local wellfield conditions because the model was not developed with that goal in mind nor were the data available on a regional basis to construct such a model for the entire area. Local wellfield simulations would benefit from a more localized model that is based on local pumping tests and calibration data.

Based on the available calibration data, the model simulates groundwater movement within the individual bolsons relatively well. However, the simulation of lateral movement between the bolsons is less defensible due to limited hydraulic property data and historic water level information.

11.0 FUTURE IMPROVEMENTS

11.1 Supporting Data

Groundwater data characterizing the West Texas Bolson aquifers are very sparse, and in some cases, nonexistent. The vertical interaction with underlying geologic units is not understood. Lateral eastward flow out of the Eagle Flat and into the Salt Basin through Cretaceous and Paleozoic rocks is not well understood. Therefore, continued collection of basic groundwater data (water levels, water chemistry and pumping tests) in all the aquifers would help refine the model. Because of the heterogeneity of all the aquifers, it would likely take several phased investigations to adequately characterize the distinct aquifer units so that a more detailed conceptualization could be implemented for a flow model. More characterization of the hydraulic properties of the all the aquifers, particularly the bolsons, would be helpful in refining the model. Long-term pumping tests would be advisable in the all the aquifer, but especially the Cretaceous and Paleozoic rocks.

11.2 Model Improvements

Appropriate calibration of a transient model requires a cause and effect relationship in model variables such as recharge, water levels, and production. No such data exist for the WTBGAM area. In addition to obtaining hydraulic properties for the aquifer, transient calibration data would improve the model significantly.

12.0 CONCLUSIONS

A three-dimensional groundwater model was developed for the West Texas Bolson aquifers according to a methodology prescribed by the TWDB. This modeling approach was consistent with TWDB GAM protocol and includes: (1) the development of a conceptual model of groundwater flow in the aquifer, (2) model design, (3) model calibration and verification, (4) sensitivity analysis, (5) model prediction, and (6) documentation of the model.

The model is regional in scale, and was developed with the MODFLOW-2000 flow code. The conceptual model developed for the flow model divides the aquifer system into three Layers, which incorporated the bolsons and the underlying Cretaceous and Paleozoic water-bearing zones. The conceptual model was based on data compiled from many sources and included a detailed analysis of recharge for the model area. Available hydraulic conductivity, aquifer storage properties, and water level measurements were assimilated for use in developing a representative and defensible model.

One purpose of this WTBGAM is to provide a tool for assessing impacts from production. The WTBGAM integrates all of the available hydrogeologic data for the study area into the flow model that can be used as a tool for the assessment of water management strategies. The model is publicly available and can be used by planners, Regional Water Planning Groups (RWPBs), Groundwater Conservation Districts (GCDs), and other entities to assess groundwater conditions under various scenarios.

The calibrated steady-state model reproduces the available water level measurements and flow directions relatively well, given the general lack of hydraulic properties in the model area. The model also simulates the observed radial flow pattern in the Eagle Mountains. The steady-state calibration statistics indicate that the model provides a reasonable tool for assessing groundwater flow in the model area. Sensitivity analysis indicates that the most sensitive parameters in the model are hydraulic conductivity and recharge. A transient calibration could not be completed due to the lack of significant water level change and groundwater production in the model area. However, appropriate

storage properties were incorporated in the model to ensure that the model is capable of providing reasonable estimates of water level changes due to production scenarios. The model is a valuable tool for evaluating proposed pumping in the West Texas Bolsons and underlying aquifers, and can be improved with more site-specific data.

13.0 ACKNOWLEDGEMENTS

The successful completion of a major modeling project, such as this WTBGAM, requires the cumulative knowledge, assistance, and backing of many individuals and groups outside the modeling team itself.

We would also like to thank the WTBGAM Stakeholder Group for their interest and input to the project. We thank the Texas Water Development Board for its forward thinking in developing and funding the statewide aquifer GAM program and its staff for their guidance and assistance in completing this project. Specifically, Cindy Ridgeway, who served as project manager, aided the project significantly. Ted Angle and Andy Donnelly also served as interim project managers. Jan Sherrill developed the drawings of the geologic cross-sections. Allan Standen helped assimilate the water level data for the study. Annie McCoy helped evaluate the recharge data.

Comments received from the TWDB on the Draft Conceptual Model Report can be found in Appendix E. Responses to each comment are also included in Appendix E.

14.0 REFERENCES

- Akersten, W. A., 1967, Red Light local fauna (Blancan), southeastern Hudspeth County, Texas: The University of Texas at Austin, Master's thesis, 168 p.
- Albritton, C. C., Jr., and Smith, J. F., Jr., 1965, Geology of the Sierra Blanca area, Hudspeth County, Texas: U.S. Geological Survey Professional Paper 479, 131 p.
- Anderson, M.P. and Woessner, W.W., 1992, Applied Groundwater Modeling: Academic Press, San Diego, CA, 381 p.
- Ashworth, J. B. and Hopkins, J., 1995, Aquifers of Texas: Texas Water Development Board Report 345, 69 p.
- Beach, J.A., Ashworth, J.A., Finch, Steven T., Jr., Chastain-Howley, A., Calhoun, K., Urbanczyk, K.M., Sharp, J.M., and Olson, J., 2004, Groundwater Availability Model for the Igneous and parts of the West Texas Bolsons (Wild Horse Flat, Michigan Flat, Ryan Flat and Lobo Flat) Aquifers: LBG-Guyton Associates, contract report prepared for Texas Water Development Board, 420 p.
- Bennett, J. B., and Finch, S.T., Jr., 2002, Concepts of groundwater recharge in the Trans-Pecos Region, Texas: Abstract GSA south-central spring 2002 meeting, Alpine Texas.
- Brune, G., 1975, Major and Historical Springs of Texas: Texas Water Development Board Report 189, 94 p.
- Brune, G., 1981, Springs of Texas. Volume 1: Fort Worth, Tex., Branch-Smith, Inc., 566 p.
- Collins, E. W., and Raney, J. A., 1994, Impact of late Cenozoic extension on Laramide overthrust belt and Diablo Platform margins, northwestern Trans-Pecos Texas, *in* Ahlen, Jack, Peterson, John, and Bowsher, A. L., eds., Geologic activities in the 90s: New Mexico Bureau of Mines and Mineral Resources, Bulletin No. 150, p. 71–81.

- Collins, E.W., and Raney, J.A., 1997, Quaternary faults within intermontane basins of northwest Trans-Pecos Texas and Chihuahua, Mexico: Bureau of Economic Geology Report of Investigations No. 245, University of Texas, 59 p.
- Cooper, H.H., Jr., and Jacob, C.E., 1946. A generalized graphical method for evaluating formation constants and summarizing well field history. *Trans. Amer. Geophys. Union*, 27, pp. 526-534.
- Darling, B.K., Hibbs, B.J., and Dutton, A.R., 1994, Ground-water hydrology and hydrochemistry of Eagle Flat and surrounding area: The University of Texas at Austin Bureau of Economic Geology, contract report prepared for Texas Low-Level Radioactive Waste Disposal Authority, Interagency Contract No. (92-93)-0910, 137 p.
- Darling, B.K., 1997, Delineation of the groundwater flow systems of the Eagle Flat and Red Light basins of Trans-Pecos Texas: The University of Texas at Austin, Ph.D. dissertation, 179 p.
- Darling, B.K., and Hibbs, B.J., 2001, The aquifers of Red Light Draw, Green River Valley, and Eagle Flat, *Section 16 in* Mace, R.E., Mullican, W.F., and Angle, E.S., eds., *Aquifers of West Texas*, Texas Water Development Board, p.226-240.
- DeFord, R. K., and Bridges, L. W., 1959, Tarantula Gravel, northern Rim Rock country, Trans-Pecos Texas: *Texas Journal of Science*, v. 11, p. 268-295.
- DeFord, R. K., and Haenggi, W. T., 1971, Stratigraphic nomenclature of Cretaceous rocks in northeastern Chihuahua, *in* Seewald, Ken, and Sundeen, Dan, eds., *The geologic framework of the Chihuahua tectonic belt: West Texas Geological Society Publication 71-59*, p. 175–196.
- Dietrich, J. W., Owen, D. E., Shelby, C. A., and Barnes, V. E., 1983, Van Horn–El Paso sheet: The University of Texas at Austin, Bureau of Economic Geology, *Geologic Atlas of Texas*, scale 1:250,000.

- Driscoll, F.G., 1986, *Groundwater and Wells*, Second Edition: Johnson Filtration Systems, St. Paul, MN, 1,089 p.
- Doherty, J., 2002. *Manual for PEST*, 5th edition. Watermark Numerical Computing, Brisbane, Australia.
- Fenneman, N. M., 1931, *Physiography of the Western United States*; McGraw-Hill, New York, 534 p.
- Finch, S.T., Jr., and Armour, J., 2001, Hydrogeologic analysis and groundwater flow model of the Wild Horse Flat area, Culberson County, Texas: consultant's report prepared by John Shomaker & Associates, Inc., for Beldon Foundation (administered by Christian Life Commission) and Culberson County Groundwater Conservation District, 37 p. plus figures and appendices.
- Finch, S.T., Jr., McCoy, A.M., Luna, M.L., 2005, 2nd annual progress report in support of Chino Mines Company Supplemental Discharge Permit for Closure, DP-1340, Condition 86: consultant's report prepared by John Shomaker & Associates, Inc., for Chino Mines Company, 36 p. plus figures and appendices.
- Freeze, R. A., and Cherry, J. A., 1979. *Groundwater*, Prentice-Hall, Inc., 604 p.
- Freeze, R.A., and P.A. Witherspoon, 1967, Theoretical analysis of regional groundwater flow: effects of water-table configuration and subsurface variation: *Water Resources Research*, Vol. 3, p. 623-34.
- Gates, J.S., and Smith, J.T., 1975, Exploration for fresh water in the Eagle Mountains area, Hudspeth County, Texas; *in* *Geology of the Eagle Mountains and Vicinity, Trans-Pecos Texas: Permian Basin Section Guidebook Publication 75-15*, p. 129-134.
- Gates, J.S., and White, D.E., 1976, Test drilling for ground water in Hudspeth, Culberson, and Presidio Counties in westernmost Texas: U.S. Geol. Survey Open-File Rept. 76-338, 76 p.

- Gates, J.S., White, D.E., Stanley, W.D., and Ackermann, H.D., 1980, Availability of fresh and slightly saline ground water in basins of westernmost Texas: Texas Department of Water Resources Report No. 256, 108 p.
- George, P., Mace, R.E., and Mullican, W.F., 2005, The hydrogeology of Hudspeth County, Texas: Texas Water Development Board Report 364.
- Gries, J. G., and Haenggi, W. T., 1971, Structural evolution of the eastern Chihuahua Tectonic Belt, *in* Seewald, Ken, and Sundeen, Dan, eds., The geologic framework of the Chihuahua Tectonic Belt: West Texas Geological Society, p. 119-138.
- Gries, J. G., 1980, Laramide evaporite tectonics along the Texas–northern Chihuahua border, *in* Dickerson, P. W., Hoffer, J. M., and Callender, J. F., eds., Trans-Pecos region, southeastern New Mexico and West Texas: New Mexico Geological Society, 31st Annual Field Conference, p. 93–100.
- Henry, C.D., 1979, Geologic setting and geochemistry of thermal water and geothermal assessment, Trans-Pecos Texas: Bureau of Economic Geology Report of Investigations No. 96, University of Texas.
- Henry, C.D. and McDowell, F.W., 1986, Geochronology of magmatism in the Tertiary volcanic field, Trans-Pecos Texas, *in* Price, J.G., Henry, C.D., Parker, D.F., and Barker, D.S., eds., Igneous geology of Trans-Pecos Texas: Field trip guide and research articles: The University of Texas, Bureau of Economic Geology Guidebook 23, pp. 99-122.
- Henry, C. D., and Price, J. G., 1984, Variations in caldera development in the mid-Tertiary volcanic field of Trans-Pecos Texas: *Journal of Geophysical Research*, v. 89, no. B10, p. 8765-8786.
- Henry, C. D., and Price, J. F., 1985, Summary of the tectonic development of Trans-Pecos Texas: The University of Texas at Austin, Bureau of Economic Geology, Miscellaneous Map No. 36, scale 1:500,000, 8-p. text.
- Henry, C. D., McDowell, F. W., Price, J. G., and Smyth, R. C., 1986, Compilation of

potassium-argon ages of Tertiary igneous rocks, Trans-Pecos Texas: The University of Texas at Austin, Bureau of Economic Geology, Geological Circular 86-2, 34 p.

Henry, C. D., and Price, J. F., 1986, Early Basin and Range development in Trans-Pecos Texas and adjacent Chihuahua: magmatism and orientation, timing, and style of extension: *Journal of Geophysical Research*, v. 91, no. B6, p. 6213-6224.

Henry, C. D., and Price, J. F., 1989, Characterization of the Trans-Pecos region, Texas: geology, in Bedinger, M. S., Sargent, K. A., and Langer, W. H., eds., *Studies of geology and hydrology in the Basin and Range Province, southwestern United States, for isolation of high-level radioactive waste- characterization of the Trans-Pecos region, Texas*: U.S. Geological Survey Professional Paper 1370-B, p. B4-B22.

Hibbs, B.J., Darling, B.K., and Ashworth, J.B., 1995, Interbasin movement of groundwater and vertical ground-water flow in Hudspeth County, Texas: *Proceedings of Texas Water 95, a Component Conference of the First International Conference on Water Resources Engineering*, American Society of Civil Engineers, San Antonio, TX, p. 267 - 277.

Hibbs, B.J., and Darling, B.K., 1995, Salinization of the Rio Grande alluvial aquifer in Trans-Pecos, Texas: *Proceedings of the 24th Water for Texas Conference, Research Leads the Way*, Austin, TX, p.157-161.

Hibbs, B.J., and Darling, B.K., 2005, Revisiting a classification scheme for U.S.-Mexico alluvial basin-fill aquifers: *Ground Water*, vol. 43, no. 5, pp. 750-763.

Horak, R. L., 1985, Trans-Pecos tectonism and its effect on the Permian Basin, *in* Dickerson, P. W., and Muehlberger, W. R., eds., *Structure and tectonics of Trans-Pecos Texas*: West Texas Geological Society Publication 85-81, p. 81-87.

- Huff, G.F., 2004, Simulation of groundwater flow in the Tularosa Basin, south-central New Mexico, 1948-95, with projections to 2040: U.S. Geological Survey Water Resources Investigations Report 2004-5197, 108 p.
- Jackson, M. L. W., and Whitelaw, M. J., 1992, Characteristics and paleomagnetic dating of thick buried vertisols, Trans-Pecos Texas (abs.): Geological Society of America Abstracts with Programs, v. 24, no. 7, p. A286.
- Jackson, M. L. W., Langford, R. P., and Whitelaw, M. J., and Whitelaw, 1993, Basin-fill stratigraphy, Quaternary history, and paleomagnetism of the Eagle Flat study area, southern Hudspeth County, Texas: The University of Texas at Austin, Bureau of Economic Geology, final report prepared for the Texas Low-Level Radioactive Waste Disposal Authority under interagency contract no. IAC(92-93)-0910, 137 p.
- Jones, B. R., and Reasor, D. F., 1970, Geology of southern Quitman Mountains, Hudspeth County, Texas: The University of Texas at Austin, Bureau of Economic Geology Geologic Quadrangle Map No. 39, scale 1:48,000, 24-p. text.
- JSAI, 2006, Report on Water Treatment System Sustainability, Chino Mines Company, DP-1340, Condition 86: consultant's report prepared by John Shomaker & Associates, Inc., for Chino Mines Company, 47 p. plus figures and appendices.
- King, P. B., and Flawn, P. T., 1953, Geology and mineral deposits of the Precambrian rocks of the Van Horn area, Texas: University of Texas, Austin, Bureau of Economic Geology Publication 5301, 218 p.
- King, P. B., 1965, Geology of the Sierra Diablo region, Texas: U.S. Geological Survey Professional Paper 480, 185 p.

- Kreitler, C.W., Raney, J.A., Nativ, R., Collins, E.W., Mullican, W.F., Gustavson, T.C., and Henry, C.D., 1987, Siting a low-level radioactive waste disposal facility in Texas, volume four - geologic and hydrologic investigations of State of Texas and University of Texas Lands: The University of Texas at Austin, Bureau of Economic Geology, report prepared for the Texas Low-Level Radioactive Waste Disposal Authority under Interagency Contract No IAC(86-87) 1790, 330 p.
- Langford, R. P., 1993, Landscape evolution of the Eagle Flat and Red Light Basins, Chihuahuan Desert, South-Central Trans-Pecos Texas: The University of Texas at Austin, Bureau of Economic Geology, final report prepared for the Texas Low-level Radioactive Waste Disposal Authority under interagency contract no. IAC(92-93)-0910, 153 p.
- Larkin, T. J. and Bomar, G. W., 1983, Climatic Atlas of Texas: Texas Department of Water Resources Report LP-192, 151 p.
- LBG-Guyton Associates, 1998, Evaluation of the potential impact of the application of biosolids on surface-water and ground-water resources in the vicinity of the Pinon Ranch, Hudspeth County, Texas: contract report prepared for EPIC, Inc., 29 p.
- LBG-Guyton Associates, Freese and Nichols, Inc., Moreno Cardenas, Inc., M3H Consulting, Inc., 2001, Far West Texas Regional Water Plan: consultant's report prepared for Texas Water Development Board.
- Mack, G. H., and Seager, W. R., 1990, Tectonic control on facies distribution of the Camp Rice and Palomas Formations (Plio-Pleistocene) in the southern Rio Grande rift: Geological Society of America Bulletin, v. 102, p. 45–53.
- Mack, G. H., Kottlowski, F. E., and Seager, W. R., 1998, The stratigraphy of south-central New Mexico, *in* Mack, G. H., Austin, G. S., and Barker, J. M., eds., Las Cruces country II: New Mexico Geological Society Guidebook, 49th Field Conference, p. 135–154.

- Maxey, G.B., and M.D. Mifflin, 1966, Occurrence and movement of groundwater in carbonate rocks of Nevada: National Speleol. Soc. Bulletin, Vol. 28, no. 3, p. 141-157.
- McAda, D.P., and Wasiolek, M., 1988, Simulation of the regional geohydrology of the Tesuque aquifer system near Santa Fe, New Mexico: U.S. Geological Survey Water Resources Investigations Report 87-4056, 71 p.
- Meyer, W.R., 1976, Digital model for simulating effects of ground-water pumping in the Hueco Bolson, El Paso area, Texas, New Mexico, and Mexico: U.S. Geological Survey Water Resources Investigations Report 85-4219, 94 p.
- Mifflin, M.D., 1968, Delineation of ground-water flow systems in Nevada: Univ. of Nevada at Reno, Center for Water Resources Research and Desert Research Institute Technical Rept. Series H-W, No. 4. 112 p
- Muehlberger, W. R., 1980, Texas lineament revisited, *in* Dickerson, P. W., Hoffer, J. M., and Callender, J. F., eds., Trans-Pecos region, southeastern New Mexico and West Texas: New Mexico Geological Society Guidebook No. 31, p. 113–121.
- Muehlberger, W.R. and Dickerson, P.W., 1989, A tectonic history of Trans-Pecos Texas: *in* Muehlberger, W.R. and Dickerson, P.W. (editors), Structure and Stratigraphy of Trans-Pecos Texas: American Geophysical Union field trip Guidebook T317, pp. 35-54.
- Nativ, R., and Riggio, R., 1989, Meteorologic and isotopic characteristics of precipitation events with implications for groundwater recharge, southern High Plains: Atmospheric Research, v. 23, pp. 51 – 82.
- Nativ, R., and Riggio, R., 1990, Precipitation in the southern High Plains – Influences and isotopic features: Journal of Geophysical Research, v. 95.
- Nichols, W. D., 2000, Regional groundwater evapotranspiration and groundwater budgets, Great Basin, Nevada: U. S. Geological Survey Professional Paper 1628.

- Osburg, Cliff, Berge, Tim, Dowse, Mary, and Dickerson, Ed, 1985, Third day road log from Van Horn to Devil Ridge, to Malone Mountains to Sierra San Ignacio, and on to Alpine, *in* Dickerson, P. W., and Muehlberger, W. R., eds., Structure and tectonics of Trans-Pecos Texas: West Texas Geological Society Publication 85-81, p. 17- 24.
- Price, J. G., and Henry, C. D., 1984, Stress orientations during Oligocene volcanism in Trans-Pecos Texas: timing the transition from Laramide compression of Basin and Range tension: *Geology*, v. 12, no. 4, p. 238-241.
- Price, J. G., and Henry, 1985, Summary of Tertiary stress orientations and tectonic history of Trans-Pecos Texas, *in* Dickerson, P. W., and Muehlberger, W. R., eds., Structure and tectonics of Trans-Pecos Texas: West Texas Geological Society Publication 85-81, p. 149-151.
- Price, J. G., Henry, C. D., Parker, D. F., and Barker, D. S., 1986, Igneous geology of Trans-Pecos Texas: The University of Texas at Austin, Bureau of Economic Geology Guidebook 23, 360 p.
- Raney, J. A., and Collins, E. W., 1993, Regional geologic setting of the Eagle Flat study area, Hudspeth County, Texas: The University of Texas at Austin, Bureau of Economic Geology, final report prepared for the Texas Low-level Radioactive Waste Disposal Authority under interagency contract no. IAC(92-93)-0910, 53 p.
- Reaser, D.F., Underwood, J.R., and Jones, B.R., J.T., 1975, Geothermal prospects of the Eagle-Mountains vicinity Trans-Pecos Texas; *in* Geology of the Eagle Mountains and Vicinity, Trans-Pecos Texas: Permian Basin Section Guidebook Publication 75-15, p. 129-134.
- Scanlon, B. R., Darling, B. K., and Mullican, W. F., 2001, Evaluation of groundwater recharge in basins in Trans-Pecos Texas: *in* Aquifers of West Texas: Texas Water Development Board Report 356, pp. 26-40.

- Schmidt, R. H., 1995, The climate of Trans-Pecos Texas: *in* The Changing Climate of Texas; predictability and implications for the future: Texas A&M University, GeoBooks, pp. 122 – 137.
- Seager, W. R., Shafiqullah, M., Hawley, J. W., and Marvin, R. F., 1984, New K-Ar dates from basalts and the evolution of the southern Rio Grande rift: Geological Society of America Bulletin, v. 95, no. 1, p. 87-99.
- Sears, J. W., and Price, R. A., 1978, The Siberian connection: a case for Precambrian separation of the North American and Siberian cratons: *Geology*, v. 6, no. 5, p. 267-270.
- Snyder, C.T. 1962. A hydrologic classification of valleys in the Great Basin, western United States. *Bulletin of the International Association of Scientific Hydrology* 7, no. 3: 53–59.
- Stevens, J. B., and Stevens, M. S., 1985, Basin and Range deformation and depositional timing, Trans-Pecos Texas, *in* Dickerson, P. W., and Muehlberger, W. R., eds., Structure and tectonics of Trans-Pecos Texas: West Texas Geological Society Field Conference, Publication 85-81, p. 157-163.
- Stone, D B., Moomaw, C. L., and Davis, A., 2001, Estimating recharge distribution by incorporating runoff from mountainous areas in an alluvial basin in the Great Basin region of the southwestern United States: *Groundwater*, v. 39, no. 6, pp. 807-818.
- Strain, W. S., 1966, Blancan mammalian fauna and Pleistocene formations, Hudspeth County, Texas: Texas Memorial Museum Bulletin No. 10, 55 p.
- Strain, W. S., 1971, Late Cenozoic bolson integration in the Chihuahua tectonic belt, *in* Hoffer, J. M., ed., Geologic framework of the Chihuahua tectonic belt: West Texas Geological Society Publication 71-59, p. 167–173.
- Thornbury, W. D., 1965, Regional Geomorphology of the United States: John Wiley & Sons, New York, 609 p.

- Twiss, P. C., 1959, Geology of Van Horn Mountains, Texas: University of Texas, Austin, Bureau of Economic Geology Geologic Quadrangle Map No. 23, scale 1:48,000.
- Twiss, P. C., 1979, Marfa sheet, Barnes, V. E., project director: The University of Texas at Austin, Bureau of Economic Geology geologic Atlas of Texas, scale 1:250,000.
- USGS, 2003, Heitmuller, F. T., and B.D. Reece. Database of Historically Documented Springs and Spring Flow Measurements in Texas, Open-File Report 03-315.
- Underwood, J. R., Jr., 1963, Geology of the Eagle Mountains and vicinity, Hudspeth County, Texas: University of Texas, Austin, Bureau of Economic Geology, Geologic Quadrangle Map No. 26, scale 1:48,000, 32-p. text.
- Utah State University Climate Center, 2006, climate.usu.edu/weather/dataserv.htm
- Wasiolek, M., 1995, Subsurface recharge to the Tesuque aquifer system from selected drainage basins along the western side of the Sangre de Cristo Mountains near Santa Fe, New Mexico: U.S. Geological Survey, Water Resource Investigations Report 94-4072, 57 p.
- Waltemeyer, S.D., 2001, Estimates of mountain-front streamflow available for potential recharge to the Tularosa Basin, New Mexico: U.S. Geological Survey, Water-Resources Investigations Report 01-4013, 8 p.
- White, D.E., Gates, J.J., Smith, M.T., and Fry, B.J., 1980, Groundwater data for Salt Basin, Eagle Flat, Red Light Draw, Green River Valley, and Presidio Bolson in westernmost Texas: Texas Department of Water Resources Report 259, 97 p. (Also published as U.S. Geological Survey Open-File Report 77-575.)
- White, D.E., J.S. Gates, J.T. Smith, and B.J. Fry, 1980, Ground-water data for the Salt Basin, Eagle Flat, Red Light Draw, Green River Valley, and Presidio Bolson in westernmost Texas: Texas Dept. of Water Res. Rept. 259, 97 p.
- Winograd, I.A., 1962, Interbasin movement of ground water at the Nevada Test Site, Nevada: U.S. Geol. Survey Professional Paper 45-C, p. C108-C111.

Winograd, I.A., and W. Thodarson, 1975, Hydrogeological and hydrochemical framework, south central Great Basin, with special reference to the Nevada Test Site: U.S. Geol. Survey Professional Paper 712-C.

Wilson, J. A., 1970, Vertebrate biostratigraphy of Trans-Pecos Texas and northern Mexico, *in* Seewald, Ken, and Sundeen, Dan, eds., The geologic framework of the Chihuahua tectonic belt-a symposium in honor of Professor R. K. DeFord: West Texas Geological Society Publication 71-59, p. 159-166.

Wilson, J.D. and Naff, R.L., 2004, The U.S. Geological Survey modular ground-water model -- GMG linear equation solver package documentation: U.S. Geological Survey Open-File Report 2004-1261, 47 p.

APPENDIX A

DETAILED GEOLOGIC MAPS AND DEFINITIONS

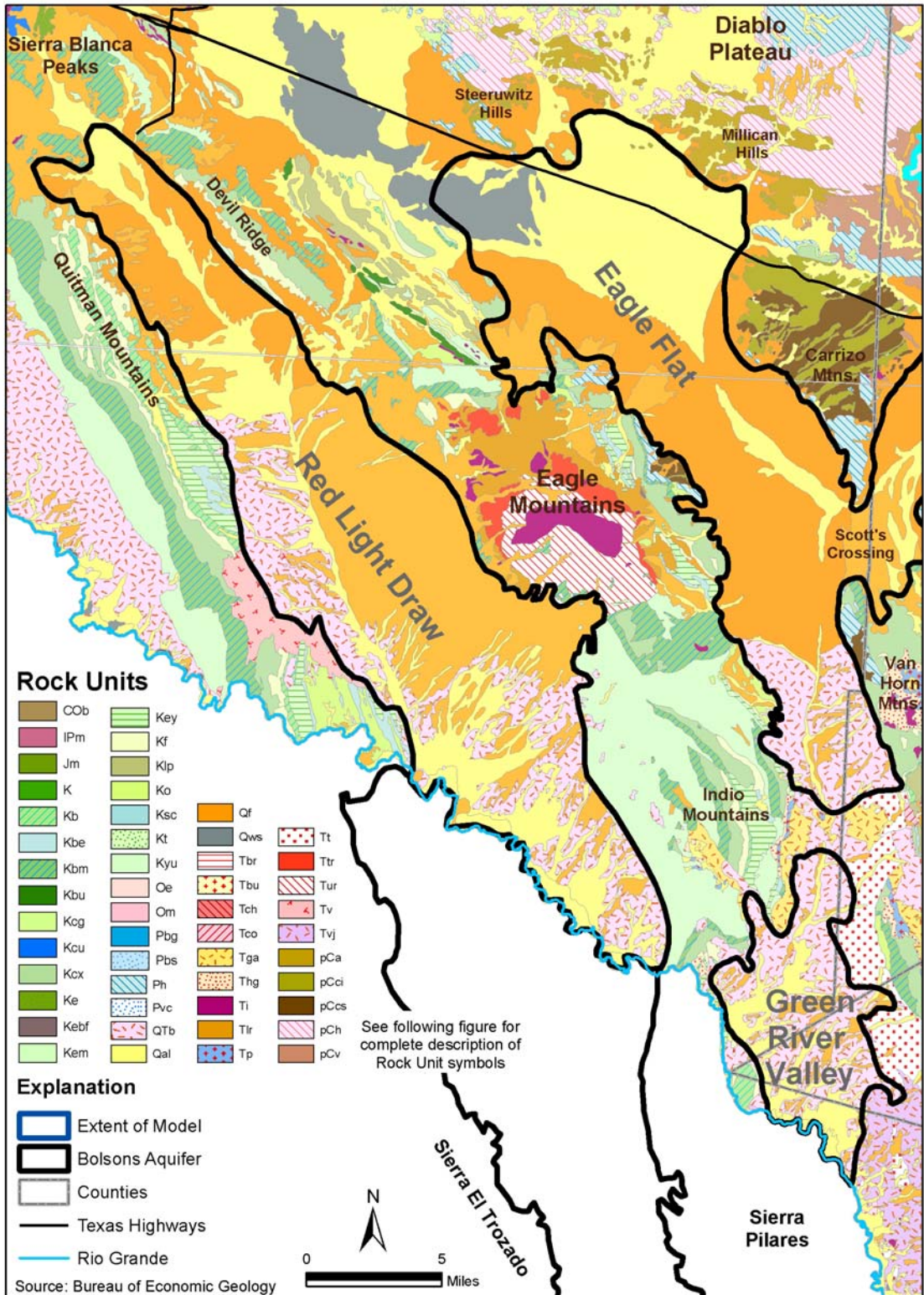


Figure A.1 – Detailed geology of the West Texas Bolson study area (BEG)



Figure A.2 – Geology symbol explanation (BEG)

Table A.1 – Geology definitions (BEG)

Rock Unit Code	Short Name	Long Name	Domain	Description	Epoch	Period
COb	Bliss	Bliss Sandstone	COb - Bliss Sandstone	Franklin Mountains, sandstone, mostly fine grained, medium to thick bedded, a few beds quartzitic, some glauconitic beds in upper half: weathers dark reddish brown; maximum thickness 250 feet, locally absent. Hueco Mountains, sandstone, in part coarse gr	Lower Ordovician and Upper Cambrian	Ordovician and Cambrian
DM	Devonian and Mississippian rocks	Devonian and Mississippian rocks undivided	DM - Devonian and Mississippian rocks undivided	Limestone, shale, and chert. Franklin Mountains, five units not separately mapped (Mississippian-(1) Helms Shale, (2) Rancheria Formation, (3) Las Cruces Limestone; Devonian-(4)Percha Shale, (5) Canutillo Formation), from the top down: (1) gray and green		Mississippian and Devonian
IPm	Magdalena	Magdalena Formation	IPm - Magdalena Formation	Limestone, shale, and marl. Franklin Mountains, four units not separately mapped (from top unnamed unit, Bishops Cap, Berino, and La Tuna), mostly limestone, mostly fine grained, in part cherty particularly in basal unit, very thick bedded, basal unit ma		Pennsylvanian
Jm	Malone	Malone Formation	Jm - Malone Formation	Limestone, shale, siltstone, sandstone, gypsum, and conglomerate. Upper part, mostly limestone, aphanitic, beds 3-7 feet thick, black, weathers gray; up to 25 feet of brownish-yellow sandstone and limestone at top. Lower part, complexly interfingered san	Upper Jurassic	Jurassic
K	Cretaceous rocks	Cretaceous rocks undivided	K - Cretaceous rocks undivided	Franklin Mountains area, small outcrops of limestone, marl, shale, and sandstone; mostly Comanchean, some Gulfian. Northern Diablo Plateau, basal clastic rocks including Cox Sandstone and Campagrande Formation undivided. Sierra Blanca area, Gulfian sand	Upper and Lower Cretaceous	Cretaceous
Kb	Benevides	Benevides Formation	Kb - Benevides Formation	in Quitman Mountains, upper part: shale, gray, fissile, a few thin limestone interbeds, nodular, gray; middle part: limestone, thick bedded, probably rudistid reef; lower part: shale, dark gray,	Lower Cretaceous	Cretaceous

Rock Unit Code	Short Name	Long Name	Domain	Description	Epoch	Period
				calcareous, interbedded with sandstone, fine grained, thin		
Kbd	Buda and Del Rio	Buda Limestone and Del Rio Clay undivided	Kbd - Buda Limestone and Del Rio Clay undivided	Buda Limestone and Del Rio Clay undivided, Kbd, in Pinto Canyon area. Buda Limestone, in Quitman Mountains, upper part: limestone, thin to thick bedded, resistant, a few chert nodules; middle part: interbedded gray limestone, marl, and calcareous shale,	Lower Cretaceous	Cretaceous
Kbe	Buda and Eagle Mountain	Buda Limestone and Eagle Mountain Sandstone	Kbe - Buda Limestone and Eagle Mountain Sandstone	Buda Limestone and Eagle Mountain Sandstone undivided, Kbe, in Quitman, Eagle, and Van Horn Mountains areas. Buda Limestone, in Quitman Mountains, upper part: limestone, thin to thick bedded, resistant, a few chert nodules; middle part: interbedded gray	Lower Cretaceous	Cretaceous
Kbh	Boracho	Boracho Limestone	Kbh - Boracho Limestone	in Wiley Mountains, upper part (San Martine Limestone Member): microgranular, hard, thick bedded, fossiliferous, pale yellowish brown; lower part (Levinson Limestone Member): marl, mostly covered; thickness of formation 180 to 330 feet.	Lower Cretaceous	Cretaceous
Kbl	Levinson	Levinson Limestone	Kbl - Levinson Limestone	limestone, marl, shale, and sandstone. Upper two-thirds, limestone, thin to thick bedded, light gray to light olive gray; interbeds of yellowish marl and shale. Lower one-third, shale, light to dark gray; a few thin to thick beds of limestone; sandstone	Lower Cretaceous	Cretaceous
Kbm	Bluff Mesa	Bluff Mesa Formation	Kbm - Bluff Mesa Formation	in Quitman Mountains, upper part: limestone, fine grained, massive to thick bedded, dark gray, Orb;to;ma-bearing, at top thin bedded, thickness 600+ feet; middle part: interbedded shale, black-gray, calcareous, limestone, thin bedded, fossiliferous, and	Lower Cretaceous	Cretaceous
Kbo	Boquillas	Boquillas Formation	Kbo - Boquillas Formation	limestone, marl, and shale; upper part: interbedded marl and shale; lower part: limestone, silty to sandy, flaggy, dark grayish orange near base; marine megafossils; confined to a few thin outcrops in the northeastern corner of sheet	Upper Cretaceous	Cretaceous
Kbs	San Martine	San Martine	Kbs - San	San Martine Limestone Member, Kbs, mapped	Lower	Cretaceous

Rock Unit Code	Short Name	Long Name	Domain	Description	Epoch	Period
		Limestone Member	Martine Limestone Member	separately northwest of Boracho Peak	Cretaceous	
Kbu	Buda	Buda Limestone	Kbu - Buda Limestone	in Quitman Mountains, upper part: limestone, thin to thick bedded, resistant, a few chert nodules; middle part: interbedded gray limestone, marl, and calcareous shale, recessive, limonite nodules common; lower part: limestone, aphanitic, thin to thick be	Lower Cretaceous	Cretaceous
Kbus	Buda and San Martine	Buda Limestone and San Martine Member	Kbus - Buda Limestone and San Martine Member	of Boracho Formation undivided	Lower Cretaceous	Cretaceous
Kcg	Campagrande	Campagrande Formation	Kcg - Campagrande Formation	Limestone, marl, conglomerate, sandstone, siltstone, and shale; thins northeastward. Finlay Mountains, upper 200-250 feet, alternating marl and limestone thin to thick bedded, gray; abundant marine megafossils and foraminifers; lower part interbedded sand	Lower Cretaceous	Cretaceous
Kcu	Comanchean	Comanchean (Washita) rocks undivided	Kcu - Comanchean (Washita) rocks undivided	West of Arroyo Campo Grande, pre-Finlay(?) limestone and shale. Quitman Mountains and Sierra Blanca area, marl, clay, and limestone younger than Finlay Limestone. Sneed (Cox) Mountain, Finlay Formation and overlying marl and clay. Diablo Plateau, marl	Lower Cretaceous	Cretaceous
Kcx	Cox	Cox Sandstone	Kcx - Cox Sandstone	In Quitman Mountains, upper part: interbedded sandstone, fine grained, calcareous, siltstone, shale, limestone, sandy, nodular, fossiliferous, thickness 360 feet; middle part: limestone, thick-bedded, reefy, rudistid-bearing, thickness 250 feet; lower part	Lower Cretaceous	Cretaceous
Ke	Etholen	Etholen Conglomerate	Ke - Etholen Conglomerate	Mostly conglomerate composed of gray to black well-rounded limestone blocks and fragments up to 18 inches across and chert fragments, generally black, up to 6 inches across in a gray to white limestone and sparry calcite matrix. A few angular	Lower Cretaceous	Cretaceous

Rock Unit Code	Short Name	Long Name	Domain	Description	Epoch	Period
				blocks of l		
Kebf	Benevides and Espy	Benevides Formation and Finlay Limestone undivided	Kebf - Benevides Formation and Finlay Limestone undivided	Benevides Formation, Kb, in Quitman Mountains, upper part: shale, gray, fissile, a few thin limestone interbeds, nodular, gray; middle part: limestone, thick bedded, probably a rudistid reef; lower part: shale, dark gray, calcareous, interbedded with san	Lower Cretaceous	Cretaceous
Kem	Eagle Mountains	Eagle Mountains Sandstone	Kem - Eagle Mountains Sandstone	Quartz sandstone, very fine grained, calcareous, ferruginous, crossbedded in part, thin bedded; some sandy limestone and shale interbeds; weathers shades of orange and brown, outcrop littered by angular, platy fragments of sandstone; thickness 130 feet	Lower Cretaceous	Cretaceous
Key	Espy	Espy Limestone	Key - Espy Limestone	in Quitman Mountains, upper part: limestone, recessive, thin to thick bedded, fossiliferous, interbedded with limestone, in part nodular, in part flaggy, sandy, and shale, calcareous; lower part: limestone, resistant, thin to thick bedded, with marl and	Lower Cretaceous	Cretaceous
Kf	Finlay	Finlay Limestone	Kf - Finlay Limestone	in Quitman and Eagle Mountains, alternating resistant and recessive units, limestone, fine grained, some beds cherty, thick bedded, fossiliferous, medium gray, weathers pale yellowish brown; shale, silty, calcareous; toward base some siltstone and sandst	Lower Cretaceous	Cretaceous
Kg	Gulfian rocks	Gulfian rocks undivided	Kg - Gulfian rocks undivided	marl, shale, and argillaceous limestone. Fossils indicate correlation with Central Texas units-Taylor, Austin, upper opart of Eagle Ford; thickness 300+/-feet	Upper Cretaceous	Cretaceous
Klp	Loma Plata	Loma Plata Limestone	Klp - Loma Plata Limestone	in Van Horn Mountain area, upper part: fine grained, thick to very thick bedded, medium light gray, fossiliferous; thickness 400 feet; lower part: fine grained, nodular, thin to thick bedded, medium gray, some interbeds of shale, laminated, calcareous, t	Lower Cretaceous	Cretaceous
Ko	Ojinaga	Ojinaga	Ko - Ojinaga	in Quitman Mountains, shale, black, fissile; a few	Upper	Cretaceous

Rock Unit Code	Short Name	Long Name	Domain	Description	Epoch	Period
		Formation	Formation	beds of sandstone and limestone, basal 50 feet flaggy; thickness 2,000+ feet. In Eagle Mountains area, shale, brown, fissile, calcareous, in part sandy; shale, black, fissile; and sandstone, calcareous,	Cretaceous	
Kpi	El Picacho	El Picacho Formation	Kpi - El Picacho Formation	Claystone, sandstone, and lignite; upper part: claystone, massive, purplish gray, white, pale red, a few yellowish gray sandstone beds; middle part, sandstone, forms prominent ledges, about 175 feet thick; lower part: claystone, alternations of bright pu	Upper Cretaceous	Cretaceous
Ksc	San Carlos	San Carlos Sandstone	Ksc - San Carlos Sandstone	Fossiliferous sandstone and clay containing coal; thickness at least 1,400 feet	Upper Cretaceous	Cretaceous
Kt	Torcer	Torcer Formation	Kt - Torcer Formation	Limestone, sandstone, shale, and conglomerate. Mostly limestone, fine grained, argillaceous, sandy, contains scattered limestone pebbles, mostly medium to thick bedded, dark gray to black, weathers light gray. Sandstone, medium grained, thin bedded, cr	Lower Cretaceous	Cretaceous
Kye	Yearwood	Yearwood Formation	Kye - Yearwood Formation	south of Kent area Van Horn sheet, limestone and interbedded shale, thin to thick bedded, light gray	Lower Cretaceous	Cretaceous
Kyu	Yucca	Yucca Formation	Kyu - Yucca Formation	In Quitman Mountains, upper part: limestone, microgranular, gray, yellow, mudstone, soft, calcareous, nodules of green weathering microgranular calcite common, a few beds of limestone-pebble conglomerate near base, gray-maroon, thickness 400 to 1,100 fee	Lower Cretaceous	Cretaceous
Oe	El Paso	El Paso Formation	Oe - El Paso Formation	Limestone, dolomite, and sandstone. Franklin Mountains, upper 1,050 feet, mostly limestone, inequigranular, in part cherty; lower 540 feet, dolomite, in part sandy; thickness 1,590 feet Hueco Mountains, upper two-thirds, mostly limestone, granular, impur	Lower Ordovician	Ordovician
Om	Montoya	Montoya Dolomite	Om - Montoya Dolomite	Dolomite, limestone, and sandstone, four units not separately mapped: Cutter Member, Aleman Chert	Upper and Middle	Ordovician

Rock Unit Code	Short Name	Long Name	Domain	Description	Epoch	Period
				Member, Upham Member, and Cable Canyon Sandstone Member. Upper part, dolomite and limestone, aphanitic to medium grained, thin to thick bedded, white to dar	Ordovician	
Os	Simpson	Simpson Group rocks undivided	Os - Simpson Group rocks undivided	Sandstone, green shale, and dolomite; thickness 60-80 feet; mapped with Montoya Dolomite	Upper and Middle Ordovician	Ordovician
Pa	Alta	Alta Formation	Pa - Alta Formation	in Pinto Canyon area, mudstone, thin bedded, dark gray, and sandstone beds every few feet, fine grained, calcareous, in 6- to 12-inch ledges, dark gray, submarine slump features common; thickness 610 to 1,300 feet, thins northwestward. In northern Chinat	Wolfcamp	Permian
Pal	Paleozoic rocks	Paleozoic rocks undivided	Pal - Paleozoic rocks undivided	Fusselman Dolomite, Montoya Dolomite, and a small outcrop of the Magdalena Formation in Crazy Cat Mountain near south end of Franklin Mountains		Pennsylvanian, Silurian, and Ordovician
Pbc	Bell Canyon	Bell Canyon Formation	Pbc - Bell Canyon Formation	sandstone and limestone. Mostly sandstone, very fine grained, very thin to thick bedded, in part massive, brownish yellow. Limestone, five units not separately mapped (from topùLamar, McCombs, Rader, Pinery, and Hegler), fine grained, mostly thin bedded,	Guadalupe	Permian
Pbcd	Bell Canyon, Cherry Canyon, and Brushy Canyon	Bell Canyon, Cherry Canyon, and Brushy Canyon Formations undivided	Pbcd - Bell Canyon, Cherry Canyon, and Brushy Canyon Formations undivided	Bell Canyon Formation, Pbc, sandstone and limestone. Mostly sandstone, very fine grained, very thin to thick bedded, in part massive, brownish yellow. Limestone, five units not separately mapped (from topùLamar, McCombs, Rader, Pinery, and Hegler), fine	Guadalupe	Permian
Pbg	Briggs	Briggs Formation	Pbg - Briggs Formation	mostly gypsum; some carbonate rocks. Gypsum, sparry, granular, white. Carbonate rocks: in upper part, limestone and pisolitic dolomite interbedded with gypsum; at base, persistent 25-foot unit of brownish-yellow, sandy dolomite; in middle part, mostly d	Leonard	Permian
Pbs	Bone Spring	Bone Spring	Pbs - Bone	limestone, dolomite, sandstone, and shale. Mostly	Leonard	Permian

Rock Unit Code	Short Name	Long Name	Domain	Description	Epoch	Period
		Limestone	Spring Limestone	limestone, in part cherty, thin bedded, dark gray to black, marine megafossils scarce; some beds of siliceous shale and shaly limestone; a few thin beds of platy, fine-grained, calcareous, quartz sandston		
Pc	Capitan	Capitan Limestone	Pc - Capitan Limestone	Guadalupe Mountains, reef limestone, in shelfward part dolomitic, massive, beds mostly 15-100 feet thick, white, light gray, grayish yellow, brownish yellow; grades to Carlsbad Group shelfward, to Bell Canyon Formation basinward (southeastward); marine f	Guadalupe	Permian
pCa	Allamoore	Allamoore Formation	pCa - Allamoore Formation	interbedded cherty limestone, limestone-pebble conglomerate, phyllite, pyroclastic rock, and lava flows; numerous shallow intrusions of igneous rock; thickness several thousand feet		PreCambrian
Pcb	Carlsbad	Carlsbad Group	Pcb - Carlsbad Group	Limestone and sandstone, three units not separately mapped: Tansill Formation, Yates Formation, and Seven Rivers Formation. Limestone, mostly dolomitic, in part pisolitic, thin bedded, light gray to white becoming varicolored northwestward (shelfward). S	Guadalupe	Permian
Pcc	Cherry Canyon	Cherry Canyon Formation	Pcc - Cherry Canyon Formation	sandstone, siltstone, and limestone. Mostly very fine grained quartz sandstone and siltstone, mostly noncalcareous, in part shaly, mostly thin bedded, some varvelike bedding and ripple marks, irregularly bedded channel fillings common in lower two-thirds	Guadalupe	Permian
pCci	Meta-igneous rocks	Meta-igneous rocks	pCci - Meta-igneous rocks	include amphibolite in the Eagle Mountains and Wiley Mountains areas; and pegmatite in the Mica Mine locality of the Van Horn Mountains area		PreCambrian
pCcs	Metasedimentary rocks	Metasedimentary rocks	pCcs - Metasedimentary rocks	include, in the Eagle Mountains area, feldspathic meta-quartzite, thickness 3,200 to 3,400 feet; metaquartzite, phyllite, and mica schist, thickness about 600 feet; dark slate, dark phyllite, and black limestone, thickness not given. In the Van Horn Moun		PreCambrian
pCg	Granite	Granite	pCg - Granite	Franklin Mountains, Red Bluff Granite, medium to		PreCambrian

Rock Unit Code	Short Name	Long Name	Domain	Description	Epoch	Period
				coarse grained, massive, pink to red disintegrates readily on weathering; intrudes all other Precambrian rocks. Southern Hueco Mountains, granite, coarse grained, red		
pCh	Hazel	Hazel Formation	pCh - Hazel Formation	interbedded sandstone and conglomerate. Mostly indistinctly bedded sandstone in northern outcrops, conglomeratic in basal part; mostly conglomerate in southern outcrops, sandstone in upper part. Sandstone, mostly fine to very finegrained, mostly tightly		PreCambrian
Pci	Cibolo	Cibolo Formation	Pci - Cibolo Formation	in northern Chinati Mountains, from top down: limestone, dolomitic, hard, yellow, thickness 650 feet; limestone, cherty, compact, evenly bedded, in part sandy, dark colored, thickness 470 feet; limestone, somewhat thinner bedded than above, sponge spicul	Leonard	Permian
pCl	Lanoria	Lanoria Quartzite	pCl - Lanoria Quartzite	sandstone, quartzite, siltstone, and shale. Upper part, sandstone, fine grained, thin bedded, gray, weathers brown; siltstone, thin bedded; and shale; metamorphism slight; thickness 550-700 feet. Middle part, quartzite, fine grained, thick bedded, cross-		PreCambrian
pCmc	Mundy and Castner	Mundy Breccia and Castner Limestone undivided	pCmc - Mundy Breccia and Castner Limestone undivided	Mundy Breccia, randomly oriented, black basalt boulders, angular to slightly rounded, in matrix of dark-gray mudstone; thickness 250 feet maximum. Castner Limestone, limestone, hornfels, conglomerate, dolomite, and diabase. Mostly limestone, fine to coar		PreCambrian
Pco	Cutoff	Cutoff Shale	Pco - Cutoff Shale	shale, siltstone, sandstone, and limestone; meager marine megafossils. West side of Guadalupe Mountains, discontinuous outcrops mapped with Victorio Peak Limestone; mostly shale, in part siliceous and black, in part sandy and brown; some soft sandstone;	Leonard	Permian
pCr	Rhyolite	Rhyolite	pCr - Rhyolite	Franklin Mountains, rhyolite, porphyritic, feldspar and quartz phenocrysts, widely spaced but well-		PreCambrian

Rock Unit Code	Short Name	Long Name	Domain	Description	Epoch	Period
				defined layering, massive, dark red to black, rounded quartzite pebbles near base-thickness 1,400 feet maximum. Pump Station Hills, rhyolite porphyry, phen		
Pcs	Castile	Castile Formation	Pcs - Castile Formation	Gypsum, anhydrite, and limestone. Mostly anhydrite at depth and gypsum at surface, banded, commonly 5 to 30 alternating laminae of brown calcite and white gypsum per inch, gypsum layers 3 to 20 times as thick as calcite; highly contorted, commonly brecci	Ochoa	Permian
pCv	Van Horn	Van Horn Sandstone	pCv - Van Horn Sandstone	In Carrizo Mountains, feldspathic sandstone and arkose, medium to coarse grained, crossbedded, red, brown; pebble and cobble conglomerate in lower part		PreCambrian
Pdb	Brushy Creek	Brushy Creek Formation	Pdb - Brushy Creek Formation	mostly sandstone (discontinuous Pipeline Shale Member at base not separately mapped). Sandstone, in part medium grained, thick bedded, a few persistent massive units, brownish yellow, yellowish gray; in part fine grained, thin bedded, beds in part varvel	Guadalupe	Permian
Pdl	Dewey Lake	Dewey Lake Redbeds	Pdl - Dewey Lake Redbeds	Siltstone, sandstone, clay, and gypsum. Siltstone and fine-grained quartz sandstone, reddish orange, reddish brown, and brownish yellow. Clay, silty, red and grayish green, gypsiferous, numerous thin beds. Gypsum in white to red masses up to 5 feet across	Ochoa	Permian
Pgrc	Rustler and Castile	Gypsum of Rustler and Castile Formations Undivided	Pgrc - Gypsum of Rustler and Castile Formations Undivided	Gypsum in collapse structures, white, banded with thin layers of brown calcite; brecciated as much as 30 feet below the surface, mostly from uppermost part of Rustler Formation; may include gypsum and limestone residual from Salado Formation	Ochoa	Permian
Pgs	Goat Seep	Goat Seep Limestone	Pgs - Goat Seep Limestone	(tongue of Cherry Canyon sandstone at base not separately mapped). Upper unit (Goat Seep Limestone), mostly limestone, in part dolomitic, in part sandy, mostly thick bedded, massive, light gray to brownish yellow; sandstone interbeds more	Guadalupe	Permian

Rock Unit Code	Short Name	Long Name	Domain	Description	Epoch	Period
				abundant downwa		
Ph	Hueco	Hueco Limestone	Ph - Hueco Limestone	in Eagle Mountains area, mostly limestone, very fine grained, compact, thin bedded, medium gray to medium dark gray, fetid odor when fractured, irregular patches and nodules of chert in upper half, calcite veins common in lower half, thickness 1,060 feet	Wolfcamp	Permian
Pl	Leonardian rocks	Leonardian rocks undivided	Pl - Leonardian rocks undivided	locally includes Wolfcampian Hueco Limestone. Finlay Mountains, marlstone, limestone, limestone-pebble conglomerate; mostly marlstone, in part silty, well indurated, thin bedded and laminated, large-scale crossbedding in places, weathers light gray; lime	Leonard	Permian
Pm	Munn	Munn Formation	Pm - Munn Formation	dolomite, limestone, siltstone, and sandstone. Upper part, mostly dolomite and limestone, fine to coarse grained, in part oolitic, medium to thick bedded, white to grayish orange; some siltstone and fine-grained quartz sandstone, proportion increases sou	Guadalupe	Permian
Pmg	Mina Grande	Mina Grande Formation	Pmg - Mina Grande Formation	Limestone, hard, massive, dolomitic, reefy, surface rough and hackly with brecciated appearance, gray to yellow to yellowish brown; serves as chief lead and silver host rock in Shatter district to the south; thickness up to 200 feet, feathers out both to	Guadalupe	Permian
Pp	Pinto Canyon	Pinto Canyon Formation	Pp - Pinto Canyon Formation	In Pinto Canyon area, from top down: siltstone, dolomitic, cherty, pyritiferous, bituminous, thin to medium bedded, microgranular limestone concretions up to 4 feet long, weathers reddish brown, thickness 93 feet in type section, probably correlates with	Guadalupe and Leonard	Permian
Prm	Ross Mine	Ross Mine Formation	Prm - Ross Mine Formation	northern Chinati Mountains, sandstone, shale, chert, and limestone; thickness 100 to 600 feet, thins northwestward	Guadalupe	Permian
Pru	Rustler	Rustler Formation	Pru - Rustler Formation	Limestone, siltstone, sandstone, gypsum, and clay. Near Kent, limestone, dolomitic, thin bedded, light greenish gray to yellowish gray, some beds	Ohcoa	Permian

Rock Unit Code	Short Name	Long Name	Domain	Description	Epoch	Period
				brecciated; thickness 140+ feet. Near Cottonwood Draw, upper part, limestone and dolomitic limestone similar		
Psr	Seven Rivers	Seven Rivers Formation	Psr - Seven Rivers Formation	in Wiley Mountains area, limestone, fine grained, hard, thick bedded, nonfossiliferous, light colored; thickness 160 feet	Guadalupe	Permian
Pt	Tansill	Tansill Formation	Pt - Tansill Formation	mostly dolomite, fine grained, very thick to medium bedded, pale yellowish brown; weathers very pale orange, small anhydrite crystal molds common on weathered surfaces; some fossiliferous limestone in northern Apache Mountains; thickness 75-100+feet	Guadalupe	Permian
Pvc	Victorio Peak	Victorio Peak Formation	Pvc - Victorio Peak Formation	in Van Horn Mountains area, upper part: limestone, dolomitic, fine grained, medium to thick bedded, unfossiliferous, brownish black to medium gray, weathers pale orange, thickness about 180 feet; lower part: probably medium grained dolomite sand cemented	Leonard	Permian
Py	Yates	Yates Formation	Py - Yates Formation	siltstone, shale, limestone, and dolomite. In southern area siltstone, very fine grained sandstone, and shale, thin to medium bedded, some thin beds of sandy limestone, dolomite, and locally redbeds; grades to limestone and dolomite northward (reefward)	Guadalupe	Permian
Qaf	Flat deposits	Alkali flat deposits	Qaf - Alkali flat deposits	Alkali and salt impregnated clay, dolomite, and very fine grained sand, some intermittent salt lakes	Holocene	Quaternary
Qal	Quaternary deposits	Young Quaternary deposits	Qal - Young Quaternary deposits	alluvium and low terrace deposits along other streams	Holocene	Quaternary
Qalr	Quaternary deposits	Young Quaternary deposits	Qalr - Young Quaternary deposits	alluvium along the Rio Grande	Holocene	Quaternary
Qao	Quaternary deposits	Old Quaternary deposits	Qao - Old Quaternary deposits	Alluvium, colluvium, caliche, and gypsite on surfaces dissected by modern drainage. Kent Area, includes Gozar and Bigtank Gravels. Terraces along the Rio Grande. Sierra Blanca area, includes Balluco, Ramey, Gills, Madden, and Miser Gravels	Pleistocene	Quaternary

Rock Unit Code	Short Name	Long Name	Domain	Description	Epoch	Period
Qb	Quaternary deposits	Young Quaternary deposits	Qb - Young Quaternary deposits	lacustrine and fluvial deposits of clay, silt, sand, and gypsum in bolsons	Holocene	Quaternary
Qf	Quaternary deposits	Young Quaternary deposits	Qf - Young Quaternary deposits	colluvium and fans	Holocene	Quaternary
Qgt	Toy	Toy Limestone	Qgt - Toy Limestone	nonmarine limestone, mostly in southwestern Reeves County	Pleistocene	Quaternary
Ql	Landslide deposits	Landslide deposits	Ql - Landslide deposits	Displaced bouldery masses of rock	Holocene and Pleistocene	Quaternary
QTb	Bolson	Bolson deposits	QTb - Bolson deposits	Clay, sand, and gravel, in part gypsiferous, some caliche; includes Gatuna Formation of Kent area	Oligocene	Tertiary
QTg	Bolson	Bolson deposits and other similar deposits	QTg - Bolson deposits and other similar deposits	consolidated valley fill, in Musgrave Canyon	Pleistocene	Quaternary
Qws	Windblown sand	Windblown sand	Qws - Windblown sand	Windblown sand	Holocene	Quaternary
Qwsd	Windblown sand	Windblown sand	Qwsd - Windblown sand	Areas of large dunes	Holocene	Quaternary
Sf	Fusselman	Fusselman Dolomite	Sf - Fusselman Dolomite	Dolomite, dolomitic limestone, and locally limestone, aphanitic to coarse grained, thick to very thick bedded, massive, white to light gray, some beds medium dark gray; marine fossils in a few limestone beds. Thickness: Franklin Mountains, 600-900+ feet;	Middle Silurian	Silurian
Tac	Adobe Canyon	Adobe Canyon	Tac - Adobe Canyon	rhyolite and trachyte flows with a basal trachyte porphyry ("Big Brown Porphyry" Member) up to 425 feet thick with anorthoclase phenocrysts up to 8 mm in diameter and clinopyroxene microphenocrysts; rest of formation multiple flow units, massive at base,	Oligocene	Tertiary
Tbm	Brooks Mountain	Brooks Mountain	Tbm - Brooks Mountain	porphyritic trachyte, with colorless to gray alkali feldspar phenocrysts, aphanitic to very fine grained	Oligocene	Tertiary

Rock Unit Code	Short Name	Long Name	Domain	Description	Epoch	Period
		Formation	Formation	in lower part, fine grained in upper part, weathers grayish brown; forms steep, locally vertical cliffs; in Brooks Mountain area of southern Davis Mo		
Tbr	Bracks	Bracks Rhyolite	Tbr - Bracks Rhyolite	slightly porphyritic with rhombic anorthoclase phenocrysts up to 3 mm in diameter, matrix alkalic feldspar, quartz, and mafic minerals; dark reddish brown to grayish olive; thickness up to 360 feet; K-Ar ages 36.5 ± 1.2 m.y., 36.8 m.y.	Oligocene	Tertiary
Tbs	Barrel Springs	Barrel Springs Formation	Tbs - Barrel Springs Formation	from top down: indurated to friable, fine-grained vitric tuff; nonfoliated porphyritic rhyolite; pinkish gray to purplish brown, foliated porphyritic rhyolite; black, foliated vitrophyre; thickness about 105 feet at type locality, thickens eastward to 25	Oligocene	Tertiary
Tbu	Buckshot	Buckshot Ignimbrite	Tbu - Buckshot Ignimbrite	rhyolitic, slightly porphyritic, vitric, contains very dark red spheres 2 to 10 mm in diameter; black vitrophyre at base in many places; grayish red, weathers pale to dark reddish brown; many blister cones, 6 feet high and up to 45 feet in diameter, on u	Eocene	Tertiary
Tca	Capote Mountain	Capote Mountain Tuff	Tca - Capote Mountain Tuff	fine-grained, vitric, tuffaceous sandstone and siltstone, a few interbeds of conglomerate; on the north very light gray a few pale red beds, on the south lower 2/3 pale red, upper 1/3 very light gray; thickness 600 to 2,100 feet; contains Oligocene verte	Oligocene	Tertiary
Tch	Chambers	Chambers Tuff	Tch - Chambers Tuff	fine grained, crystal-vitric tuff, moderate to well bedded, pale red, grayish pink, grayish green, pale purple, and grayish orange pink; a persistent layer of coarse sandstone in southern area with some conglomerate 130 feet above base; thickness 105 to	Oligocene	Tertiary
Tco	Colmena	Colmena Tuff	Tco - Colmena Tuff	fine-grained, thin-bedded tuffaceous sandstone and pebble-to-boulder limestone-and-sandstone conglomerate; some nonmarine limestone, silty claystone, and glassy flow-rock, pale red to white; mostly tuffaceous sandstone and limestone on	Eocene	Tertiary

Rock Unit Code	Short Name	Long Name	Domain	Description	Epoch	Period
				south, mostly cong		
Td	Duff	Duff Tuff	Td - Duff Tuff	chiefly rhyolitic ruff with minor breccia and conglomerate; tuff fine grained, well indurated, massive, mostly white, light shades of red and yellow common; conglomerate in lenticular beds up to 40 feet thick, crossbedded, dark brown; thickness up to 1,4	Oligocene	Tertiary
Tdp	Duff and Pruett	Duff Tuff and Pruett Formations undivided in Cuesto del Burro area	Tdp - Duff Tuff and Pruett Formations undivided in Cuesto del Burro area	rhyolitic tuff and intercalated tuffaceous clay, silt, sandstone, and conglomerate, moderate to well indurated, white, gray, red, and yellow; thickness up to 1,500 feet	Oligocene	Tertiary
Ter	Eppenauer Ranch	Eppenauer Ranch Formation	Ter - Eppenauer Ranch Formation	basalt, aphanitic, hard, massive to vesicular, dark brown to black; thickness probably exceeds 100 feet	Oligocene	Tertiary
Tfc	Frazier Canyon	Frazier Canyon Formation	Tfc - Frazier Canyon Formation	vitric-lithic-crystal tuff and lapilli tuff, locally contains conglomerate and sandstone, poorly bedded; white to light brown, gray, yellow, or green; up to 340 feet thick	Oligocene	Tertiary
Tg	Gomez	Gomez Tuff	Tg - Gomez Tuff	peralkaline ash-flow tuff, densely welded to friable, one cooling unit; contains 1.5 mm phenocrysts of anorthoclase and some quartz, and micro-phenocrysts of aegirinaugite and some fayalite; abundant xenoliths of mafic lava, limestone, sandstone, biotite	Oligocene	Tertiary
Tga	Garren	Garren Group	Tga - Garren Group	in Wiley Mountains area, from top down includes Zopilote Breccia, trachyte lithic flow-breccia, hard, massive, grayish red, thickness approximately 150 feet; Means Trachyte, aphanitic, vesicular, hard, dark gray to black, thickness 530 feet; Fairbury Tra	Oligocene	Tertiary
Tgc	Goat Canyon	Goat Canyon Formation	Tgc - Goat Canyon Formation	porphyritic-aphanitic trachyte, with white alkali feldspar phenocrysts, hard, gray to greenish gray; weathers platy, grayish white to yellow brown; thickness 515 feet in type section in Goat Canyon,	Oligocene	Tertiary

Rock Unit Code	Short Name	Long Name	Domain	Description	Epoch	Period
				southern Davis Mountains, 8 miles to east thins to 100		
Tgi	Gill	Gill Breccia	Tgi - Gill Breccia	flow breccias of three types; medium gray fragments in a grayish-red matrix; variegated mottled fragments in a dark greenish-gray to orange-pink matrix; and brecciated to massive light-olive-green to greenish-gray, fine-grained rock; deposited on irregular	Eocene	Tertiary
Th	Heulster	Heulster Formation	Th - Heulster Formation	mostly tuff, thin layers of sandstone and conglomerate, lenses of fresh-water limestone, and trachydoleritic lava; forms landslide terrain of hummocky, grass-covered hills, includes displaced blocks of overlying flow-rock units; thickness up to 490 feet	Oligocene	Tertiary
Thg	Hogeye	Hogeye Tuff	Thg - Hogeye Tuff	in Eagle Mountains area, southern Indio Mountains, composed of an upper tuff, middle trachyte, and lower tuff; thickness 75, 170 to 250, and 30 feet, respectively; in Van Horn Mountains, composed of an upper sandstone, 7 to 80 feet thick, and a lower vit	Oligocene	Tertiary
Ti	Igneous rocks	Intrusive igneous rocks	Ti - Intrusive igneous rocks	Stocks, laccoliths, sills, and dikes of rhyolite, rhyolite porphyry, quartz monzonite, monzonite, granodiorite, granite, syenite, trachyte, basalt, and altered diabase		Tertiary
Tlr	Rhyolite	Lower Rhyolite	Tlr - Lower Rhyolite	a sequence of tuff, flow breccia, volcanic breccia, extrusive and intrusive rhyolite, with sedimentary rock at the base; thickness more than 1,000 feet	Eocene	Tertiary
Tm	Merrill	Merrill Formation	Tm - Merrill Formation	latite porphyry, hard, reddish brown, weathers with pitted surface, brown to yellowish brown, locally fine- to coarse-grained, vitric-lithic tuff at top; thickness about 130 feet, pinches out rapidly eastward	Oligocene	Tertiary
Tme	Medley	Medley Formation	Tme - Medley Formation	latite porphyry, vesicular, gray; weathers brownish gray to reddish gray; in southern Davis Mountains; thickness uncertain as upper portion covered by talus from Goat Canyon Formation, maximum	Oligocene	Tertiary

Rock Unit Code	Short Name	Long Name	Domain	Description	Epoch	Period
				measureable section 22 feet		
Tml	Mount Locke	Mount Locke Formation	Tml - Mount Locke Formation	quartz trachyte and rhyolite porphyry, gray, weathered surface rough, brownish gray to reddish brown; thickness 580 feet at type locality, thins rapidly westward and southwestward	Oligocene	Tertiary
Tmm	Mitchell Mesa	Mitchell Mesa Welded Tuff	Tmm - Mitchell Mesa Welded Tuff	cliff-forming ash flow, generally non welded to slightly welded, where more than 30 feet thick pronounced foliation in a broad zone about midway between base and center; in type area porphyritic, phenocrysts of quartz and chatoyant sanidine up to 0.2 inc	Oligocene	Tertiary
Tp	Pantera	Pantera Trachyte	Tp - Pantera Trachyte	in Eagle Mountains, resistant, pale red or grayish red, with 6 feet of black- to light-gray welded crystal tuff at base, thickness 45 feet; in Van Horn Mountains, light brownish gray to grayish red, thickness about 40 feet; in Wiley Mountains, hard, nonv	Oligocene	Tertiary
Tpc	Perdiz	Perdiz Conglomerate	Tpc - Perdiz Conglomerate	fanglomerate of highly variable composition shed mostly northeastward from Chinati Mountains in Cuesta del Burro region; thickness up to about 500 feet		Tertiary
Tpe	Petan	Petan Basalt	Tpe - Petan Basalt	trachyandesite porphyry, dark greenish gray to brownish gray; thickness up to 510 feet (includes Bell Valley Andesite of the Wiley Mountains area and the Jones Formation of the southern Davis Mountains)	Oligocene	Tertiary
Tsh1	Shelly	Shelly Group	Tsh1 - Shelly Group	trachyte tuff and red siltstone	Oligocene	Tertiary
Tsh2	Shelly	Shelly Group	Tsh2 - Shelly Group	Trachyte, consists of numerous separate tongues of breccia and massive lava composed of plagioclase trachyte porphyry and vitrophyre, medium purplish gray to grayish red, thickness up to 400 feet, crops out at north end of Chinati Mountains	Oligocene	Tertiary
Tsh3-5	Shelly	Shelly Group	Tsh3-5 - Shelly Group	Upper third of unit 5, tuff, thin bedded, conglomeratic, very light gray to white, locally perlite at top up to 100 feet thick; middle third, a wedge of	Oligocene	Tertiary

Rock Unit Code	Short Name	Long Name	Domain	Description	Epoch	Period
				conglomerate, pebbles, cobbles, and boulders of igneous rock in a matrix of tuffaceous sand; lower th		
Tsh5	Shelly	Shelly Group	Tsh5 - Shelly Group	Upper third of unit 5, tuff, thin bedded, conglomeratic, very light gray to white, locally perlite at top up to 100 feet thick; middle third, a wedge of conglomerate, pebbles, cobbles, and boulders of igneous rock in a matrix of tuffaceous sand; lower th	Oligocene	Tertiary
Tsh6	Shelly	Shelly Group - Ignimbrite	Tsh6 - Shelly Group - Ignimbrite	rhyolitic, very fine grained, hard, slightly vesicular, medium grayish red, medium brownish gray in middle, abundant angular xenoliths of light gray, very fine grained trachyte(?), thickness 200 to 250 feet	Oligocene	Tertiary
Tsh7	Shelly	Shelly Group - Ignimbrite	Tsh7 - Shelly Group - Ignimbrite	rhyolitic, very fine grained, hard, partly devitrified, various shades of "brown, gray, and pink, thickness up to 75 feet	Oligocene	Tertiary
Tsh8	Shelly	Shelly Group - Spherulitic rhyolite	Tsh8 - Shelly Group - Spherulitic rhyolite	excellent flow banding, aegirine-bearing, slightly porphyritic, medium bluish gray to green-speckled yellowish gray, thickness up to 250 feet	Oligocene	Tertiary
Tsp	Sheep Pasture	Sheep Pasture Formation	Tsp - Sheep Pasture Formation	slightly porphyritic rhyolite, indurated to friable, grayish purple to brown; fine-grained vitric tuff locally near top; thickness at type section 510 feet; K-Ar age, 36.2 ± 0.4 m.y. (2 samples)	Oligocene	Tertiary
Tt	Tarantula	Tarantula Gravel	Tt - Tarantula Gravel	composition related to rock types in nearby areas; upper part: fragments of subrounded tuff, trachyte, basalt, and ignimbrite; lower part: subrounded to rounded quartzite and limestone pebbles and cobbles probably derived from basal conglomerate of Colmen		Tertiary
Tta	Tascotal	Tascotal Formation	Tta - Tascotal Formation	upper part: sandstone, tuffaceous sandstone, and conglomerate; sandstone medium to coarse grained with lenses, beds, and channel fillings of pebble to cobble conglomerate, mostly limestone, some igneous rocks and chert, about half of interval is tuff and	Oligocene	Tertiary
Ttr	Trachyte	Trachyte	Ttr - Trachyte	hard, compact, weathers to angular blocks, various	Eocene	Tertiary

Rock Unit Code	Short Name	Long Name	Domain	Description	Epoch	Period
		porphyry	porphyry	shades of grayish red, pale red, pale brown, with very pale orange phenocrysts of alkali feldspar; thickness up to approximately 750 feet		
Tur	Rhyolite	Upper rhyolite	Tur - Upper rhyolite	Upper rhyolite, Tur, rhyolite including an upper volcanic breccia, flow breccia, and patches of basal conglomerate; volcanic breccia, fragments of volcanic rock, quartzite, and limestone in aphanitic matrix, white to light gray to very pale orange; rhyol	Eocene	Tertiary
Tv	Igneous rocks	Extrusive igneous rocks undivided	Tv - Extrusive igneous rocks undivided	in Quitman Mountains, interbedded flows and pyroclastic rocks of the Square Peak Volcanics in SNeed (Cox) Mountains and west of Victoria Peak, small basalt flow remnants	Oligocene	Tertiary
Tvj	Vieja	Vieja Group undivided	Tvj - Vieja Group undivided	West of Sierra Vieja, where Bracks Rhyolite absent, Vieja Group, undivided	Eocene	Tertiary
Twb	Wild Cherry and Barrel Springs	Wild Cherry and Barrel Springs Formation undivided	Twb - Wild Cherry and Barrel Springs Formation undivided	where Mount Locke Formation is absent and the remaining formations become similar in appearance	Oligocene	Tertiary
Twc	Wild Cherry	Wild Cherry Formation	Twc - Wild Cherry Formation	from top down: indurated to friable, fine-grained vitric tuff; foliated, porphyritic rhyolite; black, foliated vitrophyre; thickness 355 feet at type locality, thins southward	Oligocene	Tertiary
Wa	water	water	Wa - water	body of water		

APPENDIX B

RECHARGE ESTIMATION METHODOLOGY

TABLE OF CONTENTS

1.0	INTRODUCTION	B-4
2.0	METHODS	B-7
2.1	Delineating Sub-Basins.....	B-7
2.2	Analysis of Precipitation Data	B-7
2.3	Estimating Areal Recharge	B-12
2.4	Estimating Runoff.....	B-14
3.0	RESULTS	B-16
4.0	REFERENCES	B-23

TABLES

Table B.1. Basins and sub-basins of the Red Light Draw-Green River Valley groundwater availability model study area, Trans-Pecos Texas	B-9
Table B.2. Weather stations in and around Red Light Draw-Green River Valley groundwater availability model study area, Trans-Pecos Texas	B-11
Table B.3. 24-hour storm events recorded at the Van Horn and Sierra Blanca 2 E weather stations in the Red Light Draw-Green River Valley groundwater availability model study area, Trans-Pecos	B-13
Table B.4. Summary of coefficients used to estimate areal recharge, and corresponding elevation, average annual precipitation, and areal recharge.....	B-13
Table B.5. Summary of lower-than-average and greater-than-average precipitation and potential runoff-generating events at the Van Horn and Sierra Blanca 2 E weather stations	B-16
Table B.6. Summary of recharge estimates for Red Light Draw-Green River Valley groundwater availability model study area	B-17
Table B.7. Recharge for Red Light Draw	B-18
Table B.8. Recharge for Green River Valley and Eagle Canyon	B-19
Table B.9. Recharge for Eagle Flat Draw	B-19
Table B.10. Recharge for Blanca Draw	B-20
Table B.11. Comparison of recharge methods for Red Light Draw-Green River Valley groundwater availability model study area	B-21

LIST OF FIGURES

Figure B. 1 Schematic of recharge processes and methods used to estimate recharge	B-26
Figure B. 2 Basins and sub-basins in the study area.....	B-27
Figure B. 3 Elevation and average water year precipitation for the period of record at 14 weather stations in the Red Light Draw-Green River Valley groundwater availability model study area, Trans-Pecos Texas	B-28
Figure B. 4 Elevation and average water year precipitation with linear trend, Red Light Draw-Green River Valley groundwater availability model study area, Trans- Pecos Texas	B-29
Figure B. 5 Graph showing areal recharge coefficient versus average annual precipitation....	B-30
Figure B. 6 Average magnitude of 24-hour precipitation events that exceed 0.67 inches (runoff-producing events) for the period of record at weather stations, Red Light Draw-Green River Valley groundwater availability model study area, Trans-Pecos Texas	B-31
Figure B. 7 Average magnitude of 24-hour precipitation events that exceed 1.58 inches (runoff-producing events) for the period of record at weather stations, Red Light Draw-Green River Valley groundwater availability model study area, Trans-Pecos Texas	B-32
Figure B. 8 Average number of 24-hour precipitation events that exceed 0.67 inches (runoff-producing events) annually at weather stations, Red Light Draw-Green River Valley groundwater availability model study area	B-33
Figure B. 9 Average number of 24-hour precipitation events that exceed 1.58 inches (runoff- producing events) annually at weather stations, Red Light Draw-Green River Valley groundwater availability model study area.....	B-34
Figure B. 10 Annual precipitation at the Van Horn weather station for the period of record 1939 to 2005.....	B-35
Figure B. 11 Annual precipitation at the Sierra Blanca 2 E weather station for the period of record 1950 to 2000.....	B-36
Figure B. 12 Number of potential runoff-generating events for period of record 1939 to 2005 at Van Horn weather station.....	B-37
Figure B. 13 Number of potential runoff-generating events for period of record 1950 to 2000 at Sierra Blanca 2 E weather station.....	B-38

RECHARGE ESTIMATION METHODOLOGY

1.0 INTRODUCTION

In the Red Light Draw-Green River Valley groundwater availability model study area, groundwater recharge primarily occurs as 1) direct recharge from infiltration of precipitation on the mountain block (i.e., Quitman Mountains, Eagle Mountains, Carrizo Mountains, and Van Horn Mountains), and 2) as bolson-fringe recharge (also termed mountain-front recharge) from infiltration of storm-water runoff in channels of ephemeral streams on alluvial fans along the bolson perimeter (Gates and others, 1980; Scanlon and others, 2001; Finch and Armour, 2001). Due to semi-arid to arid climatic characteristics and depth to water (> 100 ft), little or no recharge occurs on the bolsons. Instead, most of the precipitation that falls directly on the bolsons is removed very quickly by evaporation (Darling, 1997). This recharge concept is depicted in Figure B1.

Previous investigators have made estimates of recharge to the bolsons in the Red Light Draw-Green River Valley groundwater availability model study area based on 1 percent of average annual precipitation (Gates and others, 1980), radioactive isotope analysis and cross-sectional numerical flow modeling (Darling, 1997), storm-water runoff and infiltration, and watershed analysis. The USGS recharge study (Gates and others, 1980) estimated average annual recharge as high as 2,000 acre-feet per year (ac-ft/yr) in Red Light Draw, 1,000 ac-ft/yr in Green River Valley, and 3,000 ac-ft/yr in Eagle Flat Draw. Based on analysis of radioactive isotopes carbon-14 and tritium, and cross-sectional numerical flow modeling, Darling (1997) estimated average annual recharge as low as 280 ac-ft/yr in Red Light Draw, 120 ac-ft/yr in Green River Valley, and 430 ac-ft/yr in Eagle Flat Draw. Using a modification of the USGS approach, LBG-Guyton Associates and others (2001) estimated average annual recharge of 700 ac-ft/yr in Red Light Draw, 700 ac-ft/yr in Green River Valley, and 1,000 ac-ft/yr in the southeastern part of Eagle Flat Draw. Using watershed topographic analysis, the assumption that a runoff-generating storm event occurs only once every 2 years, and 35 percent of runoff becomes recharge, Finch and Armour (2001) estimated average annual recharge of 4,119 ac-ft/yr in Eagle Flat Draw. Based on watershed topographic analysis, and a modified version of the

runoff redistribution method of Stone and others (2001), LBG-Guyton Associates and others (2004) estimated average annual recharge of 3,036 ac-ft/yr in Eagle Flat Draw.

In the current study, the method selected to calculate initial recharge estimates for the study area was based on previous studies completed by Nichols (2000), Stone and others (2001), Bennett and Finch (2002), and LBG-Guyton Associates and others (2004). This approach to determining recharge and distribution of recharge takes into account climate, watershed, and geologic characteristics for each sub-basin defined in the study area. The method includes the following analyses:

1. Delineating mountain and bolson sub-basins within the study area, and their hydrologic characteristics;
2. Calculating topographic statistics for each sub-basin;
3. Estimating areal recharge (corrected for elevation zones and evaporation) for each sub-basin;
4. Determining runoff from each sub-basin by analyzing the magnitude of precipitation events that result in runoff (scaled to elevation); and,
5. Determining the amount of runoff that leaves mountain sub-basins and enters the bolsons, thus contributing recharge to the bolsons (corrected for evaporation).

The assumptions made for calculating recharge and recharge distribution include the following:

1. Direct precipitation on the bolsons does not infiltrate and become recharge;
2. Precipitation increases with elevation as defined by existing data;
3. There is no areal recharge for areas with less than 12 inches per year average precipitation (this correlates to elevations < 4,700 ft amsl);
4. Dry soil conditions are used for estimating the runoff curve number; and,
5. Approximately 30 percent of the runoff infiltrates at the alluvial fan and the remaining 70 percent evaporates or flows out of the model domain.

The first step in determining areal recharge is to develop a relationship between precipitation and elevation for weather stations within, and surrounding, the study area (Figure 2.3.1). Average annual and daily precipitation data for the period of record were collected for 14 weather stations (Figure 2.3.1; Utah State University Climate Center, 2006). For each weather station, we determined the frequency of 24-hour precipitation events of specified magnitudes that could potentially generate storm-water runoff. We used the linear relationship between elevation and frequency of runoff events at the weather stations to calculate runoff for each sub-basin in the study area. Calculated runoff for the mountain (topographically up-gradient) sub-basins was assumed to leave the mountain sub-basins and enter the bolsons, thus representing potential recharge to the bolsons.

It is important that the effects of evapotranspiration and other losses be considered when estimating recharge; otherwise the recharge values are overestimated. Bolson-fringe recharge was estimated as 30 percent of runoff entering the bolsons from the mountain sub-basins. This percentage is consistent with 35 percent of runoff used by Finch and Armour (2001) and 30 percent of runoff used by LBG-Guyton Associates and others (2004).

2.0 METHODS

2.1 Delineating Sub-Basins

The five major basins that encompass the study area are Red Light Draw, Green River Valley, Eagle Flat Draw, Blanca Draw, and Eagle Canyon (Figure 4.4.2). Smaller sub-basins within these major basins (Table B.1; Figure B.2) were delineated. Topographic statistics, such as areas within given elevation intervals, were determined for each sub-basin based on 1:100,000 scale and 1:24,000 scale U.S. Geological Survey topographic maps for the region.

2.2 Analysis of Precipitation Data

Daily precipitation data for the period of record for 14 weather stations in and around the study area were obtained (Utah State University Climate Center, 2006) and used to develop a relationship between precipitation and elevation (Table B.2; Figure B.3).

In Figure B.3, standard deviations associated with average water year (October through September) precipitation values overlap with the trend line, except for Salt Flat CAA. The Salt Flat CAA weather station has the shortest period of record (9 years, from 1948 to 1957) and the period of record coincided with the drought of the 1950s (see time-series precipitation graphs for Van Horn, Valentine 10 WSW, and Cornudas SS weather stations in Figure 2.3.2). Thus, the Salt Flat CAA weather station was removed from the analysis. The Candelaria and El Paso 32 ENE weather stations are outliers and represent the extreme south and northwest stations considered for the analysis (Figure 2.3.1), and are therefore removed from the analysis. The Candelaria station is at a relatively low elevation of 2,881 ft amsl, south of the study area along the Rio Grande, whereas the basin floors within the study area are higher than 3,000 ft amsl. The El Paso 32 ENE station is the farthest away from the study area. Removing only the El Paso 32 ENE station from the analysis has little effect on the r^2 value, improving it from 0.39 to 0.42. The other weather stations included in the analysis show a strong linear trend on graphs of elevation versus frequency of high-magnitude precipitation events. The Candelaria station has a much higher frequency, and the El Paso station a much lower frequency of high-magnitude precipitation events than what would be expected for the study area (Figure B.8 and B.9). In general, the climate data for the Candelaria and El Paso stations indicate that different climate

dynamics are at work in these areas, and these stations should not be used to characterize the study area. The removal of these three weather stations increases the r-squared value for the linear fit from 0.39 to 0.73 (Figure B.4). The weather stations show a variation in annual precipitation of about 8 inches over an elevation range of 2,108 ft. As suggested by Figure B.4, the relationship between elevation and precipitation for the study area is likely more complicated than a simple linear relationship. However, the relationship can generally be approximated by a simple linear relationship.

Table B.1. Basins and sub-basins of the Red Light Draw-Green River Valley groundwater availability model study area, Trans-Pecos Texas

basin	sub-basin	sub-basin type	geology	CN ¹	CN, ¹ dry conditions	weather station	I _a , ² dry conditions, inches
Red Light Draw	Red Light Bolson	bolson	Quaternary-age alluvium and fans	88/74	74.8/55.8	Sierra Blanca 2 E	0.67/1.58
	Cedar Arroyo	mountain	Cretaceous-age Espy Fm	88/74	74.8/55.8	Sierra Blanca 2 E	0.67/1.58
	Babb Tank	mountain	Cretaceous-age Espy Fm	88/74	74.8/55.8	Sierra Blanca 2 E	0.67/1.58
	Smuggler's Gap	mountain	Cretaceous-age Benevides Fm	88/74	74.8/55.8	Sierra Blanca 2 E	0.67/1.58
	Upper Red Light Draw West	mountain	Cretaceous-age Benevides Fm and Cox Sandstn	88/74	74.8/55.8	Sierra Blanca 2 E	0.67/1.58
	Upper Red Light Draw	mountain	Tertiary-age intrusives, Ti, Cretaceous-age Comanchean rocks	88/74	74.8/55.8	Sierra Blanca 2 E	0.67/1.58
	Texas Mountain	mountain	Quaternary-age fans, Cretaceous-age Bluff Mesa Fm and Yucca Fm	88/74	74.8/55.8	Sierra Blanca 2 E	0.67/1.58
	Devil Ridge	mountain	Cretaceous-age Cox Sandstn	88/74	74.8/55.8	Sierra Blanca 2 E	0.67/1.58
	Red Hills Arroyo	mountain	Cretaceous-age Loma Plata Fm and Bluff Mesa Fm	88/74	74.8/55.8	Sierra Blanca 2 E	0.67/1.58
	Eagle Mountains Other 5	mountain	Quaternary-age older deposits, Cretaceous-age Finley Limestn and Bluff Mesa Fm	88/74	74.8/55.8	Sierra Blanca 2 E	0.67/1.58
	Eagle Mountains Other 4	mountain	Quaternary-age older deposits, Tertiary-age intrusives and lower rhyolite	88/74	74.8/55.8	Sierra Blanca 2 E	0.67/1.58
	Eagle Mountains Other 3	mountain	Quaternary-age older deposits, Tertiary-age lower rhyolite	88/74	74.8/55.8	Sierra Blanca 2 E	0.67/1.58
	Eagle Mountains Other 2	mountain	Quaternary-age older deposits, Tertiary-age lower rhyolite	88/74	74.8/55.8	Sierra Blanca 2 E	0.67/1.58
	Frenchman's Canyon	mountain	Tertiary-age upper rhyolite and trachyte porphyry ⁶	88/74	74.8/55.8	Sierra Blanca 2 E	0.67/1.58
	Eagle Peak	mountain	Tertiary-age upper rhyolite	88/74	74.8/55.8	Sierra Blanca 2 E	0.67/1.58
	Cottonwood Canyon	mountain	Tertiary-age upper rhyolite	88/74	74.8/55.8	Sierra Blanca 2 E	0.67/1.58
	Oxford Canyon	mountain	Cretaceous-age Cox Sandstn, Bluff Mesa Fm, and Yucca Fm	88/74	74.8/55.8	Sierra Blanca 2 E	0.67/1.58
	Squaw Pass	mountain	Cretaceous-age Yucca Fm	88/74	74.8/55.8	Sierra Blanca 2 E	0.67/1.58
	Squaw Creek	mountain	Cretaceous-age Yucca Fm	88/74	74.8/55.8	Sierra Blanca 2 E	0.67/1.58
	Echo Canyon	mountain	Cretaceous-age Bluff Mesa Fm and Yucca Fm	88/74	74.8/55.8	Sierra Blanca 2 E	0.67/1.58
	Eagle Mountains Other 1	mountain	Cretaceous-age Bluff Mesa Fm and Yucca Fm	88/74	74.8/55.8	Sierra Blanca 2 E	0.67/1.58
	Eagle Mountains Other 7	mountain	Cretaceous-age Yucca Fm	88/74	74.8/55.8	Sierra Blanca 2 E	0.67/1.58
Eagle Mountains Other 6	mountain	Quaternary-age older deposits, Cretaceous-age Bluff Mesa Fm	88/74	74.8/55.8	Sierra Blanca 2 E	0.67/1.58	

¹CN is the Curve Number, as defined by U.S. Department of Agriculture (1986). CN value of 88 represents the most common CN value for the study area, and the CN value of 74 represents the most conservative CN value for the study area. Runoff was calculated according to both values. CN values adjusted for dry conditions from Wanielista and others (1997).

²I_a is the initial abstraction for a 24-hour storm event; it is assumed that precipitation events with magnitudes below the I_a do not generate runoff. The I_a was calculated based on the CN values for dry conditions.

³rhyolite is a fine-grained, light gray-colored volcanic rock with abundant quartz

⁴intrusive rocks form from magmas that cooled slowly beneath Earth's surface, unlike volcanic rocks, which form from eruption of magmas at Earth's surface.

⁵consolidated volcanic ash deposit

⁶trachyte is a fine-grained, gray or red-colored volcanic rock with no quartz and abundant alkali feldspars and feldspathoids

Table B.1. Basins and sub-basins of the Red Light Draw-Green River Valley groundwater availability model study area, Trans-Pecos Texas (continued)

basin	sub-basin	sub-basin type	geology	CN ¹	CN, ¹ dry conditions	weather station	I _a , ² dry conditions, inches
Green River Valley	Green River Bolson	bolson	Quaternary-age alluvium and fans	88/74	74.8/55.8	Van Horn	0.67/1.58
	Green River West	mountain	Tertiary-age Garren Grp, Cretaceous-age Espy Fm and Yucca Fm	88/74	74.8/55.8	Van Horn	0.67/1.58
	High Lonesome Peak	mountain	Tertiary-age Hogeeye Tuff, ⁵ Cretaceous-age Cox Sandstn	88/74	74.8/55.8	Van Horn	0.67/1.58
	China Canyon	mountain	Tertiary-age Tarantula Gravel, Loma Plata Fm, and Benevides Fm	88/74	74.8/55.8	Van Horn	0.67/1.58
	Lower China Canyon	mountain	Quaternary-age bolson	88/74	74.8/55.8	Van Horn	0.67/1.58
	Van Horn Other 1	mountain	Quaternary-age bolson, Tertiary-age Tarantula Gravel, Cretaceous-age Loma Plata Fm	88/74	74.8/55.8	Van Horn	0.67/1.58
	Wilson Canyon	mountain	Tertiary-age Tarantula Gravel and Garren Grp, Cretaceous-age Cox Sandstn and Bluff Mesa Fm	88/74	74.8/55.8	Van Horn	0.67/1.58
	Sand Creek	mountain	Cretaceous-age Cox Sandstn and Bluff Mesa Fm	88/74	74.8/55.8	Van Horn	0.67/1.58
	Van Horn Other 3	mountain	Tertiary-age Tarantula Gravel	88/74	74.8/55.8	Van Horn	0.67/1.58
	Hog Canyon	mountain	Tertiary-age volcanics and Tarantula Gravel	88/74	74.8/55.8	Van Horn	0.67/1.58
Eagle Canyon	Eagle Canyon	mountain	Cretaceous-age Benevides Fm, Finley Limestn, Cox Sandstn, Bluff Mesa Fm, and Yucca Fm	88/74	74.8/55.8	Sierra Blanca 2 E	0.67/1.58
Eagle Flat Draw	Eagle Flat Bolson	bolson	Quaternary-age alluvium and fans	88/74	74.8/55.8	Van Horn	0.67/1.58
	Eagle Mountains Other 1	mountain	Cretaceous-age Cox Sandstn, Bluff Mesa Fm, and Yucca Fm	88/74	74.8/55.8	Van Horn	0.67/1.58
	Lower Cypress Canyon	mountain	Cretaceous-age Espy Fm, Finley Limestn, and Cox Sandstn	88/74	74.8/55.8	Van Horn	0.67/1.58
	Cypress Canyon	mountain	Tertiary-age intrusives, ⁴ rhyolites ³	88/74	74.8/55.8	Van Horn	0.67/1.58
	Carpenter Canyon	mountain	Tertiary-age rhyolite, ³ Cretaceous-age Espy Fm, Permian-age Hueco Limestn	88/74	74.8/55.8	Van Horn	0.67/1.58
	Panther Peak	mountain	Tertiary-age rhyolite, ³ Cretaceous-age Cox Sandstn, Permian-age Hueco Limestn	88/74	74.8/55.8	Van Horn	0.67/1.58
	Goat Canyon	mountain	Tertiary-age rhyolite, ³ Cretaceous-age Cox Sandstn and Bluff Mesa Fm	88/74	74.8/55.8	Van Horn	0.67/1.58
	Horse Canyon	mountain	Quaternary-age older deposits, Cretaceous-age Cox Sandstn and Yucca Fm	88/74	74.8/55.8	Van Horn	0.67/1.58
	Camel Draw	mountain	Cretaceous-age Campagrande Fm, Precambrian-age rocks	88/74	74.8/55.8	Van Horn	0.67/1.58
	Seventeen Draw	mountain	Quaternary-age alluvium, Permian-age Hueco Limestn, Precambrian-age rocks	88/74	74.8/55.8	Van Horn	0.67/1.58
	Millican Hills	mountain	Precambrian-age rocks	88/74	74.8/55.8	Van Horn	0.67/1.58
	Millican Hills 2	mountain	Precambrian-age rocks	88/74	74.8/55.8	Van Horn	0.67/1.58
	Mineral Creek	mountain	Precambrian-age rocks	88/74	74.8/55.8	Van Horn	0.67/1.58
	Hackett Peak	mountain	Precambrian-age rocks	88/74	74.8/55.8	Van Horn	0.67/1.58
Carrizo Peak	mountain	Permian-age Hueco Limestn, Precambrian-age rocks	88/74	74.8/55.8	Van Horn	0.67/1.58	

¹CN is the Curve Number, as defined by U.S. Department of Agriculture (1986). CN value of 88 represents the most common CN value for the study area, and the CN value of 74 represents the most conservative CN value for the study area. Runoff was calculated according to both values. CN values adjusted for dry conditions from Wanielista and others (1997).

²I_a is the initial abstraction for a 24-hour storm event; it is assumed that precipitation events with magnitudes below the I_a do not generate runoff. The I_a was calculated based on the CN values for dry conditions.

³rhyolite is a fine-grained, light gray-colored volcanic rock with abundant quartz

⁴intrusive rocks form from magmas that cooled slowly beneath Earth's surface, unlike volcanic rocks, which form from eruption of magmas at Earth's surface.

⁵consolidated volcanic ash deposit

Table B.1. Basins and sub-basins of the Red Light Draw-Green River Valley groundwater availability model study area, Trans-Pecos Texas (concluded)

basin	sub-basin	sub-basin type	geology	CN ¹	CN, ¹ dry conditions	weather station	I _a , ² dry conditions, inches
Blanca Draw	Blanca Draw Bolson	bolson	Quaternary-age alluvium and fans	88/74	74.8/55.8	Sierra Blanca 2 E	0.67/1.58
	Yucca Mesa	mountain	Cretaceous-age Finley Limestn and Yucca Fm	88/74	74.8/55.8	Sierra Blanca 2 E	0.67/1.58
	Little Hills	mountain	Quaternary-age older deposits	88/74	74.8/55.8	Sierra Blanca 2 E	0.67/1.58
	Upper Sierra Blanca	mountain	Tertiary-age intrusives, ⁴ Cretaceous-age Finley Limestn and Cox Sandstn	88/74	74.8/55.8	Sierra Blanca 2 E	0.67/1.58
	Upper Blanca Flat	mountain	Quaternary-age alluvium, Cretaceous-age Finley Limestn and Cox Sandstn	88/74	74.8/55.8	Sierra Blanca 2 E	0.67/1.58
	Blanca Flat	mountain	Quaternary-age alluvium, Cretaceous-age Cox Sandstn	88/74	74.8/55.8	Sierra Blanca 2 E	0.67/1.58
	Davis Tank	mountain	Quaternary-age alluvium, Cretaceous-age Cox Sandstn and Campagrande Fm	88/74	74.8/55.8	Sierra Blanca 2 E	0.67/1.58
	Streeruwitz Other 1	mountain	Cretaceous-age Campagrande Fm, Permian-age Hueco Limestn, Precambrian-age rocks	88/74	74.8/55.8	Sierra Blanca 2 E	0.67/1.58
	Streeruwitz Other 2	mountain	Cretaceous-age Campagrande Fm, Permian-age Hueco Limestn, Precambrian-age rocks	88/74	74.8/55.8	Sierra Blanca 2 E	0.67/1.58
	Streeruwitz Hills	mountain	Permian-age Hueco Limestn, Precambrian-age rocks	88/74	74.8/55.8	Sierra Blanca 2 E	0.67/1.58

¹CN is the Curve Number, as defined by U.S. Department of Agriculture (1986). CN value of 88 represents the most common CN value for the study area, and the CN value of 74 represents the most conservative CN value for the study area. Runoff was calculated according to both values. CN values adjusted for dry conditions from Wanielista and others (1997).

²I_a is the initial abstraction for a 24-hour storm event; it is assumed that precipitation events with magnitudes below the I_a do not generate runoff. The I_a was calculated based on the CN values for dry conditions.

³rhyolite is a fine-grained, light gray-colored volcanic rock with abundant quartz

⁴intrusive rocks form from magmas that cooled slowly beneath Earth's surface, unlike volcanic rocks, which form from eruption of magmas at Earth's surface.

Table B.2. Weather stations in and around Red Light Draw-Green River Valley groundwater availability model study area, Trans-Pecos Texas

weather station	county	period of record	number of years ^a	elevation, ft amsl
Candelaria	Presidio	1948-2006	56	2,881
Cornudas Service Station	Hudspeth	1948-2006	51	4,482
Dell City 5 SSW	Hudspeth	1979-2006	26	3,734
El Paso 32 ENE	Hudspeth	1983-2005	20	5,241
Fabens	El Paso	1948-1977	28	3,612
Fort Hancock 8 SSE	Hudspeth	1966-2006	34	3,914
Pine Springs	Culberson	1939-2005	24	5,634
Salt Flat 10 ENE	Culberson	1959-1977	19	3,891
Salt Flat CAA Airport	Hudspeth	1948-1957	9	3,717
Sierra Blanca 2 E	Hudspeth	1897-2002	37	4,554
Tornillo 2 SSE	El Paso	1946-2006	26	3,526
Valentine	Jeff Davis	1960-2006	26	4,432
Valentine 10 WSW	Presidio	1897-2006	56	4,423
Van Horn	Culberson	1943-2005	52	4,052

ft amsl feet above mean sea level

^ayears with 3 or more months of missing data were omitted

Daily precipitation data for the period of record for two weather stations, Sierra Blanca 2 E (within the study area) and Van Horn (adjacent to the study area to the east), were analyzed to determine the frequency distribution of 24-hour storm events (for example, precipitation events of 0.01 to 0.10 inch magnitudes, 0.11 to 0.50 inch magnitudes, and so on). The results of this analysis are presented in Table B.3, and show similar distributions for the two weather stations.

2.3 Estimating Areal Recharge

The effects of evapotranspiration and other losses need to be considered when estimating recharge; otherwise the recharge values for the sub-basins are overestimated. To do this, the areal recharge is estimated from empirical relationships (coefficients) described by Nichols (2000). The coefficients from Nichols (2000) were developed using multiple linear regression methods for similar basins in Nevada, and adjusted to reflect Trans-Pecos climate conditions (see Figure B.5). The coefficients used to estimate areal recharge, summarized in Table B.4, result in a range of 0 to 7 percent of total precipitation becoming areal recharge, with the percentage increasing with increasing elevation. The areal recharge rate is equal to the average precipitation multiplied by the modified coefficient, using the following relationship:

$$\text{AREAL RECHARGE} = C * \text{PRECIPITATION}$$

where,

PRECIPITATION is equal to average annual precipitation (inches/year) and C is equal to $(0.00874) * (\text{PRECIPITATION}) - (0.105)$.

Table B.3. 24-hour storm events recorded at the Van Horn and Sierra Blanca 2 E weather stations in the Red Light Draw-Green River Valley groundwater availability model study area, Trans-Pecos

magnitude of 24-hour storm event, inches	percent of total precipitation events at Van Horn weather station	percent of total precipitation events at Sierra Blanca 2 E weather station
0.01 to 0.10	62	47
0.11 to 0.5	28	40
0.51 to 1.00	7	9
1.01 to 1.58	2	3
above 1.58	1	1

Table B.4. Summary of coefficients used to estimate areal recharge, and corresponding elevation, average annual precipitation, and areal recharge

average annual precipitation, inches per year	potential recharge coefficient	potential recharge, inches per year	elevation, ft amsl
12	0.000	0.00	3,000
14	0.018	0.25	3,870
16	0.035	0.56	4,740
18	0.052	0.94	5,600
20	0.070	1.40	6,475

ft amsl feet above mean sea level

2.4 Estimating Runoff

To calculate the average amount of runoff based on average precipitation, the magnitude that must be reached by a precipitation event in order for runoff to occur was determined. Runoff does not occur in a 24-hour precipitation event until the amount of precipitation has exceeded an initial abstraction (I_a), which is influenced by vegetative cover, vegetation density, permeability of the soil surface, and the condition of the soil prior to the precipitation event (Stone and others, 2001; Wanielista and others, 1997; USDA, 1973). I_a is equal to S (the amount of water retained in a drainage basin in a long precipitation event) multiplied by 0.2. S is related to soil and cover conditions according to the following:

$$S = (1,000 / CN) - 10$$

where,

CN is the curve number, which represents the effect of the hydrologic soil group classification and landcover type on the amount of rainfall that runs off (USDA, 1986). Soils in hydrologic group 'A' have low run-off potential. These soils have high infiltration rates when thoroughly wet. The depth to any restrictive layer is greater than 40 inches and the depth to a permanent water table is deeper than 6 ft (USDA, 1986). Hydrologic group 'A' is rare in Trans-Pecos Texas. Soils in hydrologic group 'B' have moderate infiltration rates when thoroughly wet. The depth to any restrictive layer is greater than 20 inches and the depth to a permanent water table is deeper than 2 ft (USDA, 1986). Soils in hydrologic group 'C' have low infiltration rates when thoroughly wet. The depth to any restrictive layer is greater than 20 inches and the depth to a permanent water table is deeper than 2 ft (USDA, 1986). Soils in hydrologic group 'D' have high runoff potential. These soils have very low infiltration rates when thoroughly wet, and water movement through the soil is slow to very slow. The depth to a restrictive layer is 20 inches or less and the depth to a permanent water table is shallower than 2 ft (USDA, 1986).

Runoff was calculated for each sub-basin according to two CN values. The higher CN value, 88, represents the most common value for the current study area and the adjacent Igneous

and Salt Basin Bolson groundwater availability model study area (LBG-Guyton and others, 2004). The lower CN value, 74, represents the most conservative value for the current study area and the adjacent Igneous and Salt Basin Bolson groundwater availability model study area (LBG-Guyton and others, 2004). In the absence of detailed soil cover data or multiple types of soil cover in one sub-basin, runoff was calculated for each sub-basin using these two CN values, and the intermediate runoff value (the average of the two values) was used to estimate recharge. Desert brush landcover, at a 25 percent density, was assumed. In most watersheds of the southwestern U.S., the cover density for desert brush cover ranges from zero to 50 percent. Thus, the cover densities assumed in the current study are ‘middle-of-the-road’ assumptions. The CN value was adjusted based on the assumptions that dry conditions, in which soils are dry but not to the wilting point, exist prior to each precipitation event (Wanielista and others, 1997).

The total amount of precipitation that occurred during events that exceeded I_a (in the period of record for each weather station) was divided by the number of events that exceeded I_a . The resulting value (denoted as P , representing the average precipitation event that exceeds I_a) was used to calculate runoff (Q) in the following equation:

$$Q = (P - I_a)^2 / (P - I_a) + S$$

Analysis of 24-hour storm events that exceed 0.67 inches and 1.58 inches in magnitude (potential runoff-generating events) shows that the average magnitude of runoff events does not show linear variation with respect to elevation (Figures B.6 and B.7). Thus, the average magnitude of runoff events (as recorded at the weather stations) cannot be adjusted according to elevation. However, the frequency of runoff events does have a general linear increasing trend with increasing elevation (Figures B.8 and B.9). Note that the Salt Flat CAA weather station was only removed from the analysis of elevation versus water year precipitation (Figure B.4), due to the fact that it has a short period of record coinciding with the Drought of Record. However, the station was included in the evaluation of elevation versus magnitude of precipitation events (Figures B.8 and B.9) because it agrees closely with the trend defined by the rest of the data, suggesting that the drought period affected total water year precipitation but not the frequency of high magnitude precipitation events. The Candelaria and El Paso 32 ENE weather stations are outliers and represent the extreme south and northwest stations considered for the analysis (Figure 2.3.3), and are therefore removed from the analysis. The removal of

these two weather stations increases the r-squared value for the linear fit from 0.27 to 0.76. We use the general linear relationship between frequency of runoff events and elevation to determine the annual number of runoff events for each sub-basin.

Annual precipitation and the number of potential runoff-generating precipitation events vary considerably from year to year (Figures B.10 through B.13). The mid-1940s to the late-1960s was a period of lower-than-average precipitation and potential runoff-generating events at the Van Horn and Sierra Blanca 2 E weather stations. From about 1995 to 2005 was also a period of lower-than-average precipitation. From the late-1960s to 1994 was a period of greater-than-average precipitation and runoff. Precipitation trends do not necessarily correspond with trends in potential runoff-generating events. Table B.5 summarizes the periods of lower-than-average and greater-than-average precipitation and potential runoff-generating events for the periods of record at the Van Horn and Sierra Blanca 2 E weather stations.

Table B.5. Summary of lower-than-average and greater-than-average precipitation and potential runoff-generating events at the Van Horn and Sierra Blanca 2 E weather stations

weather station	period of lower-than-average precipitation	period of greater-than-average precipitation	period of lower-than-average runoff-generating events	period of greater-than-average runoff-generating events
Van Horn ^a	1946-1965, 1976, 1977, 1995-2005	1939-1945, 1966-1973, 1978-1994	1950-1968, 1995-2005	1939-1949, 1969-1994
Sierra Blanca 2 E ^b	1963-1969, 1979, 1980, 1995-2000	1970-1978, 1981-1994	1963-1968, 1977-1983, 1995-2000	1969-1976, 1984-1994

^a missing 1970, 1974, 1975, and 1982 to 1986

^b missing 1951-1962, 1987, and 1988

3.0 RESULTS

The results of the recharge analysis are summarized in Table B.6. Recharge values for individual sub-basins of Red Light Draw, Green River Valley, Eagle Flat Draw, Blanca Draw, and Eagle Canyon are presented in Tables B.7 through B.10. Total recharge to the Red Light Draw-Green River Valley groundwater availability model study area is estimated at 5,214 ac-ft/yr, which is about 0.8 percent of the total precipitation. Most of the recharge to the

bolson is from infiltration of precipitation on the mountain block, and from infiltration of storm-water runoff along the bolson fringe.

If Darling (1997) is correct in reasoning that little or no recharge occurs along the bolson fringe in the Eagle Mountains, this type of recharge would be reduced from 441 ac-ft/yr to 231 ac-ft/yr in Red Light Draw, from 168 ac-ft/yr to 126 ac-ft/yr in Green River Valley, and from 489 ac-ft/yr to 342 ac-ft/yr in Eagle Flat Draw. Thus, total recharge to the study area would be reduced from 5,214 ac-ft/yr to 4,815 ac-ft/yr.

Table B.6. Summary of recharge estimates for Red Light Draw-Green River Valley groundwater availability model study area

parameter	unit	Red Light Draw	Green River Valley	Eagle Flat Draw	Blanca Draw	Eagle Canyon	study area
area	acres	227,430	103,210	200,850	131,380	9,530	672,400
total precipitation	ac-ft/yr	203,640	87,780	209,740	125,130	7,070	633,360
estimated areal recharge to mountain block	ac-ft/yr	1,190	80	2,380	130	0	3,780
runoff from mountain block	ac-ft/yr	1,470	560	1,630	1,030	90	4,780
estimated recharge along bolson fringe ^a	ac-ft/yr	441	168	489	309	27	1,434
total estimated recharge to watershed area encompassing bolson	ac-ft/yr	1,631	248	2,869	439	27	5,214
	in/yr	0.09	0.03	0.17	0.04	0.03	0.09
total precipitation that becomes recharge	percent	0.8	0.3	1.4	0.4	0.4	0.8

^a 30 percent of runoff from mountain block
ac-ft/yr acre-feet per year
in/yr inches per year

Table B.7. Recharge for Red Light Draw

sub-basin	sub-basin area, acres	precipitation, ac-ft/yr	areal recharge, ac-ft/yr	runoff generated within sub-basin that contributes to recharge along bolson fringe, ac-ft/yr	estimated recharge along basin fringe, ac-ft/yr ^a
Red Light Bolson	120,667	98,375	0	0	0
Cedar Arroyo	2,908	2,964	10	36	11
Babb Tank	4,159	2,271	5	53	16
Smuggler's Gap	2,105	2,265	22	30	9
Upper Red Light Draw West	7,505	7,906	54	110	33
Upper Red Light Draw	9,422	9,837	56	158	47
Texas Mountain	7,400	7,474	10	100	29
Devil Ridge	7,567	7,601	3	95	29
Red Hills Arroyo	17,960	17,860	36	195	58
Eagle Mountains Other 5	1,900	1,194	0	21	6
Eagle Mountains Other 4	3,492	3,333	35	55	16
Eagle Mountains Other 3	1,275	1,570	45	22	7
Eagle Mountains Other 2	2,522	2,706	102	43	13
Frenchman's Canyon	3,523	5,054	245	70	21
Eagle Peak	7,432	9,877	380	142	43
Cottonwood Canyon	1,084	1,582	53	21	6
Oxford Canyon	7,869	7,467	96	123	37
Squaw Pass	4,107	2,751	2	45	14
Squaw Creek	4,200	3,895	2	46	14
Echo Canyon	3,523	2,522	0	35	11
Eagle Mountains Other 1	3,148	1,940	2	31	9
Eagle Mountains Other 7	2,303	1,636	0	23	7
Eagle Mountains Other 6	1,359	1,560	32	16	5
Red Light Draw TOTAL	227,430	203,640	1,190	1,470	441
leaves model area through evaporation	1,867^b				

^a 30 percent of runoff

^b 70 percent of runoff plus all runoff generated within bolson

Table B.8. Recharge for Green River Valley and Eagle Canyon

sub-basin	sub-basin area, acres	precipitation, ac-ft/yr	areal recharge, ac-ft/yr	runoff generated within sub-basin that contributes to recharge along bolson fringe, ac-ft/yr	estimated recharge along basin fringe, ac-ft/yr ^a
Green River Bolson	48,540	38,705	0	0	0
Green River West	13,540	13,144	7	146	44
High Lonesome Peak	7,734	7,315	45	100	30
China Canyon	6,921	6,958	10	78	23
Lower China Canyon	1,543	1,545	0	13	4
Van Horn Other 1	5,118	3,767	18	55	17
Wilson Canyon	7,130	6,623	0	73	22
Sand Creek	5,347	4,807	0	50	15
Van Horn Other 3	1,365	636	0	10	3
Hog Canyon	5,972	4,280	0	35	10
Green River Valley TOTAL	103,210	87,780	80	560	168
leaves model area through evaporation	736 ^b				
Eagle Canyon TOTAL	9,530	7,070	0	90	27
leaves model area through evaporation	63 ^b				

^a 30 percent of runoff

^b 70 percent of runoff plus all runoff generated within bolson

Table B.9. Recharge for Eagle Flat Draw

sub-basin	sub-basin area, acres	precipitation, ac-ft/yr	areal recharge, ac-ft/yr	runoff generated within sub-basin that contributes to recharge along bolson fringe, ac-ft/yr	estimated recharge along basin fringe, ac-ft/yr ^a
Eagle Flat Bolson	93,320	93,460	0	0	0
Eagle Mountains Other 1	6,483	5,185	129	110	33
Lower Cypress Canyon	3,586	3,896	42	52	16
Cypress Canyon	4,628	6,589	310	88	26
Carpenter Canyon	4,346	5,702	195	76	23
Panther Peak	5,441	5,484	108	87	26
Goat Canyon	2,596	3,257	95	44	13
Horse Canyon	2,289	2,845	87	40	12
Camel Draw	20,398	19,478	214	273	82
Seventeen Draw	27,266	33,650	934	445	133
Millican Hills	9,193	10,108	125	130	39
Millican Hills 2	9,329	10,309	134	135	40
Mineral Creek	1,595	1,476	0	19	6
Hackett Peak	4,470	2,333	0	56	17
Carrizo Peak	5,910	5,968	7	75	23
Eagle Flat Draw TOTAL	200,850	209,740	2,380	1,630	489
leaves model area through evaporation	2,127 ^b				

^a 30 percent of runoff

^b 70 percent of runoff plus all runoff generated within bolson

Table B.10. Recharge for Blanca Draw

sub-basin	sub-basin area, acres	precipitation, ac-ft/yr	areal recharge, ac-ft/yr	runoff generated within sub-basin that contributes to recharge along bolson fringe, ac-ft/yr	estimated recharge along basin fringe, ac-ft/yr ^a
Blanca Draw Bolson	58,640	58,730	0	0	0
Yucca Mesa	10,110	5,613	5	129	39
Little Hills	2,261	2,265	0	28	8
Upper Sierra Blanca	17,698	16,738	40	307	92
Upper Blanca Flat	22,472	22,542	5	298	89
Blanca Flat	9,686	10,276	80	131	39
Davis Tank	4,206	4,213	0	57	17
Streeruwitz Other 1	1,526	1,528	0	20	6
Streeruwitz Other 2	1,606	1,609	0	20	6
Streeruwitz Hills	3,179	1,615	0	40	12
Blanca Draw TOTAL	131,384	125,129	130	1,030	309
leaves model area through evaporation	1,343^b				

^a 30 percent of runoff

^b 70 percent of runoff plus all runoff generated within bolson

DISCUSSION

A comparison of other recharge methods with the re-distribution method, and estimates of ground-water outflow using Darcy's Law, is provided for the study area in Table B.11. The runoff-redistribution method appears to be an appropriate method for the Red Light Draw-Green River Valley groundwater availability model study area because it considers the runoff characteristics of each sub-basin and the variable precipitation received by each sub-basin. Previous recharge estimates that used a flat percentage of precipitation (Gates and others, 1980; Meyer, 1976) did not consider components of the conceptual model, such as geographic and geologic characteristics for infiltration and areas on the bolsons where recharge likely does not occur. Therefore, the runoff-redistribution method provides constraints on a sensitive model parameter consistent with the conceptual model, and helps minimize the inherent non-uniqueness associated with parameterization in numerical models.

Table B.11. Comparison of recharge methods for Red Light Draw-Green River Valley groundwater availability model study area

Method	Estimated Recharge, ac-ft/yr		
	Red Light Draw	Green River Valley	Eagle Flat Draw
Previous work (Table 4.1)	280 to 2,000	120 to 1,000	430 to 4,119
Darcy flux check (this study)	915 to 4,576 ^a	1,365 to 6,823 ^a	53 to 266 ^a
Modified runoff redistribution (this study)	1,631	248	2,869

^a Considers cross sectional area of bolson and low and high range of hydraulic conductivity value of 1 and 5 feet per day, respectively.

ac-ft/yr = acre-feet per year

Groundwater flow models are sensitive to the quantity and distribution of recharge, and given the uncertainties in recharge estimates for the study area, the runoff-redistribution method provides estimates of quantity and distribution that would otherwise be difficult or impossible to obtain.

In general, recharge estimates (using methods similar to the runoff-redistribution method) for regional modeling studies have resulted in recharge values slightly higher than those obtained from final groundwater flow model calibration. The USGS Española Basin model prepared by McAda and Wasiolek (1988) calibrated to 9,600 ac-ft/yr of recharge for selected drainages along

the western side of the Sangre de Cristo Mountains. A very detailed recharge analysis of the same area by the USGS (Wasiolek, 1995) resulted in an estimate of average recharge of 14,700 ac-ft/yr; the model-calibrated recharge resulted in approximately 66 percent of the estimated recharge. Similar results have been realized from recent studies of the Tularosa Basin in southern New Mexico, where the estimated recharge (Waltemeyer, 2001) was approximately 60 percent of the model-calibrated recharge (Huff, 2004), and of the Mimbres Basin in southwestern New Mexico, where the estimated recharge was 69 percent of the model-calibrated recharge (Finch and others, 2005; JSAI, 2006).

There is likely some rejected recharge that is not accounted for in the recharge estimates that causes the model-calibrated recharge to be less than the estimated recharge. One example of rejected recharge would be recharge to a perched groundwater system that is discharged to a spring or by evapotranspiration. There are several springs on the west side of the Eagle Mountains (Oxford and Squaw Springs), on the east side of the Eagle Mountains (Eagle, Carpenter, and Cypress Springs, and several unnamed springs), and on the west side of the Van Horn Mountains (Mesquite, Catclaw, and Ash Springs, and several unnamed springs), where this may be occurring. Although discharge rates have not been documented for these springs, the lower part of the Green River Valley appears to have perennial streamflow fed in part by Mesquite Spring.

Other possibilities for the recharge discrepancy may be related to the lack of long-term climate data (i.e., comparing 60 years of climate data to a regional hydrologic system that takes thousands of years for water to be recharged and ultimately discharged), and the lack of detail in the regional model to account for conveyance of all the estimated recharge through the groundwater system.

Recharge to the Red Light Draw-Green River Valley groundwater availability model study area may occur by processes other than infiltration of precipitation on the mountain block and infiltration of storm-water runoff along the bolson fringe, such as a deep groundwater flow system and upwelling of geothermal waters. Some research has suggested that the aquifer of Eagle Flat Draw is linked to a deep regional flow system that transports groundwater toward the east (Nielson and Sharp, 1985; Sharp, 1989). Upwelling of geothermal waters is evidenced by hot springs on the west side of the Quitman Mountains, just west of the Red Light Draw-Green River Valley groundwater availability model study area.

4.0 REFERENCES

- Bennett, J.B., and Finch, S.T., Jr., 2002, Concepts of ground-water recharge in the Trans-Pecos Region, Texas: Abstract GSA south-central spring 2002 meeting, Alpine Texas.
- Collins, E.W., and Raney, J.A., 1997, Quaternary faults within intermontane basins of northwest Trans-Pecos Texas and Chihuahua, Mexico: Bureau of Economic Geology Report of Investigations No. 245, University of Texas, 59 p.
- Darling, B.K., 1997, Delineation of the ground-water flow systems of the Eagle Flat and Red Light basins of Trans-Pecos Texas: The University of Texas at Austin, Ph.D. dissertation, 179 p.
- Finch, S.T., Jr., and Armour, J., 2001, Hydrogeologic analysis and ground-water flow model of the Wild Horse Flat area, Culberson County, Texas: consultant's report prepared by John Shomaker & Associates, Inc., for Beldon Foundation (administered by Christian Life Commission) and Culberson County Groundwater Conservation District, 37 p. plus figures and appendices.
- Finch, S.T., Jr., McCoy, A.M., and Luna, M.L., 2005, 2nd annual progress report in support of Chino Mines Company Supplemental Discharge Permit for Closure, DP-1340, Condition 86: consultant's report prepared by John Shomaker & Associates, Inc., for Chino Mines Company, 36 p. plus figures and appendices.
- Gates, J.S., White, D.E., Stanley, W.D., and Ackermann, H.D., 1980, Availability of fresh and slightly saline groundwater in basins of westernmost Texas: Texas Department of Water Resources Report No. 256, 108 p.
- Henry, C.D., 1979, Geologic setting and geochemistry of thermal water and geothermal assessment, Trans-Pecos Texas: Bureau of Economic Geology Report of Investigations No. 96, University of Texas.
- Hibbs, B.J., and Darling, B.K., 2005, Revisiting a classification scheme for U.S.-Mexico alluvial basin-fill aquifers: *Ground Water*, vol. 43, no. 5, pp. 750-763.
- Huff, G.F., 2004, Simulation of ground-water flow in the Tularosa Basin, south-central New Mexico, 1948-95, with projections to 2040: U.S. Geological Survey Water Resources Investigations Report 02-XXXX, draft report, 66 p.
- John Shomaker & Associates, Inc., 2006, Report on water treatment system sustainability, Chino Mines Company, DP-1340, Condition 86: consultant's report prepared by John Shomaker & Associates, Inc., for Chino Mines Company, 47 p. plus figures and appendices.

- Langford, R.P., 1993, Landscape evolution of Eagle Flat and Red Light basins, Chihuahuan Desert, South-Central Trans-Pecos Texas: The University of Texas at Austin, Bureau of Economic Geology contract report, prepared for Texas Low-Level Radioactive Waste Disposal Authority under Interagency Contract IAC (92-93)-0910.
- LBG-Guyton Associates; Freese and Nichols, Inc.; Moreno Cardenas, Inc.; and M3H Consulting, Inc., 2001, Far West Texas regional water plan: consultant's report prepared for Texas Water Development Board.
- LBG-Guyton Associates; Water Prospecting and Resource Consulting, LLC; John Shomaker & Associates, Inc.; Daniel B. Stephens & Associates, Inc.; Urbanczyk, K.; Sharp, J.; and Olson, J., 2004, Groundwater availability model for the Igneous and Salt Basin Bolson aquifers of the Davis Mountains Region of Texas: consultant's report prepared for Texas Water Development Board.
- McAda, D.P., and Wasiolek, M., 1988, Simulation of the regional geohydrology of the Tesuque aquifer system near Santa Fe, New Mexico: U.S. Geological Survey Water Resources Investigations Report 87-4056, 71 p.
- Meyer, W.R., 1976, Digital model for simulating effects of ground-water pumping in the Hueco Bolson, El Paso area, Texas, New Mexico, and Mexico: U.S. Geological Survey Water Resources Investigations Report 85-4219, 94 p.
- Nielson, P.M., and Sharp, J.M., Jr., 1985, Tectonic controls on the hydrogeology of the Salt Basin, Trans-Pecos Texas: *in* Dickerson, P.W., and Muehlberger, W.R., eds., Structure and tectonics of Trans-Pecos Texas: West Texas Geological Society Publication 95-81, pp. 231-234.
- Nichols, W.D., 2000, Regional ground-water evapotranspiration and ground-water budgets, Great Basin, Nevada: U. S. Geological Survey Professional Paper 1628.
- Scanlon, B.R., Darling, B.K., and Mullican, W.F., III, 2001, Evaluation of groundwater recharge in basins in Trans-Pecos Texas: *in* Aquifers of West Texas, Texas Water Development Board Report No. 356, edited by R.E. Mace, W.F. Mullican III, E.S. Angle, 272 p.
- Sharp, J.M., Jr., 1989, Regional ground-water systems in northern Trans-Pecos Texas: *in* Structural geology and stratigraphy of Trans-Pecos Texas, 1989: 28th International Geological Congress Guidebook T-317, p. 123-130.
- Stone, D.B., Moomaw, C.L., Davis, A., 2001, Estimating recharge distribution by incorporating runoff from mountainous areas in an alluvial basin in the Great Basin region of the southwestern United States: *Ground Water*, vol. 39, no. 6, pp. 807-818.
- Texas Office of the State Climatologist, 2003, digital files of weather station data conveyed upon request: <http://www.met.tamu.edu/met/osc/osc.html>

- U.S. Department of Agriculture, 1972, General soil map of Presidio County, Texas: Soil Conservation Service, U.S. Department of Agriculture Soil Conservation Service.
- U.S. Department of Agriculture, 1973, Peak rates of discharge for small watersheds, chapter 2 (revised 10/73 for New Mexico), engineering field manual for conservation practices, U.S. Department of Agriculture Soil Conservation Service.
- U.S. Department of Agriculture, 1974, General soil map of Culberson County, Texas: Soil Conservation Service, U.S. Department of Agriculture Soil Conservation Service.
- U.S. Department of Agriculture, 1977, Soil survey of Jeff Davis County, Texas: Soil Conservation Service, U.S. Department of Agriculture Soil Conservation Service.
- U.S. Department of Agriculture, 1986, Urban hydrology for small watersheds: Soil Conservation Service technical Release 55, U.S. Department of Agriculture Soil Conservation Service.
- Utah State University Climate Center, 2006, climate.usu.edu/weather/dataserv.htm
- Waltemeyer, S.D., 2001, Estimates of mountain-front streamflow available for potential recharge to the Tularosa Basin, New Mexico: U.S. Geological Survey, Water-Resources Investigations Report 01-4013, 8 p.
- Wanielista, M. P., Ealgin, R., and Kersten, R. D., 1997, Hydrology: water quantity and quality control; 2nd edition. J. Wiley & Sons, New York, 567 p.
- Wasiolek, M., 1995, Subsurface recharge to the Tesuque aquifer system from selected drainage basins along the western side of the Sangre de Cristo Mountains near Santa Fe, New Mexico: U.S. Geological Survey, Water Resource Investigations Report 94-4072, 57 p.

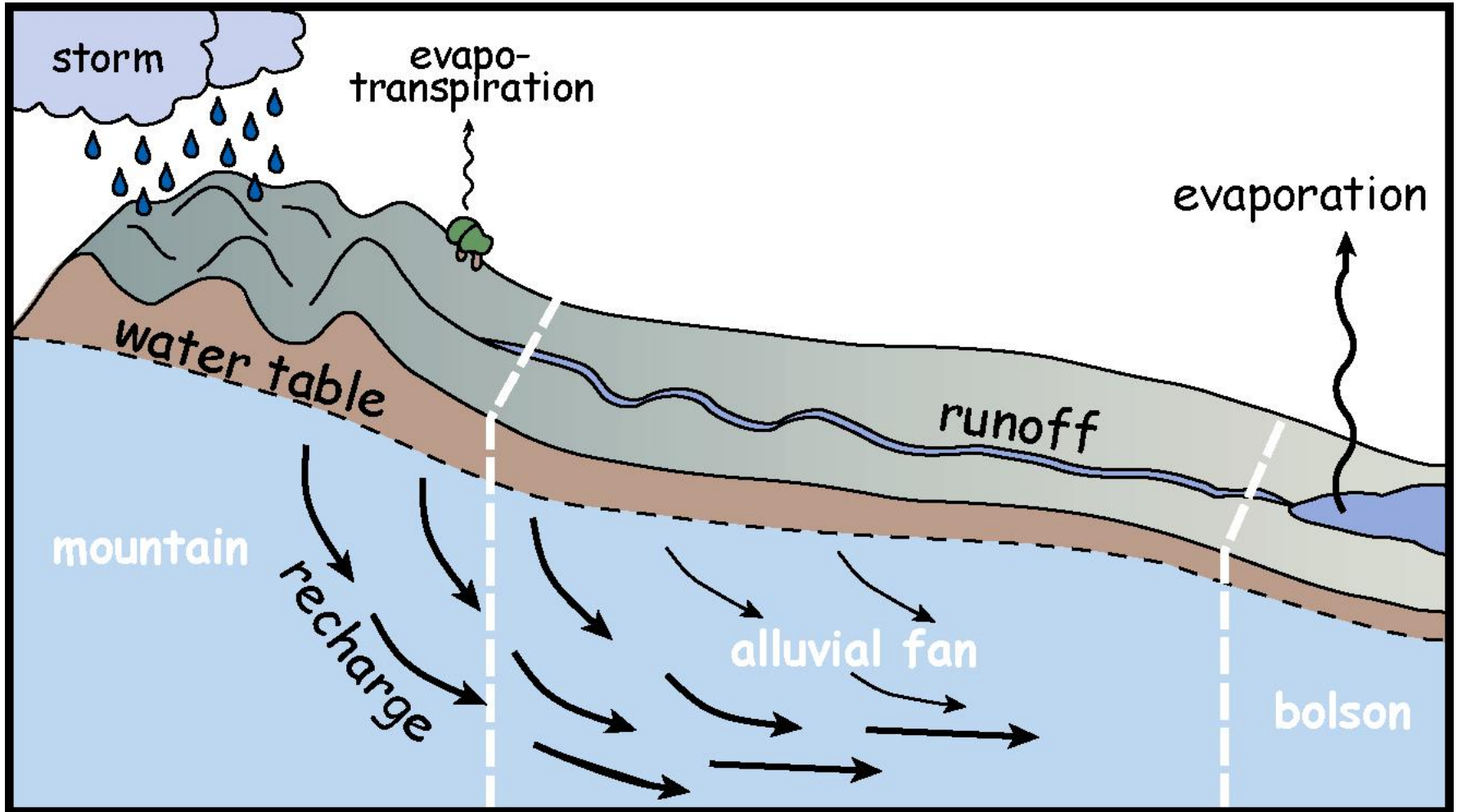


Figure B.1. Schematic of recharge processes and methods used to estimate recharge.

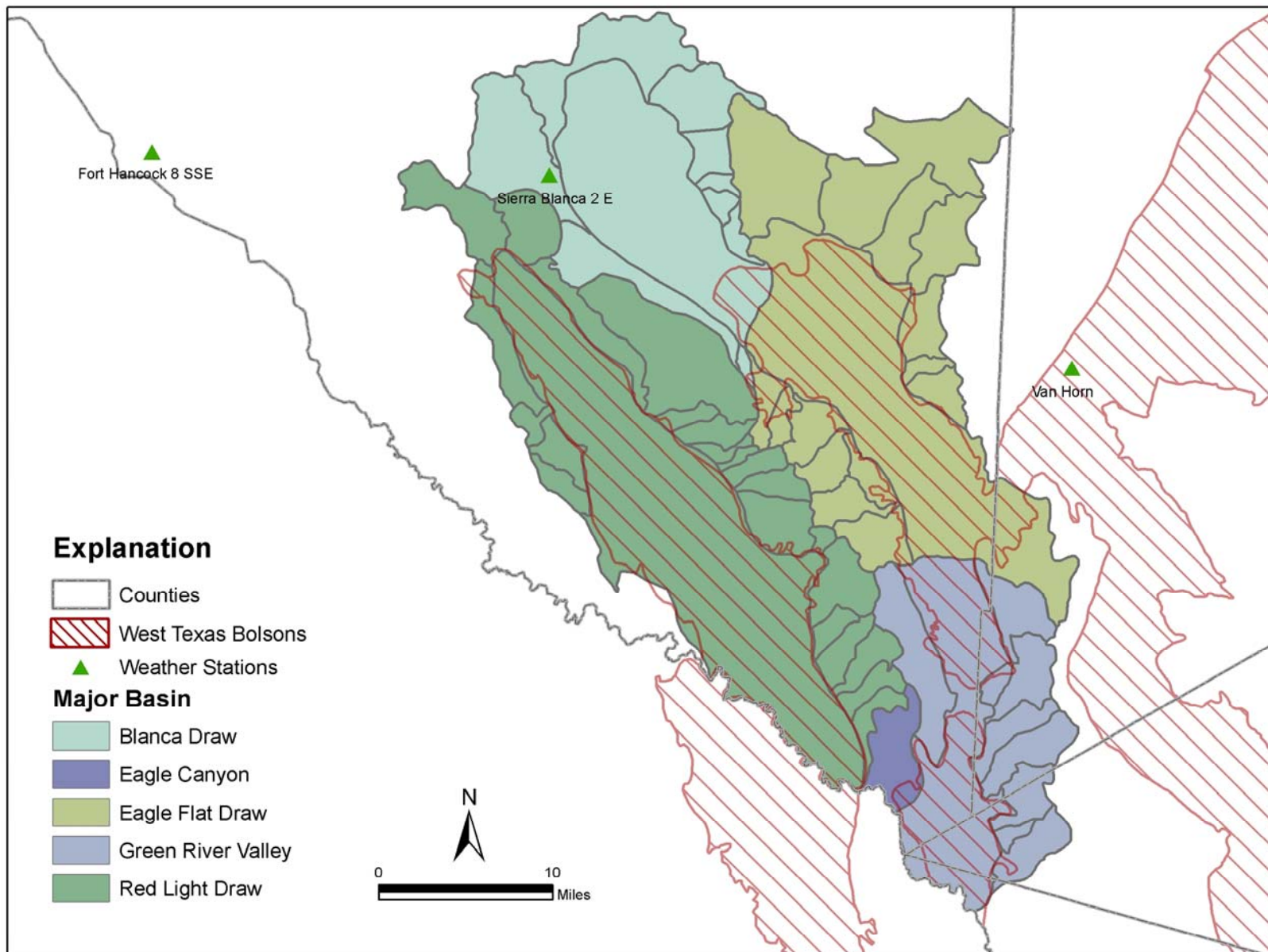


Figure B.2. Basins and sub-basins in the study area (shapefile will be provided).

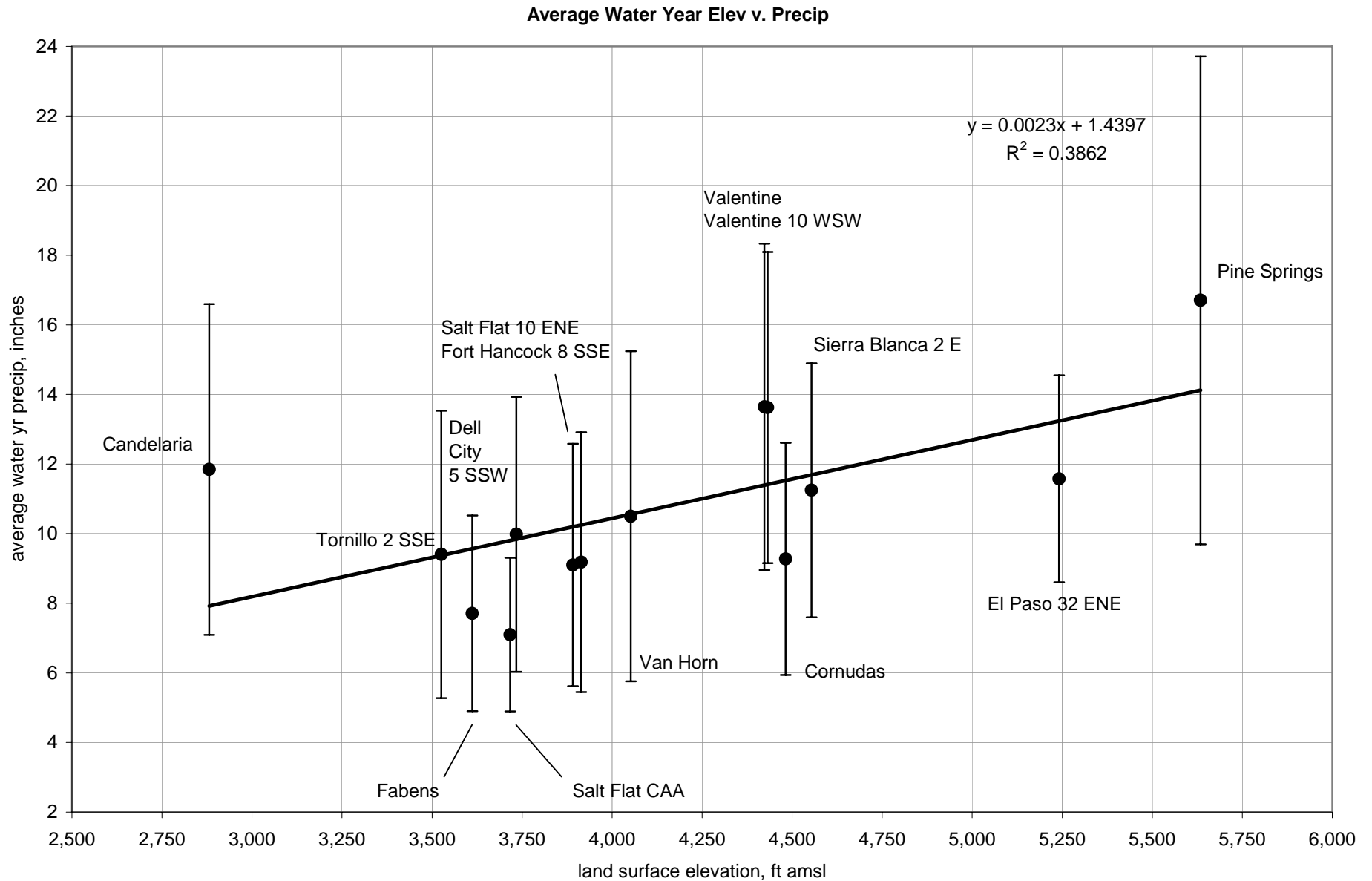


Figure B.3. Elevation and average water year precipitation for the period of record at 14 weather stations in the Red Light Draw-Green River Valley groundwater availability model study area, Trans-Pecos Texas.

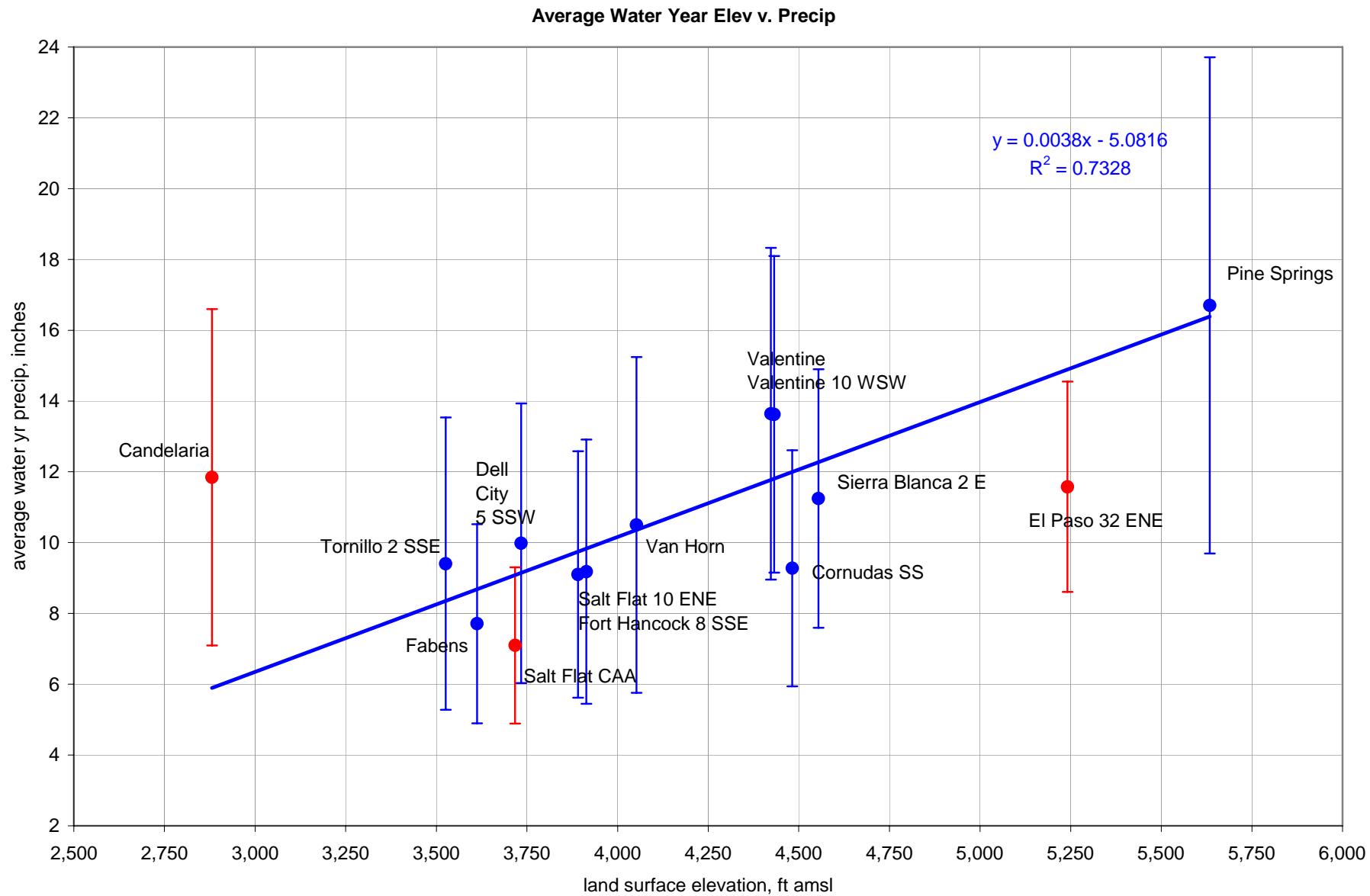


Figure B.4. Elevation and average water year precipitation with linear trend, Red Light Draw-Green River Valley groundwater availability model study area, Trans-Pecos Texas.

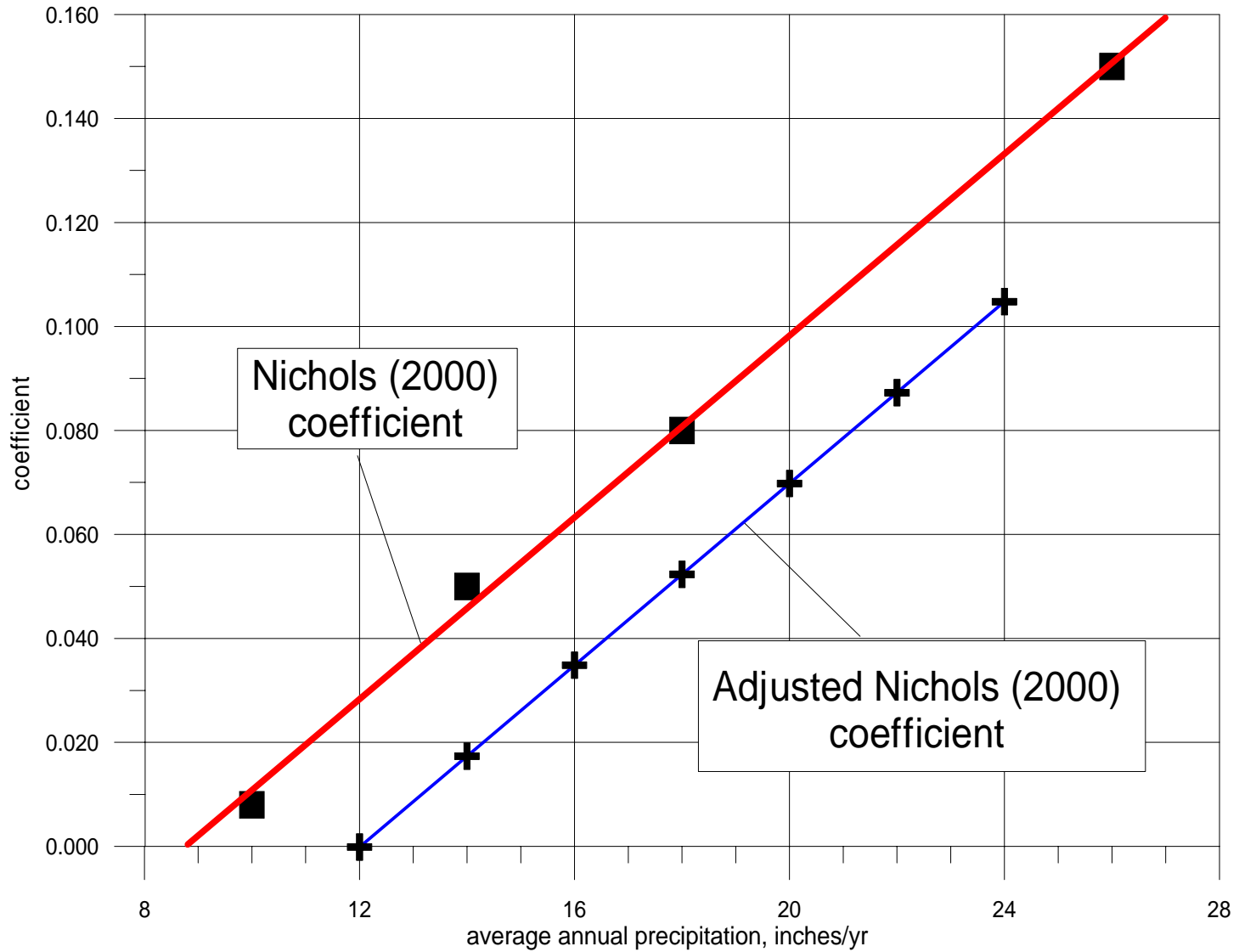


Figure B.5. Graph showing areal recharge coefficient versus average annual precipitation.

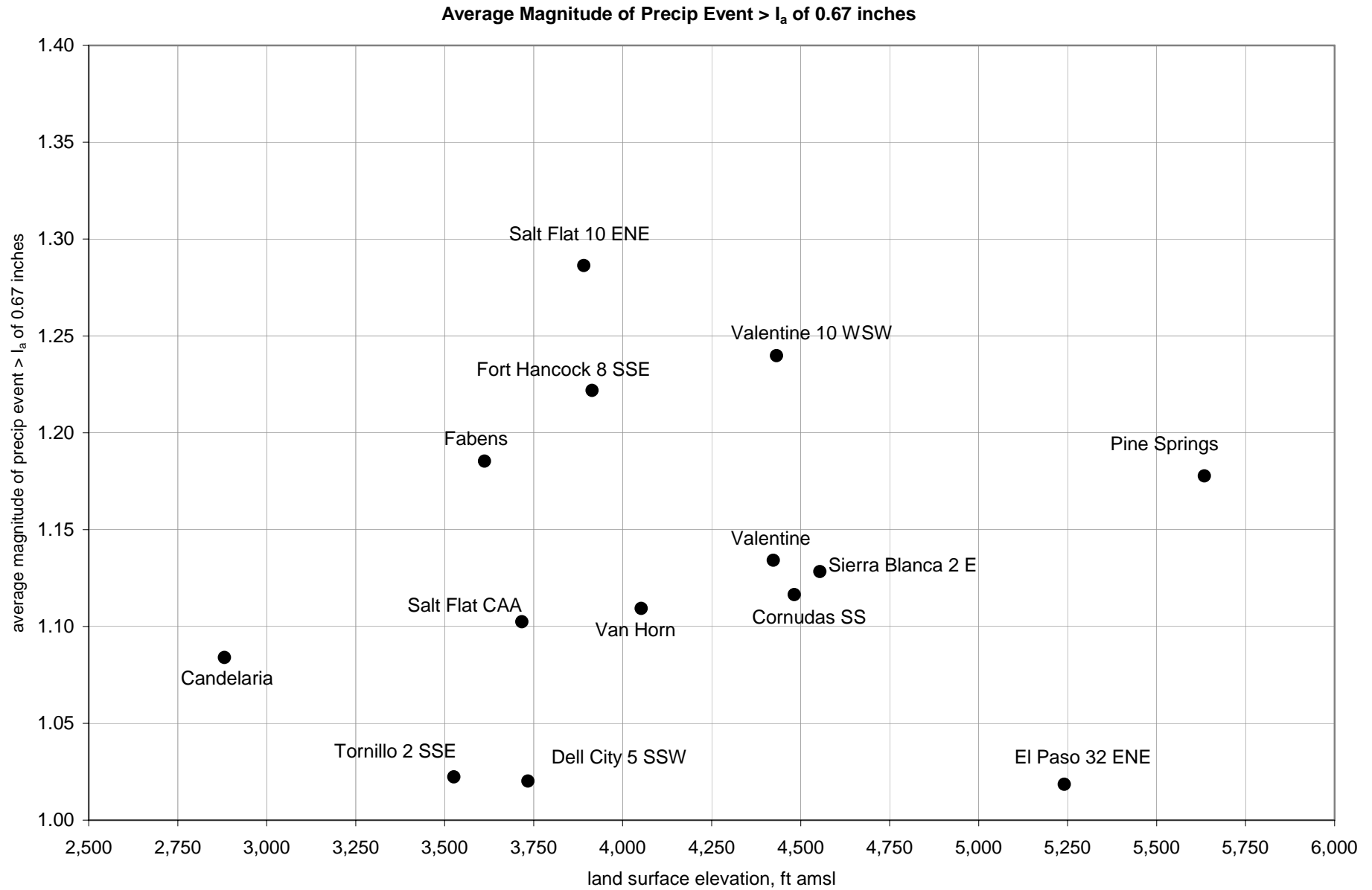


Figure B.6. Average magnitude of 24-hour precipitation events that exceed 0.67 inches (runoff-producing events) for the period of record at weather stations, Red Light Draw-Green River Valley groundwater availability model study area, Trans-Pecos Texas.

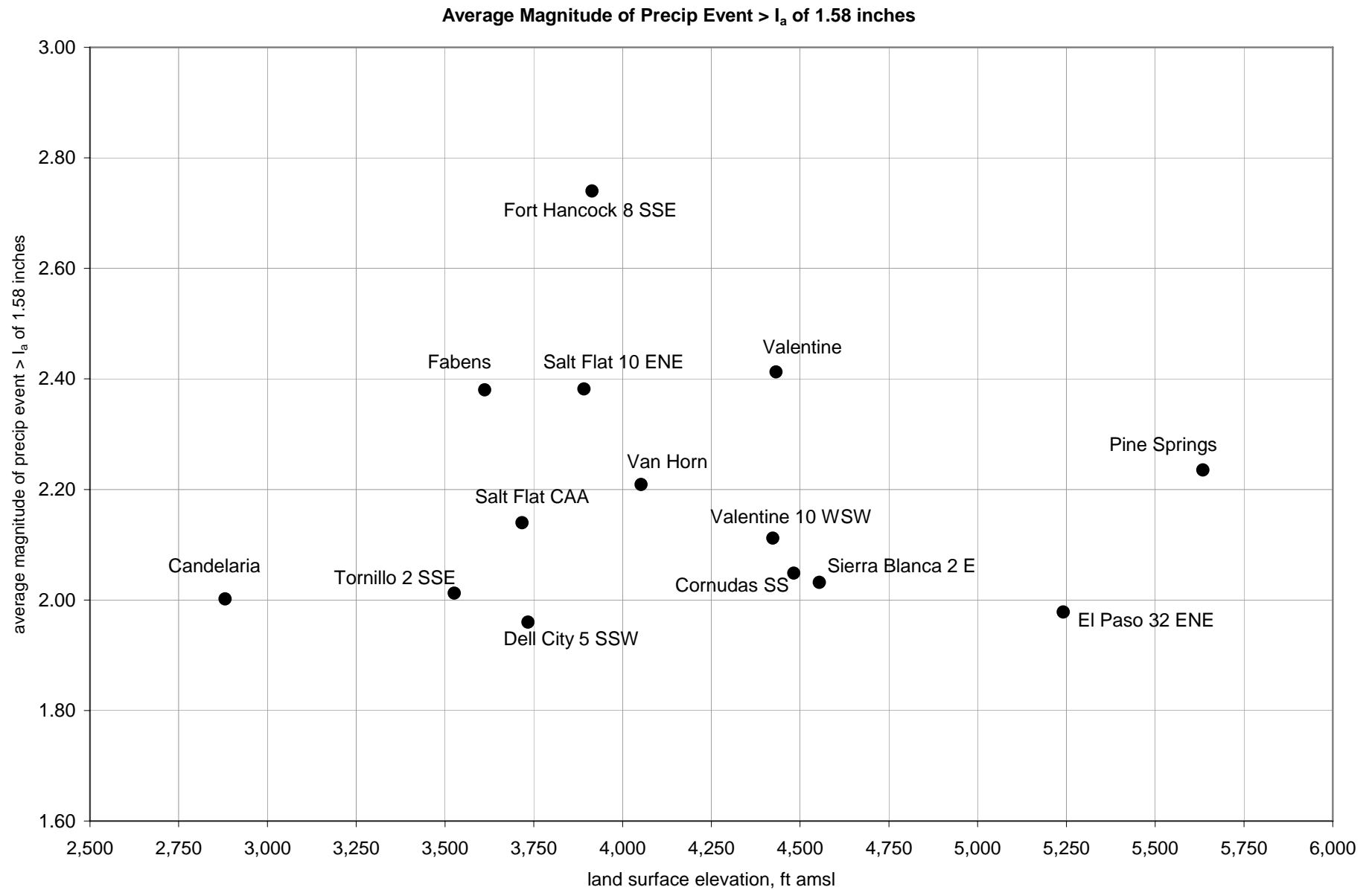


Figure B.7. Average magnitude of 24-hour precipitation events that exceed 1.58 inches (runoff-producing events) for the period of record at weather stations, Red Light Draw-Green River Valley groundwater availability model study area, Trans-Pecos Texas.

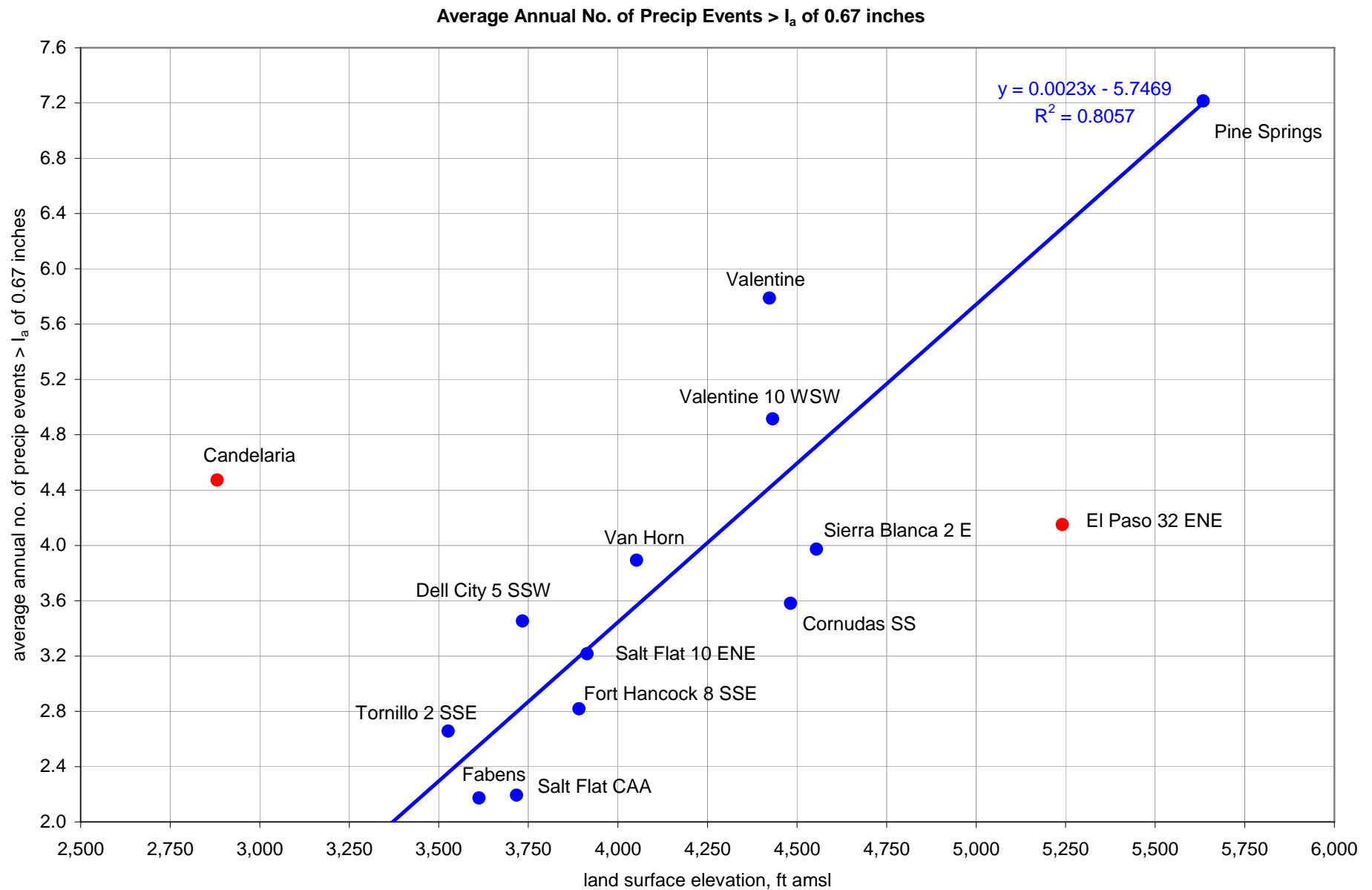


Figure B.8. Average number of 24-hour precipitation events that exceed 0.67 inches (runoff-producing events) annually at weather stations, Red Light Draw-Green River Valley groundwater availability model study area, Trans-Pecos Texas.

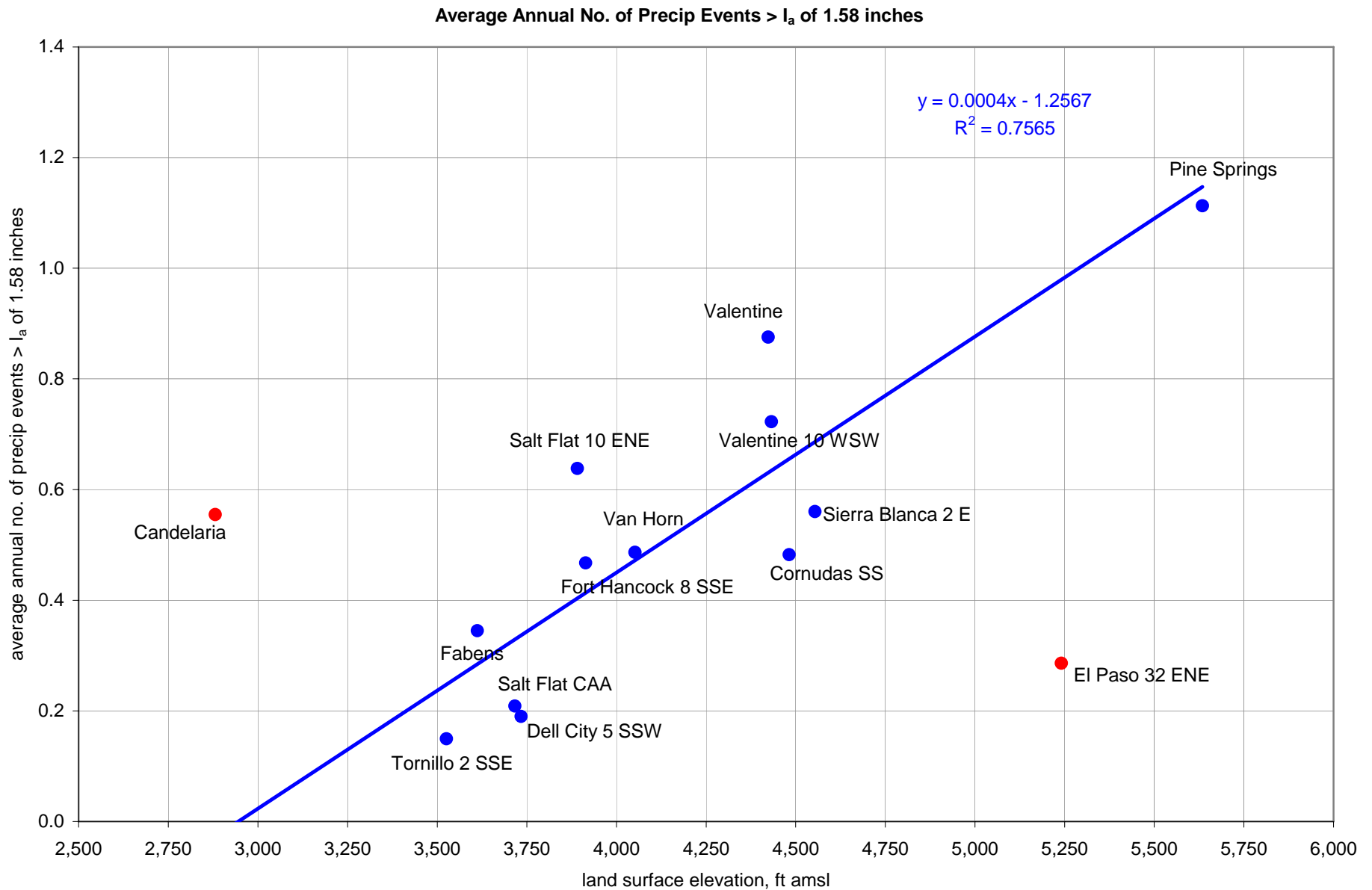


Figure B.9. Average number of 24-hour precipitation events that exceed 1.58 inches (runoff-producing events) annually at weather stations, Red Light Draw-Green River Valley groundwater availability model study area, Trans-Pecos Texas.

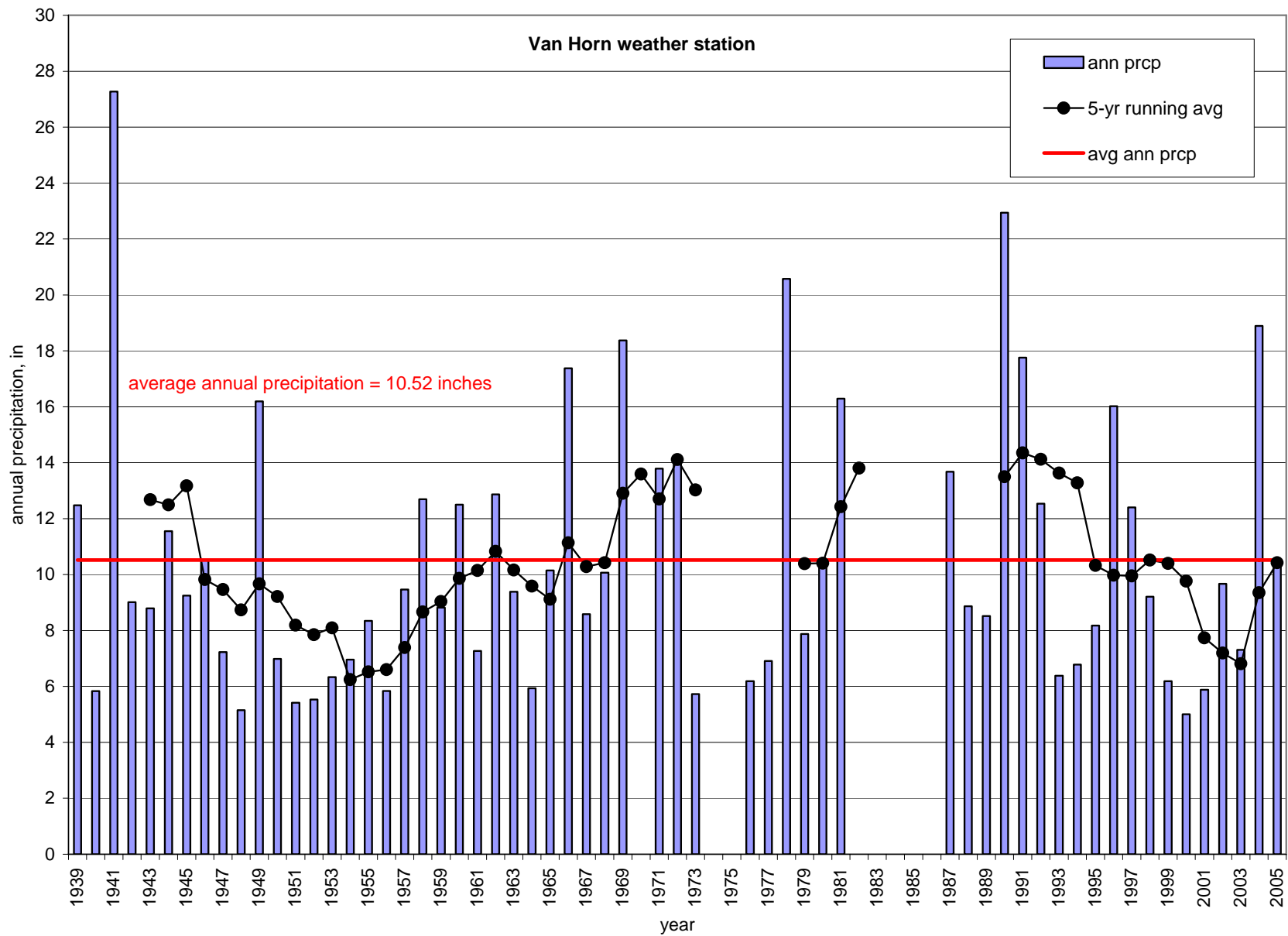


Figure B.10. Annual precipitation at the Van Horn weather station for the period of record 1939 to 2005.

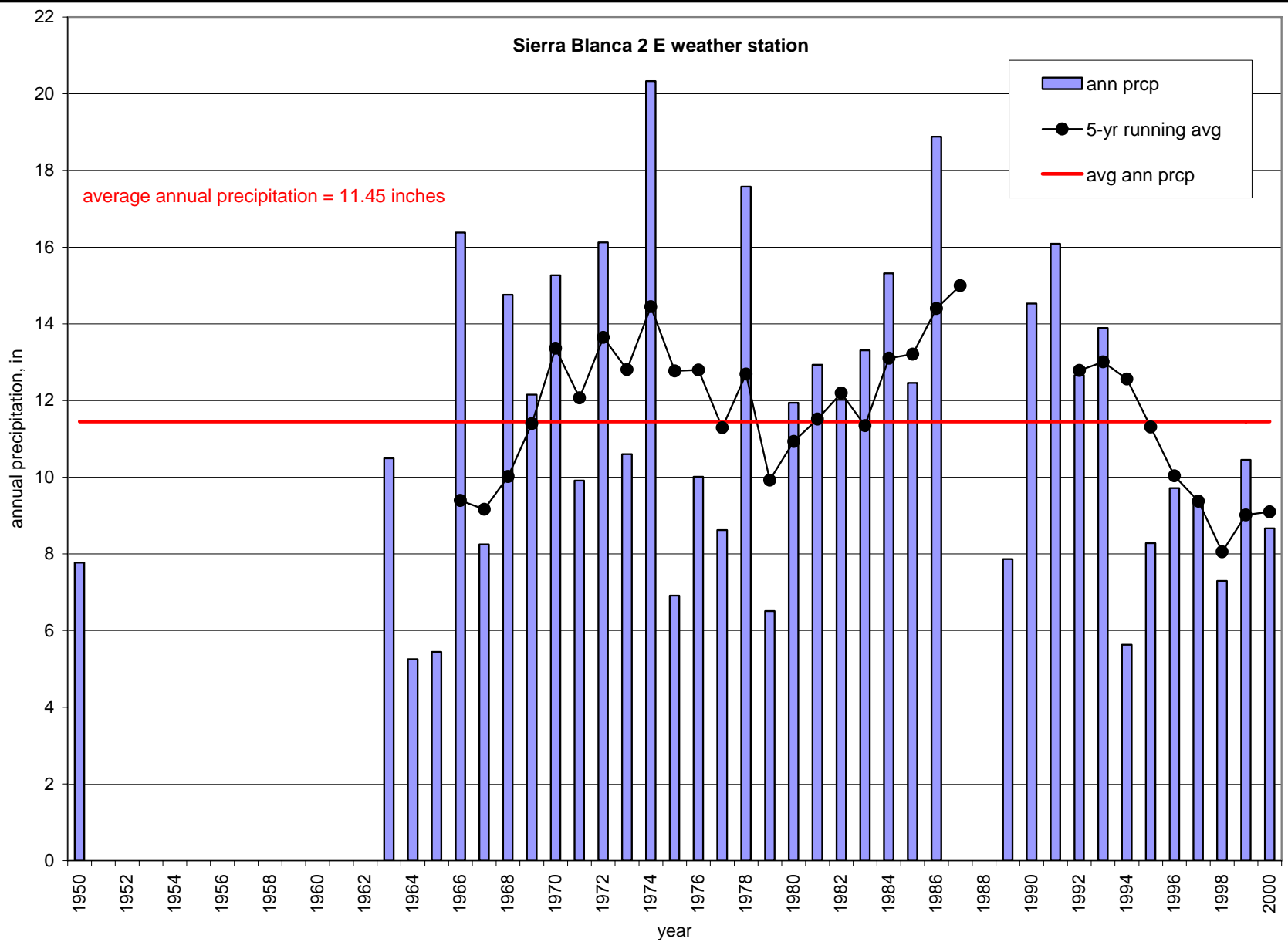


Figure B.11. Annual precipitation at the Sierra Blanca 2 E weather station for the period of record 1950 to 2000.

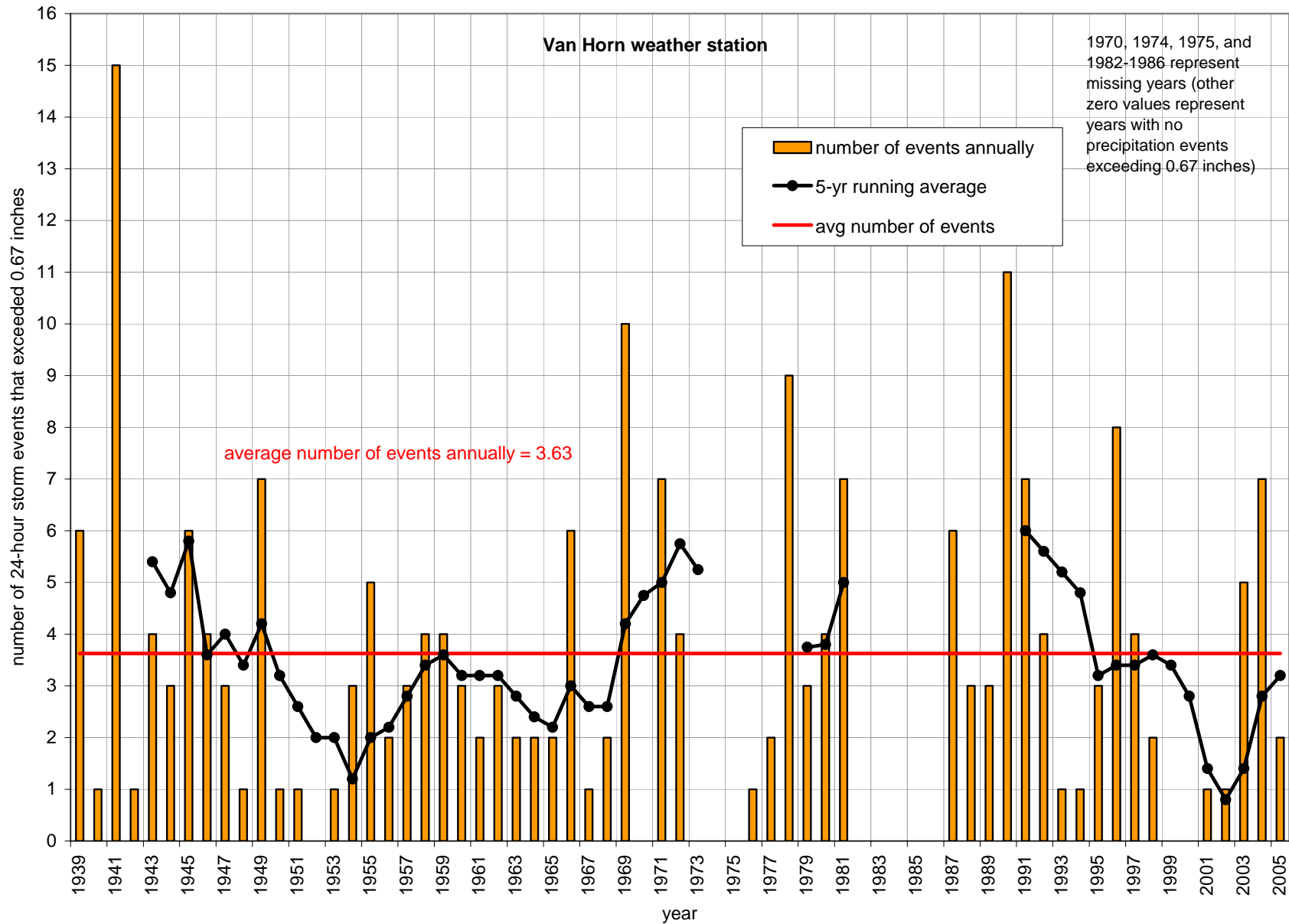


Figure B.12. Number of potential runoff-generating events for period of record 1939 to 2005 at Van Horn weather station.

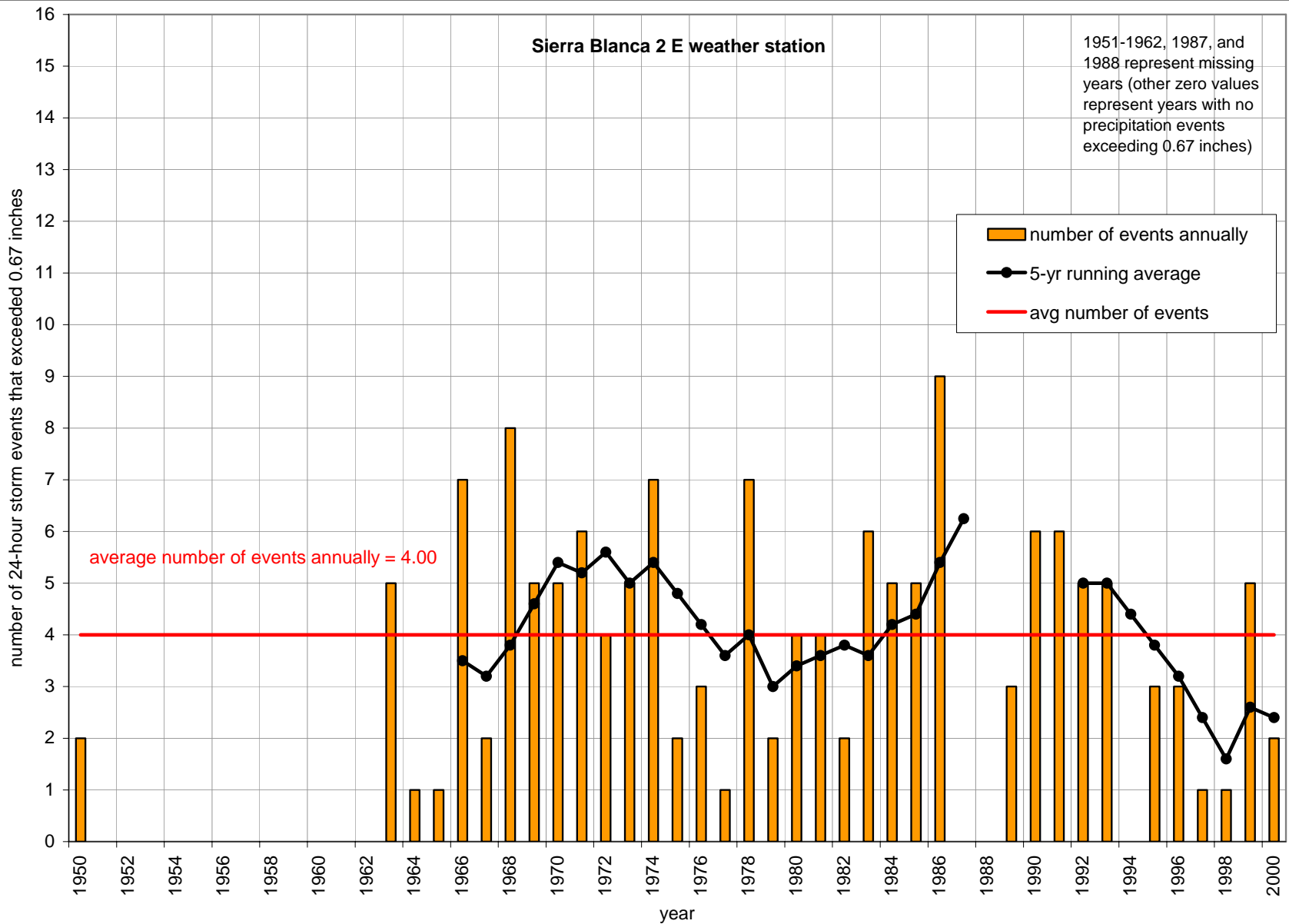


Figure B.13. Number of potential runoff-generating events for period of record 1950 to 2000 at Sierra Blanca 2 E weather station.

APPENDIX C

TEXAS AND MEXICO PUMPING DATA

Included below is a discussion of each type of pumping that was assessed in the model area included in the TWDB Pumpamatic database. Specific notes on details for each county are also included.

Rural Domestic

During the conceptual model report we reported only totals for rural domestic pumping. Some of those values changed for the steady state model so values are different from the 1980 total given in the conceptual model report. Generally, when rural domestic data is interpolated, census data is used. However, the census data must be “clipped out” or deleted wherever there is a city with municipal pumping, so that domestic pumping isn’t inadvertently doubled up. For the conceptual model, we simply totaled #s and cities were not clipped out for rural domestic pumping. We refined it for the actual pumping distribution done for the Steady State. So a total of 117.9 acre-feet was shown instead of 39.1. Rural domestic pumping was not assigned based on aquifer. Census data was used to calculate rural water demands and distribute pumping by population.

Irrigated Agricultural Pumping

The TWDB GAM Pumpamatic procedures allow irrigated agricultural pumping to be assigned as point or non-point. There is no “Irrigated-Ag” based on the Land Use coverage in the study area. Irrigated agricultural pumping was assigned directly to the cells where pumping occurred.

Culberson County

There are two Culberson County Lobo wells (From previous GAM) at the Eastern edge of the study area. Based on the research from the previous West Texas Bolsons GAM, these wells produced in 1978, 1979, and 1980. Pumping was assigned to the two model grid cells that these two wells fall within only for 1980. The same pumping values that were assigned to the wells in the previous GAM are assigned for 1980 in this GAM. (Well IDs 4758703 and 5102101 each have 168 acre-feet assigned to their corresponding grid cells, row 58 col 78 and row 62 col 78).

Hudspeth County

All Hudspeth County/West Texas Bolson irrigated values were assigned to our model since no portion of the West Texas Bolson in Hudspeth County falls outside of our study area.

Several wells along the Rio Grande show irrigated pumping with drill dates dating to the 1950s. There was no way to tell when they were in operation. The Board provided us with TIFF images that showed irrigated areas for 1979 and 1984. We used the 1979 maps to locate irrigated agricultural pumping. In Hudspeth County, the one small area with irrigated agricultural pumping (near the river) based on the maps, has two of the irrigated wells. Both wells fall within the same grid cell. Hudspeth County's 3500 acre-feet of irrigated pumping, minus the 336 acre-feet from the 2 Lobo wells, is 3164 acre-feet and was assigned to that single grid cell. According to the notes on the 1979 TIFF files, there was 2,730 acre-feet used in this small area in 1979.

Presidio County

The TWDB did not provide us with 1979 agricultural TIFF images for Presidio County. There are two irrigation wells along the river in Presidio county. These lie in two different grid cells, slightly less than one mile apart. The 182.4 acre-feet of pumping was distributed evenly among the two cells that the two irrigated wells lie within (91.2 acre-feet each)

Presidio County was originally assigned 1.6% of the total pumping in the Conceptual model report based on the fact that 1.6% of the county's portion of the West Texas Bolson lies within the study area. In order to better match the results from the previous West Texas Bolson GAM, the pumping for Presidion County was assigned the same values in the small area of the county (along the Rio Grande) where both model grids overlap. 182 ac/ft were assigned in the conceptual model report, though only 60 acre-feet, within the same area were assigned during the previous model. The 60 acre-feet will be distributed evenly (30 acre-feet each) to the 2 cells with irrigation wells along the river.

Jeff Davis County

Since no irrigated agricultural pumping exists in Jeff Davis county based on the Land Use or well locations, no irrigated agricultural pumping was assigned to the county.

Manufacturing

A single record for manufacturing exists for Hudspeth County in 1980, at the Allamore Aggregate Plant. There is a well location (Pioneer Talk) that coincides with a manufacturing polygon within the landuse file (in row 50 col 62). However, researching the actual location of the plant in aerial photos places it approximately 3600 feet to the SE of the well location and one grid cell over (row 51 col 63).

Stock (livestock)

Stock is the only pumping type that contributes pumping into the “Other” category. Therefore, it is the only well with pumping in layer 2.

27 of 28 stock wells identified as drilled in the bolsons, lie within the bolson boundary. The 28th is a Green River Bolson well in SW Culberson County that is less than 1/2 mile from the bolson boundary. Therefore, bolson-stock pumping was evenly distributed to the non-irrigated - Agriculture Land-use polygons that lie within the bolson boundary. The same methodology was used to distribute Stock pumping to the Hueco-Bolsons

Other Stock pumping was distributed to all non-irrigated agricultural lands that are not within an aquifer boundary. Factors were calculated that show the percentage of non-irrigated agricultural lands for each county/aquifer that are in the study area. The factors used are:

County	Percent of study area with Other Stock pumping
Culberson county	7.85%
Hudspeth	41%
Jeff Davis	29.10%
Presidio	12.60%
County	Percent of study area with West Texas Bolson Stock Pumping
Hudspeth	100%
Culberson	9.22%
Jeff Davis	5.40%
Presidio	1.60%
Hudspeth - Hueco Bolson	13.40%

Approximately 15 acre-feet was distributed among the non-irrigated agricultural cells in Hudspeth County that overlay the Hueco-Bolson aquifer.

Mexico Pumping

As stated in the report, in an effort to assess irrigation pumping in Mexico south of Red Light Draw we reviewed the pumping permit database from the Comisión Nacional del Agua (CONAGUA). (<http://siga.cna.gob.mx/ArcIMS/Website/REPDA/Localizador/viewer.htm>)

Figure C.1 locates permits found in and around the model area. Table C.1 lists accompanying data for these permits. The accuracy of this data could not be verified and the clarity of the units for the pumping rates was uncertain. In addition, it was uncertain whether the amount permitted by the Mexican government was actually pumped from each well. There is also little data on well completion in this area. In order to perform a proper calibration in this area, good estimates of production and transient water levels would be required, and because neither of these were available, the pumping data from Mexico was not incorporated into the model.

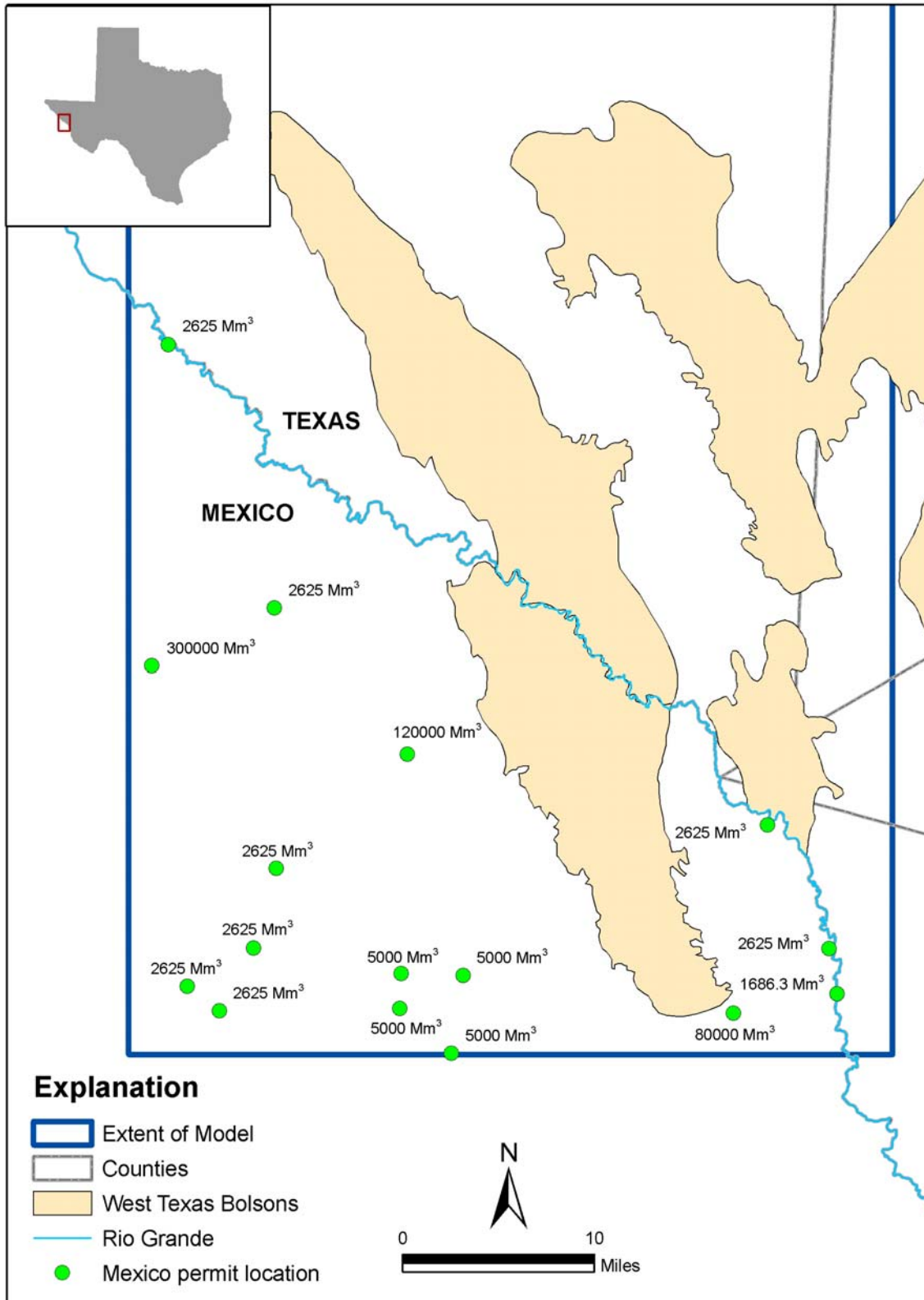


Figure C.1 – Location of Mexican pumping permits

Table C.1 - Mexican pumping permit data searched in the Comisión Nacional del Agua - CONAGUA database

NUMERO DE TITULO	LONGITUD DECIMAL	LATITUD DECIMAL	TITULAR	REGIÓN HIDROLÓGICA	NOMBRE DE CUENCA HIDROLÓGICA	NOMBRE DE ESTADO	NOMBRE DE MUNICIPIO	VOLUMEN ANUAL [Mm3]	VOLUMEN ANUAL 2 [Mm3]	VOLUMEN ANUAL 3 [Mm3]	ACUIFERO	USO DEL AGUA SUBTERRÁNEA
06CHI121404 /34AMGE98	-105.25556	30.635556	PEDRO GIESBRECHT F ROESE	CUENCA S CERRADAS D EL NORTE	RÍO CASAS GRANDES	CHIHUAHUA	JANOS	120000	0	0	JANOS	AGRICOLA
06CHI126546 /24HMGE98	-105.36583	30.543889	PRESIDENCIA MUNICIPAL DE GUADALUPE, LO C.: SAN FRANCISCO	RÍO BRAVO	RÍO BRAVO-CIUDAD JUÁREZ	CHIHUAHUA	GUADALUPE	2625	0	0	VALLE DE JUAREZ	PUBLICO URBANO
06CHI126942 /24HMGE98	-105.40972	30.433611	PRESIDENCIA MUNICIPAL DE GUADALUPE, LO C.: AGUA BLANCA	RÍO BRAVO	RÍO BRAVO-CIUDAD JUÁREZ	CHIHUAHUA	GUADALUPE	2625	0	0	VALLE DE JUAREZ	PUBLICO URBANO
06CHI126956 /24HMGE98	-105.48333	30.9375	PRESIDENCIA MUNICIPAL DE GUADALUPE, LO C.: CAJONCITOS	RÍO BRAVO	RÍO BRAVO-CIUDAD JUÁREZ	CHIHUAHUA	GUADALUPE	2625	0	0	VALLE DE JUAREZ	PUBLICO URBANO
06CHI127057 /24HMGE99	-105.38222	30.4825	PRESIDENCIA MUNICIPAL DE GUADALUPE, LO C.: LAS PALMAS	RÍO BRAVO	RÍO BRAVO-CIUDAD JUÁREZ	CHIHUAHUA	GUADALUPE	2625	0	0	LAGUNA DEL CUERVO	PUBLICO URBANO
06CHI127058 /24HMGE99	-105.37861	30.741389	PRESIDENCIA MUNICIPAL DE GUADALUPE, LO C.: LA PARRA	RÍO BRAVO	RÍO BRAVO-CIUDAD JUÁREZ	CHIHUAHUA	GUADALUPE	2625	0	0	BOSQUE BONITO-OJINAGA	PUBLICO URBANO
06CHI127062 /24HMGE98	-104.93583	30.594167	PRESIDENCIA MUNICIPAL DE GUADALUPE, LO C.: LOMAS DE ARENA	RÍO BRAVO	RÍO BRAVO-OJINAGA	CHIHUAHUA	GUADALUPE	2625	0	0	BOSQUE BONITO-OJINAGA	PUBLICO URBANO
06CHI127076 /24HMGE98	-104.87694	30.502222	PRESIDENCIA MUNICIPAL DE GUADALUPE, LO C.: TRES ALAMOS	RÍO BRAVO	RÍO BRAVO-OJINAGA	CHIHUAHUA	GUADALUPE	2625	0	0	BOSQUE BONITO-OJINAGA	PUBLICO URBANO
06CHI127084 /24HMGE99	-105.43889	30.451111	PRESIDENCIA MUNICIPAL DE GUADALUPE, LO C.: RANCHO BRACAMONTES	RÍO BRAVO	RÍO BRAVO-CIUDAD JUÁREZ	CHIHUAHUA	GUADALUPE	2625	0	0	LOS LAMENTOS	PUBLICO URBANO
06CHI128121 /24GMGE99	-105.19722	30.469444	GEORGINA FIERRO ARCHULETA	RÍO BRAVO	RÍO BRAVO-CIUDAD JUÁREZ	CHIHUAHUA	COYAME	5000	0	0	LAGUNA EL CUERVO	PECUARIO
06CHI128525 /24GMGE99	-105.25139	30.441944	ANA MARIA FIERRO ARCHULETA	RÍO BRAVO	RÍO BRAVO-CIUDAD JUÁREZ	CHIHUAHUA	GUADALUPE	5000	0	0	LAGUNA EL CUERVO	PECUARIO
06CHI128526 /24GMGE99	-105.25139	30.468611	ANA MARIA FIERRO ARCHULETA	CUENCA S CERRADAS D EL NORTE	ARROYO EL CARRIZO Y OTROS	CHIHUAHUA	GUADALUPE	5000	0	0	LAGUNA EL CUERVO	PECUARIO

NUMERO DE TITULO	LONGITUD DECIMAL	LATITUD DECIMAL	TITULAR	REGIÓN HIDROLÓGICA	NOMBRE DE CUENCA HIDROLÓGICA	NOMBRE DE ESTADO	NOMBRE DE MUNICIPIO	VOLUMEN ANUAL [Mm3]	VOLUMEN ANUAL 2 [Mm3]	VOLUMEN ANUAL 3 [Mm3]	ACUIFERO	USO DEL AGUA SUBTERRÁNEA
06CHI128527 /24GMGE99	-105.20417	30.409722	GEORGINA FIERRO ARCHULETA	CUENCAS CERRADAS DEL NORTE	ARROYO EL CARRIZO Y OTROS	CHIHUAHUA	COYAME	5000	0	0	LAGUNA EL CUERVO	PECUARIO
06CHI129447 /24HPGE99	-104.86806	30.468056	PRESIDENCIA MUNICIPAL DE OJINAGA, LOC.: TRES HERMANOS I	RÍO BRAVO	RÍO BRAVO-CIUDAD JUÁREZ	CHIHUAHUA	OJINAGA	1686.3	0	0	BOSQUE BONITO-OJINAGA	PUBLICO URBANO
06CHI134843 /24APGE00	-104.95833	30.45	MARTHA JUAREZ ZUBI A	RÍO BRAVO	RÍO BRAVO-CIUDAD JUÁREZ	CHIHUAHUA	OJINAGA	80000	0	0	BOSQUE BONITO-OJINAGA	AGRICOLA
06CHI136829 /34AMGE05	-105.48417	30.693056	ABRAHAM BERG MARTENS	CUENCAS CERRADAS DEL NORTE	ARROYO EL CARRIZO Y OTROS	CHIHUAHUA	AHUMADA	300000	0	0	LOS LAMENTOS	AGRICOLA

Table C.2 – Explanation of field headings in Table C.1.

Label	Description
NUMERO DE TITULO	Title number
LONGITUD DECIMAL	Longitude (decimal degrees)
LATITUD DECIMAL	Latitude (decimal degrees)
TITULAR	Owner
REGIÓN HIDRO-LÓGICA	Hydrologic region
NOMBRE DE CUENCA HIDROLÓGICA	Watershed
NOMBRE DE ESTADO	State
NOMBRE DE MUNICIPIO	Municipality
VOLUMEN ANUAL [Mm3]	Annual volume
VOLUMEN ANUAL 2 [Mm3]	Annual volume 2
VOLUMEN ANUAL 3 [Mm3]	Annual volume 3
ACUIFERO	Aquifer
USO DEL AGUA SUBTERRÁNEA	Groundwater use

APPENDIX D
COUNTYWIDE WATER BUDGETS

County	Layer	West	East	North	South	Top	Bottom	Recharge	ET	GHB	Stream	TOTAL	
Hudspeth	IN	1	233	2	0	30	0	3,108	1	0	0	119	3,494
		2	102	27	0	61	524	2,269	5,858	0	0	233	9,073
		3	75	228	0	36	2,586	0	0	0	0	0	2,924
		All	410	256	0	127			5,859	0	0	352	15,491
	OUT	1	59	0	0	296		524	0	1,972	0	643	3,494
		2	25	64	0	183	3,108	2,586	0	2,730	0	377	9,073
		3	147	65	0	443	2,269	0	0	0	0	0	2,924
		All	231	129	0	923			0	4,702	0	1,020	15,491
Culberson	IN	1	0	0	0	0	0	165	167	0	0	0	331
		2	51	2	25	0	331	205	453	0	0	0	1,066
		3	48	9	48	0	329	0	0	0	0	0	435
		All	98	11	73	0			620	0	0	0	1,832
	OUT	1	1	0	0	0	0	331	0	0	0	0	331
		2	34	0	0	12	165	329	0	145	381	0	1,066
		3	160	0	0	73	205	0	0	0	0	0	435
		All	195	0	0	85			0	145	381		1,832
Jeff Davis	IN	1	0	0	0	0	0	11	0	0	0	0	11
		2	0	0	15	1	0	34	61	0	0	0	111
		3	10	0	331	0	36	0	0	0	0	0	377
		All	10	0	346	1	36	45	61	0	0	0	499
	OUT	1	1	0	0	2	0	0	0	9	0	0	11
		2	18	0	0	34			0	13	0	0	111
		3	78	0	0	265	34	0	0	0	0	0	377
		All	97	0	0	300	45	36	0	22	0	0	499
Presidio	IN	1	0	0	2	0	0	18	3	0	0	54	76
		2	82	8	32	23	0	312	426	0	0	253	1,136
		3	109	6	281	0	64	0	0	0	0	0	460
		All	191	14	315	23			429	0	0	307	1,671
	OUT	1	0	0	0	0		0	0	72	0	4	76
		2	66	1	1	14	18	64	0	794	0	178	1,136
		3	32	10	0	107	312	0	0	0	0	0	460
		All	61	11	0	155			0	873		248	1,671

County	Layer	West	East	North	South	Top	Bottom	Recharge	ET	GHB	Stream	TOTAL	
Mexico	IN	1	0	260	483	0	0	1,139	0	0	0	51	1,933
		2	2	57	253	0	2	896	5,402	0	0	248	6,859
		3	2	179	383	0	607	0	0	0	0	0	1,170
		All	4	496	1,119	0			5,402	0	0	299	9,962
	OUT	1	0	48	7	0		2	0	1,442	0	434	1,933
		2	0	231	77	0	1,139	607	0	4,318	0	489	6,859
		3	0	239	36	0	896	0	0	0	0	0	1,170
		All	0	518	120	0			0	5,760	0	922	9,962

- All values recorded in acre-feet/year

Explanation of Water Budget Components

- West, East, North, or South – Water that flows into and out of the specific area from the west, east, north and south side of that area.
- Top or Bottom – Water that flows into and out of the specific area from the top or the bottom boundary.
- Recharge – Areally distributed recharge due to precipitation.
- ET – Water that flows out of the aquifer due to evaporation and transpiration. This component of the budget will always be shown as outflow.
- GHB – General head boundary. Used in the model to simulate the flow between the Salt Basin Bolson and the Eagle Flat Bolson.
- Streams – Water exchange between streams and the aquifer. Water that flows into the aquifer is shown as inflow.

APPENDIX E

RESPONSE TO TWDB COMMENTS

Table of Contents

1.0	RESPONSE TO CONCEPTUAL MODEL COMMENTS.....	1
1.1	Conceptual Model Report Comments.....	1
1.2	Conceptual Model Source Data Comments.....	14
2.0	RESPONSE TO DRAFT FINAL COMMENTS	16
2.1	Draft Final Report Comments.....	16
2.2	Appendix E: Response to comments from the conceptual model report.....	23
2.3	Model Comments.....	26
2.4	Geodatabase Comments.....	27
2.5	Suggestions	31

Appendix E

Response To TWDB Comments

This appendix contains responses to all the comments received from the TWDB on the conceptual model report and the draft final report.

1.0 RESPONSE TO CONCEPTUAL MODEL COMMENTS

1.1 Conceptual Model Report Comments

Comment: Per contract, Exhibit B, Attachment 1, Section 4.4.2 Report Deliverables, last paragraph: Each report shall have an authorship list of persons responsible for the studies: firms or agency names as authors will not be acceptable.

Response: *Authorship has been clarified.*

Comment: Per contract, Exhibit B, Attachment 1, Section 4.4.3 Report Deliverables: For the conceptual report, and then later for the draft report, the contractor shall deliver to the TWDB: all the related documented source and derived data in the appropriate geodatabase (see Attachment 2).

Response: *Completed.*

Comment: Page v. Executive summary needs to be re-written after the model has been developed

Response: *Executive summary has been re-written to include model details.*

Comment: Introduction: Please clarify what new field data was collected and analyzed to assess hydraulic properties and current water levels as noted on page 1-1. Also please remove or explain predictive simulations referenced on page 1-2 as this is outside the scope of work.

Response: *New field data was not collected. Other text was corrected.*

Comment: Section 2.1, page 2-1, paragraph 2: Please re-phrase last sentence since it appears contradictory. The basin fill and aquifer appear to extend into Mexico even if the 'name' of the aquifer may change or not be referenced as Red Light Draw in Mexico. Also Section 2.1 pages 2-1 through 2-2 describe the study area boundaries using mountains and highways. Suggest adding these features with labels to figure 2.1.1 or figure 2.1.2 and referencing the figure in the text.

Response: *Sentence has been clarified.*

Comment: Figure 2.1.2: Suggest re-aligning the location of the Culberson County label in figure 2.1.2 since it is truncated by the inset box. Text refers to Presidio-Redford Bolson however; figure 2.1.2 does not include this part of the West Texas Bolsons. Suggest labeling the 'Salt Basin' bolsons in figure 2.1.2 and adding Presidio-Redford Bolsons to figure.

Response: *Figure has been updated with area aquifers and appropriate labels.*

Comment: Figure 2.1.1: Suggest adding label to Interstate-10 since text uses this to identify the location of Sierra Blanca.

Response: *Figure has been labeled.*

Comment: Figure 2.1.4: Suggest including within figure or in the caption the date of the source reference since district boundaries may change during the course of the project.

Response: *Figure has been updated.*

Comment: Figure 2.2.3: Suggest adding location of Indian Hot Springs referenced in text on page 2-11 to figure 2.2.3.

Response: *Figure has been updated.*

Comment: Section 2.2, page 2-9, paragraph 1 reference Thornbury, 1965 which is not listed in references. Please update references as applicable.

Response: *Reference has been added to references section.*

Comment : Page 2-9. Text in Local Setting subsection (pages 2-9 to 2-10) there are numerous landmarks referenced that are not included in the figure referenced. This includes the Steeruwitz Hills, Millican Hills, Scott's Crossing, Wildhorse Flat, Allamoore, etc. Be sure to include a figure with landmarks if you are going to refer to these landmarks in your text. Include landmarks not delineated in figure 2.2.2. Suggest updating figure with missing landmarks described in text. Topographic map does not agree with statement that water discharges from Green River Valley to Eagle Flat since it appears water would flow uphill. Topographic map suggests predominant flow towards the Rio Grande. Please clarify

Response : *Landmarks referenced have been added to Figure 2.2.2.*

Comment: Page 2-10. Previously the report stated that the Red Light Draw wash does not extend to the other side of the Rio Grande, but here it implies that it does.

Response: *Sentence has been clarified.*

Comment: Page 2-12. The hatching on the figure makes it difficult to look at, county names can't be read, etc... If the entire area is Basin and Range, suggest stating this in the text and/or figure title and not putting a hatch pattern on the entire figure. If a hatch should remain, suggest a less distracting one.

Response: *Figure has been clarified by removing hatch pattern and updating text and figure caption.*

Comment: Fig 2.2.2: Please correct spelling of Quitman Mountains and include landmarks described in text.

Response: *Figure label has been corrected and landmarks referenced have been added.*

Comment: Section 2.3: Please update report with a map of climate classification for the study per Contract Exhibit B, Attachment 1, Section 4.4.2 page 20 of 26 and reference in text.

Response: *Text has been updated to clarify study area as arid to semi-arid.*

Comment: Section 2.3, page 2-15, paragraph 2 references Nativ and Riggio, 1989 and 1990 which 1990 is not listed in references. Please update references as applicable.

Response: *Reference has been added to references section.*

Comment: Fig 2.3.1: Please clarify and document the years used to calculate the mean annual precipitation

Response: *The average annual precipitation contours are from 1971-2000 annual precipitation data gridded using the PRISM (Parameter-elevation regressions on independent slopes model) climate mapping system, at an 800-meter (30-arcsec) resolution (www.prism.oregonstate.edu)*

Comment: Figure 2.3.2: Suggest using same x-axis scale and using a larger font on graphs.

Response: *Figure will be corrected in final report.*

Comment: Section 2.3, page 2-16 describes spatial variability of temperature, please update text to include description of temporal variability per Contract Exhibit B, Attachment 1, Section 3.1.1 page 4 of 26.

Response: *Text has been updated to include temporal variability of temperature.*

Comment: Page 2-17. Suggest coloring the precipitation to more easily show readers the values. Coloration of bolsons can be eliminated.

Response: *Figure has been updated.*

Comment: Page 2-21. Hatch pattern on figure very difficult to read.

Response: *Figure has been updated.*

Comment: Observation--Figure 2.3.3 is averaged from 1954 to 2004 which includes drought of record and therefore may represent a higher than normal evaporation average.

Response: *Text has been updated*

Comment: Section 2.5, Geology, page 2-1, 2nd paragraph and page 2-2, 3rd paragraph references Dietrich and others, 1987; however, references only list Dietrich and others 1968, please clarify and correct as needed. 2nd paragraph-Line 1: Landmarks referenced in text not included on figure. Also, the complexity of the figure makes it almost impossible to easily see what the text is referring to. Can a simpler version of surface geology be made as a supplement to Figure 2.5.1?.

Response: *Text has been corrected to Dietrich and others, 1983. Figure 2.5.1 has been updated to clarify geology and landmarks referenced have been added.*

Comment: Text in Geology Section describes stratigraphy however Geology section (2.5) is missing stratigraphic chart showing systems and ages of units described per Contract Exhibit B, Attachment 1, Section 4.4.2 page 21 of 26. Suggest organizing and labeling figure 2.5.1b to include this information or cross-reference to figures located elsewhere in the report

Response: *Table 4.1 has been moved to this section and renamed Table 2.1; table explanation has been added to the text.*

Comment: Figure 2.5.1b please clarify spelling of 'Etholean' to coincide with Table 4.1 which lists this as 'Etholen' as well as 'Trachyte porphery, Garren Group' which table 4.1 lists as Trachyte Porphyry.

Response: *Corrected as requested.*

Comment: Geology section (2.5) is missing maps of spatially distributed geologic information used during the modeling study (showing the control data if possible) per Contract Exhibit B, Attachment 1, Section 4.4.2 page 21 of 26. Please add or cross-reference to figures located elsewhere in the report

Response: *Geology of the study area is detailed in Section 4 of this report. Text has been added to clarify.*

Comment: Geology section (2.5) is missing a map of the major structural and tectonic features in the area per Contract Exhibit B, Attachment 1, Section 4.4.2 page 21 of 26. Please add or cross-reference to figures located elsewhere in the report.

Response: *Geology of the study area is detailed in Section 4 of this report. Text has been added to clarify.*

Comment: Geology section (2.5) is missing several geologic cross-sections through the study area per Contract Exhibit B, Attachment 1, Section 4.4.2 page 21 of 26. Please add or cross-reference to figures located elsewhere in the report.

Response: *Geology of the study area is detailed in Section 4 of this report. Text has been added to clarify.*

Comment: Pages 3-2 to 3-3. What kind of model? All that is stated is "numerical model", which is non-specific. The figure shows a straight line for the model area (see comment below). How did this steady-state model come up with model-estimated residence times and how accurate were these estimates?

Response: *The model was a two-dimensional, cross-section MODFLOW model. The line represents the linear extent of the cross-section model, and does not have a lateral extent.*

Comment: Figure refers to a model extent as a single line? Also, figure refers to Darling, Hibbs, and Dutton (1994) while text on page 3-2 refers to Hibbs and Darling (1995)

Response: *Model extent is described by a single line because it was a two-dimensional cross-section model. Reference in the text has been corrected.*

Comment: Missing introduction to Hydrologic Setting section 4.0 that should set up and introduce the following subsections in the chapter and how or why they are important to the modeling project.

Response: *Introduction has been added.*

Comment: Text in Section 4.1 appears to discuss mostly geology and some discussion of water in the bolsons. Unclear if units below bolsons are confining, part of the flow

system, or a combination of both. The terminology with Red Light Draw and what does and does not extend into Mexico should be straightened out. "Draw", "bolson", "wash", "aquifer". Here it says the "Bolson" (but not the draw itself) extends into Mexico. What does and does not extend into Mexico? And is it really necessary to include at all? Please clarify, move geology information to geology section (including stratigraphic cross-sections and structural faulting figures), and discuss the layering of the aquifers and confining units for the study area per Contract Exhibit B, Attachment 1, Section 3.1.3 page 5 of 26.

Response: *Hydrogeologic cross-sections and discussion have been moved to Section 2.5. Text has been clarified where possible.*

Comment: Text in Section 4.1 does not explain the rationale of model layers 2 and 3 or what they hydrostratigraphically are representing. Please update section 4.0 with a discussion on the rationale for the hydrostratigraphic units per Contract Exhibit B, Attachment 1, Section 3.1.3 page 5 of 26.

Response: *Completed, see section 4.1. Vertical discretization of the complex system was difficult because the elevation of the contacts between the conceptualized hydrogeologic units varies significantly over short distances. In addition, due to the faulting and complex geology, it is impossible to follow the layering concepts used in the MODFLOW formulation without simplifying the hydrogeologic setting. Layer 1 represents the Bolson aquifer and is only active in those areas where the bolson deposits are present. Layers 2 and 3 represent the Cretaceous, Paleozoic, Tertiary, Permian and other units in the model area. Because of the complexity of the hydrogeology and the uncertainty regarding precise elevations of geologic contacts and hydraulic properties of various hydrogeologic units, the total thickness of the underlying rocks was split between Layer 2 and Layer 3 in most areas.*

Comment: Pg 4-4, para 2, line 3. I am still not sure I have seen a figure with Scott's Crossing identified, even though this is a frequently mentioned landmark. It isn't on any of the cross-sections either.

Response: *Figure has been updated with landmarks referenced.*

Comment: Pg 4-4, para 3, line 4. It says Tertiary intrusive rocks are exposed along the axis of GRV, but nothing like this is shown in the F-F' cross-section, which appears to be along the axis of GRV. And as noted above, Figure 2.5.1 is not usable to see if Tertiary volcanics are shown in that figure, the patterns are not discernable in that figure.

Response: *Text has been corrected and Figure 2.5.1 has been clarified.*

Comment: Table 4.1. This table is dropped in here without any reference in the text. This is a critical table and warrants significant discussion. And it would be appropriate to either show the breakout of Layers 2 and 3 or explain in detail why they are lumped. At some point they have to be split out.

Response: *Table 4.1 has been moved to Section 2 and described there. Regarding layer 2 and 3, see Section 4.1.*

Comment: Pg 4-6. On all figures the E' and D labels are reversed and the page numbers are not located at the bottom of the page.

Response: *Figure 4.1.1 labels have been corrected.*

Comment: Pg 4-13. For figures such as this suggest zooming into the model extent. This figure is very detailed and difficult to read all of the detail, and it would seem appropriate not to zoom out well beyond the model extent when detail is lost.

Response: *Figure has been corrected as requested.*

Comment: Pages 4-14 to 4-16. Section 4.2: Text states delineation of underlying Tertiary, Cretaceous, Jurassic, and Permian formations into 2 layers will occur during model development. This information needs to be included in the report, as well as, description of rationale, units combined, and structure maps with control points showing the elevation of the top and bottom of each of the hydrostratigraphic units per Contract Exhibit B, Attachment 1, Section 3.1.4 page 5 of 26.

Response: *Text now includes rationale.*

Comment: Page 4-14 section 4.2.1. Is this text where it is supposed to be? The intro to the structure section does not seem to be an appropriate place for describing the three layers in the model.

Response: *Text remains.*

Comment: Section 4.2: Text states delineation of underlying Tertiary, Cretaceous, Jurassic, and Permian formations into 2 layers will occur during model development. Please describe for the downdip model areas, the relationship of structural delineations and assumed confining layers, as applicable, per Contract Exhibit B, Attachment 1, Section 3.1.4 page 5 of 26.

Response: *Text modified.*

Comment: Section 4.2: Please clarify conceptually what information will be used to delineate layers 2 and 3 and why, per Contract Exhibit B, Attachment 1, Section 3.1.4 page 5 of 26.

Response: *Section 4.2 now contains more descriptive text.*

Comment: Figures 4.2.2 and 4.2.4 do not appear to reflect control points, please include control points. Missing figure for base of layer 2 and/or top of layer 3. Text states this will be determined during model development. This information needs to be included in the report, as well as, rationale and control points. Also base of model does not appear to coincide with cross-sections. For example A to A' indicates the Precambrian basement rocks elevations are greater than -10,000 msl however figure 4.2.4 lowest elevation is -8719. Please clarify and correct as needed.

Response: *Layer thickness for this model was derived using digitized structural contours; therefore no control points are necessary. Layer 2 and 3 rationale included in Section 4.2. New figures included. The base of Layer 3 is consistent with the base of the Cretaceous formations in cross-section A-A', which are above 10000 feet msl.*

Comment: Figures 4.2.1 and 4.2.4 missing control points. Section 4.2 missing thickness maps for layer 2 and 3. Text and figure 2.5.1 indicate Precambrian at surface in the Carrizo Mountains. Figure 4.2.3 shows thickness at zero around the Eagle Mountains between Red Light and Eagle Flat, please redo.

Response: *Layer thickness for this model was derived using digitized structural contours; therefore no control points are necessary. Thickness maps for 2 and 3 have been added. Thickness of underlying Paleozoic and Cretaceous rocks north of Eagle Mts. does thin significantly, which is consistent with cross-section B-B'. The thickness of Layers 2 and 3 have been increased in that area to account for the presence of underlying Precambrian basement rocks which are a part of the aquifer system in that area.*

Comment: Section 4.3, page 4-21, 1st paragraph, 1st sentence: Please re-write introduction sentence, it appears the sentence structure is convoluted.

Response: *Corrected as requested.*

Comment: Pg 4-25, Para 2, line 3. What does "This surface is consistent with Darling (1997)" mean?

Response: *Text has been corrected to read, "This potentiometric surface is consistent with interpretation made by Darling (1997)."*

Comment: Pg 4-25, Para 2, line 5. The figure does not show 800-900' bgl anywhere in Eagle Flat as defined by the outline shown in the figure. The deepest within the extent of Eagle Flat in the figure is 600-800'.

Response: *Text has been corrected to reflect figure.*

Comment: Pg 4-25, Para 3, line 5. Groups 1 and 2 are not shown in the figure, the text here is not possible to verify with the figure.

Response: *Here, groups 1 and 2 refer to groups denoted in Figure 4.3.3.*

Comment: Figure 4.3.5, suggest labeling the groundwater divides and/or color coding each divide described on page 4-26 as it is difficult to correlate groundwater divides in the figure to the description in the text without landmarks labeled on the figure.

Response: *Figure has been updated with labels as requested.*

Comment: Section 4.3.4.2, page 4-29, 1st paragraph, 2nd sentence: please clarify sentence that begins, "The each system, the depth to the potentiometric surface..."

Response: *Text has been clarified.*

Comment: Please include map showing the location of the wells for the hydrographs in figure 4.3.2 per Contract Exhibit B, Attachment 1, Section 4.4.2 page 21 of 26 (figures for section 4.3).

Response: *Figure has been updated with map of well locations.*

Comment: Pg 4-28: Text is very difficult to follow because--as mentioned numerous times in this review--features, divide names, and flow system names are not included on any of the figures. There is nothing for the reader to reference to help get oriented.

Response: *Figure has been updated with landmarks referenced.*

Comment: Pg 4-28, para 3, line 1. The potentiometric surface map does not indicate that groundwater in the Allamoore system flows east toward Lobo Valley because neither the Allamoore Flow System nor Lobo Valley is shown on the figure. This is becoming a common issue with this report, I suggest reviewing ALL figures with their associated discussion in the text to be sure that landmarks, system/divide names, etc. discussed in the text are included in the figure.

Response: *Figure has been updated with landmarks referenced.*

Comment: Pg 4-32. Please label the groundwater divide names as they are referred to later on. Also the groundwater flow system names would be helpful, if necessary perhaps on a separate figure. As before, label other landmarks discussed in text, like Eagle Mountains and other mtns. and hills. Placement of groundwater divides are not supported by data included in this figure. The first one is the long one at the top, with no data included for it at all. What relevance does including this have on your figure? Why is no data included in this area if it is to be included in model? The second if the one to the left below the long one, and the contours do not justify all of this divide. The third and fourth look OK.

Response: *Figure has been updated with labels landmarks referenced. The text indicates that the groundwater divides are those estimated by Darling (1997).*

Comment: Pg 4-33. Why does one of the flowlines go right past a closed 3800-foot contour? Should there also not be a D next to this depression?

Response: *The closed contour is based on one data point, but the flowlines are "generalized" groundwater flow directions, which adhere to the regional flow gradients in Eagle Flat. A "D" was not used in that depression because it was based on only one data point over a very large area.*

Comment: Why are all figures zoomed out beyond the model extent? There is plenty of empty space in figures like 4.3.5 and 4.3.6 to include a legend, scale, and north arrow even if the model extent was the full extent of the figure. Each figure doesn't require a location reference in the upper left corner.

Response: *Suggestion noted.*

Comment: Table 4.2, page 4-35: Please clarify comments that suggest radioactive isotopes approach over estimates recharge or "under" estimates since values are lower than other approaches. Section 4.4.3, page 4-38 references 14 weather stations and figure 2.3.2 which only shows 5 stations, please update report with location of the 14 stations or reference Table B.2 on page B-11, Appendix B.

Response: *Table 4.2 has been corrected. Text on page 4-38 has been corrected and re-referenced.*

Comment: Pg 4-34, Para 1, line 7. Why is depth to water listed as a cause of little to no recharge in the Bolson?

Response: *Text has been corrected.*

Comment: Pg 4-34, Para 4. As above, much of this is difficult for someone without inherent knowledge of the area to understand. Many references are made to locations and faults and fault zones without benefit of a figure to reference one's self.

Response: *Figure 4.1.8, which includes features referenced in this paragraph, has been referenced.*

Comment: Please clarify, figure 4.4.2 does not appear related to Table 4.4 or text which states total recharge is estimated at 4,905 acft/yr while figure 4.4.2 sums to 5,204 acft/yr.

Response: *Figure 4.4.2 has the correct recharge values, except “238” to Green River Valley should be “248.” Table 4.4 is erroneous – the entire table has been updated to match Table B.6 in Recharge Appendix.*

Comment: Section 4.5: Per Contract Exhibit B, Attachment 1, Section 3.1.7 page 6 of 26, please address any specific or general information on streambed conductance for Rio Grande.

Response: *Text added.*

Comment: Section 4.5: Per Contract Exhibit B, Attachment 1, Section 3.1.7 page 6 of 26, please address information needed for the MODFLOW streamflow-routing package (Prudic and others, 2004), that is, streambed top and bottom, channel width and slope, and Manning's roughness coefficient for Rio Grande.

Response: *Text added.*

Comment: Section 4.5: Per Contract Exhibit B, Attachment 1, Section 4.4.2 page 21 of 26, please include representative stream-flow hydrographs for the major streams in the study area with a map indicating gage locations on Rio Grande.

Response: *Text has been updated to reference Figure 2.2.3, which shows stream gage locations along the Rio Grande.*

Comment: Page 4-48, para 1-3. There are so few data that it would seem appropriate to just include everything in a table. As it is I have to comment that three wells were noted in this paragraph and not shown anywhere on a map or in a table to help understand where they are located. Please comment how these values compare with other bolsons not in this study area, and how comparable they should be. Because there is a distinct lack of data, you will have to make some assumptions on T or K values, so present some analogies that you may use to base assumptions on. Are values from the other West Texas Bolsons useful? If so, what are the values?

Response: *Table 4.6 has been added. Labels have been added to reference wells in the text. Values for other bolsons useful ?*

Comment: Figure 4.6.1 is missing a caption, please update.

Response: *Caption lost to next page due to formatting. Formatting has been corrected.*

Comment: Section 4.6 missing specific/general information on vertical hydraulic conductivity for each layer compiled and/or calculated & related to known geologic & hydrogeologic conditions per Contract Exhibit B, Attachment 1, Section 3.1.8 page 7 of 26. Suggest adding text stating insufficient information.

Response: *Text added.*

Comment: Section 4.6 missing vertical hydraulic conductivity & storativity distributed according to geologic information per Contract Exhibit B, Attachment 1, Section 3.1.8 page 7 of 26. Suggest adding text stating insufficient information.

Response: *Text added.*

Comment: Section 4.6 missing Horizontal anisotropy defined, discussed, and estimated per Contract Exhibit B, Attachment 1, Section 3.1.8 page 7 of 26. Suggest adding text stating insufficient information.

Response: *Text added.*

Comment: Pg 4-51. Section 4.7: please note that the trend of irrigation in Hudspeth County from 1980 to 1984 was because the irrigation survey showed surface water/groundwater mixed use in Red Light and Green River Valley in 1974 and 1979; however the following survey in 1984 indicated farming had stopped in the study area. It is unknown what year farming ceased between 1979 and 1984. Anomalies like this should always be discussed as to whether they are real, as these types of numbers will always be questioned.

Response: *Text added.*

Comment: Pg 4-51, para 1, line 1. The opening sentence is unrelated to the rest of the discussion. What was it prior to 1980? There must be something to discuss if this statement is included. In general this paragraph is hard to follow, it is a series of generic statements strung together. And why is this the first thing discussed in this section? It seems that paragraph 2 should be first.

Response: *Text modified.*

Comment: Section 4.7 missing identification, discussion, and if possible, quantified cross-formational flow, baseflow to streams, and discharge to springs per Contract Exhibit B, Attachment 1, Section 3.1.9 page 7 of 26. Suggest adding text stating insufficient information.

Response: *Text added.*

Comment: Section 4.7 may need to include additional information of estimates of early aquifer use of irrigation in Hudspeth County.

Response: *No change.*

Comment: Section 4.7: need to discuss what information, if any, exists for pumpage that may have occurred in the Red Light portion of the model in Mexico. Per Contract Exhibit B, Attachment 1, Section 3.1.9 page 7 of 26: for model areas outside Texas, the contractor is expected to compile and use pumping estimates from outside sources, as appropriate.

Response: *Text added.*

Comment: Per Contract Exhibit B, Attachment 1, Section 3.1.9 page 7 of 26: tables of the historical pumping data according to major user group and summed over each county shall be included in the report.

Response: *Table included.*

Comment: Section 5.1, page 5-1, paragraph 3: states figure 5.1.1 shows two different depictions of the conceptual model. Please update text or figure 5.1.1 so they agree.

Response: *Text modified.*

Comment: Pg 5-2, para 1, line 8. The text says that some of the recharge moves laterally and discharges as underground flow to the bolsons, although the figure does not include arrows between the bolsons and the adjacent green layer to the side. These conceptual models always seem vastly over-simplified and/or generalized. For example, an important part of the conceptual model in this aquifer is the movement of groundwater in portions of the bolson to the middle and then downward to underlying units, yet this is undiscussed here.

Response: *Text modified.*

Comment: Figure 5.1.1: Suggest adding a symbol for recharge entering the system through the groundwater-surface water interaction (combine recharge symbol with gw-sw symbol). Also this is the first indication that basement rock will be included in the model as opposed to forming the lower boundary. Please clarify. There is a recharge arrow for the bolson formation, please explain.

Response: *Text modified.*

Comment: Pg 4-60. Why are the color designations in this figure different from what is discussed in the text? TWDB breakdowns are 1000, 3000, and 10000 as stated on page 4-58, but in this figure the brackish breakdowns are 5000 and 10000. Consider using the same color scheme from the brackish water report (i.e. slightly saline = yellow, moderately saline = orange).

Response: *Figure has been corrected as requested.*

Comment: Appendix B, Section 1.0, page B-7, 1st paragraph: references figure 2.3.1 for relationship of precipitation and elevation. Figure 2.3.1 just shows precipitation. Suggest adding figure with weather stations and elevation. Same paragraph also references figure 2.3.3 which shows evaporation not 14 weather stations. Suggest adding figure showing 14 weather stations or reference Table B.2. Table B.1, CN, CN dry conditions and Dry conditions inches all repeat the same values, suggest eliminating these fields and just note the results in the Table caption or footer. Figure B.2 missing.

Response: *Figure 2.3.1 has been modified and referenced for locations of 14 weather stations. Table B.1 correct, no changes made. Figure B.2 has been added to the report.*

1.2 Conceptual Model Source Data Comments

Comment: The spatial extents of many of the feature classes in the source geodatabase do not match the spatial extent of the figures in the draft report. Please revise either the source geodatabase or the appropriate figures so that the two match.

Response: *Corrected as requested.*

Comment: The boundaries of the City of Sierra Blanca in the submitted source geodatabase do not match the city boundaries that appear in many of the figures. Please revise for consistency.

Response: *Corrected as requested.*

Comment: Please add the feature class of *West Texas Bolson Aquifer within the study area* to the source geodatabase to correspond to the labeled bolsons in Figure 2.1.2.

Response: *Corrected as requested.*

Comment: Please add the weather stations in Figure 2.3.2 to the source geodatabase.

Response: *Corrected as requested.*

Comment: The spatial extent of *veg_cover* feature class differs from Figure 2.4.1, please revise.

Response: *Spatial extent corrected as requested.*

Comment: Please add the names of the different bolsons in Figure 2.4.2 to the attributes of the West Texas Bolsons Aquifer feature class included in the source geodatabase. Need to add land uses to the attributes of the *landuse* feature class.

Response: *Names of aquifers added. Land uses added to attributes table of Landuse feature class.*

Comment: Please fill in the attribute table for the feature class *geomap*.

Response: *Corrected as requested.*

Comment: Please add the location of the model by Daring, Hibbs, and Dutton (1994) that appears in Figure 3.2.1 to the source geodatabase.

Response: *Corrected as requested.*

Comment: Please add the fault type data that appears in Figure 4.1.8 to the attributes of the *faults* feature class.

Response: *Corrected as requested.*

Comment: The wells in feature class *Wells_TWDB_AnnWL* are not the same as the wells in Figure 4.3.4. Please revise.

Response: *Wells in Figure 4.3.4 correspond to feature class *Wells_WLdata*.*

Comment: Please add the *Blanco Bolson* feature class that appears in Figure 4.4.1 to the source geodatabase.

Response: *Corrected as requested.*

2.0 RESPONSE TO DRAFT FINAL COMMENTS

2.1 Draft Final Report Comments

Comment: Page 2-5, Figure 2.1.2: Please shade other bolsons consistent with figure legend (light tan color) instead of the same shade as the study area bolsons.

Response: *Figure updated to match legend.*

Comment: Page 2-15, Section 2.3: Please add a map of climate classification(s) for the study area per contract Exhibit B, Attachment 1, Section 4.4.2 page. 20 of 26. Though the text states that the area is semi-arid to arid, it is not clear spatially where these two climate areas exist.

Response: *Figure added (Figure 2.3.1)*

Comment: Page 2-16, Paragraph 4: Please add discussion on the spatial and temporal variability of evapotranspiration. At a minimum, if evapotranspiration information is not available, please support why it is not available. Contract Exhibit B, Attachment 1, Section 3.1 states that “Each element of the conceptual model shall be thoroughly described, documented, and referenced in the final report.” Evapotranspiration is an important part of the physiography and climate section of the conceptual model.

Response: *Text added.*

Comment: Page 2-18, Figure 2.3.1: Please clarify in the text and the figure which years were used to calculate the mean annual precipitation. Per contract Exhibit B, Attachment 3, Section 2.2.2, graphics need to include support material for the reader to understand what is shown.

Response: *Text and figure updated with data time period (1971-2000).*

Comment: Page 2-21, Figure 2.3.4: Please redo this map for the average annual temperature from 1971 to 2000 (and state this on the figure) and separate into 1 degree intervals or a continuous color scale as is it is impossible to interpret the contrast between temperatures per contract Exhibit B, Attachment 1, Section 4.4.2.

Response: *Figure has been revised to show*

Comment: Page 2-25, Section 2.5: The text references Dietrich and others, 1987, but the References section only contains Dietrich and others, 1983. Please correct as needed per contract Exhibit B, Attachment 3, Section 4.2.

Response: *Text corrected to reference Dietrich and others, 1983*

Comment: Page 2-30, 3rd paragraph: Maps of structure and cross-sections are referenced to section 4.0, but these figures are in this section (2.5). Please update the text to reflect this.

Response: *Text corrected to reflect new figure placement in Section 2.5*

Comment: Page 2-32, Figure 2.5.1: Please label surface geologic features in the figure or simplify the figure somehow to make it readable per contract Exhibit B, Attachment 3, Section 2.2.2. Comparing colors and patterns is impossible when dealing with 50 categories.

Response: *Figure 2.5.1 has been simplified for ease of viewing and a geology appendix added (Appendix A) showing the more complex nature of geology in the area.*

Comment: Page 3-2, Section 3.2: Please expand on how the new model compares to previous modeling efforts in extent and applicability per contract Exhibit B, Attachment 1, Sections. 3.1 and 4.4.1. As is, the need for a new model is not conveyed. For instance, cross-sectional models are 2-dimensional and not useful for estimating groundwater availability.

Response: *Text added.*

Comment: Page 4-5, Section 4.0: Please start page numbers with 4-1 and adjust Table of Contents appropriately.

Response: *Page numbers corrected.*

Comment: Page 4-5, Section 4.1: Please significantly expand discussion to justify why and how the model was divided up into three layers per contract Exhibit B, attachment 1, Section 3.1.3, page. 5 of 26. Stating what was done without explaining the rationale is insufficient.

Response: *Text added and re-organized (also per the next comment).*

Comment: Page 4-5, Section 4.1: Please move the geology information in this section to section 2.5 and focus this section (4-1) on the hydrostratigraphy per contract Exhibit B, attachment 1, Sections. 3.1.2 and 4.4.1.

Response: *Text reflects geology in Section 2.5 and important hydrostratigraphic information for each aquifer basin in Section 4.1. Text was added in Section 2.5 to accompany figure 2.5.9, but no other changes were made.*

Comment: Page 4-5, Section 4.1: Please add a schematic of the hydrostratigraphic units per contract Exhibit B, Attachment 1, Section 4.4.2.

Response: *A schematic added.*

Comment: Page 4-9, Section 4.2, paragraph 1: Please update the introduction to this section to reflect the contents of the structure section as described in the contract Exhibit B, Attachment 1, Section 3.1.4 as opposed to the layering of the model.

Response: *Text revised.*

Comment: Page 4-9, 5th paragraph, 1st line: Please change to “Section 2.5 discusses the”

Response: *Text corrected.*

Comment: Page 4-11, paragraph 3: Please expand the justification for how the model was divided into the 3 layers and move to Section 4.1 per contract Exhibit B, Attachment 1, Sections 3.1.3 and 4.4.1.

Response: *Text added and re-organized.*

Comment: Page 4-11, paragraph 2: Refers to Table 4.1, which addresses recharge. Please update to reference table or figure on structure.

Response: *Text updated to reference Table 2.1.*

Comment: Page 4-17, Section 4.2, Figure 4.2.5: The caption on this figure and the legend do not match up. Please update this figure to reflect the thickness of layer 3, not layer 2 per contract Exhibit B, Attachment 1, Section 4.4.2.

Response: *Figures 4.2.2 through 4.2.6 modified and/or deleted in order to be consistent with report specifications. All captions and figure labels have been updated to reflect this change.*

Comment: Page 4-24, Figure 4.3.4: Please add a legend and labeled contour lines.

Response: *Figure corrected.*

Comment: Page 4-25, Figure 4.3.4: Please add a legend to this figure per contract Exhibit B, Attachment 3, Section 2.2.2.

Response: *Figure corrected.*

Comment: Page 4-30, Figure 4.3.5: Please add a legend to this figure per contract Exhibit B, Attachment 3, Section 2.2.2.

Response: *Figure corrected.*

Comment: Page 4-32, last paragraph, 2nd line: Refers to Figure 4.1.1 which does not exist; please add the correct figure number.

Response: *Text updated to reference Figure 2.5.9.*

Comment: Page 4-32: Second type of bolson refers to the Sierra Blanca area as being in the Northeast Eagle Flat; please update appropriately.

Response: *Text updated to describe Sierra Blanca as being in the Northwest Eagle Flat.*

Comment: Page 4-33: Please replace “et al.” with “and others” here and wherever else it appears in the report.

Response: *Text updated.*

Comment: Section 4.4.2: cites Table 4.2, please update to Table 4.1.

Response: *Text corrected.*

Comment: Page 4-36, 1st paragraph, 4th line down: Please change Table A.2 to Table B.2.

Response: *Reference corrected.*

Comment: Page 4-37, paragraph 1: Refers to Table 4.4 as a summary instead of a comparison table; please revise text to reflect this.

Response: *Text corrected to refer to Table 4.4 as a comparison table.*

Comment: Page 4-40, 1st paragraph, 2nd line: Please refer to Table 4.4 (rather than 4.5).

Response: *Text corrected to reference correct table.*

Comment: Page 4-40, Table 4.4: Values for Modified Runoff method (row 3) do not agree with Table 4.3 (row 6). Please update table or explain in text what the difference is.

Response: *Tables 4.4 and B.11 have been updated and should be identical. Note that the “modified runoff redistribution (this study)” values are incorrect for all three sub-basins in Table 4.4, and for Green River Valley in Table B.11. “Previous work” should refer to Table 4.1 (not 4.4.1 as in Table B.11). “Previous work” range in values for Eagle Flat Draw should range from 430 to 4,119 (not 3,000 as in Table 4.4).*

Comment: Table 4.6 comes before Table 4.5: Please revise and fix misspellings, capitalization, and abbreviations

Response: *Table numbers switched to reflect proper order and content revised for grammar.*

Comment: Page 4-41, 1st paragraph: Says in general recharge estimates for regional modeling studies using redistribution have resulted in recharge values slightly greater than those obtained from final model calibration. Then three examples are given, for the estimate is greater than the model, but for the second and third the estimates are less than the model. This contradicts the beginning general statement. Please clarify.

Response: *Text modified for consistency.*

Comment: Page 4-42, paragraph 5: Figure 4.5.2 shows Mesquite Spring in the same category as Indian Hot Springs, contradicting the first statement in the paragraph, please revise text or figure for consistency.

Response: *Text revised for clarity.*

Comment: Page 4-45, Section 4.6.1, paragraph 1, line 6: Please change “Darling, et al (1994)” to “Darling and others (1994)” per contract Exhibit B, Attachment 3, Section 4.1. Please also update this on page 4-46, paragraph 4, line 2.

Response: *Text revised.*

Comment: Page 4-49, Figure 4.7.4: Please clarify if the values show in Figure 4.7.4 county totals or for just the study area.

Response: *Caption revised for clarity to indicate values are for study area.*

Comment: Page 4-50, last paragraph: Was there information available in the CNA database for Mexico irrigation south of Red Light Draw? If so, please update the text accordingly.

Response: *Text was added to reflect Comisión Nacional del Agua - CONAGUA database search for Mexico pumping and results of that search. (Appendix C shows results of search).*

Comment: Page 4-54, Table 4.5: Please include county totals in the table.

Response: *Table updated with county totals by year.*

Comment: Page 4-56, 1st paragraph, 5th line: “Several other parameters maybe be of interest ...including nitrate” However, nitrate data are not shown or discussed. Please include nitrate data or remove this line.

Response: *Table 4.7 and related text added that includes data on Nitrates and other constituents of concern.*

Comment: Page 5-1, Section 5.1, paragraph 2, lines 5 and 6: Please add quotes around the phrase “a pictorial representation of...or a cross section” since it is a direct quote from Anderson and Woessner (1992) per contract Exhibit B, Attachment 3, Section 4.0.

Response: *Text corrected.*

Comment: Section 6.3 to Section 6.0: Page numbers missing. Please update with appropriate pagination.

Response: *Pagination corrected.*

Comment: Section 6.3.1: This section seems to primarily be a description of how the hydraulic conductivity data was limited and not applicable. However, a value must have been assigned to the model prior to calibration. Please explain and justify what was assigned and the range of values that would be considered normal for this system (i.e. the range within which calibration can occur) per contract Exhibit B, Attachment 1, Section 3.2.1.

Response: *Text added for justification.*

Comment: Section 6.3.2, paragraph 2, line 3: Please add reference and/or justification for assigning a specific yield of 0.01 for “rocks” in layers 2 and 3 per contract Exhibit B, Attachment 1, Section 3.1.8. Also, suggest replacing the term “rocks” with a more specific description of what is being referenced.

Response: *Text modified as suggested.*

Comment: Section 6.4 1st paragraph, line seven: “In MODFLOW, a stress period is a period of time over which is assumed ...” is an incomplete sentence. Please re-phrase.

Response: *Text corrected.*

Comment: Section 6.4.4, 2nd paragraph: Please state in text what the basis for using 10 inches per year for the potential evapotranspiration rate.

Response: *Text added for justification.*

Comment: Section 6.4.4, paragraph 2: A single sentence is insufficient to adequately address how evapotranspiration was applied to the model. Please expand to document the sources of the evapotranspiration information and justify how it was applied to the model per contract Exhibit B, Attachment 1, Section 3.1, paragraph 2.

Response: *Text added.*

Comment: Section 7.1.2: Please add a paragraph to discuss that the model mass balance (inflows – outflows) shall be less than 1 percent and ideally less than 0.1 percent per contract Exhibit B, Attachment 1, Section 3.3, paragraph 1.

Response: *Text added.*

Comment: End of Section 7.1.2: You are incorrectly stating that the RMS error is the standard deviation (SD) of errors. SD measures deviation (root-mean-square deviation) from the mean. This is not apparent in any of the formulas. Please revise.

Response: *Text modified as suggested.*

Comment: Section 7.2: Please expand this discussion of sensitivity analyses to be more specific. Describe what factors were used and how they were applied.

Response: *Text modified. However, we still keep it as general discussion in this chapter and more specific information is given in chapters where analyses are done.*

Comment: Page 8-10, Section 8.1.6, paragraph 4, line 3: Please expand the justification for why you believe the dry zones are actually dry as opposed to an artifact of model instability. Per contract Exhibit B, Attachment 1, Section 3.3, paragraph 4, the performance of the model and strategies used to improve fit must be thoroughly documented. Saying that the simulated water table is smooth is not a clear justification.

Response: *Text revised to provide justification.*

Comment: Page 8-14, Figure 8.1.9: Please display dry cells on the figure and add the appropriate symbol to the figure.

Response: *Figure updated with dry cells.*

Comment: Page 8-21, Section 8.2: Suggest creating a plot similar to figure 8.2.1 showing the sensitivity in each layer instead of just layer 1 and all layers averaged together.

Response: *Figures added for each layer as suggested.*

Comment: Page 8-21, Section 8.2: Please add the value of the General Head Boundary (GHB) simulating the connection between Salt Basin Bolson and Eagle Flat Bolson to the sensitivity analysis per contract Exhibit B, Attachment 1, Section 3.4.

Response: *Modified as suggested.*

Comment: Page 9-1, Section 9.0, paragraph 3: Please provide a more complete presentation of the transient model developed to test its ability to make transient simulations reasonably. This should include: how pumping was applied spatially, maps of water levels at 0, 15, and 30 years, and a discussion of the results that explains to the reader *why* the results were reasonable.

Response: *Text and figures added. Since this is a test simulation run, we still keep it as minimal.*

Comment: Page B-8: The removal of the Candelaria and El Paso 32 ENE weather stations from the analysis (in order to improve r^2) appears arbitrary. There are five weather stations that are further away from the study area than the Candelaria weather station. The Fabens weather station (which was included in the analysis) is 36 miles away from the study area while El Paso 32 ENE is at 38 miles. Please re-justify removal or re-evaluate analysis.

Response: *Text updated for clarity and/or justification.*

Comment: Table B.11 refers to Table 4.4.1 which doesn't exist; please revise.

Response: *Table revised to reference Table 4.1*

Comment: Figure pages in Appendix B are not numbered and the List of Figures does not contain page number references.

Response: *Revised to include page numbers on figure pages and in List of Figures.*

Comment: Salt Flat CAA weather station is claimed to be removed from the analysis (section 2.2), yet figures show that it is included (see Figures B.8 and B.9); please revise.

Response: *Text revised for clarity and/or justification.*

2.2 Appendix E: Response to comments from the conceptual model report.

(The following comments have not been completely addressed in the draft final report). Please address the following comments in the final report:

Comment: *Introduction: Please clarify what new field data was collected and analyzed to assess hydraulic properties and current water levels as noted on page 1-1. Also please remove or explain predictive simulations referenced on page 1-2 as this is outside the scope of work.*

Response: *Text revised.*

Comment: *Section 2.3: Please update report with a map of climate classification for the study per Contract Exhibit B, Attachment 1, Section 4.4.2 page 20 of 26 and reference in text.*

Response: *Climate classification map has been added (Figure 2.3.1).*

Comment: *Figure 2.3.1: Please clarify and document the years used to calculate the mean annual precipitation.*

The response is provided in the “response to comments”; however, please also add it to the figure caption.

Response: *Figure caption has been updated with data time period.*

Comment: *Figure 2.3.2: Suggest using same x-axis scale and using a larger font on graphs.*

Response: *Figure number 2.3.3 now and x-axis scales and font size have been revised.*

Comment: *Section 2.5, Geology, page 2-1, 2nd paragraph and page 2-2, 3rd paragraph: References Dietrich and others, 1987; however, references only list Dietrich and others 1968, please clarify and correct as needed. 2nd paragraph-Line 1: Landmarks referenced in text not included on figure. Also, the complexity of the figure makes it almost impossible to easily see what the text is referring to. Can a simpler version of surface geology be made as a supplement to Figure 2.5.1?*

There is also another reference to Dietrich and others, 1983, on page 2-27 and Dietrich and others, 1968 on page 2-29. Please clarify all of these and verify that they are in the references.

Response: *All such references have been corrected.*

Comment: *Geology section (2.5) is missing several geologic cross-sections through the study area per Contract Exhibit B, Attachment 1, Section 4.4.2 page 21 of 26. Please add or cross-reference to figures located elsewhere in the report.*

Response referred to Section 4 of the report addressing this comment. Did you mean Figures 2.5.2 through 2.5.8?

Response: *Cross-sections were originally placed in Section 4, but were moved to Section 2.5 for the Draft Final report. These have been re-referenced in Section 4 as well.*

Comment: *Page 4-4, paragraph 3, line 4: It says Tertiary intrusive rocks are exposed along the axis of GRV, but nothing like this is shown in the F-F' cross-section, which appears to be along the axis of GRV. And as noted above, Figure 2.5.1 is not usable to see if Tertiary volcanics are shown in that figure, the patterns are not discernable in that figure.*

Response: *Text was corrected in the Draft Final report to clarify that Tertiary volcanics lie directly north of the Green River Valley and not within, therefore the exclusion of these formations in F-F' is legitimate.*

Comment: *Page 4-25, Paragraph 2, line 5: The figure does not show 800-900' bgl anywhere in Eagle Flat as defined by the outline shown in the figure. The deepest within the extent of Eagle Flat in the figure is 600-800'.*

The figure has no legend or contours, so it is difficult to verify the text against the figure. Please add contours and legend to the figure and verify that text is consistent.

Response: *Text and figure corrected as requested.*

Comment: *Why does one of the flowlines go right past a closed 3800-foot contour? Should there also not be a D next to this depression?*

The response states that contour is based on one data point. Suggest removing that closed contour, to reduce confusion.

Response: *Contour was an artifact of gridding methodology; it was removed to eliminate confusion.*

Comment: *Page 4-34, Paragraph 4: As above, much of this is difficult for someone without inherent knowledge of the area to understand. Many references are made to locations and faults and fault zones without benefit of a figure to reference one's self.*

Response states that Figure 4.1.8 has been added with the features, but there is no Figure 4.1.8 in the report. Please add Figure 4.1.8 with the features.

Response: *Response is supposed to read Figure 4.1.1. The figure number is correct in the report text.*

Comment: Section 4.7: Please discuss what information, if any, exists for pumpage that may have occurred in the Red Light portion of the model in Mexico. Per Contract Exhibit B, Attachment 1, Section 3.1.9 page 7 of 26: for model areas outside Texas, the contractor is expected to compile and use pumping estimates from outside sources, as appropriate.

Please discuss what information, if any, is available from the Comisión Nacional del Agua - CONAGUA online pumping permit database:
http://portaltransparencia.gob.mx/pot/concesion/begin.do?method=begin&_idDependencia=16101

Response: *Text was added to reflect Comisión Nacional del Agua - CONAGUA database search for Mexico pumping and results of that search. (Appendix C shows results of search).*

2.3 Model Comments

Comment: From the contract, Exhibit B, Attachment 1, Section 4.3, MODFLOW input files: future users shall be able to run the model using MODFLOW 2000 from the DOS prompt with the files provided. The submitted MODFLOW files do not converge outside of Groundwater Vistas. The mf2k.exe executable does not run successfully (the script stops at time step 1). Please either submit new MODFLOW solver inputs which allow the model to converge using USGS standard MODFLOW2000 or please provide a MODFLOW2000 executable that can be run from the command line, and that we have permission to distribute, that will allow these model files to converge.

Response: *Problem corrected by implementing GMG solver.*

Comment: Appendix A: Countywide Water Budgets: Please check the budget terms especially the top and bottom fluxes in Hudspeth County. They are much greater than any of the other budget terms in the table and they do not agree with the results that we see from the model. We get 527 and 3,101 acre-feet per year in and out respectively of the top of layer 2 in Hudspeth County, rather than 37,819 and 50,871 listed in Appendix A.

Response: *Text corrected.*

Comment: We also recommend listing the mass balance for the Mexico portion of the model as well so that the total of all zones can be checked against the model-wide budget.

Response: *Added the mass balance for the Mexico portion of the model as suggested.*

Comment: Please also perform and document in the report an analysis of sensitivity to storage properties (based on the test transient scenario), since this model will be used to run predictive scenarios.

Response: *Added sensitivity to storage properties and to pumping as suggested.*

Comment: Please add a readme.txt file to the folder containing the model files with instructions specific instructions on running the model and any other important information necessary to use the model properly.

Response: *A readme file is added.*

2.4 Geodatabase Comments

Comment: Contract specifies in Attachment 2, Section 1.2 Data Documentation, Metadata shall be created using Federal geographic Data Committee (FGDC) metadata editor within ESRI's ArcCatalog. The TWDB-provided schemas include some basic metadata, which shall be extended by the contractor to completely document all source and derived data.

The metadata for all feature classes provided is incomplete and at the very minimum, should include: the spatial projection name, parameters, datum, and altitude system definition if appropriate; the purpose and a description of the data set; the source(s) of the data set; and definitions and/or units of measurement for each of the attributes.

Response: *Metadata has been completed for all features, tables, and datasets used in the source geodatabase.*

Comment: Contract specifies in Attachment 2, Section 1.1 Data Content and Organization, part 1.11 Source and derivative geodatabase schema: Depending on the aquifer and methodologies used, we recognize that source and derivative data will be different for each project. Therefore, TWDB staff will review final contracts to identify the appropriate source and derivative data needed for the source geodatabase to reproduce the critical model input.

The geology feature datasets provide contoured data digitized from scanned unpublished maps. Please provide the scanned map(s) source data for each of these contoured data sets.

The geology feature datasets provide location of cross-sections but actual cross-section data was not found in geodatabase. Please provide vector and/or scanned raster data for these cross-sections.

Response: *All scanned maps (including cross-sections and structural contour maps) have been added to the geology dataset and described individually in the metadata accompanying.*

Comment: Contract specifies in Attachment 2, Section 1.1 Data Content and Organization, part 1.12 Pumpage geodatabase schema: Pumpage shall be processed and distributed spatially within the GAM pumpage geodatabase.

No Pumpage geodatabase found. Please provide Pumpage geodatabase.

Response: *Pumpage geodatabase has been provided for steady state model. Since no pumping was used for the model, pumpage geodatabase may be incomplete (no transient pumping). (See comments in Appendix C)*

Comment: Contract specifies in Attachment 2, Section 1.1 Data Content and Organization, part 1.14 Model grid feature dataset: A unique, Cell_ID or relationship/index key consisting of a seven-digit integer based on layer, row, and column shall be used to link the polygon and point feature classes with any parameter values and time-series variables.

The model grid polygon and point files are not attributed with Cell_ID as specified above.

Response: *Cell_ID fields have been added to all relevant features and tables.*

Comment: A request was made during the conceptual model comments phase that a feature class be added for *West Texas Bolson Aquifer within the study area*. If not included, please add. If it is included, please group under boundaries.

Response: *Feature class has been added to illustrate only the bolsons in the model.*

Comment: Though fault type data is included in the attributes of the *faults* feature class, not all fault types in the legend are included in the attributes. If these fault types are not present in the study area, please add a note to the figure clarifying this. If these fault types are present, please update the attribute table.

Response: *Legend has been simplified to only include those fault types that exist in the study area.*

Comment: Comment #2 from the Conceptual geodatabase review: The following figures are still inconsistent with 'TexasCities' layer: 2.1.2, 2.1.3, 2.1.4, 2.1.5, 2.2.2, 2.5.2, 4.7.1, and 4.7.5.

Response: *All above figures corrected to include the cities of Sierra Blanca and Allamore.*

Comment: Comment #4 from the Conceptual geodatabase review: Please include the data associated with the weather stations that was used to create the graphs.

Response: *Table PRECIP_data includes precipitation data used to create graphs in Figure 2.3.2.*

Comment: Please update CONT_Precip' feature class metadata with units of measurement.

Response: *Units of measurement are now included in the attributes description of metadata.*

Comment: Figure 2.2.3 is inconsistent with 'StreamGage' and 'Springs' feature classes (please revise the figure, including the legend).

Response: *Figure revised for clarity of point locations as to which are gauging stations or springs.*

Comment: Figure 2.3.3: Please update figure with aquifer layers and please include the quad numbers (from the figure) in the attribute table.

Response: *Figure has been updated with aquifer layers and quad numbers.*

Comment: Table 2.2.1: Please fix the numbering and the text where the table is mentioned and please fix abbreviations.

Response: *Table number has been changed to Table 2.1 and abbreviations corrected.*

Comment: Figure 2.5.9: Numerous types of faults in this figure cannot be found in the 'Faults' feature class, please revise; also please adjust formatting so caption and figure are on the same page.

Response: *Legend has been simplified to only include those fault types that exist in the study area.*

Comment: Figure 4.2.4: The 'base_lay2' raster dataset shows a maximum elevation of 3500 feet while the contours show a maximum of above 4000 feet; please clarify.

Response: *Figure (now 6.2.2) has been revised to eliminate confusion and 4000' contour deleted.*

Comment: Figure 4.3.4: Please include legend to show class breaks.

Response: *Legend has been added to the figure.*

Comment: Figure 4.3.5: Please include a legend and please include in the geodatabase the contours feature class used in this figure.

Response: *Legend has been added to the figure and contours feature class added to geodatabase.*

Comment: Figure 4.3.6: Please include in the geodatabase the flow direction feature class.

Response: *Flow direction was digitized and added to geodatabase.*

Comment: Figure 4.7.4 suggestion: It would help readers to have identical scales for the Culberson, Presidio, and Jeff Davis county graphs.

Response: *Y-axis scales have been revised for Culberson and Jeff Davis Counties to extend to 300 af/yr but no change was made to the y-axis for Hudspeth County in order to retain all data in the chart.*

Comment: Figure 4.8.1: Legend and figure symbology do not match (aquifer); please revise so they match.

Response: *Legend has been rearranged for clarity of map symbolism. No change has been made to the rest of the map.*

Comment: Figure 8.1.6: ET is not categorical data according to the attribute table; please revise the figure and the legend (in its current state, the figure doesn't match the data).

Response: *Figure has been updated and legend revised to quantitatively describe ET data.*

Comment: Figure 8.1.10: Aquifer symbology in the legend does not match aquifer symbology in the map, please revise for consistency.

Response: *Aquifer symbol has been revised for clarity.*

Comment: Figures 8.1.11- to 8.1.12: Please fix the figure borders.

Response: *Report figures corrected.*

Comment: Figure B.2: Aquifer symbology in the legend doesn't match aquifer symbology in the map, please revise for consistency.

Response: *Figure legend revised for clarity.*

Comment: Because control points were not included, please include the original scanned and geo-referenced hand-drawn contour maps in the geodatabase.

Response: *All maps used for digitizing contours have been added to the geodatabase Geology dataset.*

Comment: Metadata needs to be edited with a proper editor such as the ArcCatalog built-in metadata editor. Please include brief descriptions/definitions (with measurement units where applicable) for each attribute of a feature class under the ‘Attributes’ tab of metadata. Many feature classes/raster catalogs/tables lack this kind of information. Raster catalogs metadata needs to include a brief description of each raster by specifying the name of the raster and what it represents. ‘SubSurfaceHydroWaterLevels’ raster catalog has such descriptions; you just need to add measurement units. Please use it as a guide for the other raster catalogs.

- ‘CONT_Base_lay2’ feature class has no metadata.
- ‘CONT_Thick_lay2’ feature class has no metadata.
- ‘CONT_Thick_lay3’ feature class has no metadata.
- ‘CONT_ss_Head_lay1_200’ feature class has no metadata.
- ‘CONT_ss_Head_lay1_50’ feature class has no metadata.
- ‘CONT_ss_Head_lay2_200’ feature class has no metadata.
- ‘CONT_ss_Head_lay3_200’ feature class has no metadata.
- ‘Model_SS_Heads_lay1_poly’ feature class has no metadata.
- ‘Model_SS_Heads_lay2_poly’ feature class has no metadata.
- ‘Model_SS_Heads_lay3_poly’ feature class has no metadata.
- ‘Model_SS_targets_residuals’ feature class has no metadata.
- ‘Saturation_extent’ feature class has no metadata.
- ‘WELLS_Quality_Bolsons’ feature class has no metadata.
- ‘WELLS_Quality_NonBolsons’ feature class has no metadata.
- ‘WELLS_WLdata’ feature class has no metadata.
- ‘MODEL_Data’ table has no metadata.

Response: *All feature dataset, feature, and table metadata has been updated using ArcCatalog’s metadata editor. This includes raster explanations and units of measurement included in the attributes description of metadata.*

2.5 Suggestions

Requests for discussion or clarification should be addressed within the text and figures, as appropriate.

Comment: List of Figures, page iv: Please remove extra spaces in caption for Figure 8.1.6.

Response: *Corrected as requested.*

Comment: List of Figures: Figure 2.5.1b does not appear in the list of figures, please update.

Response: *Corrected as requested, Figure 2.5.1b is now a continuation of Figure 2.5.1.*

Comment: List of Figures: Figure 2.5.9 is listed on the wrong page in the list of figures, please update.

Response: *Corrected as requested.*

Comment: List of Tables and page 2-30: Numbering of Table 2.2.1 is inconsistent with other tables, please update accordingly.

Response: *Corrected as requested Table is now 2.1..*

Comment: List of Tables: Table 4.6 is not listed in the List of Tables, please update. List of Tables and caption for Table 4.2: Please check spelling and update accordingly.

Response: *Corrected as requested.*

Comment: Executive Summary, 2nd paragraph, 3rd line: “bolsons” should not be capitalized. It is only capitalized when referring to a specific bolson.

Response: *Corrected as requested.*

Comment: Executive Summary, 2nd paragraph: Please add commas separating 1,000’s to numbers greater than 999.

Response: *Corrected as requested.*

Comment: Executive Summary, 3rd paragraph 3rd line from bottom: Please change “indicated” to “indicate”.

Response: *Corrected as requested.*

Comment: Section 1.0, page 1-2, 1st paragraph, 1st line: Please briefly describe MODFLOW when it is mentioned for the first time. For example, finite difference code developed by USGS, etc.

Response: *Corrected as requested.*

Comment: Page 2-9, 3rd paragraph, 4th line: Suggest changing text to “...Eagle Mountains to the west, and by Southeast Eagle Flat to the south...”

Response: *Corrected as requested.*

Comment: Page 2-10, paragraph 1, 2nd line: Suggest changing text to “..., and by the Indio Mountains and Green River Valley to..”

Response: *Text revised for clarity.*

Comment: Page 2-10, paragraph 2, 2nd line: Suggest changing to “Ridge to the northeast, ...”

Response: *Corrected as requested.*

Comment: Page 2-10, paragraph 3, 1st line: Suggest changing to “Green River Valley is bound to the northwest by the Indio Mountains ...”

Response: *Corrected as requested.*

Comment: Page 2-10, paragraph 3 3rd line: Suggest changing to “..Valley’s northern and southern boundaries respectively...”

Response: *Corrected as requested.*

Comment: Page 2-34, Table 2.2.1: Please renumber table 2.2.1 to be consistent with text on page 2-30 and numbering of other tables throughout the report.

Response: *Corrected as requested.*

Comment: Page 2-41, Section 2.5, Figure 2.5.8: Please update figure caption to reflect F-F’ instead of F-F.

Response: *Corrected as requested.*

Comment: Page 2-43: Please move title for Figure 2.5.9 “Structural Faulting” to page 2-42 over the correct figure.

Response: *Corrected as requested.*

Comment: Page 2-32, Figure 2.5.1: Please add a label for Bean Hills which is referenced in the text but not shown in the figure.

Response: *Location description in text sufficient without mention of Bean Hills, text deleted for clarity.*

Comment: Page 3-4, Section 3.2, Figure 3.2.1: Please clarify which model(s) are referenced in this figure and that the Darling and others (1994) model is a 2-dimensional cross-section model. This is an issue of clarity, not accuracy.

Response: *Clarified as requested.*

Comment: Page 4-5, Section 4.0, paragraph 1: Please replace the phrase “GAM model” with “groundwater availability model” or “GAM.” As is, “GAM model” is redundant

Response: *Corrected to read “GAM” as requested.*

Comment: Page 4-8, Section 4.1, paragraph 3, line 3: Please update figure 2.5.8 to reflect the presence of tertiary volcanics described in this section, if present. At a minimum, explain in text why tertiary volcanics are not shown in the F-F’ cross section.

Response: *Text clarified as requested to recall no tertiary volcanics within the Green River Valley.*

Comment: Page 4-8, 4th paragraph: Suggest changing sentence to “Green River Valley is bound to the northwest by the Indio Mountains

Response: *Corrected as requested.*

Comment: Page 4-9, Section 4.2.1: Please replace the word “show” to “shown.”

Response: *Corrected as requested.*

Comment: Page 4-11, paragraph 2, sentence 2: Please change “where” to “were.”

Response: *Corrected as requested.*

Comment: Page 4-20, Section 4.3.1, paragraph 1: Please change “this probably” to “this is probably.”

Response: *Corrected as requested.*

Comment: Pages 4-20 to 4-22, Section 4.3.2: Suggest rewriting the equations in this section with Microsoft Equation Editor for a cleaner appearance.

Response: *Corrected as requested.*

Comment: Page 4-23, paragraph 2, sentence 5: Please add the word “surface” after “potentiometric.”

Response: *Corrected as requested.*

Comment: Page 4-27, Section 4.3.4.2, last sentence: Please change “though” to “thought.”

Response: *Corrected as requested.*

Comment: Page 4-34, Table 4-1: Please increase the font size.

Response: *Corrected as requested.*

Comment: Page 4-36, Table 4-2 Heading: Please change Foefficients to Coefficients.

Response: *Corrected as requested.*

Comment: Page 4-38, Figure 4.4.1: Please re-label legend item “Blanco Bolson Poly” to a more descriptive name.

Response: *Legend corrected as requested.*

Comment: Page 4-41, paragraph 1, 3rd line: Please change Espanola to Española.

Response: *Corrected as requested.*

Comment: Page 4-45, Section 4.6.1, paragraph 2, line 6: Please add a period after “Driscoll (1986).”

Response: *Corrected as requested.*

Comment: Page 4-46, 2nd paragraph, last line: Please change 1 feet per day to one foot per day.

Response: *Corrected as requested.*

Comment: Page xxx, Section 4.6.1, paragraph 2: Please fix punctuation.

Response: *Corrected as requested.*

Comment: Page 4-46, Section 4.6.2, paragraph 2, line 3: Please clarify whether the range in porosity states as “0.0 to 0.10” is from “zero to 0.10” or from some smaller decimal to 0.10.

Response: *Corrected to read “zero to 0.10”.*

Comment: Page 4-48, Table 4.6: Please increase font to 12 point.

Response: *Font size was not changed at the discretion of LBG-Guyton.*

Comment: Pages 4-52 and 4-53: Please increase the font on the figure captions.

Response: *Font size was not changed at the discretion of LBG-Guyton.*

Comment: Page 6-1, Section 6.1, paragraph 2, line 6: Please correct the end of the sentence to read “that is used.”

Response: *Corrected as requested.*

Comment: Page 6-1, 2nd paragraph, 2nd line from bottom: “(4) there are a several graphical user..” please remove “a”.

Response: *Corrected as requested.*

Comment: Page 6-1, paragraph 3: second to last sentence is incomplete. Please revise.

Response: *Sentence revised as requested.*

Comment: Page 6-1, 3rd paragraph, last line: “...~~were~~[are] used” Please add are.

Response: *Corrected as requested.*

Comment: Section 6.3 to Section 7.2: Please add page numbers to these sections.

Response: *Corrected as requested.*

Comment: Section 6.3, paragraph 1: Suggest adding additional information to focus on what “model parameters” are. For instance, explain that they describe the characteristics of the aquifer that determine how water moves through it.

Response: *Text clarified as requested.*

Comment: Section 6.3.1, paragraph 1, line 1: Please change phrase to “there *are* only.”

Response: *Corrected as requested.*

Comment: Page 6-4, 1st paragraph, 2nd line: “..contain ¼ square mile” Please remove “s”.

Response: *Corrected as requested.*

Comment: Section 6.4.2: Please change phrase in second sentence to read "...bottom of the aquifers..."

Response: *Corrected as requested.*

Comment: Section 6.4.2, 2nd line: "...bottom of the aquifers.." Please add "of".

Response: *Corrected as requested.*

Comment: Section 6.4.2: Last sentence is incomplete; please revise.

Response: *Sentence revised as requested.*

Comment: Section 6.4.3, 4th line: "... Stream boundaries are a head-dependant....." Please add "a" .

Response: *Corrected as requested.*

Comment: Section 6.4.4, 1st paragraph, second line: "...redistribution analysis that is detailed...". Please add "is".

Response: *Corrected as requested.*

Comment: Page 8-1, 3rd paragraph, 2nd to last line: Please replace "...layer 1, 2, and 3..." with layers 1, 2, and 3.

Response: *Corrected as requested.*

Comment: Table 8.3: Please add commas to separate 1,000's in numbers greater than 999.

Response: *Corrected as requested.*

Comment: Page 10-2, Section 10.1, paragraph 1, line 1: Please remove the word "is." Page 10-2, paragraph 1, Please replace "A groundwater model is simulates..." with "A groundwater model simulates..." .

Response: *Corrected as requested.*

Comment: Page 10-2, paragraph 1: Please clarify or revise sentence containing "is simulates".

Response: *Corrected as requested.*

Comment: Page 11-1, 3rd paragraph, 1st line: Please replace “Appropriate calibration of transient model ...” with “Appropriate calibration of a transient model...”.

Response: *Corrected as requested.*

Comment: Appendix B, general: Please replace all “et al.” in reference citations with “and others”.

Response: *Corrected as requested.*